Characterization of the role of TRAPPC2/Trs20p-related and associated proteins in membrane traffic

Nassim Shahrzad

A Thesis in

The Department

of

Biology

Presented in Partial Fulfillment of the Requirements

for the Degree of Doctor of Philosophy at

Concordia University

Montreal, Quebec, Canada

February 2014

CONCORDIA UNIVERSITY

SCHOOL OF GRADUATION STUDIES

This is to certify that the thesis prepared

By: **Nassim Shahrzad**

Entitled: Characterization of the role of TRAPPC2/Trs20p-related and associated proteins in membrane traffic

and submitted in partial fulfillment of the requirements for the degree of

DOCTOR OF PHILOSOPHY (Biology)

complies with the regulations of the University and meets the accepted standards with respect to originality and quality.

Signed by the final examining committee:

_____ Chair

Dr. C. Kalman

_____ External Examiner

Dr. J. Presley

_____ External to Program

Dr. P. Darlington

_____ Examiner

Dr. R. Storms

_____ Examiner

Dr. P. Pawelek

_____ Thesis Supervisor

Dr. M. Sacher

Approved by _____

Dr. Selvadurai Dayanandan, Graduate Program Director

Abstract

In the process of intracellular trafficking, fidelity of delivering proteins and lipids across the secretory pathway is of critical importance. Any failure in this highly regulated event could have severe consequences to the cell. Various human diseases arise from mutations affecting membrane trafficking. In this regard, vesicle tethering complexes serve as key factors for the maintenance of cellular function. The transport protein particle (TRAPP) is one such factor which provides specificity in delivering proteins and lipids. TRAPP is found in three related complexes sharing core subunits, each governing different transport steps. *TRAPPC2,* a mammalian ortholog of yeast *TRS20*, is an essential gene that codes for a protein that exists in all forms of the TRAPP complexes. My research has focused on elucidating the cellular function of TRAPPC2 and proteins that associate with it.

Substitution of an aspartic acid residue at position 47 of TRAPPC2 to tyrosine has been shown to cause a skeletal disorder known as spondyloepiphyseal dysplasia tarda (SEDT), a disorder which is believed to be due to a defect in collagen secretion. In Chapter 2 I demonstrate that aspartic acid residue 47 is absolutely invariant across taxa suggesting that this amino acid plays an important role in the function of the TRAPP complex. Even though TRAPPC2 is ubiquitously expressed the SEDT phenotype is manifested in only in specific tissue. Thus, we rationalised a search for homologs of TRAPPC2/Trs20p, hoping to provide an answer to the tissue-specificity of SEDT. We identified two novel proteins; TRAPPC2L and its yeast counterpart Tca17p. The

position for the novel TRAPPC2L protein is postulated to be opposite to the region where TRAPPC2/Trs20p incorporates into the TRAPP complex.

In Chapter 3 I demonstrate a direct interaction between the TRAPP complex and the SNARE fusion machinery. This binding is lost in the pathogenic TRAPPC2D47Y mutant. Subsequently, we revealed that an SEDT-analogous mutation in Trs20p (*trs20D46Y*) resulted in deficiency in autophagy rather than defects in endoplasmic reticulum to Golgi trafficking. Chapter 4 describes the discovery of the association between TRAPP and the tethering factor p115. By using the TRAPPC2D47Y mutant I showed that p115 could not efficiently dissociate from membranes, thereby showing that a TRAPP-p115 interaction is critical for p115 membrane recognition. Furthermore, I provide evidence that TRAPP associates with p115 and SNAREs in a Brefeldin A-resistant manner. I propose placing this association at the ER-Golgi intermediate compartment (ERGIC) membranes, a compartment that lacks in lower eukaryotic cells, at the very early stage of the secretory pathway.

Previous work by our laboratory found several novel mammalian TRAPP components including TRAPPC11. Chapter 5 discusses our discoveries into the function of TRAPPC11, a TRAPPC2 protein partner. The genetic component of this work was conducted by our collaborators from Alberta who used homozygosity mapping in combination with exome sequencing in two siblings from a Hutterite family. They found that the candidate gene mutation affects the *foie gras* domain of TRAPPC11 in these brothers. The deletion mutation accounts for the array of phenotypes including myopathy, ataxia, and intellectual disability (ID) that is observed in these patients. I demonstrated that this mutation disrupts TRAPPC11 binding to multiple TRAPP

subunits including TRAPPC2 and compromises the integrity of the Golgi apparatus. I also showed that this mutation causes a dramatic delay in trafficking from the Golgi to the plasma membrane. Moreover, this mutation dramatically affects the localization of lysosomal membrane glycoprotein 1 (LAMP1). This is the first study to investigate the function of the *foie gras* domain of TRAPPC11 in humans. Finally, in Chapter 6 I discuss the implications of all of the studies performed in the preceding chapters and provide a working model for the function of TRAPPC11 in membrane traffic.

Acknowledgments

I would like to begin by thanking my supervisor, *Dr. Michael Sacher*, for guiding me through my graduate work, and also giving me the opportunity to incorporate my own ideas for developing the projects. I am truly grateful for his strong leadership and the way he always encouraged me to be proactive when facing challenges. His knowledge, expertise, support and advice have been critical for my achievement.

I would also like to thank all my colleagues in the Sacher laboratory, *Miroslav*, *Stephanie, Rodney*, *Audrey*, *Benedeta*, *Hartley*, *Sokunthear*, *Debora*, *James*, *Yueyun*, and *Ariel*, without whom I could not have completed my work. I would particularly like to thank *Djenann* for always being willing to take time out of her busy schedule to assist me when I was performing final experiments. Thank you for your kindness towards me. Very large thank you to *Christine Munger* for helping me run samples on the overly-crowded gel filtration chromatography system at BRI.

I would also like to express my gratitude to *Dr. Reginald Storms* and *Dr. Peter Pawelek* for accepting to be members of my program advisory committee. Their expertise, advice and comments have greatly improved both the quality of my thesis work as well as the quality of my graduate experience.

I am very grateful to all of the researchers who collaborated with us and contributed to my papers. Furthermore, thanks to *Dr. Christopher Brett* and *Gabriel Lapointe* for help acquiring the movies that were so instrumental in the identification of the traffic delay observed in patients with *TRAPPC11* mutations. Dear *Chole*, you have

gone out of your way to make things run the best they can be. Your hard work has been very much appreciated.

A special acknowledgement to *Dr. Jesse Hay*, *Dr. Peter McPherson*, *Dr. Paul Melancon, Dr. John Presley*, *Dr. Martin Lowe*, *Dr. Randy Schekman* and *Dr. James Rothman* for providing us reagents and thus helping us in our projects.

I would like to particularly thank *Dr. Alisa Piekny, Dr. Selvadurai Dayanandan*, *Dr. Hojatollah Vali, Dr. Vladimir Titorenko* and *Dr. Jack Kornblatt* for their constructive advice and suggestions.

This work could not have been completed without my family and friends who have supported me throughout my studies. A special thanks to my parents, *Darioush*, *Seyamak*, *Haneen*, *Annika*, *Sanaz, Anitta, Nellie, Sussan*, *Baraa*, *Sassan*, *Tara*, *Paknoush*, *Avid,* and *Koroush*.

I have been blessed with endless and invaluable support from my parents. You are the definition of love to me that has given me the strength to face challenges in this journey.

Finally, I would like to greatly acknowledge funding for my research from the Concordia University "*Concordia Accelerator Award* ".

Dear parents, family, friends, colleagues, committee, faculty members, and my PhD advisor, I owe you my success because of your constant support and dedication. I will commit myself to science and cherish this accomplishment with you all.

Table of Contents

List of Figures

List of Tables

List of Abbreviations

3-aminotriazole	3AT
5-fluoroorotic acid	FOA
acidic domain	AD
aminopeptidase I	Ape1
autophagy-related genes	Atg
blocked early in transport 3 protein	Bet3p
brefeldin A	BFA
bovine serum albumin	BSA
Calcofluor white	CFW
carboxypeptidase Y	CPY
chitin synthase-III	Chs3
clathrin-coated vesicle	CCV
coat protein I	COPI
conserved oligomeric Golgi	COG
creatine kinase	CK
cytoplasm-to vacuole-targeting	Cvt
dependence on SLY1–20	DSL1
dithiothreitol	DTT
Dulbecco's Modified Eagle Medium	DMEM
early endosomes	EE
electron microscopy	EM

Endoplasmic Reticulum	ER
ER-exit sites	ERES
ER-Golgi intermediate compartment	ERGIC
Ethylenediaminetetraacetic acid	EDTA
Extracellular Matrix	ECM
fetal bovine serum	FBS
fluorescence recovery after photobleaching	FRAP
GDI displacement factor	GDF
GDP-dissociation inhibitor	GDI
general-amino-acid-permease	Gap1p
globular head region	GHR
Green fluorescent protein	GFP
GTPase activating protein	GAP
Golgi-Associated Retrograde Protein	GARP
guanine nucleotide exchange factor	GEF
homotypic vacuole fusion and protein sorting	HOPS
Intellectual disability	ID
intermediate density membranes	IDM
isolation membrane	IM
Isopropyl β-D-1-thiogalactopyranoside	IPTG
lysosomal membrane proteins	LAMP1/2
lysosome-related organelles	LROs
Multisubunit Tethering Complexes	MTC

microtubule organizing center	MTOC
Microtubule-associated protein 1light chain 3 protein	LC3
microtubules	MT
Molecular weight	Mw
multivesiular bodies	MVBs
N-acetylglucosamine	GlcNAc
N-ethylmaleimide	NEM
N-ethyl-maleimide-sensitive fusion	NSF
Optical density	OD
paraformaldehyde	PFA
phagophore assembly site	PAS
phosphatidylethanolamine	PE
phosphotidylinositol 3-kinase	PI3K
Polyacrylamide gel electrophoresis	PAGE
Post-translational modification	PTM
precursor Ape1	prApe1
procollagen	PC
Revolutions per minute	Rpm
small interfering RNA	siRNA
Sodium dodecyl sulfate	SDS
Soluble N-ethylmaleimide-sensitive factor Attachment protein REceptors	SNARE
spondyloepiphysealdysplasia tarda	SEDT

Synthetic defined	SD
Sec1/Munc18 proteins	SM
Tandem affinity purification	TAP
temperature-sensitive	ts
three dimensional	3D
transferrin	Tfn
trans-Golgi network	TGN
transitional-ER	tER
transport protein particle	TRAPP
TRAPPC2	C2
TRAPPC2L	C2L
tris (hydroxymethyl)aminomethane	Tris
ubiquitin-proteasome system	UPS
very low density membranes	VLDM
Vesicular Stomatitis-Virus-Glycoprotein	VSV-G
vesicular-tubular structures	VTC
α-mannosidase 1	Ams1
α-soluble NSF attachment protein	α-SNAP
Separated proteins within a complex	-
Separate homologs	/
yeast two hybrid	Y2H

I dedicate this dissertation to my parents.

CHAPTER 1

1.1 Introduction to intracellular transport

1.1.1 Background

Organellar compartmentalization is a hallmark in all eukaryotic cells and relies on an elaborate network of endomembrane systems. These systems are composed of distinct organelles such as the endoplasmic reticulum (ER), the Golgi, endosomes and lysosomes (vacuoles in yeast). Several trafficking pathways have been established to develop communication among these organelles including the secretory pathway described by Nobel Prize winner George Palade. Palade defined protein secretion in exocrine pancreatic cells with a combination of pulse-chase, autoradiographic and electron microscopy techniques (Caro and Palade, 1964). He found that proteins to be secreted begin synthesis at the ER and traverse towards the Golgi apparatus. In the Golgi, the proteins are packaged into secretory vesicles and subsequently transported to the plasma membrane where they are released into the extracellular matrix (ECM) (Palade, 1975).

Significant insight into the molecular mechanism of vesicular trafficking was later obtained through the work of recent Nobel Prize winners Randy Schekman and James Rothman using yeast and mammalian systems, respectively (Balch et al., 1984; Novick et al., 1980). Schekman and his associate Peter Novick used genetic studies, specifically, complementation-based yeast screens, for the isolation of conditional mutants that display blocks in secretion. This led to the discovery of 23 genes required for secretion (Novick et al., 1981) and the further characterization of their corresponding gene products. Rothman's group developed a biochemical *in vitro* vesicle transport reconstitution system using isolated Golgi membranes from wild type and mutants that were lacking the glycosylation enzyme N-acetylglucosamine (GlcNAc) transferase. Mutant cells that were transfected with a secretory

pathway marker, the vesicular Stomatitis-Virus-Glycoprotein (VSV-G) in combination with a radiolabelled GlcNAc were shown to be properly glycosylated, thus leading to the discovery that vesicles containing VSV-G bud from mutant membranes and are transported across the stacks of the Golgi to fuse with the wild type membranes. The development of this assay allowed the researchers to purify cytosolic components required for budding and fusion in the secretory pathway e.g. components of the fusion machinery (Sollner et al., 1993a) (see section 1.2.4.1 for detail).

1.1.2 Secretory (biosynthetic) pathway of intracellular trafficking

The movement of proteins and lipids between different compartments in a eukaryotic cells is known as membrane trafficking and is mediated by membrane-bound transport carriers. These transport carriers may be round in shape or resemble more of a tubulo-vesicular structure. Transport intermediates (vesicles) bud from a donor compartment and subsequently fuse to a specific recipient organelle thus, interconnecting the endomembrane systems (Bonifacino and Glick, 2004). Regardless of the shape of the vesicles, vesicular transport can be classified into five events with partial overlapping steps between formation at donor and delivery to recipient organelles: (i) budding, (ii) motility, (iii) tethering, (iv) docking and (v) fusion. During the budding (vesicle biogenesis) process, selective incorporation of cargo into the growing vesicle is achieved by the collaborative action of small GTP-binding proteins, coat protein complexes COPI and COPII and accessory factors (described in later sections). The vesicles then move along cytoskeletal tracks in mammalian cells and during certain steps in yeast, with motor proteins usually facilitating their trafficking. The vesicles then tether and dock to the recipient membranes via the action of a diverse group of coiled-coil and multisubunit tethering complexes (MTCs) collectively known as tethering factors. These tethering factors are needed for vesicle grasping and establishing the first “loose” interaction between vesicles and their respective compartments, which is subsequently followed by tighter engagements of the vesicle with its

target membrane. During this docking event the two lipid bilayers undergo molecular rearrangement, presumably as a prerequisite step triggering subsequent membrane fusion. Ultimately during fusion, the soluble N-ethylmaleimide-sensitive factor attachment protein receptors (SNAREs) (see section 1.2.4) are key to allow for the merging of the bilayers thereby leading to the release of the vesicle contents into the lumen of the target organelle. The precise regulation of the biosynthetic pathway from vesicle budding to fusion ensures efficient cargo transfer to a target organelle, yet maintains the integrity of organelle identity; all this occurring while there are thousands of proteins and lipids moving through various pathways.

The complex network of endomembranes in the secretory system includes the ER, flat stacks (cisternae) of the Golgi apparatus, the *trans*-Golgi network (TGN), plasma membrane and some cell-specific secretory granules, and is evolutionarily conserved. Intracellular membrane trafficking incorporates two major routes to facilitate the transport of lipids and proteins. The secretory (anterograde) pathway operates to secrete proteins and lipids outside of the cell or to deliver them to other intracellular tragets while the endocytic pathway is devoted towards the uptake of proteins and materials from the extracellular milieu to intracellular destinations. Both pathways are finely tuned to ensure maintenance of the composition and function of the organelles.

The secretory pathway is initiated by the synthesis of many proteins destined for secretion and commences at the ER. Newly synthesized proteins must be properly folded, and in some cases proteins may undergo a series of post-translational modification (PTMs), usually N-glycosylation, prior to exit from the ER (Schegg et al., 2009). Proteins that are not folded correctly are retained in the ER and degraded. Once this initial quality control is imposed, proteins leave the ER via COPII-coated vesicles (described in 1.2.1). In mammals, COPII vesicles can fuse with each other to form an ER-Golgi intermediate compartment (ERGIC) prior

to moving to the Golgi. The vesicular-tubular structures of ERGIC (known as VTC) are the first post-ER sorting organelle in higher eukaryotes (Szul and Sztul, 2011). Although controversial, it has been suggested that COPI takes over the responsibilities for ferrying the cargo to downstream pathways and for recycling back to the ER (Martinez-Menarguez et al., 2001; Orci et al., 2000).

Highly dynamic cytoskeleton microtubules (MT), in part, are responsible for bidirectional movement of proteins between intracellular organelles. Two extremities of MTs are labelled the minus end, which is found in a perinuclear region called the microtubule organizing center (MTOC) and the plus end, which is found near the cell periphery. The position and movement of organelles and vesicles along these microtubules is achieved through the coordinated function of MTs with another group of proteins known as motor proteins. There are two classes of motor proteins, both with an intimate association with MTs: dynein-dynactin and kinesin. Dynein-dynactin delivers cargo in a retrograde fashion towards the MTOC region and is thus called a minus end directed motor protein, while kinesin is a plus end directed motor protein moving in an anterograde fashion, and thereby transporting cargos to the cell periphery (Soppina et al., 2009).

Microtubules assist COPI vesicles *en route* to the Golgi complex in higher eukaryotes (Appenzeller-Herzog and Hauri, 2006). This is followed by vectorial shuttling across the Golgi apparatus where the proteins can pass through the distinct *cis*, *medial* and *trans* sub-compartments called cisternae. The proteins once again may be subject to additional glycosylation or other PTMs such as palmitoylation (Fukuda et al., 1988; Turnbull et al., 2005). The modifications imposed on the proteins enable them to mature prior to being distributed to their final destination. Similar to endocytic trafficking, the highly dynamic TGN is a major sorting station receiving numerous transport carriers from the biosynthetic pathway and receiving those derived from the cell surface via the endocytic pathway. The TGN is responsible for packaging and

sorting cargo to ensure that the contents of the vesicle reach its specified target membrane. Finally, the TGN also plays a role in recycling transport materials that originated from endosomal compartments (Riederer et al., 1994).

Depending on the cargo's final fate, proteins can take either the constitutive or regulated secretory pathway after exiting the TGN. In the case of the constitutive pathway, vesicles harboring proteins are targeted to the cell surface where they can discharge their contents in a non-regulated fashion. In the regulated pathway, cargo proteins are stored in secretory vesicles (granules). Secretion of the contents of this vesicle is fine-tuned and triggered in response to an appropriate stimulus. Regulated secretion is observed in dedicated secretory cells of the endocrine and neuronal systems which release hormones and neurotransmitters, respectively (Bonifacino and Glick, 2004). Alternatively, some TGN-packaged cargos move toward organelles such as early/late endosomes, where the proteins can ultimately make their way to vacuoles (lysosomes). For instance, lysosomal membrane proteins LAMP1 and LAMP2 can be transported via either a direct or indirect route on their way to endosomal compartments. In the direct route, LAMP proteins use the endosomal system prior to their delivery to the lysosome. On the other hand, the indirect pathway involves the cycling of proteins to the cell surface prior to their subsequent delivery to the endosomal compartments and finally to lysosomal membranes (Janvier and Bonifacino, 2005; Kornfeld and Mellman, 1989).

1.1.3 Endocytic pathway of intracellular trafficking

The second fundamental route of intracellular trafficking is the endocytic pathway, and it is composed of three main populations of endosomes; (1) early, late and recycling endosomes, (2) lysosomes and (3) lysosome-related organelles (LROs). Like the biosynthetic pathway, endocytic transport involves multiple processes of cargo recognition which promotes vesicle formation, and then vesicle release followed by transport towards and fusion with the target

destination. While there is a flux of proteins moving towards the cell membrane in the biosynthetic pathway, the endocytic pathway involves the trafficking of material in the opposite direction. Proteins at the cell surface are collected into vesicles called endosomes which bud off from the plasma membrane via endocytosis. The endocytic pathways consist of specific sets of protein machinery and vesicles that cycle between endosomes and the TGN. Protein retrieval from endosomal organelles back to the TGN can take place either from early/recycling endosomes or from late endosomes to the Golgi. For example, the transmembrane protein TGN46 (human ortholog of rat TGN38) has an unknown function but cycles through the cell surface, early endosome and TGN. However, Shiga toxin utilizes the early/recycling endosomes subsequent to its internalization but the toxin then leaves the endocytic pathway and takes a route known as the retrograde pathway all the way towards the ER, which ultimately poisons the host cell (Johannes et al., 1997; Mallard et al., 1998). In yeast, numerous cargo proteins are directed to the endosome and the TGN via the vacuolar receptor known as Vps10p, which is a receptor for carboxypeptidase Y (CPY) (Seaman et al., 1997) (Figure 1.1). Finally, chitin synthase-III (Chs3) in yeast is another example of a cargo that exploits the retrograde pathway from the plasma membrane to the early endosome and then to the TGN (Valdivia et al., 2002).

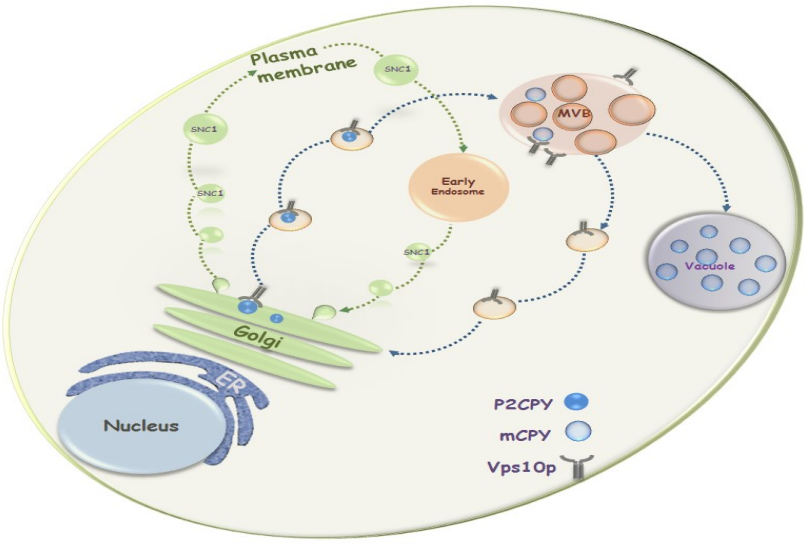

Figure 1.1 Highly coordinated bidirectional (forward and reverse) trafficking systems

interconnecting intracellular organelles. Cargo sorting from the tubular network of the *trans*-Golgi in budding yeast: Vps10p, like its mammalian counterpart mannose 6-phosphate receptor, constantly traffics from the TGN to the endosome thus, delivering its cargo. The empty receptor recycles back to the TGN for another round of biosynthetic cargo transport (Duncan and Kornfeld, 1988). In the case of the vacuolar hydrolase CPY, the cargo is secreted from the cells when its receptor Vps10p is defective (Lewis et al., 2000). Two cargo proteins Snc1p and the CPY receptor Vps10p, follow distinct recycling routes from early and late endosomes to the late Golgi, respectively.

1.2 Membrane trafficking machinery and the specificity of vesicle fusion with its appropriate compartment

In membrane trafficking, distribution of the proteins to their proper target compartments is of crucial importance and is assured by the coordination between the following cellular factors: (1) coat proteins, required to coordinate the production of transport vesicles with the selection of specific cargo; (2) tethering factors, essential for initial recognition between a vesicle and target destination, (Sztul and Lupashin, 2006); (3) GTP-binding proteins that define and localize vesicles to their appropriate organelle (Pfeffer, 2001); and (4) SNAREs (Sollner et al., 1993a), key factors for fusion of vesicles to their correct organellar destinations.

1.2.1 Coat proteins

There are three different types of well-studied coat protein complexes that are vital to membrane trafficking. The first is the COPII coat protein complex, which is involved in the early stages of the secretory pathway for transport of vesicles between the ER to either the ERGIC/VTC or the Golgi (Barlowe et al., 1994). The second is the heptameric complex COPI, also known as coatomer, that takes part in multiple transport steps including bidirectional trafficking from the VTC to the Golgi (Aridor et al., 1995), retrograde transport between Golgi cisternae and from the Golgi to the ER (Letourneur et al., 1994), and endocytic transport (Whitney et al., 1995). Finally, the clathrin protein complex acts at two distinct sites; one

emanating from the post-Golgi network to generate intermediate clathrin-coated vesicles (CCVs) *en route* to the endosomal systems, and the second CCVs originates at the cell surface and coats vesicles that travel to early endosomes (Bonifacino and Lippincott-Schwartz, 2003).

Generation of a COPII vesicle requires three main components: the small Ras-like GTPase Sar1p, the membrane-proximal layer Sec23p-Sec24p heterodimer and a second layer, membrane-distal sub-complex Sec13p-Sec31p (Figure 1.2). The formation of COPII-coated vesicles is initiated by the recruitment of the Sar1 GTPase to specialized regions of the ER membrane called ER-exit sites (ERES) (Amessou et al., 2007) also known as transitional-ER (tER) where Sar1 then becomes activated by the action of the ER-localized guanine nucleotide exchange factor (GEF) Sec12 (Figure 1.2). Following the activation of Sar1p, there is sequential recruitment of cytosolic inner and outer COPII coat proteins (Lee et al., 2005). GTP-bound Sar1p also triggers membrane curvature and fission of COPII vesicles (Bielli et al., 2005; Lee et al., 2005). Once these components of the coat have been assembled, selection and concentration of properly folded cargo, coat polymerization, membrane deformation, and finally pinching off of the vesicle can occur (Otte and Barlowe, 2004).

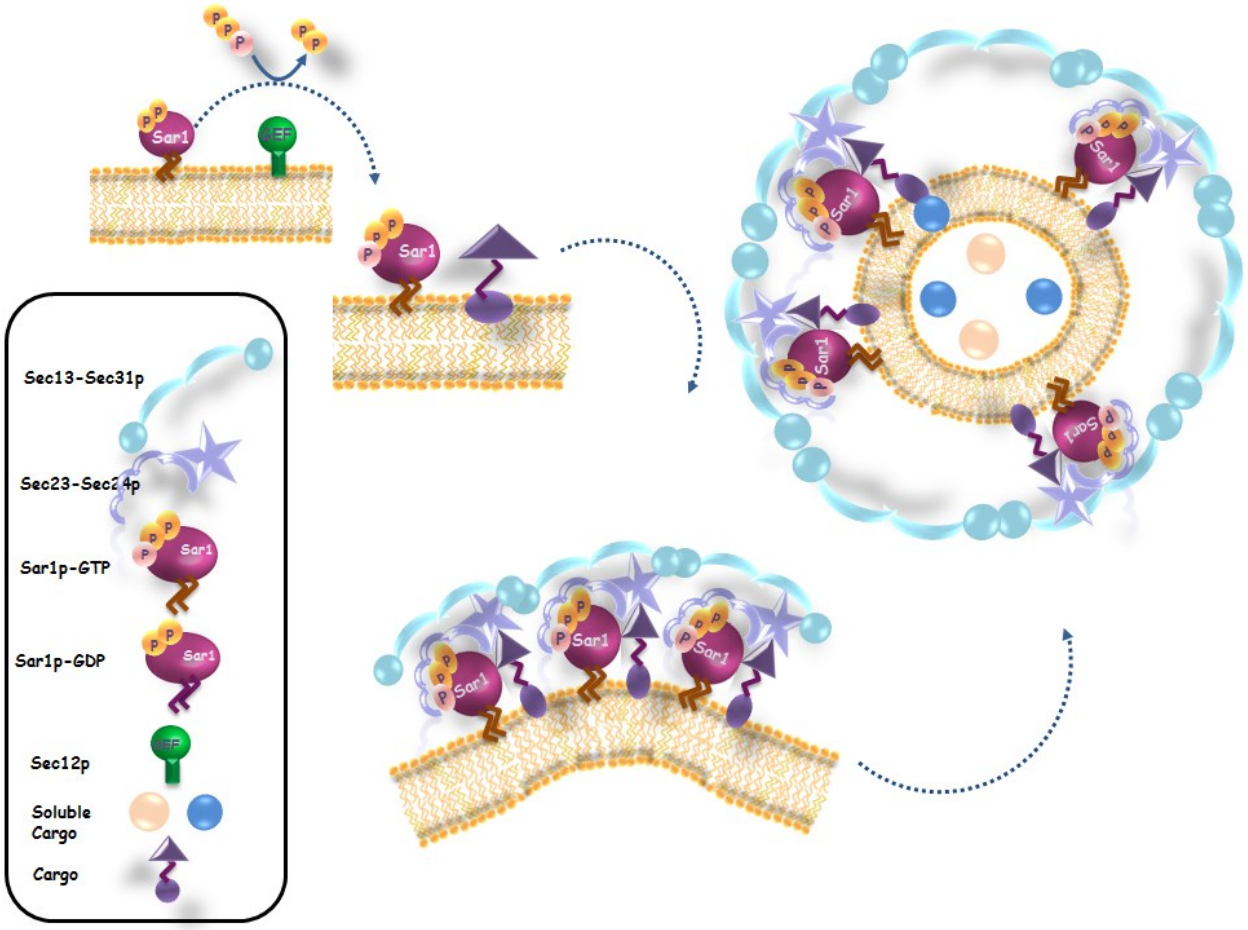

Figure 1.2 Vesicle biogenesis mediated by COPII coat protein machinery.

Typical COPII coated vesicles are estimated to be between 50-100 nm in diameter. Occasionally there are some large cargos that must exit the ER (Bachinger et al., 1982). Thus it is possible that there is an alternative mechanism for packaging these macro-cargos into vesicles destined for downstream compartments, or alternatively, the COPII coat itself is flexible enough to accommodate larger cargos. A number of laboratories recently demonstrated that the secretion of procollagen (PC), a cargo of approximately 300 nm in length, is COPII- dependent (Townley et al., 2008;O'Donnell et al., 2011) and accommodation of the large PC cargo is achieved by longer activation of Sar1 GTPase and thus longer settlement of COPII proteins on the membrane which is a requirement for PC packaging (Venditti et al., 2012).

1.2.2 Tethering factors

The initial interaction between a vesicle and its cognate membrane is a critical step for proper cell functioning. The specificity of the interaction is achieved by the action of tethers that act to initially tether (or capture) the transport vesicles to their target membrane. This occurs subsequent to the vesicle budding event. Tethering factors are localized to distinct intracellular regions where they can act upon those organelles (see Figure 1.3). Tethers can be divided into two different classes: coiled-coil proteins and multisubunit tethering complexes (MTCs) (Whyte and Munro, 2002). From a structural point of view, the elongated nature of coiled-coil tethers may allow these tethers to interact with incoming vesicles and bring them closer to the membrane on which the tether is attached. In mammals, one example of a coiled-coil tether is p115 (the mammalian homolog of yeast Uso1p) which interacts with two Golgi-localized tethers called GM130 and giantin (Beard et al., 2005).

1.2.2.1 Coiled-coil tethers

Long coiled-coil tethering factors are responsible for capturing transport intermediates in a process known as loose tethering. This is followed by vesicle docking which involves tighter interaction (Whyte and Munro, 2002). Coiled-coil proteins mostly exist in cytosolic and membrane-bound forms. This family of proteins is usually in direct contact with numerous components of the cellular trafficking machinery. One such interaction is with Ras-related GTPase which allows them to associate with the membrane. Coiled-coil tethering factors in part confer fidelity by participating in the delivery of vesicles, through the formation of physical links at relatively long-distances from the target membrane (Gillingham and Munro, 2003; Yu and Hughson, 2010). Genetic and physical interactions have been documented between a *cis*-Golgi tethering factor Uso1p/p115 and Ypt1p/Rab1 in yeast and mammalian cells enabling COPII coated vesicles to travel from the ER to the *cis* side of the Golgi (Sapperstein et al., 1995).

1.2.2.2 Multisubunit tethering complexes (MTCs)

In contrast to the coiled-coil family of tethering factors, multisubunit complexes mediate short-distance tethering events (Yu and Hughson, 2010). MTCs have been proposed to play roles at distinct trafficking steps. Some tethering factors that exist as multisubunit complexes such as TRAPP (transport protein particle) have been shown to act as Rab-activators. Other MTCs include HOPS, DSL1, COG, GARP, Exocyst and CORVET (Figure 1.3), and some these associate with and regulate the function of Rab GTPases. Tethering factors are implicated in every aspect of vesicle transport and more specifically MTCs are emerging as positive regulators of SNARE assembly (Perez-Victoria and Bonifacino, 2009;Ren et al., 2009; Shorter et al., 2002). There will be a section devoted to the TRAPP complex (see section 1.3).

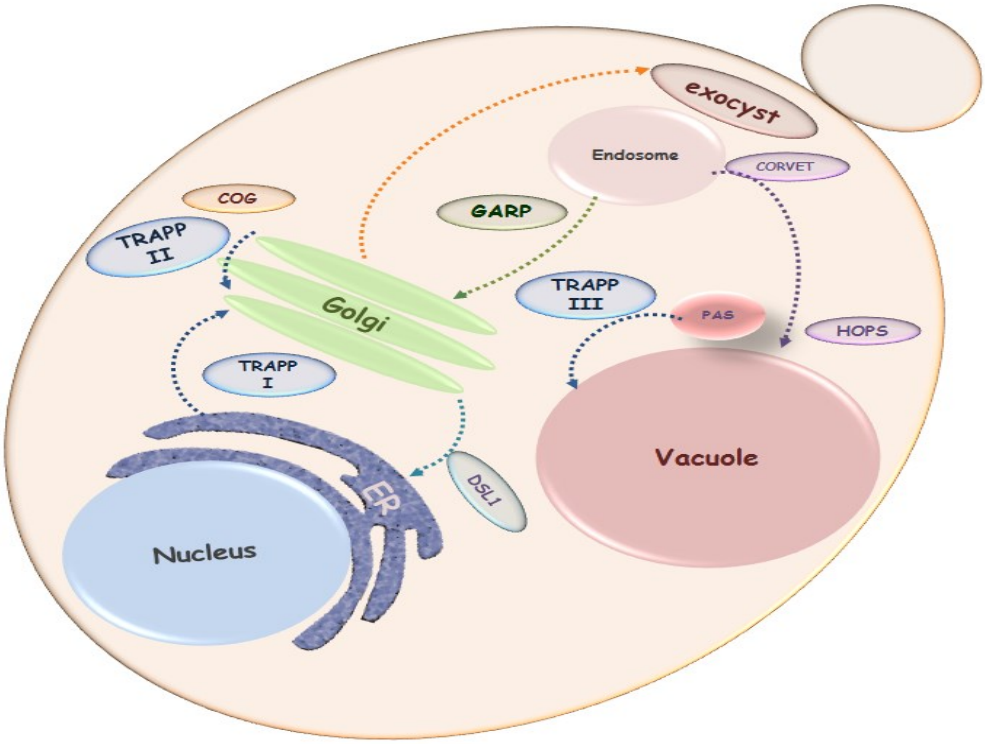

Figure 1.3 Intracellular localization of MTCs in yeast. To date, nine MTCs have been identified in budding yeast each with a distinct localization (Yu and Hughson, 2010).

1.2.3 Small GTPases as master regulators of intracellular transport

Rab GTPases are members of the Ras superfamily and are master regulators of vesicular budding, motility and fusion. These small GTPases are involved in virtually every trafficking pathway (Woollard and Moore, 2008). In eukaryotic cells, intracellular vesicle trafficking is controlled by Rab GTPases in both the secretory and endocytic pathways. In terms of vesicular trafficking events Rab GTPases are involved in vesicle biogenesis, transport, tethering and fusion events.

Once Rab proteins are activated they can then specifically interact with certain proteins or lipids referred to as effector molecules. This interaction facilitates membrane transport as the newly formed interaction can act as a scaffold for the sequential recruitment of proteins and lipids that are required in that specific process. Rab proteins cycle between an active and inactive state: the GTP- and GDP-bound forms, respectively. A general feature observed in all the GTPases is the intrinsic rates of GDP dissociation and GTP hydrolysis are slow, thus the switch between active and inactive Rab proteins requires accessory proteins (Figure 1.4). These accessory factors are collectively called guanine nucleotide exchange factors (GEFs) and GTPase activating proteins (GAPs), which stimulate activation and deactivation of Rab proteins, respectively. In addition to GEFs and GAPs, GDP-dissociation inhibitor (GDI) and GDI displacement factor (GDF) are also part of the protein machinery required for cycling of small GTPases between membrane compartments by facilitating extraction from and recruitment to specific membranes, respectively (Pfeffer and Aivazian, 2004).

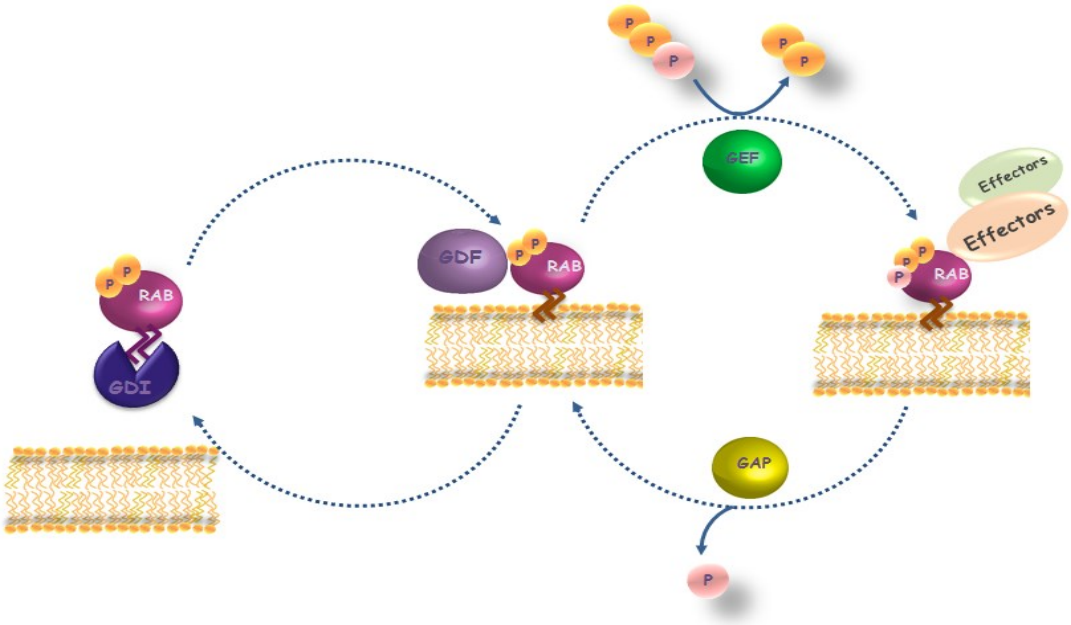

Figure 1.4 Widely accepted model of the Rab/Ypt cycle. GEFs and GAPs are responsible for the active (GTP-bound) and inactive (GDP-bound) states of small GTPases. The active form of the GTPase is competent to bind to downstream effectors. GDI extracts the GTPase from membranes while GDF mediates the dissociation of the GTPase from GDI.

1.2.4 SNARE proteins mediate intracellular fusion

SNARE (*s*oluble *N*-ethylmaleimide-sensitive factor *a*ttachment protein *re*ceptor) proteins are key to one of the fundamental processes in the fusion of eukaryotic cell membranes. In *Saccharomyces cerevisiae*, there are 25 genes encoding SNARE proteins and alternative splicing in SNARE primary transcripts in humans increases the SNARE numbers to 36 (Jahn and Scheller, 2006). All mammalian SNARE proteins of the Syntaxin family, except Syntaxin 11, are type II integral membrane proteins that are thought to be essential in anchoring the proteins by their C-terminal region. SNAREs have a broad range of protein partners within the vesicular transport machinery including coat proteins, small GTPases and tethering factors.

1.2.4.1 Discovery of SNARE proteins

As noted before, an *in vitro intra*-Golgi trafficking assay used in the Rothman lab during the 1980s led to the identification of a soluble protein called NSF (mammalian ortholog of Sec18p) and shortly after that, the identification of its adaptor molecule α-soluble NSF attachment protein (α-SNAP)/ Sec17p (Sollner et al., 1993a). Subsequently SNAREs, the receptors for α-SNAP were also discovered using methods similar to those used for NSF and α-SNAP detection. NSF and α-SNAP are important proteins in intracellular membrane fusion since four helical coiled-coil bundles of *cis*-SNARE complexes are disassembled through the action of the ATPase NSF (*N*-ethyl-maleimide-*s*ensitive *f*usion) protein in complex with α-SNAP.

1.2.4.2 SNARE hypothesis and specificity

The three SNARE proteins that were discovered as receptors for the NSF-α-SNAP complex are Syntaxin, SNAP-25 and Synaptobrevin, which had been localized to either synaptic vesicles or to presynaptic membranes (Sudhof et al., 1989). Shortly thereafter, SNARE subcellular localization studies demonstrating that distinct SNAREs are found in specific compartments led to the SNARE hypothesis that was proposed by Rothman and colleagues (Sollner et al., 1993a). It postulated that there were two different classes of SNARES: (v) - vesicle SNAREs and (t) - target SNAREs (generally corresponds to another nomenclature R- (arginine) and Q- (glutamine) SNAREs, respectively). According to this hypothesis, each v-SNARE pairs up with its unique cognate t-SNARE at the proper target membrane and this interaction is the determinant of specificity that ensures that a vesicle will fuse with its correct target membrane. Current knowledge has indicated that there is no doubt that SNAREs contribute to the specificity of membrane transport. However, it has been realized that SNAREs are not the exclusive determinants of specificity in vesicle transport. It is more likely that the specificity is defined at earlier stages upstream of SNARE complex formation *per se*, at points such as membrane targeting and vesicle tethering events where primary recognition

between vesicles and their appropriate target compartment is mediated by Rabs and tethering factors.

1.2.4.3 SNARE complex formation

Because of the similarity between eukaryotic SNAREs and viral fusion proteins (Hughson, 1999), it has been postulated that membrane fusion is caused by forcing two opposing bilayers to overcome the repulsive energy that normally keeps the two leaflets separate. Based on the zipper up model, *trans*-assembly formation (so-called SNARE-pin formation) is formed from three t-SNAREs on one membrane and one v-SNARE on the opposing membrane (Figure 1.5). The proteins initially are largely unfolded but then form a highly stable four helix bundle as the vesicle gradually approaches its target membrane (Liu and Parpura, 2010). The energy produced by the formation of a highly stable complex most likely overcomes the energy barrier that normally prevents the fusion of two separate membranes, thereby inducing fusion (Margittai et al., 2001). The nucleated *trans*-complexes arise from a so called loose form in which zipper up has just started at the N-terminal region. Once the SNARE-pin structure is completed, this then leads to pore formation and transition to a remarkably stable *cis*-SNARE complex (Otto et al., 1997), suggesting that the fusion process is associated with the release of energy. Once the fusion event takes place NSF and its adaptor α-SNAP catalyze the disassembly of the SNARE complex (Sollner et al., 1993b).

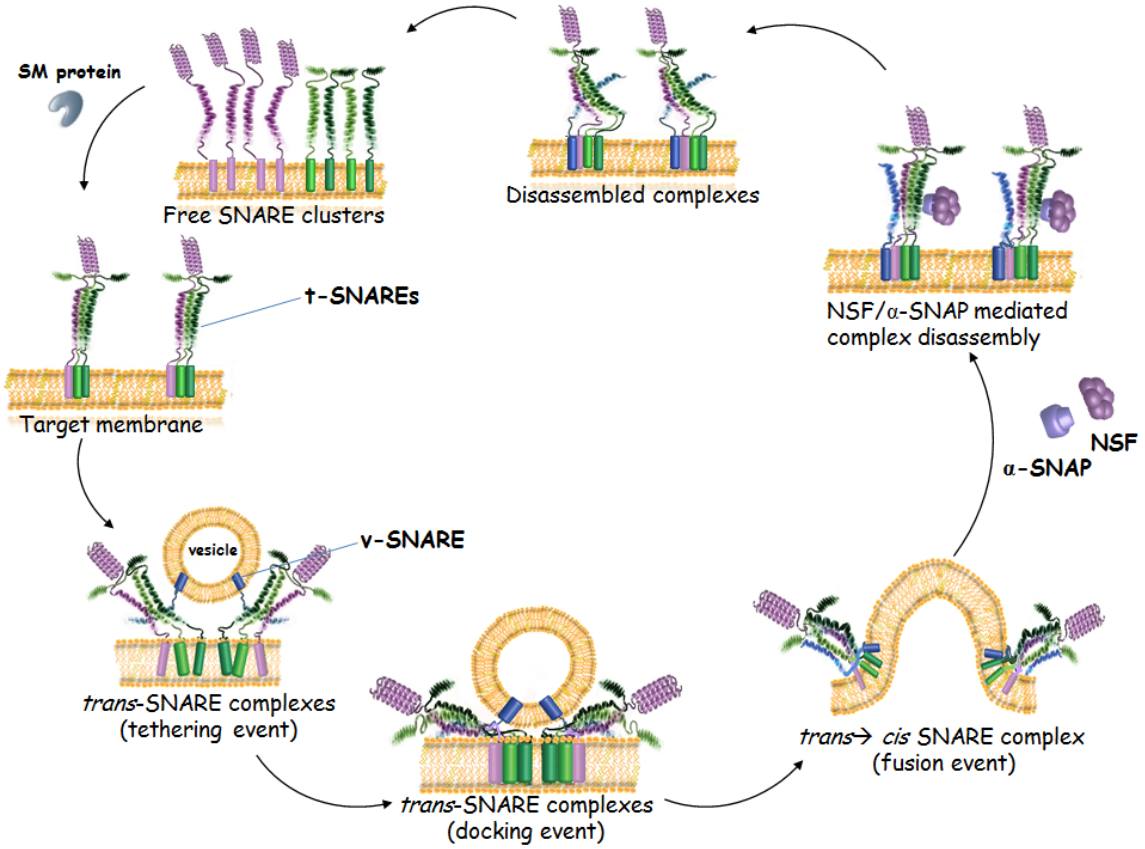

Figure 1.5 Schematic representation of the SNARE protein cycle. The cycle begins with conversion of a SNARE (t/Q-SNARE) from a closed to open conformation. Free t-SNAREs with the assistance of an SM protein (discussed in 1.2.4.4) generates clusters of three SNAREs (indicated in pink, dark and light green) that wait for an incoming vesicle. The fourth SNARE (v/R-SNARE) resides on the vesicle (depicted in blue). Transition from loose tethering of the vesicle to the docking stage allows the assembly of a four-helix bundle zipper that drives the membrane fusion (Jahn et al., 2003).The *cis*-SNARE complex disassembly is achieved by ATP hydrolysis by NSF together with its protein partner α-SNAP allowing for the SNAREs to participate in the next cycle of membrane fusion (Pratelli et al., 2004).

1.2.4.4 Sec1/Munc18 (SM) family proteins facilitate SNARE complex assembly

The evolutionarily conserved family of SM proteins has only four members: Sec1/Munc18-1, Vps45, Sly1 and Vps33, which are, thought to function in conjunction with distinct sets of SNARE proteins. All SM proteins seem to interact directly with Q-SNAREs;

however, the mode of the interaction is surprisingly diverse. For instance, neuronal Munc18-1 binds to Syntaxin 1 when the protein adopts a closed conformation, therefore preventing the exposure of the SNARE motif (60-70 amino acids near the transmembrane domain of SNAREs that participates in SNARE complex formation) and blocking its participation in SNARE complex assembly, thus negatively regulating fusion events (Dulubova et al., 1999). In contrast, other researchers have observed that Munc18-1 is essential for neurotransmitter secretion, since this process is blocked in mice lacking Munc18-1 (Verhage et al., 2000). On the other hand, the yeast homolog Sec1p interacts with the Q-SNARE Syntaxin homolog Sso1p when Sso1p is assembled in a SNARE complex as opposed to in the closed configuration (Carr et al., 1999). This second mode of SM protein binding activates SNARE-pin formation (Shen et al., 2007) (Figure 1.6).

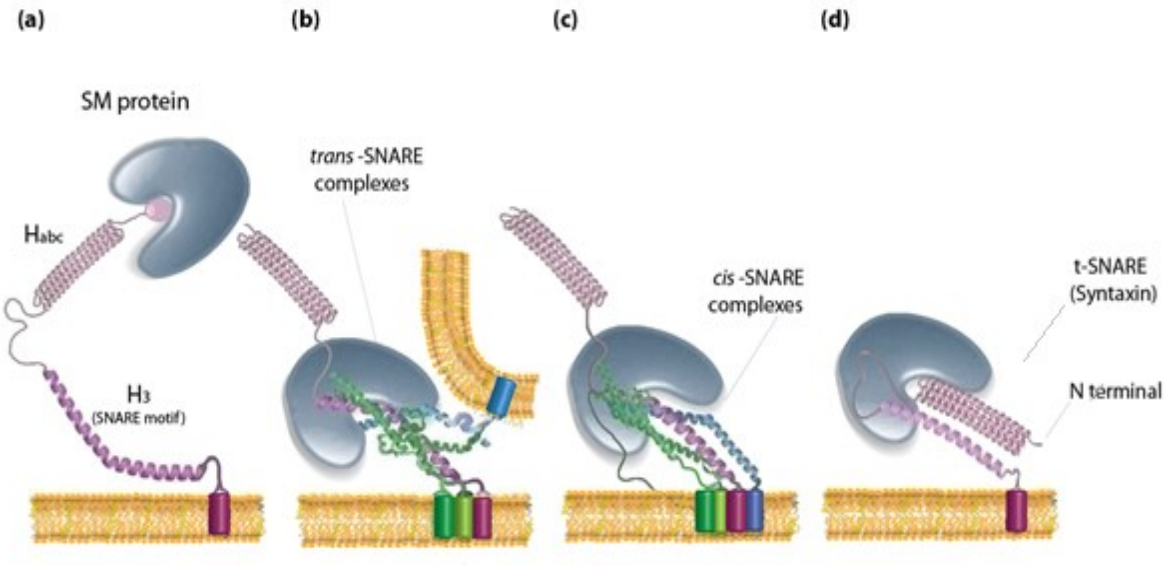

Figure 1.6 Different modes of interaction of Syntaxin and SNARE complexes with SM proteins. (a) Binding of an SM protein to an N-terminal region of Syntaxin adaptable with SNARE complex formation. (b, c) SM protein associates with SNARE complexes located in two (*trans*) or one (*cis*) membrane(s). (d) SM protein interacts with closed conformation of Syntaxin and prevents other SNARE proteins from binding. (a,d) Open and closed conformation adopted by Syntaxin, respectively; v-SNARE on the vesicle in (b) is colored in blue.

1.3 The TRAPP complex

1.3.1 Discovery of the TRAPP multisubunit complexes

The TRAPP complex in yeast is one of the best characterized multisubunit protein complexes and exists in three different compositions: TRAPP I, TRAPP II, and TRAPP III. Each of these complexes controls distinct trafficking events. TRAPP I, with seven subunits, acts in ER-to-Golgi vesicle trafficking, while TRAPP II, with its 11 subunits, governs multiple trafficking steps including *intra*-Golgi (Sacher et al., 2001), endosome-to-late Golgi (Cai et al., 2005), as well as autophagy (Zou et al., 2013). TRAPP III with 8 subunits also acts in autophagy (Lynch-Day et al., 2010). TRAPP III is discussed along with its unique subunit specific to TRAPP III, Trs85p, in section 1.4.

The first component of the yeast TRAPP complexes was identified by a synthetic lethal genetic screen designed to identify protein partners of the SNARE protein Bet1p, an ER-to-Golgi transport protein. In this screen *b*locked *e*arly in *t*ransport 3 protein (Bet3p) was identified (Rossi et al., 1995). Subsequently, *BET5* was isolated as a high copy suppressor of the temperature-sensitive (*ts*) growth phenotype of a *bet3-1* (Rossi et al., 1995). The conserved multisubunit tethering complex of TRAPP (Koumandou et al., 2007) was discovered and characterized by metabolic labelling with ^{35}S-methionine combined with immunoprecipitation of Protein A-tagged Bet3p and column chromatography techniques using *Saccharomyces cerevisiae* (Sacher et al., 1998). The TRAPP (*tra*nsport *p*rotein *p*article) complex, at this point believed to represent a single complex, was introduced to the scientific community in Susan Ferro-Novick‘s laboratory and shown to contain 10 proteins (Table 1.1) (Sacher et al., 1998).

Subsequent studies made it clear that there was more than one species of TRAPP. The first clue that there were multiple forms of the complex came from biochemical fractionation studies that initially revealed two forms of the complex: TRAPP I, with seven subunits (Bet5p,

Trs20p, two copies of Bet3p, Trs23p, Trs33p, and Trs85p,and TRAPP II, which is comprised of ten subunits including all of the subunits of TRAPP I and three TRAPP II specific subunits (Trs65p, Trs120p and Trs130p) (Sacher et al., 2001). Thus there are core subunits (Bet3p, Bet5p, Trs20p, Trs23p, Trs31p, and Trs33p) that are shared between TRAPP I and TRAPP II. Much later Tca17p was discovered in our laboratory and other laboratories through bioinformatic analysis and a genetic screen for defective SNARE recycling, respectively (Scrivens et al., 2009; Montpetit and Conibear, 2009).

Mammalian orthologs of TRAPP subunits have also been identified (Sacher et al., 1998,2000) Table 1.1. In a proteomic-based analysis using mammalian TRAPPC2 (hereafter the prefix “TRAPP” is eliminated for simplicity from the mammalian proteins) and C2L as bait, novel components of the mammalian TRAPP complex were identified. The protein partners that were identified included ones that had been previously characterized as *bona fide* TRAPP subunits including C3, C4, and C5 with the two yeast TRAPP II-specific orthologs C9 and C10. Also identified were novel proteins including the mammalian ortholog of Trs85p, C8, two proteins that are absent in the budding yeast that were named C11 and C12 (Scrivens et al., 2011) and the human homolog of Trs65p, C13 (unpublished results).

Yeast TRAPP subunit (size in kDa)	Mammalian TRAPP subunit (size in kDa)	Complex Constituent Yeast	Complex Constituent in Mammalian
Bet5p (18)	TRAPPC1 (17)	I,II, III	II, III
Trs20p (20)	**TRAPPC2** (16) **(**Sedlin**)**	I,II, III	II, III
Tca17p (17)	**TRAPPC2L** (16)	II	II, III
Bet3p (22)	TRAPPC3,C3L (20)	I,II, III	II, III
Trs23p (23)	TRAPPC4 (24)	I,II, III	II, III
Trs31p (31)	TRAPPC5 (21)	I,II, III	II, III
Trs33p (33)	TRAPPC6a,b (18)	I,II, III	II, III
Trs65p (65)	TRAPPC13 (45)	II	III
Trs85p (85)	TRAPPC8 (161)	III	III
Trs120p (120)	TRAPPC9 (140)	II	II
Trs130p (130)	TRAPPC10 (142)	II	II
none	**TRAPPC11** (129)	*	III
none	TRAPPC12 (79)	*	III

Table 1.1 Nomenclature of yeast and mammalian subunits. C11 and C12 are specific to higher eukaryotes and the star indicates that they have not been assigned to any specific complex, although one study reported that they might be part of the mammalian TRAPP III (Bassik et al., 2013). The subunits written in bold are the main focus of my research.

1.3.2 The architecture of TRAPP

The TRAPP complexes are the best-described tethering factors at the structural level, both in terms of its subunits and holocomplexes. The following sections will describe what is known to date regarding these features.

1.3.2.1 Structure of the C2 subunit

Since the identification of the TRAPP complexes, one mammalian subunit, C2, has come under scrutiny because mutations in this homolog of the yeast Trs20 protein are responsible for a skeletal disorder referred to as SEDT (*s*pondylo*e*piphyseal*d*ysplasia *t*arda)

(Gedeon et al., 1999). The single longin domain crystal structure of C2 was the first to be determined among the TRAPP subunits (Jang et al., 2002). Later it was revealed that other subunits of the TRAPP complex such as C1 and C4 (mammalian orthologs of Bet5p and Trs23p) adopt similar folds, although C4 also contains a PDZ-like domain not seen in C2 nor C1 (Kim et al., 2006). A surprising structural similarity to the N-terminal regulatory domain of two SNARE proteins was also noted, suggesting C2 may directly interact with SNARE proteins, a notion explored in Chapter 3 of this thesis.

1.3.2.2 Structure of the C3 subunit

Dimeric mouse C3 (the mammalian homolog of Bet3p) was the second subunit to have its structure determined (Kim et al., 2005b). Interestingly, C3 exhibits unique features such as a hydrophobic channel and a flat, positively charged surface. The latter characteristic appears to be critical for the membrane attachment of the Bet3p/C3 protein (Kim et al., 2005b). The monomer of C3 is composed of four β–strands on one side and five helices on the other side.The four β–strands are arranged in a twisted, antiparallel format. Interestingly the Bet3p/C3 fold is also seen in the TRAPP subunits Trs31p/C5 and Trs33p/C6 (Kim et al., 2006).

1.3.2.3 Structure of the C3-C6 heterodimer

In vitro studies using yeast subunits mapped out the various protein partners within the TRAPP complexes (Kim et al., 2005a). This ultimately led to the crystallization of the mammalian C3-C6 heterodimer. Although there is no homology between these proteins at the amino acid level, unexpectedly C6 adopts a similar fold to that of C3. Subsequently the structure of human C6 as a homodimer or heterodimer in a complex with C3 was determined (Kummel et al., 2005). The C3-C6 heterodimer was the starting point towards assembly of the TRAPP I complex.

1.3.2.4 Heterotrimeric and heterotetrameric structures of TRAPP

In vitro pull down experiments were used to examine the network of interactions within the yeast TRAPP complex. This was used to guide the recombinant co-expression of individual subunits. Subsequent work allowed for the co-expression of multiple (>2) subunits. Ultimately it was revealed that trimeric and tetrameric sub-complexes of TRAPP are composed of Bet3p-Trs31p-Trs20p and Bet3p-Trs33p-Bet5p-Trs23p. The crystal structures of the mammalian homologs of these complexes (C3-C5-C2 and C3-C6-C1-C4) were then solved. C3-C5-C2 showed that C2 interacts with the C3-C5 heterodimer in a shoulder to shoulder fashion and generates a flat sub-complex., Similarly, C3-C6-C1-C4 also associated into a flat sub-complex. (Kim et al., 2006).

1.3.2.5 Pentameric structure of yeast TRAPP complex

In yeast, the structure of the heteropentameric Bet3p-Trs33p-Trs23p-Trs31p in association with the small GTPase Ypt1p was solved (Cai et al., 2008). The structure exhibited a direct interaction between small GTPase Ypt1p with yeast Bet3p, Bet5p and Trs23p, three out of the four minimum components required for activation of Ypt1p. It was postulated that the mechanism of nucleotide exchange is obtained with the above interaction between TRAPP and Ypt1p resulting in stabilization of the Ypt1p nucleotide-binding pocket in an open conformation, followed by protrusion of the C-terminal region of Bet3p into the pocket.

1.3.3 The architecture of TRAPP I

Components of TRAPP were purified from yeast (Bet3p, Bet5p, Trs23p, Trs31p, and Trs33p) and experiments showed that Trs23p (the homolog of C4) united the two sub-complexes (Bet3p-Bet5p-Trs33p and Bet3p-Trs31p-Trs20p) together (Figure 1.7). The subunits of TRAPP I, when co-expressed in bacteria, spontaneously formed a functional TRAPP I complex (Kim et al., 2006). This complex was purified and subjected to single particle electron

microscopy to determine its low-resolution structure. This revealed a flat and elongated structure with a length of 180 A° (Kim et al., 2006) (Figure 1.8). Subsequently, the mammalian sub-complexes mentioned above were docked into this low-resolution map to generate a pseudo-atomic resolution structure of the TRAPP I complex. The fact that the yeast (electron microscopy) EM map perfectly accommodated the mammalian subunits indicates that the core of yeast and mammalian complexes are highly similar to each other. This structure has been used to elucidate the structure of TRAPP II (see below).

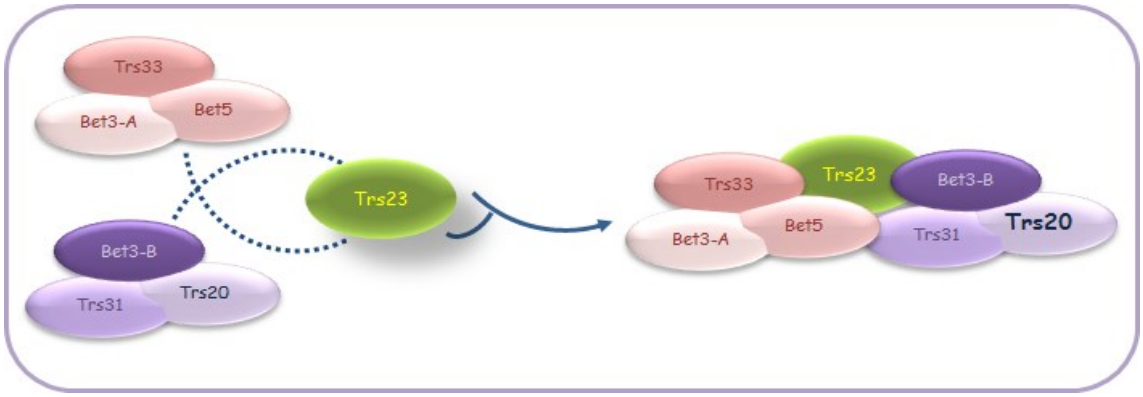

Figure 1.7 Schematic representations of two yeast heterotrimers linked together via a central Trs23p subunit.

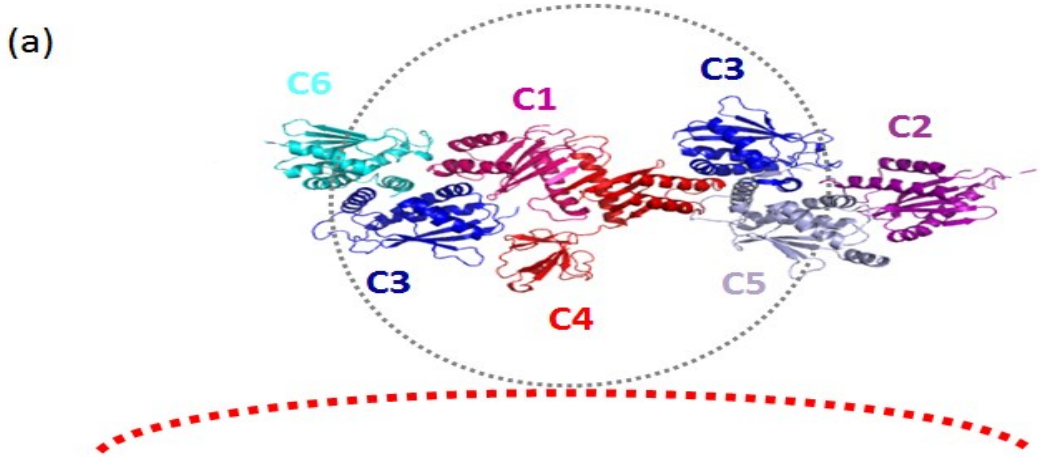

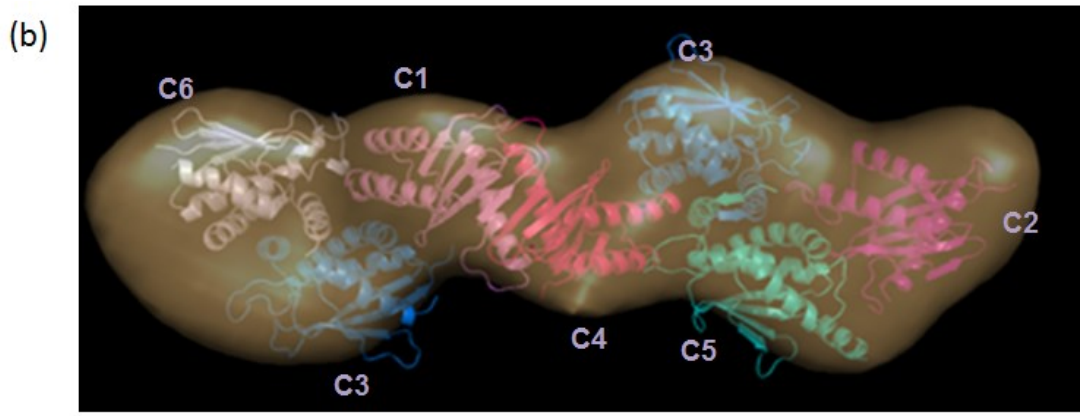

Figure 1.8 Crystal structure and subunit organization of mammalian sub-complexes and EM map of yeast TRAPP I complex. (a) Mammalian sub-complexes viewed from the putative cytosolic face. The dashed line highlighted in gray designates the minimal Ypt1 GEF. (b) The two mammalian sub-complexes docked into the EM map generated from yeast subunits (Kim et al., 2006).

Bacterially co-expressed subunits of the yeast TRAPP I led to proper assembly of a functional TRAPP I complex (Kim et al., 2006) although this was not the case for mammalian TRAPP homologs. These results suggested that there may be other protein partners, either TRAPP subunit(s) and/or unrelated protein(s) required for proper assembly of the mammalian (m)TRAPP complex. This notion formed the basis of a search for novel protein partners of mTRAPP and is presented in Chapter 2.

1.3.4 The EM structure of yeast TRAPP II

The architecture of yeast TRAPP II was predicted using the EM structure of the TRAPP I. The TRAPP II complex forms a dimer of the TRAPP I core with Trs120p and Trs130p at the ends of the core and the dimers are linked together by a central layer composed of Trs65p (Figure 1.9) (Yip et al., 2010). Indeed, deletion of Trs65p causes a shift in the components of TRAPP II to a smaller molecular size (Choi et al., 2011).

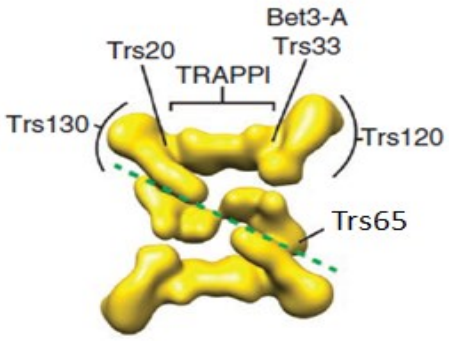

Figure 1.9 Architecture of TRAPP II in *Saccharomyces cerevisiae* (Yip et al., 2010). The shared core TRAPP I and TRAPP II components arrange side by side and generate a flat, elongated shape at the center of each monomer, consistent with Kim et al, 2006. Two specific TRAPP II components, Trs120p and Trs130p are accommodated at the extremities of the flat surface with Trs130p being adjacent to Trs20p. The dimer interface is depicted as a green dashed line where Trs65p is proposed to mediate the dimerization of TRAPP II (Choi et al., 2011; Yip et al., 2010).

1.3.5 The number and composition of yeast and mammalian TRAPP complexes

Given the limitation of using Superdex-200 to separate TRAPP complexes from cell lysates, TRAPP initially appeared as one single peak in both yeast and mammalian lysates. Co-immunoprecipitation studies showed that the mammalian homologs of the TRAPP II- (C2L and C13) and TRAPP III- (C8) specific subunits co-purified in the same complex and prompted speculation that mTRAPP might exist as a single complex (Choi et al., 2011; Scrivens et al., 2011). Recent data have strongly suggested that mTRAPP actually forms two distinct complexes. One complex, mTRAPP II, contains the core with C9 and C10 and the other complex, mTRAPP III contains the core complex plus C8, C11, C12, and C13 subunits (Figure 1.10) (Bassik et al., 2013).

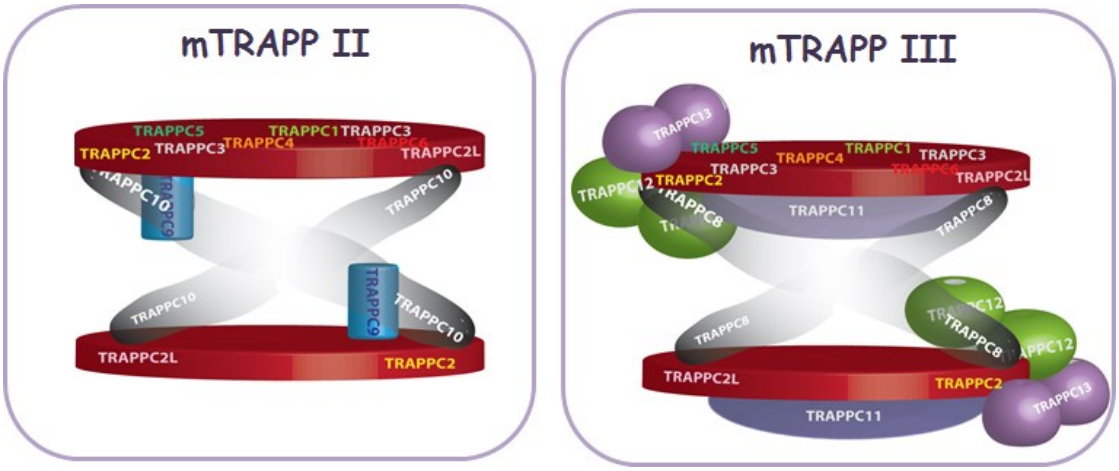

Figure 1.10 Schematic representations of mammalian TRAPP complexes. Currently identified components of the mTRAPP II and TRAPP III complexes based on Bassik et al., 2013, and yeast two-hybrid binary interactions (Scrivens et al., 2011).

All forms of yeast TRAPP contain the proteins found in TRAPP core. The structure of TRAPP II (except for the positions of Trs120p and Trs130p) has been depicted according to Yip et al., 2010, as two layers of core subunits capped by Trs120p, and Trs130p at both ends, with Trs65p in the joining part. Trs65p has been shown to interact with both Trs120p and Trs130p (Choi et al., 2011; Liang et al., 2007). Interestingly the architecture of TRAPP III was deciphered based on our Y2H analysis which is in fair agreement with very recent report on EM structure of TRAPP III (Figure 1.11).

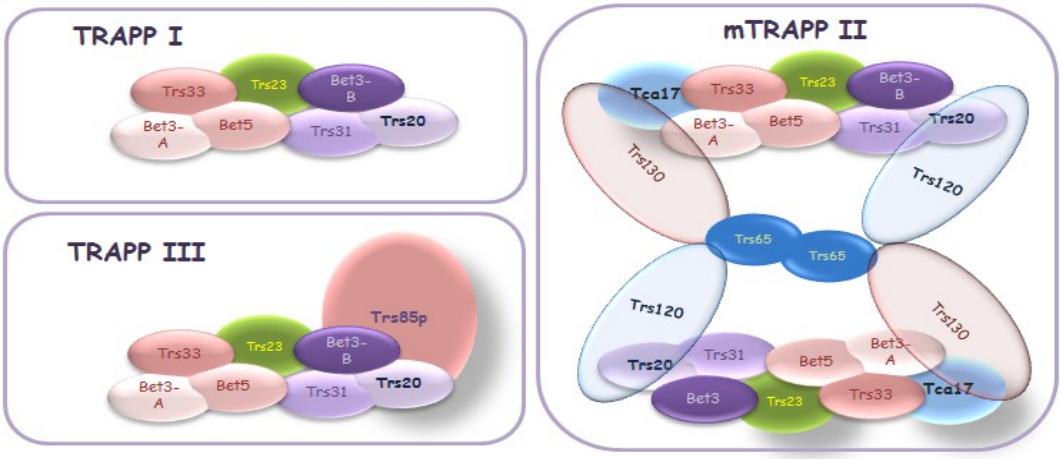

Figure 1.11 Schematic representations of the three different TRAPP complexes found in yeast.

1.3.6 Functions of the TRAPP complexes

A significant body of work has shown that TRAPP complexes cooperate with components of both the early and late secretory machinery and the mode of interaction is conserved between yeast and mammals. The two most prominent functions of the TRAPP complexes are tethering vesicles and acting as guanine nucleotide exchange factors (GEFs).

1.3.6.1 TRAPP as a GEF in yeast and mammals

Since TRAPP genes displayed genetic interactions with the gene encoding the ER-to-Golgi small GTPase Ypt1p (Rossi et al., 1995; Jiang et al. 1998) a physical interaction was between TRAPP and Ypt1p was explored. This revealed that the complex has a preference for binding to a nucleotide free form of Ypt1p which is a characteristic of nucleotide exchange factor(s). It was subsequently shown that all three forms of the TRAPP complexes stimulated the exchange of GDP for GTP on Ypt1p (Jones et al., 2000;Wang et al., 2000;Lynch-Day et al., 2010). The catalytic surfaces of TRAPP at the Ypt1p interface encompasses four subunits (Bet5p, Bet3p (A and B), Trs23p and Trs31p) common to all three forms of the complex (Kim et al., 2006). A subsequent study provided a mechanism for TRAPP-catalysed Ypt1p nucleotide exchange that involved the C-terminus of the Bet3p subunit (Cai et al., 2008). Another example of a GEF involving multiple subunits is Mon1-CCZ as a GEF for Ypt7p (Nordmann et al., 2010; Zhu et al., 2009).

Since the GEF activity is confined to the TRAPP I core, which is shared amongst all three yeast TRAPP complexes, one would suspect that all three complexes would act as Ypt1p GEFs and this has been demonstrated (Jones et al., 2000; Wang et al., 2000; Chen et al., 2011; Yamasaki et al., 2009;Lynch-Day et al., 2010). However, one group has claimed that TRAPP II acts as a GEF on Ypt31p-Ypt32p, a Rab GTPase functioning in the *trans*-Golgi (Jones et al., 2000). In contrast to the yeast controversy, mTRAPP GEF activity has been reported for Rab1

(Yamasaki et al., 2009), the mammalian homolog of Ypt1p, and not Rab11, the mammalian homologs of Ypt31p-Ypt32p.

1.3.6.2 TRAPP function as a tether in yeast and mammals

In the early secretory pathway in yeast, the TRAPP I complex, via the Bet3p core subunit, interacts physically with Sec23p, an inner layer component of the COPII coat (Cai et al., 2007b). Interestingly, Bet3p has been shown to be stably associated with the Golgi apparatus (Sacher et al., 2000), suggesting that Bet3p facilitates tethering of ER-derived vesicles to the Golgi target membrane. A recent study revealed that during the coat -TRAPP I interaction, a Golgi-associated kinase, Hrr25p, competes with TRAPP I for a Sec23p-binding site thus displacing TRAPP I. Subsequent phosphorylation of Sec23p triggers vesicle uncoating (Lord et al., 2011; Sharpe et al., 2011). Therefore phosphorylation of Sec23p by Hrr25p assures spatial and temporal regulation of vesicle transport events. While COPII vesicles are tethered to and interacted with TRAPP I, but not TRAPP II (Sacher et al., 2001;Cai et al., 2007a), COPI-coated vesicles are captured and bound to TRAPP II-specific subunits (Cai et al. 2005;Yamasaki et al., 2009). Consistent with these findings, the phenotypes of core TRAPP mutants differ from mutants defective in genes specific to TRAPP II (Cai et al., 2005; Mahfouz et al., 2012;Scrivens et al., 2009;Jian et al., 1998).

The coat-TRAPP association in the early and late biosynthetic pathways is not limited to budding yeast cells. Unlike in yeast cells, however, nascent vesicles in higher eukaryotes first fuse together to generate the intermediate ERGIC compartment prior to fusion with the Golgi. The TRAPP I subunit, C3, is necessary for homotypic fusion of COPII-coated vesicles crucial for formation of ERGIC (Yu et al., 2006). In addition, the structural integrity of both the ERGIC and Golgi apparatus is impaired upon depletion of C3. The fragmented Golgi and perturbed ERGIC structures are phenotypes that are also observed when several TRAPP subunits are mutated

(Choi et al., 2011; Scrivens et al.,2009 and 2011). The tethering action of mTRAPP is not restricted to C3; other subunits such as C9 can bind p150, a component of a microtubule (MT) motor, and C9 competes with p150 for binding to Sec23 and displace its interaction to Sec23 through tethering the vesicle toward the ERGIC (Zong et al., 2012). This consecutive process is reminiscent of the regulation of Sec23p by Hrr25p observed in yeast, which is mediated through the TRAPP I complex. The newly identified members of mTRAPP (C11 and C12) (Scrivens et al., 2011) have been found in the ERGIC as is seen with C3, suggesting its implication is consistent with the generally accepted ER-Golgi trafficking role of the yeast TRAPP I complex.

Furthermore, genome-wide studies have been implicated the TRAPP complex in membrane traffic. For example, the Golgi t-SNARE protein Syntaxin 5, and the *Drosophila* ortholog of C11, Gryzun, have been shown to be essential for secretion (Wendler et al., 2010). Moreover, high throughput analysis has revealed multiple mTRAPP proteins (C8, C11, and C12) as being important for ricin retrograde transport (Bassik et al., 2013; Moreau et al., 2011).

In addition to tethering and nucleotide binding activity, multiple subunits of mTRAPP have been identified in large-scale screens for genes involved in human autophagy (Behrends et al., 2010). Furthermore, numerous studies point to functions for the TRAPP complex in being a protein supplier and a membrane depositing factor at a very early stage of certain processes including the engagement of the Rab GEF, Rabin8 (Westlake et al., 2011), the C9-mediated recruitment of necessary components for cilia formation during ciliogenesis (Lee et al., 2012), biogenesis of melanosomes (a lysosomal-related organelle) by C6a (Gwynn et al., 2006), and autophagosome generation during autophagy (Behrends et al., 2010).

1.3.7 C2/Trs20p function in membrane trafficking

1.3.7.1 C2 function and its link to SEDT in mammals

Sedlin also known as C2 is the human ortholog of Trs20p. It was reported to reside at one end of the TRAPP core. Biochemical studies have revealed that the 140 amino acid C2 interacts with both the C3 and C5 subunits of TRAPP and possible interaction(s) with as yet to be discovered protein(s). Mutations in the C2 gene (also known as SEDL or SEDT) that encodes for C2 have been reported to be the cause of an X-linked recessive skeletal dysplasia affecting males in early adolescence known as SEDT (Gedeon et al., 1999). SEDT patients have inhibited epiphyseal bone growth leading to reduced stature among other features. The defect manifests only in skeletal tissue, suggesting an involvement of chondrocytes, cells that are involved in the synthesis of collagen for the cartilage tissue. Patients with this disease have been reported to exhibit shorter extracellular collagen fibrils compared to those of unaffected individuals.

There are a number of mutations in C2 that are associated with the disease, one being a substitution of aspartic acid at position 47 for tyrosine (Figure 1.12). This residue is highly conserved throughout metazoans (Jang et al., 2002;Scrivens et al., 2009). In addition, the wild-type C2 can complement for the loss of yeast Trs20p, while mutant D47Y has lost this ability (Gecz et al., 2000). Finally, while this residue exhibits unique features such as being a surface exposed charged residue, unlike some other missense mutations, the D47Y mutation still folds properly and more or less maintains the biophysical properties of the wild-type protein (Choi et al., 2009 and 2011; Scrivens et al., 2009). In light of the crystal structure of the TRAPP complex (Kim et al., 2006) and the mouse C2 subunit (Jang et al., 2002), researchers have suggested that the surface-exposed area of C2 is an ideal environment for protein-protein interactions with other component(s) of the membrane trafficking system (Sacher et al., 2008).

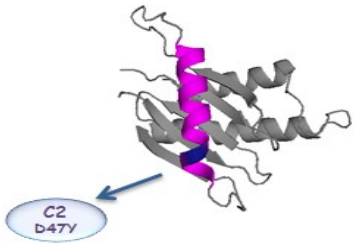

Figure 1.12 C2 structure (1H3Q). α-helix1 backbone is colored in pink using PyMOL and dark blue highlights the position of D47.

We and others have determined that C2 and C9 physically interact. This interaction is also observed between the C2 and C9 counterparts in yeast, Trs20p and Trs120p, respectively (see Table 1.1 (Jang et al., 2002;Levine et al., 2013;Taussig et al.,2013;Zong et al.,2011); see Chapter 3). This finding is not in accordance with results from single particle EM analysis presented by Yip and colleagues in 2010 who showed that, with respect to the TRAPP core, Trs20p is adjacent to the TRAPP II-specific subunit Trs130p and distant from Trs120p. The discrepancy could be explained by the possibility that TRAPP achieves a different structure upon interaction occurring inside the cells.

A recent publication suggests that C2 also acts as an adaptor for C8 and C9 (Zong et al., 2011). If C9 and C8 are in distinct sub-complexes as suggested above (Bassik et al., 2013; Zong et al., 2011) then the C2 subunit could operate as an adaptor for each of these proteins in distinct TRAPP complexes in mammals. It was recently suggested that C2 is recruited to the collagen exit site by TANGO1, a putative collagen receptor. Upon recruitment of C2 to ER exit sites, C2 regulates Sar1 GTPase activity allowing the newly formed COPII carrier to increase its size (Venditti et al., 2012). Although this finding helps to unravel the key molecular players of collagen transport, it is not clear how this relates to the pathogenesis observed in SEDT. To date, in addition to C2 mutations linked to SEDT, components of TRAPP have been linked to specific human health conditions. The table below delineates a growing list of diseases that are associated with

malfunctions of the TRAPP complex (Table 1.2).

Subunit	Associated disease	Reference
TRAPPC1	Melanoma	Chiari et al 1999
TRAPPC2	Spondyloepiphyseal dysplasia tarda (SEDT)	Gedeon et al 1999
TRAPPC4	Colon cancer	Zhao et al 2011
TRAPPC6	Mosaic-hypopigmentation	Gwynnn et al 2006
TRAPPC9	Intellectual disability (ID); Human ciliopathy	Mochida et al 2009 ; Lee et al 2012
TRAPPC10	Epilepsy holoprosencephaly candidate 1 protein (EHCO1)	Yamakawa et al 1995
TRAPPC11	Hepatic steatosis; Limb girdle muscular dystrophy, myopathy with movement disorder, and ID	Howarth et al 2011; Bogershausen et al 2013

Table 1.2 Diseases associated with disruption of normal TRAPP subunit function

1.3.7.2 Trs20p function in yeast and its implication in SEDT patients

TRS20 is an essential gene (Sacher et al.,1998 and 2000) and depletion of Trs20p results in the inhibition of trafficking from the ER to the Golgi (Sacher et al., 2001).The mammalian homolog of Trs20p (C2) can complement the lethality of the *trs20* disrupted gene product, strongly suggesting a conserved function of the gene throughout evolution (Gecz et al., 2003). In yeast, Trs20p was reported to be neither part of the GEF activity of TRAPP I nor a participant in the assembly of the complex. Although more recent work in yeast from our lab and others have suggested that Trs20p might not be critical for the assembly of TRAPP I, there is strong evidence that Trs20p is a critical component of TRAPP II and TRAPP III and could be important for the organization of these complexes (Jang et al., 2002; Levine et al., 2013; Taussig et al., 2013; Zong et al., 2011; see Chapter 3). The adaptor function might be lost along with the integrity of the TRAPP II complex in yeast harboring the D46Y mutation. The authors have shown the essential requirements for Trs20p in order for Trs120p to integrate into the

complex. The D46Y mutant was shown to prevent the normal *trans*-Golgi localization of TRAPP II components and the interaction with Trs120p is also disrupted, further supporting the conserved mode of action of C2 in the TRAPP complex from yeast to mammals (Jang et al., 2002; Levine et al., 2013; Taussig et al., 2013; Zong et al., 2011). Assessment of TRAPP II GEF activity for two small GTPases of early and late Golgi trafficking, Ypt1p and Ypt32p in the context of trs20D46Yp indicated that TRAPP II, but not TRAPP I, GEF activity was lost (Taussig et al., 2013).

Synthetic genetic interaction between *trs20* and multiple genes involved in the endocytic recycling pathway were reported (Mahfouz et al., 2012). Even though it has been reported that Trs20p links TRAPP I to the TRAPP II-specific subunit Trs130p (Yip et al., 2010), more recently it has been shown that Trs20p and Trs130p operate in distinct routes. Specifically, overexpression of Ypt32p rescues the temperature sensitivity of *trs130-HA ts*, but not *trs20ts.* Furthermore, different transport pathways including ER to Golgi, Golgi to vacuole and Golgi to cell surface monitored by Gos1p (ER-to-Golgi SNARE fusion protein), CPY (vacuolar carboxypeptidase Y), ALP (vacoular alkaline phosphatase), and Gap1p (general-amino-acid-permease) were defective in *trs130-HAts* , but not *trs20ts* (Taussig et al., 2013).

1.4 Autophagy

1.4.1 General aspects of autophagy

Two fundamental pathways can be used by eukaryotic cells for degradation of unnecessary intracellular proteins. The first is the ubiquitin-proteasome system (UPS), which degrades short-lived intracellular proteins, and the second pathway, lysosome-mediated autophagy, degrades long-lived intracellular proteins (Mizushima and Komatsu, 2011). Autophagy directly translates into self-digesting, a term coined by Christian de Duve in 1963. Autophagy is a catabolic event which is evolutionary conserved among plant, yeast and animal

cells (Klionsky, 2005). It is a tightly regulated mechanism by which obsolete components will be eliminated.Thus, at least in part, autophagy provides cellular and metabolic homeostasis through balance between synthesis and degradation of macromolecules in the cell (Komatsu et al., 2005; Shintani and Klionsky, 2004). There are three major types of autophagy in mammals that are classified based on the type of substrates targeted to lysosomes: macroautophagy, microautophagy and chaperon-mediated autophagy (Cuervo, 2004).

In microautophagy, small materials are directly delivered to the lysosomes by inward invagination of the lysosomal membrane (Wang and Klionsky, 2003). Chaperon-mediated autophagy involves the translocation of cytosolic material by a heat shock protein that recognizes the cytosolic portion of its substrate and directs it to the surface-bound lysosomal receptor LAMP2A (Massey et al., 2006). Macroautophagy involves formation of a double-membrane structure known as the autophagosome. The autophagosome removes bulk cytoplasmic material such as damaged organelles, aggregates and aberrant proteins and delivers them to the lysosome (equivalent to vacuole in yeast) for degradation via lysosomal enzymes.

Macroautophagy (hereafter autophagy) has been extensively studied and can be subclassified as non-selective (induced) or selective (basal). “Induced autophagy” is activated in response to a number of external and internal stress conditions. More specifically, in yeast and mammalian cells, nitrogen and amino acid deprivation triggers the highest response of a non-selective form of autophagy.

1.4.2 Molecular mechanism of autophagy

The molecular components involved in autophagy are known as *aut*oph*ag*y-related genes (*Atg*). There are 35 *ATG* genes identified in yeast thus far (Rubinsztein et al., 2012; Xie and

Klionsky, 2007) that can be grouped into three categories: (1) core machinery, (2) selective autophagy-specific and (3) non-selective autophagy specific genes (Lynch-Day and Klionsky, 2010). These Atg proteins are classified based on their role in starvation and/or vegetative conditions. The core Atg machinery consists of 17 proteins that are shared in both selective and non-selective autophagy. Some Atg proteins have been shown to act as binding partners of the TRAPP complex. I will therefore focus on this subset of proteins as it relates to my current research.

1.4.3 The Cytoplasm-to-vacuole (Cvt) pathway

The cytoplasm-to vacuole-targeting (Cvt) pathway is one of the best characterized types of selective autophagy observed in budding yeast. The Cvt transport system is a biosynthetic process destined for cargo delivery of inactive precursor forms of vacuolar hydrolase such as α-mannosidase (Ams1) and aminopeptidase I (Ape1), from cytosol to vacuole under log-phase growth conditions (Klionsky et al., 1992; Scott et al., 1997).

In the case of Ape1, after synthesis, precursor Ape1 (prApe1) monomers can self-assemble into a large Ape1 complex (Shintani et al., 2002) (Figure 1.13). This occurs once the complex is recognized by its receptor, Atg19p (now termed Cvt complex) that can then bind to Atg11p before its final integration into the pre-autophagosomal structure or phagophore assembly site PAS (Lynch-Day and Klionsky, 2010). In yeast, the PAS is found to be the region where most, if not all, of the Atg proteins gather (Suzuki et al., 2001). The PAS expands and generates a phagophore, which is found to be the initial sequestering site capable of enclosing the double membrane harbouring the Cvt complex. Once the ends of the phagophore are completely sealed, the Cvt complex converts into a Cvt vesicle and, in the case of bulk autophagy, becomes the autophagosome. Finally the Cvt vesicles, or the autophagosomes, fuse with the vacuole and release their contents (Cvt body or autophagic body) into the lumen. Acidic

exposure of the Cvt or autophagic bodies would then lead to the breakdown of these structures. The N-terminal cleavage of preApe1 leads to a mature form of Ape1 and the remaining non-specific contents of the autophagic bodies are degraded. Finally, the active building blocks of macromolecular by-products are recycled back to the cytoplasm to maintain cellular homeostasis and turn over (Cheong and Klionsky, 2008).

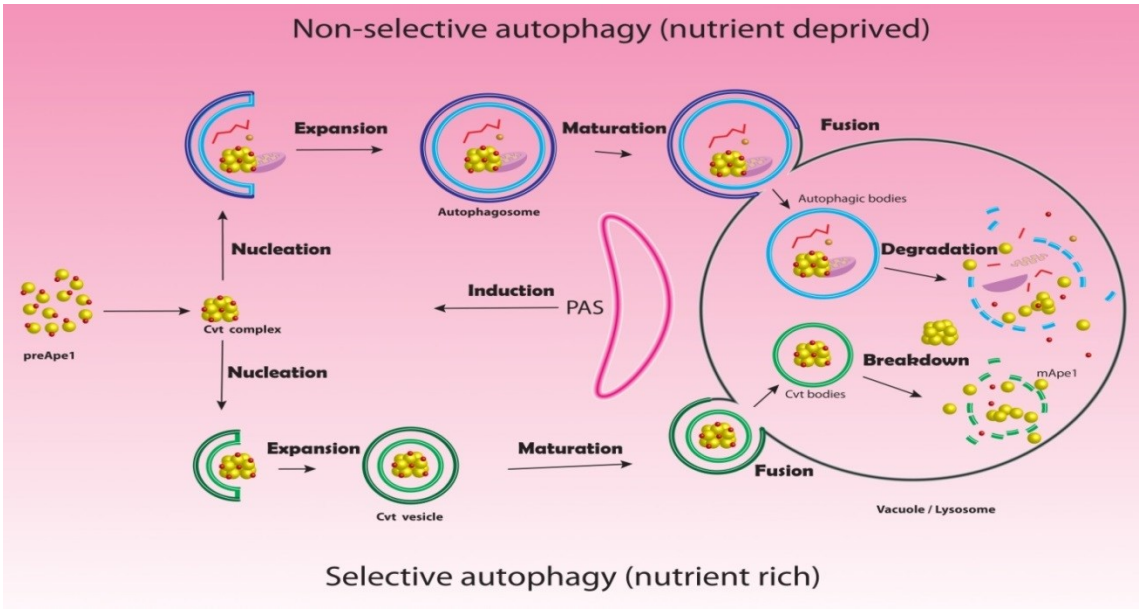

Figure 1.13 Schematic representation of Ape1 processing in selective and non-selective autophagy.

1.4.4 Molecular description of autophagy

1.4.4.1 Induction of phagophore

Initiation of autophagy in mammals begins with the isolation membrane (IM). Next, the generation of the autophagosome will arise through the elongation of the IM. In yeast, the phagophore is developed from the elongation of the PAS (Sztul and Lupashin, 2006), which later gives rise to the autophagosome (Suzuki et al., 2001). Commonly, Atg proteins are gathered in the PAS in a hierarchical fashion (Mizushima and Komatsu, 2011). To date, there are no findings demonstrating the existence of a single PAS in mammals (Young et al., 2006).

However, multiple PAS equivalents have been detected under starvation conditions (Itakura et al., 2012).

In yeast, the initiation of autophagy is hallmarked by the recruitment of Atg9p to the PAS. Atg9p is a multispanning membrane protein and an evolutionarily conserved gene involved in both selective and non-selective autophagy (Itakura et al., 2012; Orsi et al., 2012) . Upon synthesis of Atg9p, the protein is translocated to new tubulo-vesicular structures called Atg9-reservoirs in both fungi and mammals (Mari and Reggiori, 2010; Orsi et al., 2012).

1.4.4.2 Lipidation of Atg8p (LC3) along with expansion of the phagophore

The mammalian homolog of yeast Atg8p, *M*icrotubule-*a*ssociated *p*rotein 1*l*ight *c*hain *3* protein (MAP-LC3 or LC3), is the best-characterized and most extensively used marker. There are two pools of cytosolic and membrane bound LC3 (LC3-I and LC3-II).
LC3 has been used as a marker for monitoring autophagosomes and autolysosomes by microscopy or western blot analysis mainly due to its unique biochemical features (Mizushima et al., 2010). Similarly in yeast, a construct of GFP fused to Atg8p has also been used. When GFP-Atg8p is recruited to the vacuole via autophagy, the GFP fragment is released from Atg8p and Atg8p itself undergoes degradation (Shintani and Klionsky, 2004). Conversely, this process of degradation is impaired in mutants that are blocked in autophagy and can be followed by microscopy or western blot analysis.

1.4.4.3 Acquisition of components destined for degradation (autophagic cargos)

The conjugation of Atg8p to the lipid phosphatidylethanolamine (PE) of the membrane generates Atg8p-PE, which connects cargos to the cup-shaped membrane of the autophagosomes. This is accomplished either directly or indirectly through a receptor/adaptor reaction involving Atg19p and Atg11p, respectively (Cao et al., 2008; Pankiv et al., 2007). The

size of transport intermediates are determined based on the acquisition of substrates sorted to transport the intermediates. Hence, it is feasible that in non-selective autophagy, autophagosomes can range from 300-900 nm (Baba et al., 1997). On the other hand, selective autophagy, which does not comprise bulk cytosolic material and only accommodates specific cargos, generates smaller vesicles of about 150 nm in size (Scott et al., 2001).

1.4.4.4 Maturation of autophagosomes

The maturation of autophagosomes is accomplished by the fusion of autophagosomes with late endosomes and/or lysosomes, late endosomes also known as multivesiular bodies (MVBs). It is worth mentioning that the two most prominent lysosomal proteins, LAMP1 and LAMP2, are necessary for autophagosome maturation (Huynh et al., 2007). Maturation occurs by the incorporation of lysosomal/vacuolar enzymes into the autolysosomes with the aim of instigating degradative abilities for macromolecule breakdown. Finally, permeases allow the breakdown products to efflux into the intracellular milieu.

Atg8p, a PE-conjugated protein, has been shown to function in tethering and hemifusion between two opposing membranes (Nakatogawa et al., 2007) thereby mediating an emergence of a membrane and the expansion of the autophagosomes. Nevertheless, another recent study in yeast claims that under physiological conditions, Atg8p does not have the ability to drive membrane fusion and that the exocytic SNAREs (mainly Sso1/2p and Sec9p) are essential for generation of tubulo-vesicular clusters, which is a preliminary stage of PAS organization (Nair et al., 2011).

1.4.5 Autophagy implication in human disease

A great deal of our knowledge in autophagy came from the molecular studies conducted in budding yeast and subsequent identification of their mammalian homolog ATG genes.

Autophagy must be strictly regulated because any malfunction in this degradation pathway can give rise to various human diseases ranging from neurodegeneration, such as Alzheimer's and Parkinson disease, to cardiomyopathy, muscular dystrophy, inflammation and cancer (Choi et al., 2013; Komatsu et al., 2005). As a result, autophagy has received a great deal of attention over the past three decades, since it holds potential therapeutic strategies in recognizing and eliminating specific types of non-functional proteins and/or organelles. Selective autophagy acts by carefully removing specific protein aggregates through the function of mammalian Atg19 and p62, which can potentially fulfill an important role in preventing neurodegenerative disorders (Pankiv et al., 2007).

1.4.6 TRAPP implication in Autophagy

The first report indicating the involvement of the TRAPP complex in autophagy, via its growth-dispensable subunit Trs85p, came from studies conducted in *S. cerevisiae*. This study revealed that *trs85Δ* failed to transport GFP-Atg8p to and to process Ape1 in the vacuole (Meiling-Wesse et al., 2005; Nazarko et al., 2005). TRAPP complexes have been shown to bind GTP-binding proteins Ypt1p and Ypt31p-Ypt32p (Jones et al., 2000; Morozova et al., 2006). Both of these small GTPases are implicated in the process of autophagy. Given the putative link with a GEF and its corresponding GTPase, it was reasonable to ask whether the GEF could also function in autophagy. Answering this question led to the finding that yeast TRAPP II and TRAPP III are involved in both bulk and selective autophagy acting at early steps in the autophagy pathway (Lynch-Day et al., 2010; Zou et al., 2012). Interestingly, Ypt1p and Trs85p were identified in a mass spectrometry analysis of Atg9p-vesicles. Trs85p was shown to be localized at the PAS (Kakuta et al., 2012; Lynch-Day et al., 2010), the site that is highly enriched for Atg9p. Thus these results in conjunction with others led to the proposal that Trs85p is a component of Atg9p vesicles and recruits Ypt1p and TRAPP III to the PAS (Kakuta et al., 2012; Lynch-Day et al., 2010). More recently it was revealed that PAS targeting of Trs85p itself is

regulated by the scaffolding protein Atg17p (Wang et al., 2013), which is also responsible for PAS- targeting of Atg9p (Sekito et al., 2009) (Figure 1.14). In order to unravel the cross talk between TRAPP and core molecular machinery of autophagy, the PAS localization of Atg proteins during induction of autophagy was assessed using Ape1p as a marker for PAS or a cargo that utilises the Cvt pathway in a strain deleted of *trs85* or *atg* genes (Lipatova et al., 2012b). In *trs85Δ*, the defective processing of the Ape1p, assessed by the presence of the precursor form of Ape1p (prApe1p), was suppressed when *YPT1* or *ATG11* were overexpressed (Figure 1.14). Conversely, overproduction of *TRS85* had no effect on the accumulation of unprocessed Ape1p in *ypt1* or *atg11* mutant strains. Collectively, this suggests that *TRS85* functions upstream of *ATG11*, thus defining the Trs85p-Ypt1p-Atg11p module (Lipatova et al., 2012a).

Furthermore, in yeast biochemical and genetic interactions place Trs130-containing TRAPP II in both selective Cvt and non-selective bulk autophagy pathways acting through the GTPase Ypt31p-Ypt32p downstream of a Ubiquitin-like conjugating system Atg5p and upstream of Atg8p, Atg1p, Atg13p, Atg9p and Atg14p (Lynch-Day et al., 2010; Zou et al., 2012). Interestingly another study revealed the importance of Trs85p in the recruitment of Atg14p, a phosphotidylinositol 3-kinase (PI3K), to the PAS only in nutrient rich conditions but impairment of *atg14* did not alleviate the PAS localization of Trs85p suggesting that Atg14p acts downstream of Trs85p (Kakuta et al., 2012). Furthermore, in addition to TRAPP III, Ypt1p has also shown specificity towards the downstream Atg proteins. For instance, while a nutrient-rich environment permits Ypt1p-GTP to be associated with Atg11p, an Atg protein that only acts in Cvt/selective autophagy (Lipatova et al., 2012a), under nutrient deprivation, Ypt1p-GTP binds to Atg1p and further recruits other Atg proteins that are known to function in non-selective autophagy (Wang et al., 2013). In contrast, nutrient deprivation links Ypt1p-GTP to the autophagy-induced Atg1p complex, essential for autophagosome formation and recruitment of

other components of the autophagy machinery such as the heterotrimeric complex consisting of Atg17p, Atg29p and Atg31p (Wang et al., 2013) (Figure 1.14).

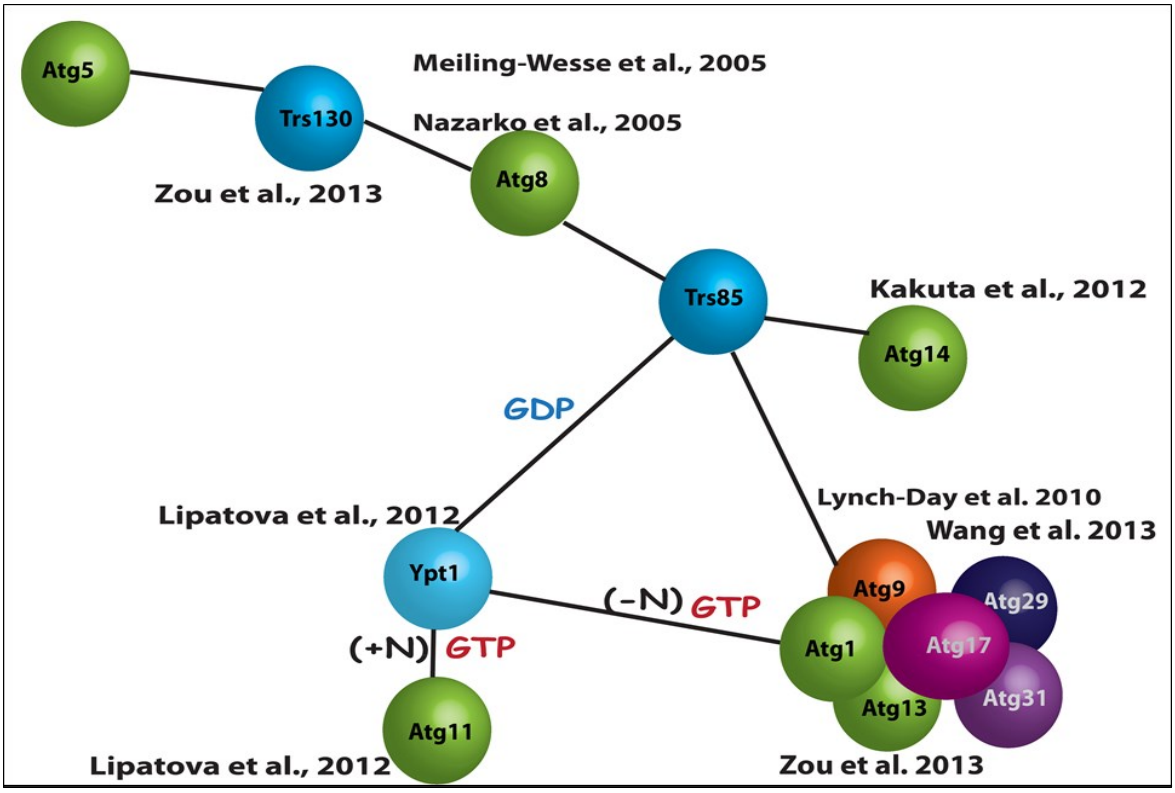

Figure 1.14 Integration of Ypt1p and the TRAPP II- and TRAPPP III-specific proteins Trs130p and Trs85p into the hierarchy of yeast Atg proteins. Note how Ypt1p-GTP stands as a hub between Cvt/nutrient rich and non-selective/nutrient deprivation routes.

Atg8p, an indicator of fusion of the autophagosome with the vacuole, is normally seen within the vacuole lumen after induction of autophagy. However, Atg8p failed to appear inside the vacuole in *trs85Δ* (Meiling-Wesse et al., 2005; Nazarko et al., 2005). In mammalian cells, the role for TRAPP in autophagy is not clearly understood. Nonetheless, components of the TRAPP complex, C11, C12, and the Trs85p homolog C8, were among the TRAPP subunits identified in a screen for components of the autophagy machinery (Behrends et al., 2010). The

C10 (mTrs130) subunit of mammalian TRAPP can activate the Ypt1p homolog Rab1. It has been suggested that C10 may tether COPI vesicles to the early Golgi membrane because depletion of C10 was shown to cause a delay in forward trafficking and resulted in an accumulation of vesicles in the Golgi membrane (Yamasaki et al., 2009). In brief, even though the small GTPase (either Ypt1p or Ypt31p-Ypt32p) upon which TRAPP II acts is controversial, the involvement of TRAPP II in autophagy in yeast and mammalian cells may be conserved. In this respect it is notable that Rab1 has also been shown to have a role in autophagosome formation in mammals.

1.5 The overall objective of my PhD dissertation

With respect to the study of multisubunit complexes of TRAPP, which are the focus in our laboratory, my PhD thesis work involved the elucidation of the cellular function of one the subunits that resides at one extremity of the core TRAPP I complex named TRAPPC2, or Sedlin, and its yeast ortholog Trs20p. In this dissertation, I have conducted experiments using two model systems, *S. cerevisiae* and human cells. I initially concentrated my efforts on understanding the function of TRAPPC2, which led to the identification of a novel TRAPPC2-related subunit that was present in both the yeast and mammalian TRAPP complexes called Tca17p and TRAPPC2L, respectively. One of the challenges in characterization of the role of TRAPPC2 is that TRAPPC2 is broadly expressed in multiple tissues, including brain, skeletal muscle and other tissues, yet the SEDT has a tissue-specific phenotype (cartilage). The rationale in searching for a protein related to TRAPPC2 was that presumably such a protein(s) may have a redundant function such that it could compensate for the loss of TRAPPC2 in the majority, but not all, tissues. This would be one possible explanation of why SEDT is tissue specific.The results of this study will be presented in Chapter 2 and were published in the journal *Traffic* in 2009.

It was determined that TRAPPC2L and TRAPPC2 expression in primary cells taken from the cartilage of SEDT patients was similar to the expression found in healthy individuals indicating

TRAPPC2L and its yeast counterpart Tca17p do not complement for the loss of TRAPPC2 and Trs20p, respectively, in chondrocytes. Thus, to investigate the function of TRAPPC2, I screened six human SNAREs involved in ER-to-Golgi transport for their potential to interact with TRAPPC2 and then continued this work in yeast. This study demonstrated that the yeast homolog of TRAPPC2, Trs20p, is not only involved in the assembly of the TRAPP III complex but is also involved in specific and non-specific autophagy. The data is presented in Chapter 3 and was published in *Traffic* in 2013.

In Chapter 4, I then present some of my unpublished findings, using mammalian cell culture, concerning the interaction between TRAPPC2 and SNARE proteins with a predominant focus on Syntaxin 5. I also describe the discovery of a novel protein partner of the TRAPP complexes, the putative coiled-coil tethering factor, p115, and will discuss the effect of the TRAPP complex on membrane and cytosol cycling of p115. I have determined that both p115 and the TRAPP complex are associated with the membrane fusion machinery and I discuss the possible functional significance of these associations.

Following the discovery of TRAPPC2L, our lab used TAP tagged TRAPPC2 and TRAPPC2L to identify novel TRAPP-associated proteins which led to the identification and characterization of other subunits including the TRAPPC11 protein. After teaming up with a group of collaborators who discovered that TRAPPC11 is mutated in several Hutterite families, I began another project with a goal of examining the effect of this deletion mutation in the *foie gras* domain on TRAPPC11 function. Through biochemical and microscopic-based analyses I demonstrated for the first time in primary human cells that the TRAPP complex is involved in a trafficking step late in the secretory pathway.The data is described in Chapter 5 and some of these findings were published in the *American Journal of Human Genetics* in 2013. Finally Chapter 6 of this dissertation includes a general summary of my studies and future perspectives.

CHAPTER 2

TRAPPC2L is a novel, highly conserved TRAPP-interacting protein

Data presented in this chapter used both the budding yeast *Saccharomyces cerevisiae* and mammalian tissue culture to identify mammalian TRAPPC2L (hereafter the prefix "TRAPP" is eliminated for simplicity from the mammalian proteins) and its yeast counterpart encoded by the *YEL048c* gene, and was published in the journal of *Traffic* (Scrivens et al. 2009). I preformed the work in Figures 2.5-2.11, 2.14 and 2.19 and I am co-first author of this manuscript. A simultaneous report also identified the product of *YEL048c* as a TRAPP component and named the gene *TCA17* (Montpetit and Conibear, 2009). I have adapted this nomenclature in subsequent chapters.

2.1 Introduction

Vesicle-mediated transport of proteins and lipids is critical to the maintenance of the distinct composition of most intracellular organelles. Many factors are required to ensure that each vesicle is recognized by and fuses with the appropriate compartment. Tethering factors are an evolutionarily conserved class of proteins that mediate the initial contact between vesicles and target membranes and are thus believed to impart the initial layer of specificity in this process (Sztul and Lupashin, 2006;Whyte and Munro, 2002;Koumandou et al., 2007). These factors can be subdivided into coiled-coil proteins and multisubunit complexes (Sztul and Lupashin, 2006;Whyte and Munro, 2002). How these two classes of tethering factors cooperate to tether a vesicle remains unclear.

TRAPP I and TRAPP II are two related multisubunit complexes acting in the yeast secretory pathway (Sacher et al., 2008). In yeast, these complexes are involved in endoplasmic

reticulum (ER) -to-Golgi transport (TRAPP I) and a transport step at the *trans*-Golgi/endosome (TRAPP II) (Cai et al., 2005; Sacher et al., 1998; Sacher et al., 2001). The complexes contain seven subunits in common (Bet5p, Trs20p, Bet3p, Trs23p, Trs31p, Trs33p and Trs85p) but TRAPP II contains three unique subunits (Trs65p, Trs120p and Trs130p; see Table 2.1 for mammalian and yeast subunit nomenclature to be used throughout this chapter). TRAPP is well-conserved through evolution and a Bet3p-like protein has even been described in prokaryotes, underlining the ancient origins and fundamental nature of this complex (Podar et al., 2008). While the yeast TRAPP complexes are readily distinguished based on their different molecular sizes and on their subunit composition (Sacher et al., 2001), no such distinction has yet been reported for mammalian TRAPP. In the limited reports on mammalian TRAPP, only a single high molecular weight pool of subunits has been described (Sacher and Ferro-Novick, 2001;Loh et al., 2005). The absence of the larger TRAPP II complex is particularly curious given that orthologs for the TRAPP II subunits Trs130p and Trs120p have been identified in mammals (Cox et al., 2007) and have been reported to co-precipitate with C3 (Gavin et al., 2002;Kummel et al., 2008).

Yeast TRAPP subunit (size in kD)	Mammalian TRAPP subunit (size in kD)
Bet5p (18)	TRAPPC1 (17)
Trs20p (20)	TRAPPC2 (16)
Bet3p (22)	TRAPPC3 (20)
Trs23p (23)	TRAPPC4 (24)
Trs31p (31)	TRAPPC5 (21)
Trs33p (33)	TRAPPC6a,b (18)
Trs65p (65)	none
Trs85p (85)	none
Trs120p (120)	TRAPPC9 (140)
Trs130p (130)	TRAPPC10 (142)

Table 2.1 Nomenclature of yeast and mammalian TRAPP subunits.

The yeast TRAPP I complex has been shown to be necessary for ER-to-Golgi transport and sufficient to interact with ER-derived transport vesicles (Sacher et al., 2001). This interaction has been proposed to be mediated by an interaction between C3 and the vesicle coat protein Sec23 (Cai et al., 2007b). Other factors needed for tethering the vesicle to the Golgi are Uso1p and the GTPase Ypt1p, and perturbation of any of these proteins abrogates efficient tethering (Cao et al., 1998). Although the sequence in which these factors function is not clear, TRAPP I has been shown to have guanine nucleotide exchange factor (GEF) activity towards Ypt1p (Jones et al., 2000;Wang et al., 2000). The TRAPP II complex has been shown to interact with components of the COP I vesicle coat (Cai et al., 2005) and has GEF activity towards the GTPases Ypt31p-Ypt32p (Jones et al., 2000;Morozova et al., 2006). Given that TRAPP I and TRAPP II share a common core, how these two highly related complexes interact with distinct proteins to mediate different transport events is unclear. One possible explanation is that other proteins that interact with the complexes regulate their function. Identification of TRAPP-interacting proteins is thus an important area of study to further our understanding of these complexes.

TRAPP is one of the best-studied of the tethering complexes at the structural level. The structures of six of the mammalian subunits and five of the yeast subunits have been solved (Cai et al., 2008;Jang et al., 2002;Kim et al., 2005a and b;Kummel et al., 2005 and 2006;Kummel et al., 2005;Turnbull et al., 2005). Interestingly, the subunits fall into two families based on their three-dimensional crystal structures: the Bet3 family containing Bet3p/C3, Trs31p/C5 and Trs33p/C6, and the Sedlin family containing Trs20p/C2, Bet5p/C1 and Trs23p/C4 (yeast/mammalian). The arrangement of the subunits within the complex produces two large, flat surfaces that may enable multiple protein-protein interactions (Kim et al., 2006).

Many factors involved in vesicle-mediated transport events have been linked to disease (Aridor and Hannan, 2000 and 2002). Mutations in the human C2 subunit have been strongly

linked to the skeletal disorder spondyloepiphyseal dysplasia tarda (SEDT) (Gedeon et al., 1999;Shaw et al., 2003). This disorder primarily affects the spine and epiphyses and has been suggested to be due to a defect in collagen secretion from chondrocytes (Sacher, 2003;Tiller et al., 2001). However, the fact that other collagen-secreting cells in SEDT patients have not been reported to be defective in the transport of this protein raises interesting questions about the specific function(s) of C2.

Here, we identify and characterize a protein, C2L, that is related to C2 and interacts with TRAPP. The protein is broadly expressed and highly conserved. We also characterize the yeast ortholog of this protein encoded by the uncharacterized open reading frame *YEL048c* and show that its genetic interactions group it with genes encoding TRAPP II subunits. C2L is in TRAPP complexes that also contain C2 indicating that the two proteins bind to different sites within TRAPP, a notion supported by biochemical studies. While C2 is found on two distinct membranes, C2L is found only on one. Finally, although functionally distinct, knockdown of the mammalian C2L and C2 proteins indicates that both are involved in Golgi dynamics. This study provides the first report of a mammalian TRAPP-interacting protein that may preferentially associate with and regulate the activity, assembly or function of a mammalian TRAPP II complex.

2.2 Materials and methods

2.2.1 Plasmids

The C2L open reading frame was amplified from cDNA obtained from OpenBiosystems. C2 was amplified from existing DNA (Kim et al., 2006). All PCR products were inserted into pRS425, pRS415 or pRS413-ADH1 (Mumberg et al., 1995) for expression in yeast and pFLAG-CMV6a (Sigma) for expression in mammalian cells. For recombinant protein expression in *E.coli* the PCR products were inserted into either pACYCDuet-1 or pRSFDuet-1 (Novagen).

2.2.2 Reverse transcriptase-PCR

Tissues were harvested and total RNA was extracted with the Nucleospin RNA II kit (Clontech). cDNA was synthesized from 1 µg of RNA using Moloney Murine Leukemia Virus reverse transcriptase (New England Biolabs). For polysome experiments, the polysomes were prepared essentially as described by Blower et al.(2007). Processing of the RNA was as described above.

2.2.3 Tissue culture

Cells were maintained in DMEM (Wisent) supplemented with 10% fetal bovine serum (FBS) in a humidified CO_2 chamber. Transfections were performed in a 10 cm dish with 10 µg of DNA by the calcium phosphate method. Cells were harvested 48 hours post-transfection using RIPA buffer (150 mM NaCl, 50 mM Tris, pH7.2, 0.1% SDS, 1% Triton X-100, 1% deoxycholate) with protease inhibitors (Roche). For gradient fractionation transfected cells were harvested in 150 mM NaCl, 50 mM Tris, pH7.2, 0.5 mM EDTA, 1 mM DTT with protease inhibitors. For size exclusion chromatography the transfected cells were harvested in RIPA without SDS and deoxycholate. A total of 30 µg of lysate was used for western analysis and detergent extraction. For size exclusion chromatography a total of 1.5 mg of lysate was fractionated and assayed by

western analysis. For purification of TAP-tagged proteins, two 15 cm dishes were transfected with 50 µg DNA each, expanded one day after transfection and purified using IgG-sepharose beads (GE Healthcare).

2.2.4 Antibodies

Polyclonal antibodies recognizing C3 and C2 were raised in rabbits using His-tagged proteins as antigen. Antibody to C4 (2D10) was purchased from Abnova. Monoclonal anti-FLAG M2 antibody was purchased from Sigma. Antibodies were used at 1:1000 dilution for western analysis or 1:250-1:1000 for immunofluorescence unless otherwise indicated. Compartment-specific markers for immunofluorescence and western analysis were: rabbit anti-Mannosidase II (Dr. Kelly Moreman, University of Georgia), mouse anti-ERGIC53 (G1/93, Cedarlane), rabbit anti-ERGIC53 (E1031, Sigma), mouse anti-GM130 (Dr. Martine Lowe, University of Manchester), mouse anti-β-COP (MAD, Sigma), rabbit anti-TAP tag (OpenBiosystems), rabbit anti-Sam68 (Dr. S. Richard). Secondary antibodies were anti-rabbit AlexaFluor 488 and anti-mouse AlexaFluor 546 (Invitrogen) or anti-mouse-Rhodamine, a kind gift from J. Uniacke.

2.2.5 Gradient fractionation

Cells were harvested and lysed as described above. The membranes were collected from the lysates by centrifugation at 100,000*g* for 1 h. Membranes were resuspended in lysis buffer and layered on top of an OptiPrep (Sigma) gradient (2.5%-40%) and centrifuged in an SW41 rotor at 156,000*g* for 16 h. Fractions of 1mL were collected from the top of the tubes and 30 µL of each fraction was used for western analysis.

2.2.6 siRNA

Small interfering RNA (siRNA) that targets either both versions of C2 (C2 and C2.19; #1: UCCAUUUUAUGAACCCAAUTT; #2: CAAUUCUCCUAUUCGAUCATT) or C2L (#1:

AGCCCUUCGAGACAACGAATT; #2: GCAUGUUCCGGAAGCUACATT) were purchased from Ambion and used at 60 nM. Introduction of the siRNA was accomplished using Oligofectamine (Invitrogen) in OptiMEM. After 24 hours the medium containing the siRNA was removed and replaced with fresh DMEM containing serum and no antibiotics. For immunofluorescence cells were first trypsinized and replated to coverslips. Cells were processed 48 hours after the medium change. Knockdown was assessed by either semi-quantitative RT-PCR (for C2L) or western analysis (for C2) as described above. The siRNAs for C3 were designed from published oligonucleotides (Yu et al., 2006).

2.2.7 Immunofluorescence microscopy

Cells were plated on coverslips in 6-well dishes. For processing, coverslips were rinsed in PBS then fixed in pre-chilled methanol: acetone (4:1) for 10 min at -20°C. Following fixation, coverslips were rinsed in PBS prior to blocking in 2% FBS, 2% BSA, and 0.2% fish skin gelatin in PBS. Primary antibodies were diluted in blocking buffer and incubated in 40 µL volumes on coverslips. The wash buffer consisted of blocking buffer progressively diluted with PBS. Secondary antibody incubation was identical to primary, except for the addition of DAPI and the fact that the incubation was conducted in the dark. Washes were as above, with the final wash being PBS alone. Slips were mounted on slides using Antifade Gold (Invitrogen) mounting medium. Samples were visualized on a Zeiss LSM510 confocal microscope using a Zeiss Planapochromat 63X N.A. 1.4 oil immersion objective. Images were adjusted for brightness and contrast and overlays created using Adobe Photoshop.

2.3 Results

2.3.1 Identification of yeast and mammalian C2-related proteins

In order to understand the function of C2 and how it is involved in the tissue-specific disorder SEDT we undertook a BLAST search of yeast and mammalian databases for C2-related proteins. Our initial hypothesis was that such proteins may compensate for a lack of C2 function in some, but not all, tissues. A BLAST search of GenBank using the yeast *S.cerevisiae* subunit Trs20p (C2 ortholog) as a query revealed two different proteins: the well-characterized C2 (33% identity, 52% similarity) and a related protein that we will call C2-like (C2L; 27% identity, 47% similarity). Using C2L as a query we found that this subunit is present throughout metazoans and is highly conserved (Figure 2.1). Of particular note is the fact that a previously uncharacterized *S.cerevisiae* open reading frame, *YEL048c*, clusters with C2L orthologs (Figure 2.1). In addition, the independent clustering of C2 and C2L indicate that these proteins are distinct and likely arose early in eukaryotic lineage. On the other hand, it appears that functional constraints may have limited the divergence of these proteins from each other as C2 and C2L display 28% identity and 50% similarity over ~100 residues. While related to C2L, the uncharacterized YEL048cp is more divergent from the mammalian protein (24% identity, 43% similarity) than is the yeast C2 ortholog from its mammalian counterpart (see above). Furthermore, YEL048cp and Trs20p are more divergent (23% identity, 43% similarity over 103 residues) than are their mammalian counterparts (see above). *YEL048c* is non-essential in yeast, and its greater divergence from its mammalian ortholog may reflect lower selective pressure in this organism relative to that operating on Trs20p/C2. The presence of C2 and C2L pairs across species suggests a conserved functional divergence between the two proteins.

A comparison between the various C2 and C2L proteins by multiple sequence alignment revealed only two invariant residues and several nearly invariant but similar residues (Figure 2.1). The invariant residues Leu46-Asp47 (human numbering) are particularly noteworthy since these are found at the surface of the protein (Jang et al., 2002;Kim et al., 2006) (Figures 2.2 and

2.3) and since an Asp47→Tyr missense mutation in C2 has been noted for one SEDT patient (Gedeon et al., 2001), suggesting a common, conserved function for this region in both C2 and C2L.

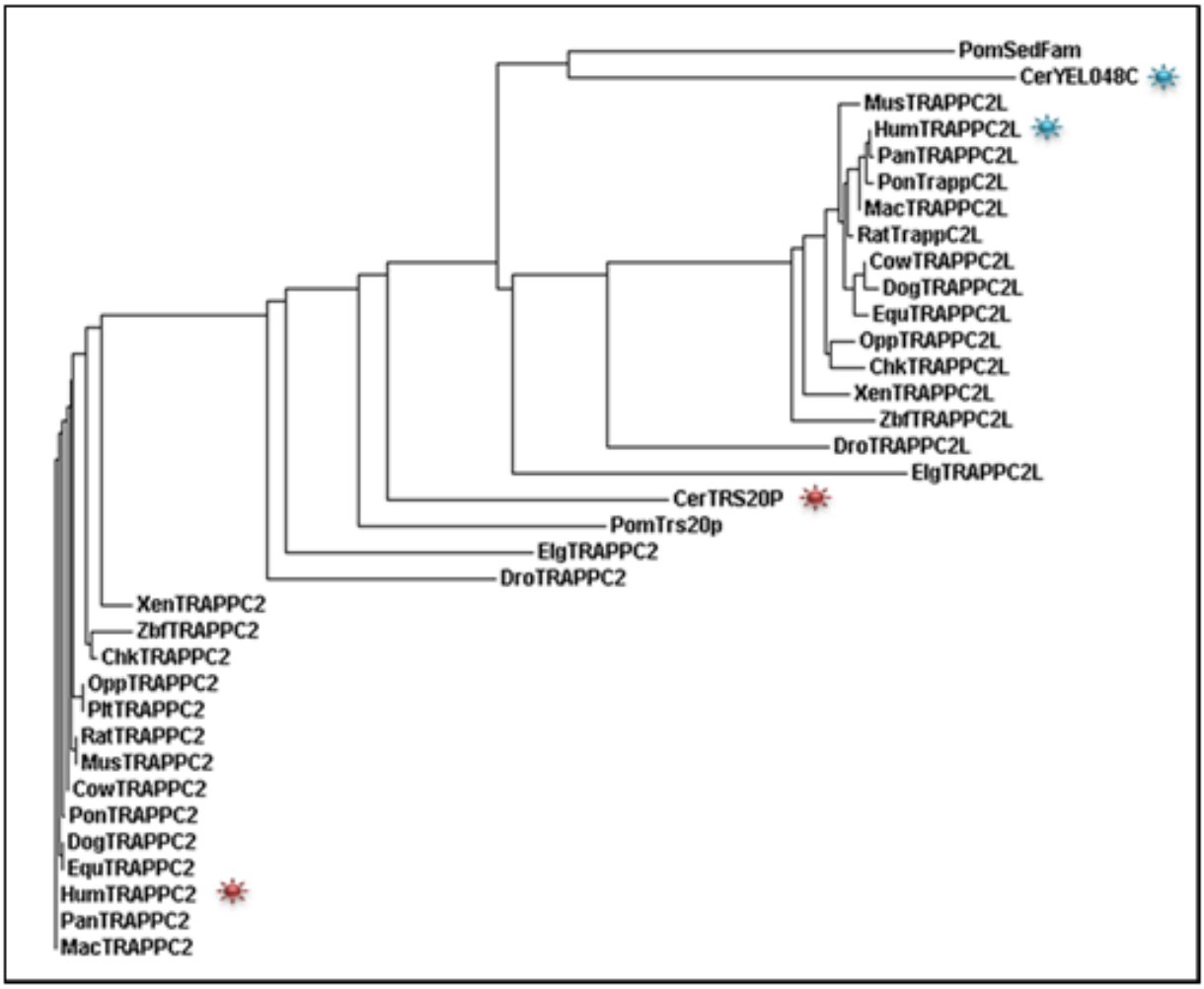

Figure 2.1 C2L is highly conserved and related to C2. Full-length sequences of C2 (indicated with a red star) or C2L proteins (indicated with a blue star) or their budding yeast orthologs were aligned using ClustalW and a phylogram generated. The independent clustering of C2 and C2L indicates these are distinct proteins. Note the clustering of the uncharacterized *S.cerevisiae* open reading frame *YEL048c* with the C2L proteins, suggesting it is the yeast ortholog of C2L.

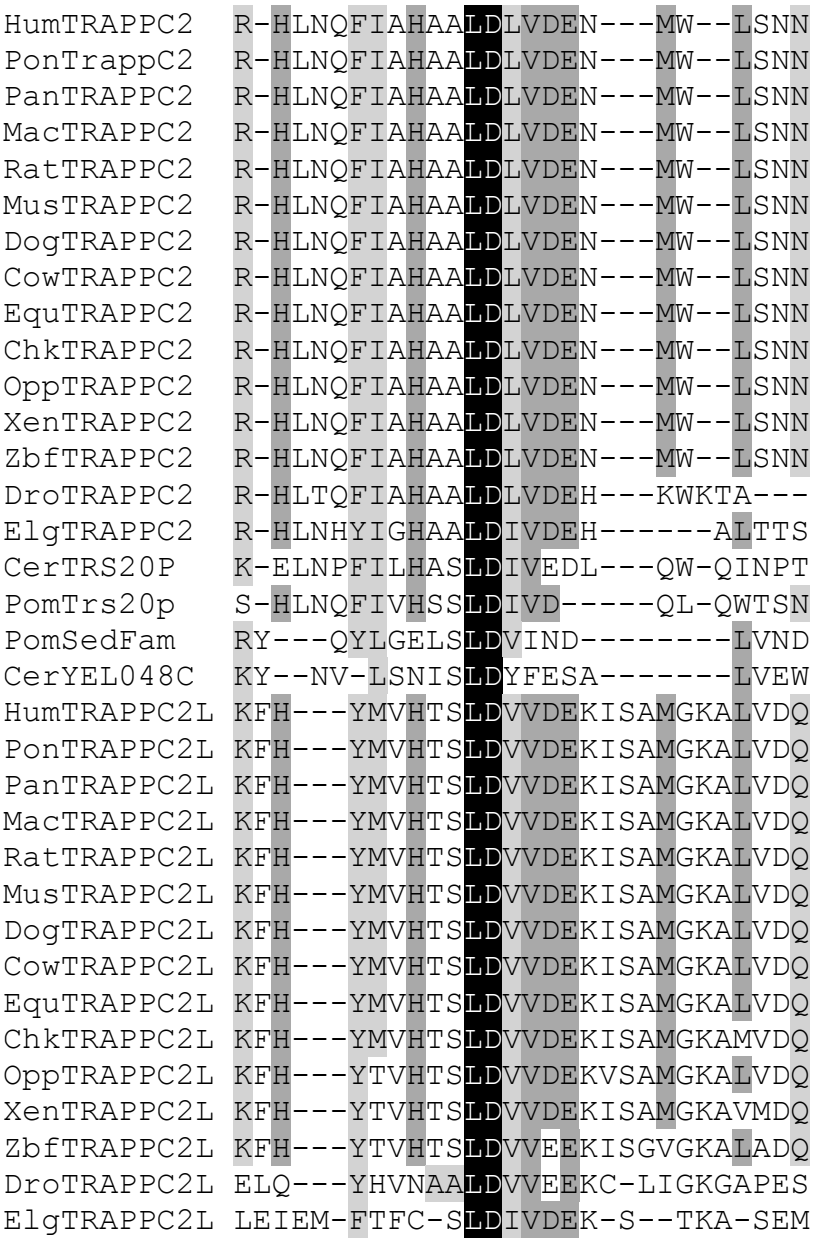

Figure 2.2 Multiple sequence alignments of C2 and C2L

When all identified C2 and C2L proteins are compared, only two amino acid residues show absolute conservation (highlighted in black). The Asp47 residue of C2 is mutated in some patients with SEDT. Residues showing 75% identity between C2 and C2L are highlighted in dark grey. Residues showing 75% similarity between C2 and C2L are highlighted in light grey.

Abbreviations and accession numbers for the proteins used in this figure are: ***C2L***- Chimpanzee (Pan), XP_001138135; Orangutan (Pon), NP_001125486; Human (Hum), NP_057293; Rhesus Macaque (Mac), XP_001090102.1; Mouse (Mus), AAI14969; Rat, AAI68734; Cow, AAI46229; Dog, XP_850022.1; Horse (Equ), XP_001488385.1; Chicken (Chk), XP_414207.1; *X. laevis* (Xen), NP_001011228.1; Zebrafish (Zbf), NP_001003506; *D. melanogaster* (Dro), NP_610662.1; *C.elegans* (Elg), NP_001033370.1; Opposum (Opp), XP_001366474.1; *S. Cerevisiae* (Cer), NP_010816.1; *S. Pombe* (Pom), NP_594299.1. ***C2***- Chimpanzee, XP_001145048.1; Orangutan, NP_001124790.1; Human, NP055371.1; Rhesus Macaque, XP001092331.1; Mouse, NP_079595.1; Rat, NP_001020136.1; Cow, NP_001029968.1; Dog, XP_537957.1; Horse, XP_001489143; Chicken, NP_001006263.1; *X. laevis*, NP_001087961.1; Zebrafish, NP_001070243.1; *D. melanogaster*, NP_648841.1; *C. elegans*, NP_508272.1; Opposum, XP_001364796.1; *S. Cerevisiae*, NP_009813; *S. Pombe*, NP_595722.

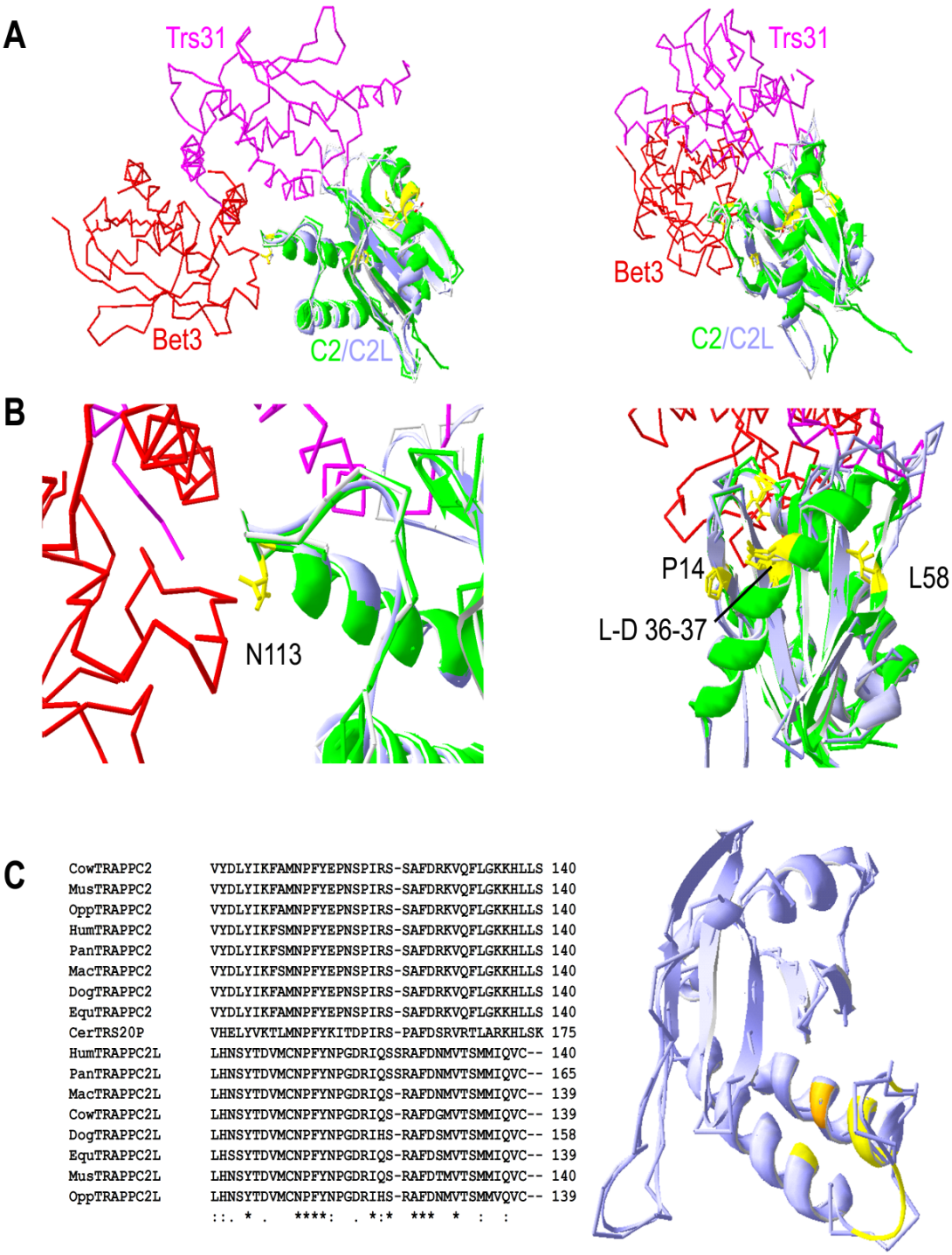

Figure 2.3 Comparison of the structures of C2 and C2L. (A) An overlay of human C2L on the previously determined structure of C2 in complex with C3 and C5 suggests possible roles for conserved amino acids. Five human C2L residues (Pro14, Leu36, Asp37, Leu58, and Asn113)

are conserved in all Trs20p-related proteins examined, with the exception of Zebrafish C2, where only Leu46 and Asp47 are conserved and are indicated in yellow along with their positions in C2. A closer view of each of these residues is shown in (B). C2 residue Asn112 (equivalent to Asn113 in C2L) was previously implicated in C3 interactions. The C2 residue Asp47 (equivalent to Asp37 in C2L) has previously been shown to be mutated in a case of spondyloepiphyseal dysplasia tarda (SEDT). The remaining residues, Pro16 (equivalent to Pro14 in C2L) and Leu61 (equivalent to Leu58 in C2L), are surface-exposed in this model suggesting a possible role in other molecular interactions. (C) *YEL048C* is non-essential in *S.cerevisiae*, and may therefore be less highly conserved than the essential Trs20p. An alignment of mammalian C2/C2L proteins versus *S.cerevisiae* Trs20p reveals a further region of homology in the carboxy-terminus. With the exception of the Asn-Pro-Phe-Tyr loop previously described to play a role in C3 interactions, these amino acids (shown in yellow) appear to be oriented towards the interior of the protein in this model, suggesting a structural role. C2 Val130 (gold) is the site of a known SEDT missense mutation.

2.3.2 Expression pattern of *C2*, *C2L* and *C2.19*

To begin characterizing C2L and C2 we examined their expression in cells using semi-quantitative reverse transcriptase (RT)-PCR. Included in these studies was the expression pattern of a gene encoded on human chromosome 19 that can potentially encode a protein identical to C2. This gene has been referred to as SEDLP1 and it was originally thought to be a pseudogene (Gecz et al., 2000) but here we refer to it as C2.19. A previous report suggested differential expression of C2 and C2.19 but the probe used was not exclusive to either of the genes (Ghosh et al., 2001). As shown in Figure 2.4 left panel, C2L, C2 and C2.19 were expressed in all cell lines examined. Of particular interest was the fact that all of these genes were expressed in primary cultures of human chondrocytes cells that are predominantly thought to be affected in SEDT patients (Figure 2.4 left panel). Previous studies demonstrated broad expression of C2 (Gedeon et al., 1999;Ghosh et al., 2003;Mumm et al., 2001) and we found that C2L was also broadly expressed (Figure 2.4 right panel top). These studies indicate that C2L

and C2 are broadly co-expressed and further provide the first evidence that both C2 and C2.19 are co-expressed within the same cell. Interestingly, C2.19 was found in polysomes (Figure 2.4 right panel bottom), suggesting that it is actively translated. The apparent broad co-expression of three Trs20p-related proteins further complicates the elucidation of the precise mechanism by which C2 mutations cause a tissue-restricted disease such as SEDT.

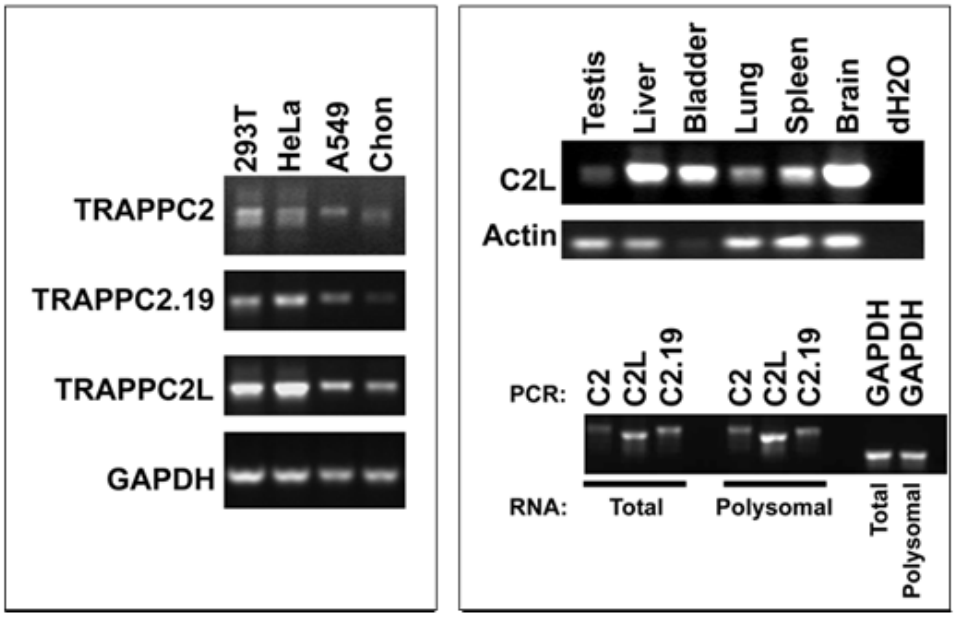

Figure 2.4 Gene expression patterns of C2, C2.19 and C2L. Total RNA from the indicated cells or tissues was subjected to RT-PCR as described in Materials and Methods. The expression of C2L, C2 and C2.19 was examined in several cell lines (HeLa, HEK293, A549) as well as in primary human chondrocytes (left panel). The expression of C2L was examined in various mouse tissues (right panel top). The presence of C2 and C2.19 in polysomes was examined by RT-PCR after collecting polysomes through a sucrose gradient as described in Materials and Methods (right panel bottom).

2.3.3 *YEL048c* displays genetic interactions with *TRAPP* genes

To begin characterizing the relationship between C2L and C2 we explored genetic interactions between the genes encoding their yeast orthologs *YEL048c* and *TRS20*, respectively. To this end we first compared suppression of temperature-sensitive alleles in genes encoding TRAPP subunits by overexpression of *YEL048c* or known TRAPP genes. For this analysis we used *bet3-5*, *bet5-2*, *trs20-1* and *trs130-1*, the latter encoding a TRAPP II-specific subunit. Overexpression of *YEL048c* suppressed the growth phenotype of each mutant except for *bet3-5* (Figures 2.5 and 2.6). In the case of *trs130-1*, *YEL048c* and two other genes encoding TRAPP II-specific proteins (*TRS65* and *TRS120*) were the only genes capable of suppressing the growth phenotype. These results clearly show genetic interactions between *YEL048c* and genes encoding TRAPP subunits.

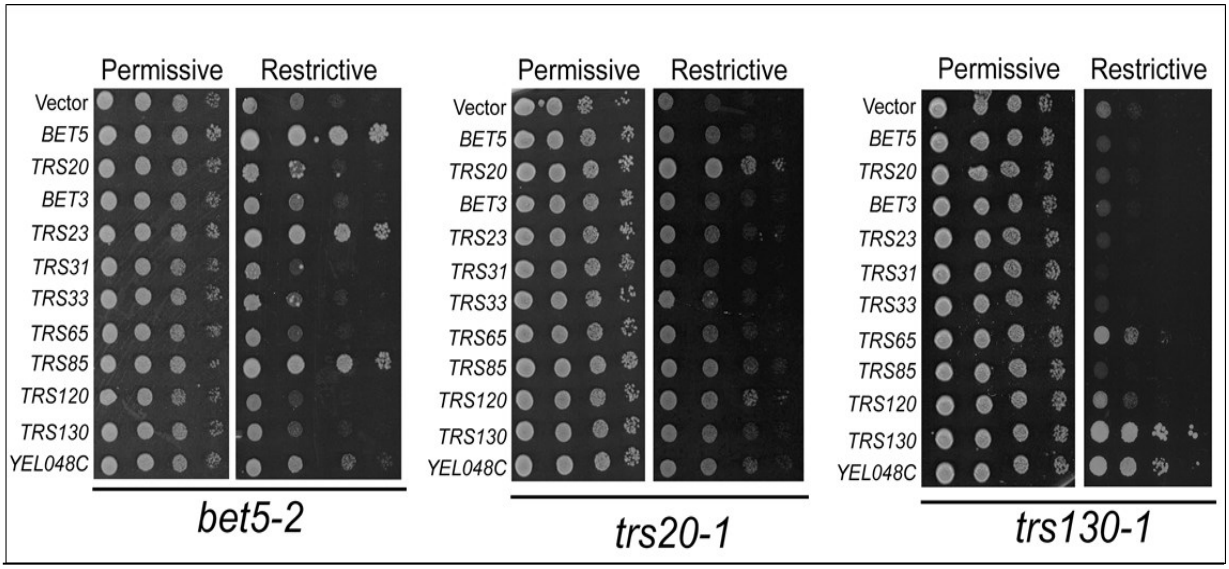

Figure 2.5 Genetic interactions between *YEL048c* and genes encoding TRAPP subunits. Yeast strains containing *bet5-2*, *trs20-1* or *trs130-1* were transformed with a pRS425-based plasmid containing either the wild type TRAPP subunit-encoding genes (*BET5*, *TRS20*, *BET3*, *TRS23*, *TRS31*, *TRS33*, *TRS65*, *TRS85*, *TRS120* and *TRS130*) or *YEL048c*. Ten-fold serial dilutions

were spotted onto rich medium and grown either at permissive temperature (25°C) or restrictive temperature. The restrictive temperature for each strain is: *bet5-2*: 34°C, *trs20-1*: 38°C, *trs130-1*: 36°C.

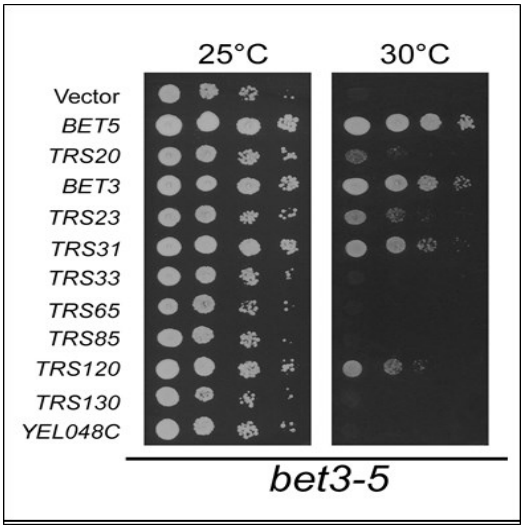

Figure 2.6 Temperature sensitivity of *bet3-5* can be suppressed by several TRAPP subunits but not with *YEL048c*. A yeast strain containing *bet3-5* was transformed with a pRS425-based plasmid containing either the wild type TRAPP subunit-encoding genes (*BET5*, *TRS20*, *BET3*, *TRS23*, *TRS31*, *TRS33*, *TRS65*, *TRS85*, *TRS120* and *TRS130*) or *YEL048c*. Ten-fold serial dilutions were spotted onto rich medium and grown either at 25°C or 30°C.

As a further measure of genetic interactions between the genes encoding TRAPP subunits and *YEL048c* we asked whether the disruption of the latter (*yel048cΔ*) displayed synthetic genetic interactions in combination with the TRAPP mutants above or with disruptions of the non-essential TRAPP genes *trs33Δ*, *trs65Δ* and *trs85Δ*. As described in Table 2.2 and *yel048cΔ* did indeed display synthetic lethality in combination with *trs20-1*, *bet3-5* and *trs65Δ* and synthetic sickness with *trs33Δ*. Interestingly, the lethality of a *yel048cΔ* /*trs65Δ* double disruption can be suppressed by overexpression of *TRS130* (Figure 2.7). Overall our analysis implicates *YEL048c* as genetically interacting with six of the TRAPP genes tested. Notably,

there is a pronounced genetic link between *YEL048c* and the genes encoding TRAPP II subunits (*TRS130*, *TRS120*, *TRS65*) suggesting that the protein encoded by *YEL048c* may interact with or modulate the activity of TRAPP II.

	synthetic lethality or sickness in a *yel048cΔ* cross[a]	suppression of single TRAPP gene alleles by *YEL048c* overexpression
bet5-2	No	yes
trs20-1	Lethal	yes
bet3-5	Lethal	no
trs33Δ	sick[b]	(not tested)
trs65Δ	Lethal	(not tested)
trs85Δ	No	(not tested)
trs130-1	No	yes

Table 2.2 Summary of *YEL048c* – TRAPP genetic interactions in yeast.
[a]A minimum of 20 dissected tetrads were examined for co-segregation of *yel048cΔ* (marked by G418 resistance) and either the temperature-sensitive phenotype (for *bet5*, *trs20*, *bet3* and *trs130*) or the His^+ phenotype (for *trs33Δ*, *trs65Δ* and *trs85Δ*). [b]All 22 colonies that displayed co-segregation of G418 resistance with the His^+ phenotype were also temperature sensitive.

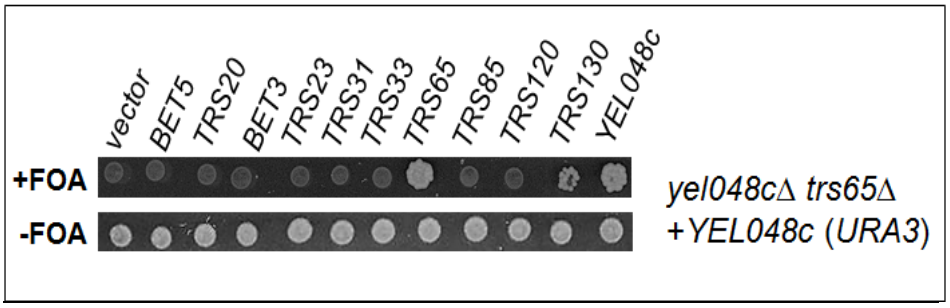

Figure 2.7 *yel048c* mutant (*yel048cΔ /trs65Δ*) is suppressed by *TRS130.* The double mutation *yel048cΔ /trs65Δ* strain was generated in which the chromosomal copy of *YEL048c* was deleted (*yel048cΔ*) and a copy of wild type *YEL048c* was maintained on a *URA3*-based plasmid. The plasmid was counter-selected on 5-fluoroorotic acid-containing plate.

2.3.4 YEL048cp and C2L physically interact with TRAPP

Given the genetic interactions presented above we next asked if the gene product of *YEL048c* can interact with TRAPP. A yeast lysate containing TAP-tagged YEL048cp was fractionated by size exclusion chromatography and YEL048cp was detected with an anti-TAP tag antibody. We also probed the fractions for the presence of Trs33p, found in both TRAPP I (low molecular weight) and TRAPP II (high molecular weight). As shown in Figure 2.8, YEL048cp was found in a high molecular weight fraction that co-fractionated with the high molecular weight peak for Trs33p. This result suggested that YEL048cp might physically interact with TRAPP and preferentially with yeast TRAPP II. Indeed, an interaction was confirmed by detection of Trs33p co-precipitating with TAP-tagged YEL048cp from a total cell lysate (Figure 2.8). It should be noted that a second pool of YEL048cp is occasionally found if cells are disrupted using a more harsh glass bead lysis procedure. This second pool is smaller than the lower molecular weight TRAPP I complex (not shown) and may result from the fragmentation of a portion of TRAPP II.

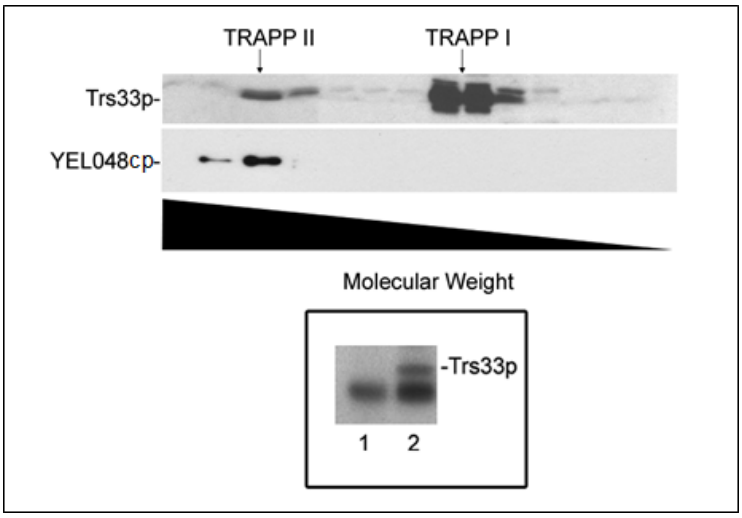

Figure 2.8 YEL048cp co-fractionates with the TRAPP II peak in yeast. A yeast lysate was prepared from spheroplasts from a strain in which YEL048cp is modified with a carboxy-terminal

TAP tag. The lysate was fractionated on a Superdex-200 size exclusion column and 1 mL fractions were collected and analyzed by western blotting using anti-Trs33p serum or anti-TAP antibody. (*Inset*) Lysates from untagged (lane 1) or TAP-tagged YEL048cp (lane 2) were treated with IgG-sepharose and the precipitates were probed with anti-Trs33p serum.

We surmised that if YEL048cp interacts with TRAPP and is related to Trs20p then it may interact with the same TRAPP subunits that interact with Trs20p. We have recently shown that the mammalian Trs20p ortholog, C2, interacts with an interface presented by the C3-C5 heterodimer (Kim et al., 2006), equivalent to yeast Bet3p-Trs31p. Therefore we co-expressed YEL048cp with 6x histidine-tagged Bet3p and Trs31p and purified the proteins on a Ni^{2+}-NTA column. We detected YEL048cp co-purifying with the Bet3p-Trs31p heterodimer (Figure 2.9, lanes 1 and 2) indicating that the protein can indeed interact in this recombinant system with the same interface that interacts with Trs20p.

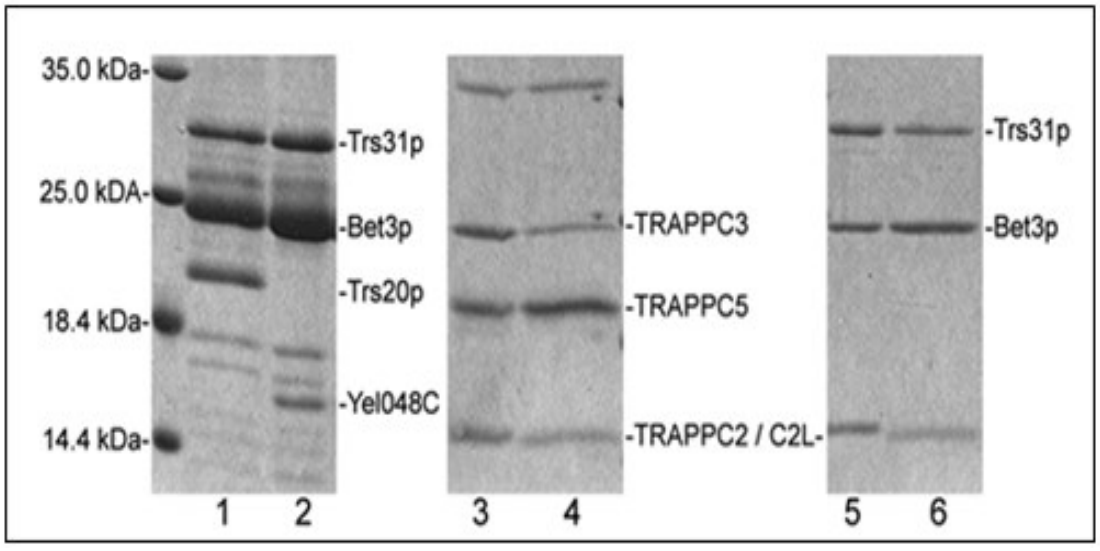

Figure 2.9 YEL048cp/C2L interacts with same interface that binds Trs20p/C2 *in vitro.* Lysates from various *E.coli* strains co-expressing yeast and mammalian TRAPP subunits were

subjected to purification over a Ni^{2+}-NTA affinity column. The strains co-expressed: His-Bet3p, Trs31p and either Trs20p (lane 1) or YEL048cp (lane 2); His-C3, C5 and either C2 (lane 3) or C2L (lane 4); His-Bet3p, Trs31p and either C2 (lane 5) or C2L (lane 6).

To assess whether C2L was behaving in a similar fashion as its yeast ortholog we transfected HEK293 cells with C2L containing a FLAG tag (FLAG-C2L) and prepared total cell lysates that were fractionated by size exclusion chromatography. In this assay, FLAG-C2L, like endogenous C2 and C3, is found in both high molecular weight and lower molecular weight fractions (Figure 2.10), the latter likely representing unassembled subunits or small heteromeric sub-complexes of TRAPP. Note that, while typical of mammalian TRAPP fractionation profiles (Loh et al., 2005;Sacher and Ferro-Novick, 2001), these results contrast with the size fractionation observed in yeast, where discrete high molecular weight TRAPP I and TRAPP II complexes are readily visualized (Sacher et al., 2001). As with the yeast results above, these results showing similar fractionation profiles of C2L, -C3 and -C2 suggested that C2L may interact with TRAPP. As shown in Figure 2.9 (lane 4), like C2 (lane 3), recombinant C2L could indeed bind to the C3-C5 heterodimer. Interestingly, the ability of the yeast and mammalian proteins to interact across species is preserved as C2 and C2L could bind to yeast Bet3p-Trs31p (Figure 2.9, lanes 5 and 6) strengthening our hypothesis of conservation of C2/Trs20p and C2L/YEL048cp functions across species.

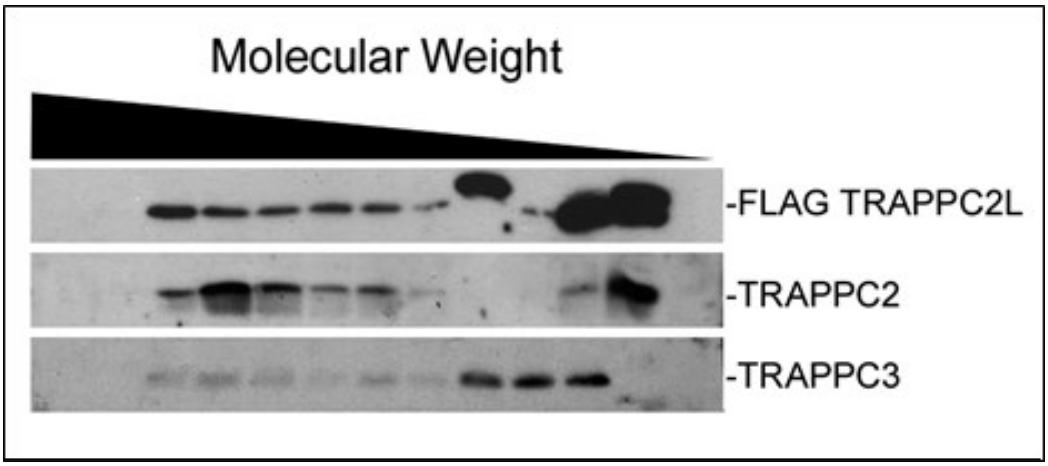

Figure 2.10 C2L co-fractionates with the high molecular weight peak of mammalian TRAPP. A lysate from HEK293 cells transfected with FLAG-C2L was fractionated on a Superdex-200 column as above. Samples were analyzed by western blotting using antibodies to the FLAG epitope (C2L), C2 and C3.

To examine whether C2L also interacts with TRAPP *in vivo* we tagged C2L and C2 with a TAP tag to allow for purification of the protein and associated proteins under native conditions. Both tagged proteins were indeed capable of co-precipitating with other TRAPP subunits (Figure 2.11). Interestingly, and somewhat unexpectedly, TAP-tagged C2L and C2 could precipitate each other (Figure 2.11). Together with the yeast results above, these results confirm that C2L/YEL048cp interact with TRAPP *in vivo* and suggests they are in the same TRAPP complex (es) as C2/Trs20p.

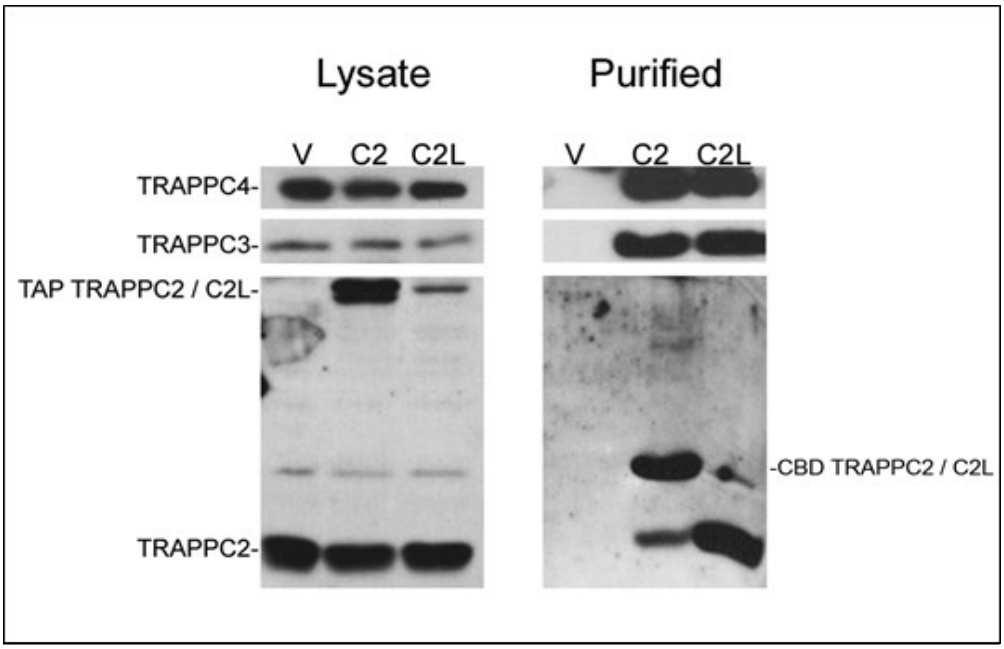

Figure 2.11 C2L binds to TRAPP *in vivo*. HEK293 cells were transfected with plasmids expressing C2-TAP or C2L-TAP, and lysates were prepared and purified on IgG-sepharose beads. Bound proteins were eluted by TEV cleavage and analyzed by western blotting for the presence of TRAPP subunits. The top panel was probed with anti-C4, the middle panel with anti C3, and the lowest panel with anti-C2. Note that the anti-C2 used weakly cross-reacts with C2L (not shown). CBD denotes the calmodulin binding domain that remains bound to the TEV-digested protein.

The latter result also suggests that, although C2L can interact with the same heterodimer as C2 *in vitro* (namely, C3-C5; see Figure 2.9), this mode of interaction may not reflect the *in vivo* situation since both subunits are found in the same complex simultaneously, suggesting discrete binding sites. We and others have shown that the C3-C5 (the C2 binding subunits) portion of the complex is structurally related to the C3-C6 dimer (Kim et al., 2005a and 2006 ;Kummel et al., 2006) found on the opposite side of the TRAPP complex (Kim et al., 2006). The C3-C6 interface equivalent to the C3-C5 interface that binds C2 is unoccupied in the current model (Kim et al., 2006) and therefore represents a likely site of C2L binding. To directly

test this possibility we co-expressed C3, C6a and C2L in our recombinant protein expression system. When 6X histidine-tagged C3-C6a was purified on Ni^{2+}-NTA beads, C2L, but not C2, co-purified (Figure 2.12) suggesting that C2L interacts with C3-C6a while C2 interacts with the opposite end of the complex through C3-C5.

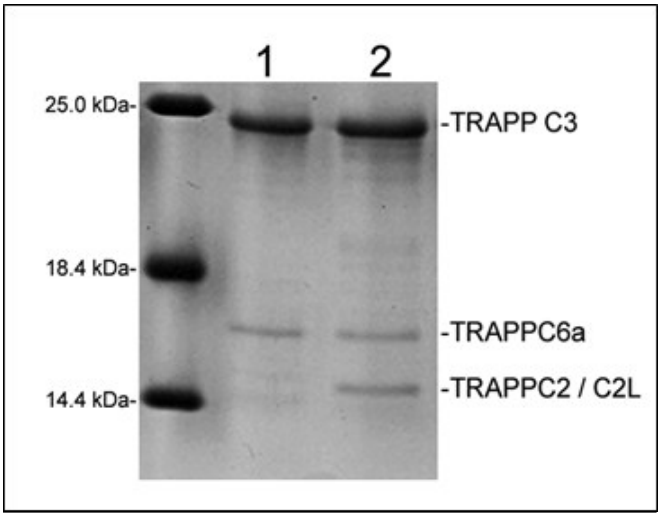

Figure 2.12 C2L interacts with the interface opposite that to which C2 binds. Lysate from an *E.coli* strain co-expressing His-C3 and C6a with either C2 (lane 1) or C2L (lane 2) were subjected to Ni^{2+}-NTA affinity purification followed by SDS-PAGE. Expression of C2 was verified by western analysis.

A tentative model of TRAPP based on these results and previous structural data (Kim et al., 2006) is presented in Figure 2.13 and shows opposite TRAPP ends occupied by C2 and C2L, respectively.

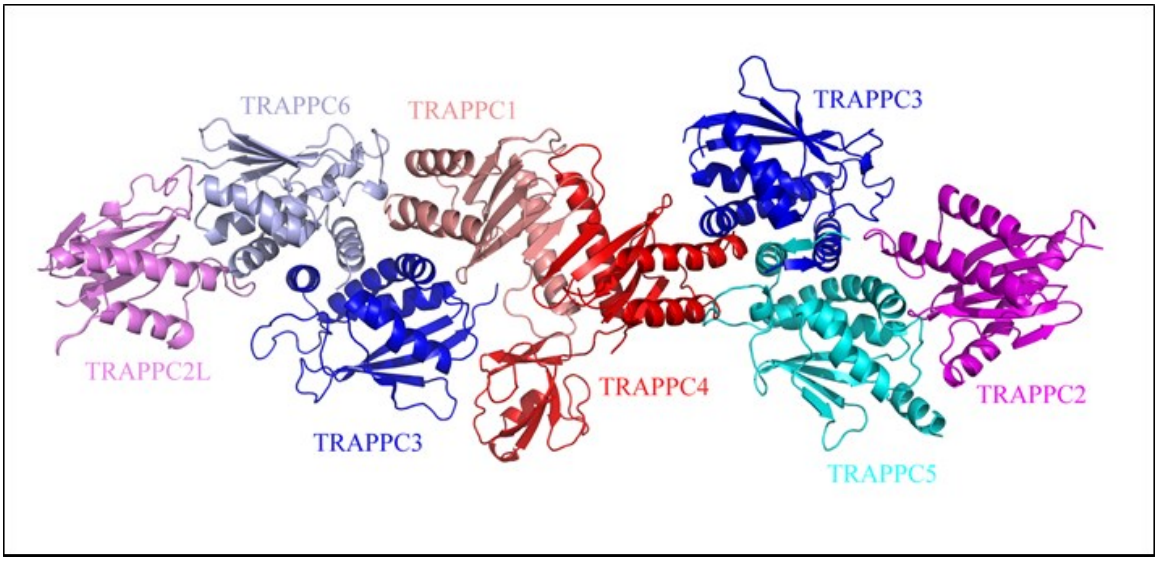

Figure 2.13 The architecture of TRAPP in complex with the C2L subunit. The structure of C2L was modeled using the known crystal structure of C2 (Jang et al., 2002). The C2L protein was then manually docked onto the previously published structure of mammalian TRAPP (Kim et al., 2006). Since C2L binds to C3-C6a (Figure 2.9) and C2 binds to C3-C5 (Kim et al., 2006), and since C2L and C2 are predicted to be structurally related, C2L was oriented to interact with C3-C6a in the same fashion as C2 interacts with C3-C5. The actual orientation of C2L with respect to the complex is unknown and hence the model presented is highly speculative.

2.3.5 Membrane distribution of C2 and C2L

We next examined whether C2 and C2L were found on similar intracellular membranes. To address this, membranes from HEK293 cells were collected by high-speed centrifugation and subjected to equilibrium-gradient centrifugation in OptiPrep. Fractions were collected and probed for C2L and TRAPP subunits. As shown in Figure 2.14, C2L was found in a single peak of very low density membranes (VLDM, peak in fraction 2). C2 and other TRAPP subunits were also found in this fraction but were further found in a second peak of intermediate density membranes (IDM, fractions 5 and 6). In order to identify the membranes in each of these

fractions we probed the gradient fractions with antibodies to various early secretory pathway marker proteins. The IDM overlapped with markers for the Golgi including Mannosidase II and GM130 (fractions 5-6; Figure 2.14). The peak of ERGIC53, the marker used to identify the ER-to-Golgi intermediate compartment (ERGIC), was separated from the peak of the Golgi markers suggesting that the IDM represents Golgi and that mammalian TRAPP is found on Golgi membranes in these cells as it is in yeast (Sacher et al., 1998;Barrowman et al., 2000). The yeast TRAPP II complex has been reported to play a role in endosome-to-Golgi trafficking (Cai et al., 2005). Since the VLDM fraction did not significantly overlap with Golgi or ERGIC markers, we asked whether this fraction contained the early endosome marker EEA1. Although partially overlapping, the peak of EEA1 was offset from the peak of C2L (Figure 2.14). The identity of the C2L-associated VLDM therefore remains unresolved at this time.

The relationship between the TRAPP complexes found in the VLDM and IDM was further characterized by overexpression of C2L (using FLAG-C2L) in HEK293 cells and examination of the distribution of the protein on membranes. We found that overexpressed C2L appeared additionally in the IDM fraction (Figure 2.14, FLAG-C2L). These results suggest that C2L can readily interact with TRAPP *in vivo* and that C2L in the VLDM fraction may reflect its interaction with a mammalian equivalent of TRAPP II.

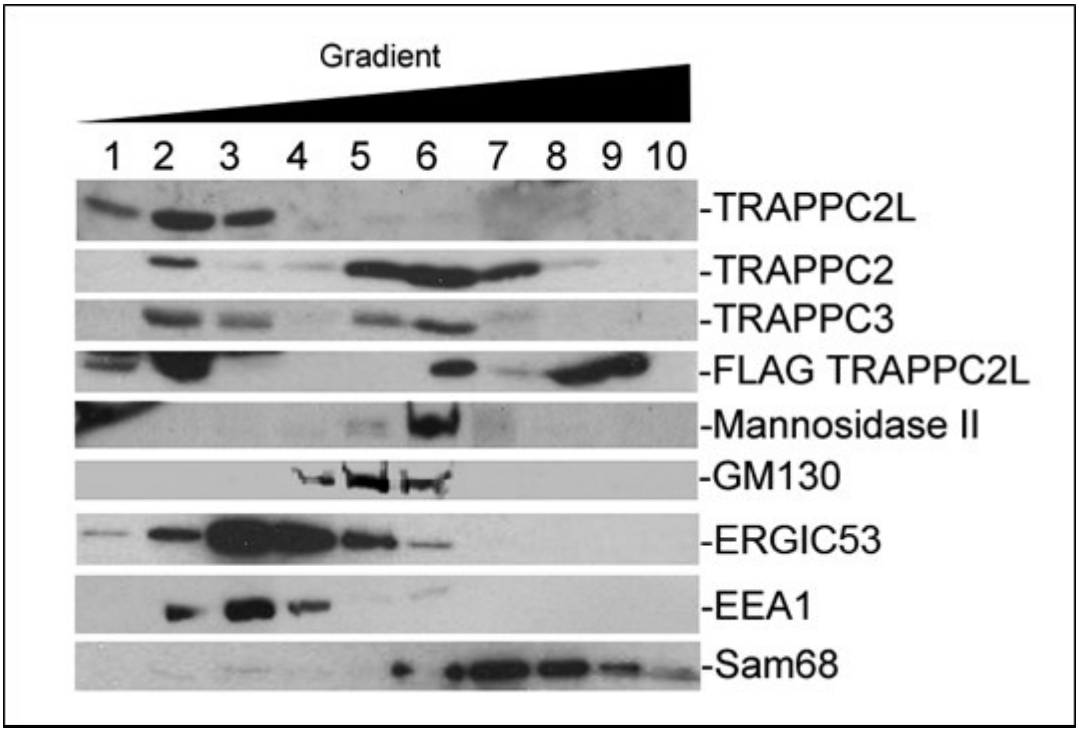

Figure 2.14 C2L resides on very low density membranes. C2L and C2 were fractionated by equilibrium gradient centrifugation. Membranes from HEK293 cells either transfected with FLAG-C2L or untransfected were subjected to equilibrium gradient centrifugation using OptiPrep for 16 h. Fractions of 1 mL were collected from the top of the gradient and analyzed by western blotting. Shown are the results for C2L, overexpressed C2L (FLAG-C2L), C2, C3 and the organelle markers GM130 and Mannosidase II for the Golgi, ERGIC53 for the ERGIC, EEA1 for endosomes and Sam68 for the nucleus.

2.3.6 C2L and C2 are required for Golgi dynamics

To begin to address the function of C2L we examined the effects of knocking down its expression using small interfering RNA (siRNA) and compared it to a C2 knockdown. We first examined the effect of knockdowns on the localization of the Golgi enzyme Mannosidase II and the Golgi matrix protein GM130 since C2L and C2 fractionate with Golgi markers (Figure 2.16) and since yeast TRAPP is implicated in Golgi dynamics (Sacher et al., 1998 and

2001;Barrowman et al., 2000). Small interfering RNA directed against C2 and C2.19 efficiently reduced the levels of the protein by 75-90% while siRNA directed against C2L drastically reduced its levels as well (Figure 2.15).

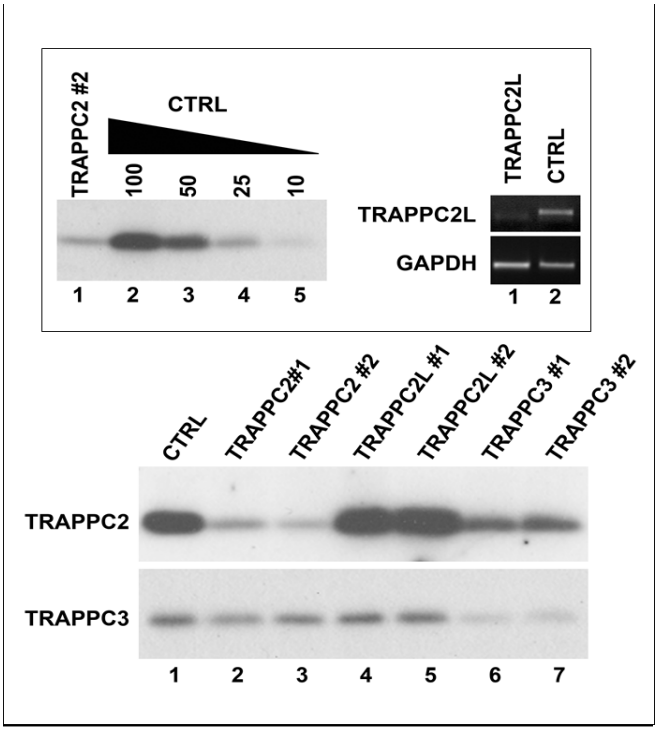

Figure 2.15 Demonstration of C2 and C2L knockdowns. HeLa cells were treated with siRNA directed against either C2 (top panel, left , lane 1) or non-specific siRNA (top panel, left, lanes 2-5) and the protein levels were analyzed by western blotting. A loading control for the non-specific knockdown was performed (indicated above lanes 2-5) to estimate the degree of C2 knockdown which was estimated to be between 75% and 90%. Cells treated with siRNA against C2L (top panel, right, lane 1) or non-specific siRNA (top panel, right, lane 2) were analyzed for C2L transcript levels by RT-PCR and normalized to GAPDH. Extracts from cells treated with non-specific siRNA (bottom panel, lane 1), or two different siRNAs directed against either C2 (bottom panel, lanes 2 and 3), C2L (bottom panel, lanes 4 and 5) or C3 (bottom panel, lanes 6 and 7) were probed for C2 and C3 levels. Note that C2 levels are reduced ~50% in the C3 knockdown but C3 levels remain unchanged in the C2 knockdown.

In cells transfected with a non-specific siRNA, Mannosidase II localizes in the Golgi and demonstrates a compact or slightly extended tubular morphology in the perinuclear region (Figures 2.16 and 2.17). Knockdown of both C2L and C2 leads to a marked increase in fragmentation of the Mannosidase II signal (Figures 2.16 and 2.17). Interestingly, these punctae co-localize well with the Golgi matrix marker GM130 (Figure 2.16).

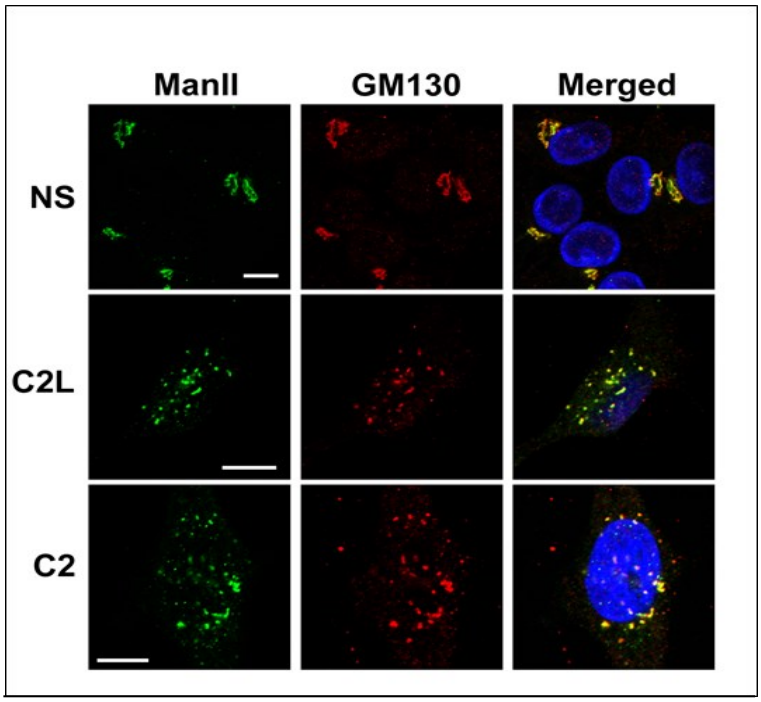

Figure 2.16 C2L and C2 knockdowns lead to Golgi fragmentation. Immunofluorescence was performed on HeLa cells following treatment with either non-specific siRNA (NS), C2L-directed siRNA (C2L) or C2-directed siRNA (C2). Localization was performed for Mannosidase II and GM130. Merged images include DAPI staining (blue) to reveal the nucleus. The increased punctate elements observed upon depletion of C2L and C2 represents the Golgi as punctate structures persist in co-localization with the Golgi markers.
The bars represent 10 μm.

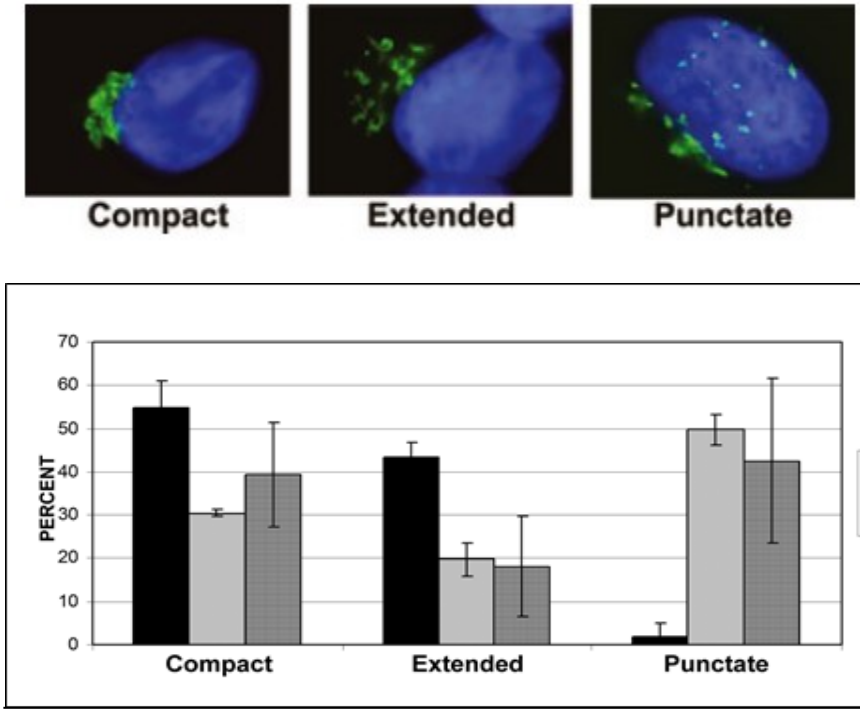

Figure 2.17 Punctate phenotype of the Golgi increases following C2L and C2 knockdowns. The fragmentation phenotype following the indicated knockdowns was quantitated for 128 (C2L knockdown), 312 (C2 knockdown) and 227 (non-specific) cells. Representative images used for scoring are shown. Note that punctate was defined as covering an area beyond the perinuclear region, while extended was largely confined to the perinuclear region but covering an area slightly larger than that in comparison to compact.

To gain better insight into the nature of these punctae, we examined the effect of the knockdowns on the localization of the ERGIC marker ERGIC53. This protein shows both perinuclear and peripheral fluorescence in cells treated with a non-specific siRNA (Figures 2.16 and 2.18). In both the C2L and C2 knockdowns there is a loss in the perinuclear ERGIC53 signal with a concomitant increase in a punctate fluorescence that continues to co-localize with the two other Golgi markers (Figures 2.16 and 2.18). However, there remains ERGIC53 staining elsewhere in the cell periphery that does not co-localize with either of the Golgi markers

suggesting that Mannosidase II and GM130 are not accumulating in the ERGIC. Importantly, there is no accumulation of any of these markers in an ER-like compartment as would be expected for proteins that recycle to the ER but encounter a block in ERGIC formation. These results implicate C2 and C2L in the same or related trafficking pathways, and demonstrate that the integrity of the Golgi is severely compromised upon ablation of either protein.

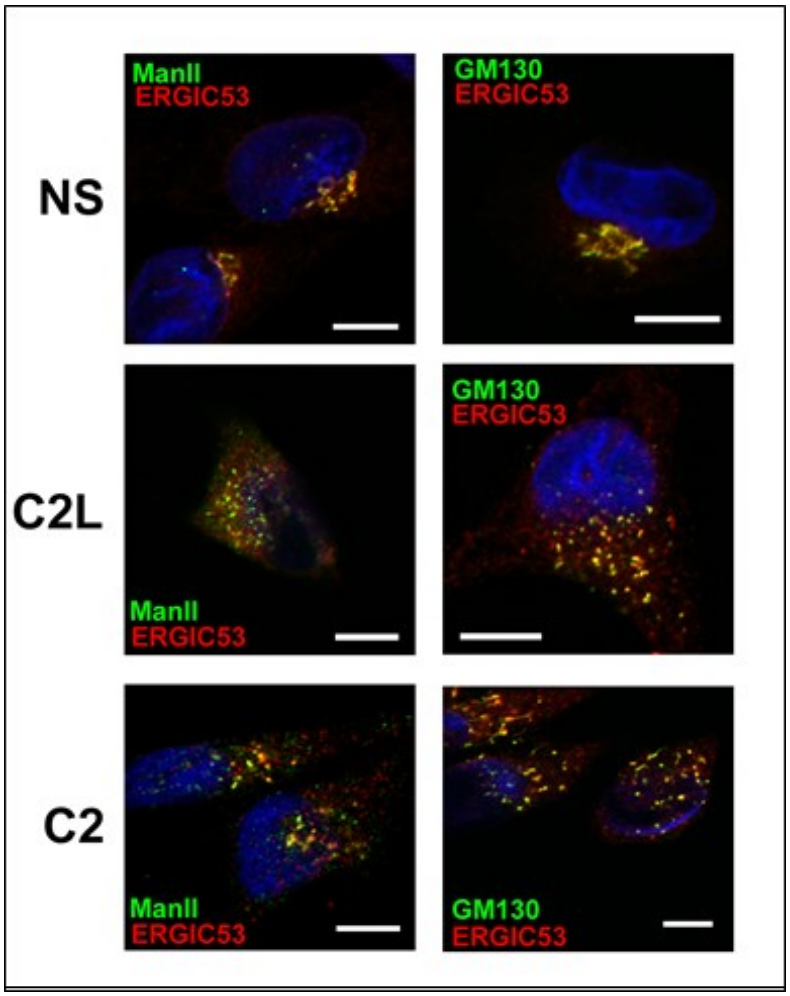

Figure 2.18 Elevated punctate phenotypes upon C2L and C2 knock down do not accumulate at ER-Golgi interface (ERGIC compartments). Immunofluorescence was performed whereby either C2L or C2 were knocked down via siRNA against the respective genes of interest. The ERCIG and Golgi localization pattern were detected by ERGIC53 and either Mannosidase II or GM130.

2.3.7 C2L cannot compensate for the loss of *trs20*

Although the results above suggest that both C2L and C2 are required for Golgi dynamics, the pairwise presence of both genes across species (Figures 2.1 and 2.2) and their overlapping expression patterns (Figure 2.4) suggest they may have distinct functions. To test this we asked whether C2 and C2L could compensate for the loss of the gene encoding the essential yeast C2 ortholog *TRS20*. We constructed a haploid yeast strain in which the genomic copy of *TRS20* is disrupted (*trs20Δ*) but the cells are kept alive with a *URA3*-based plasmid containing *TRS20*. This plasmid can be counter-selected on plates containing the compound 5-fluoroorotic acid (5-FOA). The *trs20Δ* strain was transformed with an empty vector, or a vector containing *TRS20*, *YEL048c*, C2 or C2L. As shown in Figure 2.19 only C2 and *TRS20*, but not C2L and *YEL048c*, could compensate for the loss of *trs20* as evidenced by growth on plates containing 5-FOA. This is presumably not due to an inability of C2L to interact with the yeast TRAPP complex as we previously showed this interaction takes place (see Figure 2.9 and data not shown). This result confirms that C2 is the functional ortholog of Trs20p, consistent with an earlier study that used a stronger *GAL1* promoter (Gecz et al., 2003). This result also further indicates that C2L cannot replace the function that C2 performs in the *trs20Δ* strain. Although *yel048cΔ* does not display any detectable growth phenotype (unpublished observation), the double mutant *yel048cΔ* /*trs65Δ* is lethal (see Table 2.2). However, we found that neither C2 nor C2L could complement this lethality (not shown). The inability of C2L to complement *yel048cΔ* is not entirely unexpected as the two proteins are more divergent than are C2 and *TRS20* (see Figures 2.1 and 2.2). This result indicates that the ability of C2 to compensate for a *trs20* disruption is specific to C2 and is consistent with the notion that C2L and C2 are functionally distinct.

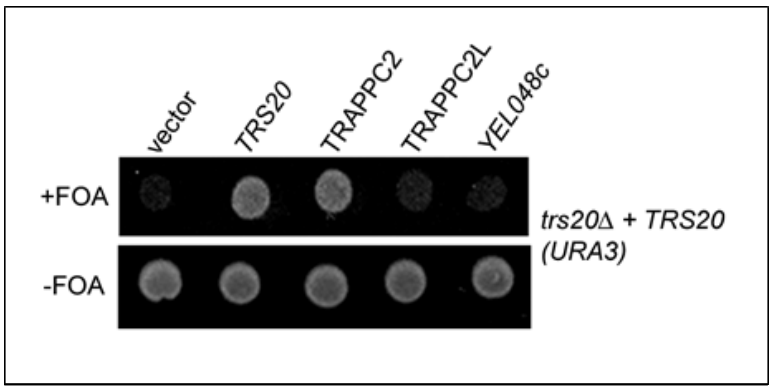

Figure 2.19 C2 and C2L are functionally distinct. A *trs20*Δ haploid strain kept alive with a *URA3*-based-*TRS20* plasmid was transformed with either an empty vector, or a vector containing either *TRS20* under its endogenous promoter, a high-copy vector containing *YEL048c* under its endogenous promoter, or either C2 or C2L under control of the *ADH1* promoter. Transformants were plated on 5-FOA to counter-select for the *URA3*-based-*TRS20* plasmid.

2.4 Discussion

We describe a novel mammalian protein, C2L that interacts with the TRAPP complex *in vitro* and *in vivo*. We show that its yeast counterpart, *YEL048c*, encodes a protein that has strong genetic interactions with genes encoding TRAPP II subunits suggesting this protein may physically interact with yeast TRAPP II. Indeed, we report a co-fractionation of YEL048cp with TRAPP II by size exclusion chromatography and an interaction between this protein and TRAPP both *in vivo* and *in vitro*. Recombinant protein expression and purification suggest that C2L binds to the TRAPP complex on a side opposite to that of C2 and adds another level of complexity to the architecture of TRAPP. Should this model be validated, the inclusion of C2L imparts a remarkable symmetry along the C1-C4 axis.

2.4.1 C2L as a marker for mammalian TRAPP II

In mammalian cells C2L is found in the VLDM fraction but overexpression leads to its appearance additionally in the IDM fraction, membranes where C2L is not normally found but which do contain other TRAPP subunits. This suggests that C2L has the ability to interact with the TRAPP complex found in the IDM fraction. The identity of the VLDM fraction is presently unknown. Given the partial overlap of this fraction with EEA1, it is tempting to speculate that the VLDM membranes are similar to the endosome-like structures with which a portion of C3 was found to associate at the ultrastructural level (Yu et al., 2006).

The two yeast TRAPP complexes are readily separated by size exclusion chromatography (Sacher et al., 2001). This is not the case in mammalian cells, suggesting that one of the complexes may be more labile or, alternatively, smaller subunits or interacting proteins dictate the distinction between the two complexes. The latter notion is supported by a recent report demonstrating the existence of multiple mammalian TRAPP complexes that can be distinguished by the subunit isoforms they contain (Kummel et al., 2008). Based on its

fractionation, interactions and effect on Golgi integrity, as well as the genetic and physical interactions between its yeast ortholog *YEL048c* and TRAPP II, we propose that C2L interacts with or is a component of a mammalian TRAPP II complex. Such a proposal implies distinct functions for C2 and C2L which is supported by their pairwise expression over multiple species and the ability of C2, but not C2L, to compensate for the loss of *TRS20*. An alternative interpretation of this latter result is the fact that C2 and C2L may be functionally redundant in mammals but divergent enough such that only C2 can compensate for the yeast *TRS20* gene. While we cannot exclude such an explanation, we note that we have identified a C2-specific interactor, using a yeast two hybrid screen, that fails to interact with C2L (S. Hul and M.S., unpublished observation), further suggesting a functional distinction between these proteins.

2.4.2 Possible function in membrane traffic

The co-localization of Mannosidase II and GM130 with a portion of ERGIC53 in both C2L and C2 knockdown cells suggests that the Golgi is disintegrating. How, precisely, do C2L and C2 regulate Golgi integrity? It is not unreasonable to speculate that, like the yeast system, C2L in the context of mammalian TRAPP II regulates traffic to or through a late Golgi compartment. Likewise, the mammalian equivalent of TRAPP I may regulate traffic between the ERGIC and Golgi. The earliest stage after ERGIC biogenesis that we envision TRAPP I involved in is the transition between what has been referred to as the late intermediate compartment and the *cis*-Golgi (Marra et al., 2001). This would again parallel the function of the highly conserved yeast TRAPP I complex that also accepts membranes (vesicles) at the *cis*-Golgi.

C3 was suggested to be involved in ERGIC biogenesis and proposed to be localized to transitional ER by immunofluorescence microscopy (Yu et al., 2006). Our studies suggest that C3 and other TRAPP subunits co-fractionate with markers for the Golgi and fractionate away

from the ERGIC marker protein ERGIC53. One explanation for this apparent discrepancy is the methodology used. Localization of TRAPP subunits to specific membranes by immunofluorescence microscopy is challenging, due to their large soluble pools. Removal of this pool by collection of membranes allowed us to visualize their co-fractionation on gradients with Golgi markers. Our fractionation results parallel those of the yeast system where TRAPP localizes to Golgi membranes (Sacher et al., 1998;Barrowman et al., 2000).

The Golgi fragmentation phenotype that we observed in the C2L and C2 knockdown is very similar to that seen for the knockdown of a subunit of the COG vesicle-tethering complex that has also been shown to function in Golgi dynamics (Zolov and Lupashin, 2005 ;Shestakova et al., 2006). Although a C3 knockdown showed GM130 fragmentation (Yu et al., 2006), we have noted that this knockdown reduces the levels of C2 (Figure 2.15), indicating this may be an indirect effect of the C3 knockdown. In addition the Golgi enzyme galactosyltransferase redistributes to the ER upon C3 inactivation (Yu et al., 2006) in contrast to the punctate, GM130-associated localization we observed for Mannosidase II. This could reflect a role of C3 in ERGIC biogenesis which may be specific to this subunit as recently suggested (Sacher et al., 2008).

Our studies suggest a site of interaction between C2L and the TRAPP complex. The simplest model (Figure 2.13) places C2L on the side of the complex opposite that of C2. Consistent with this notion are the findings that residues important for C2 binding to the complex are conserved in C2L (Figure 2.3) and *yel048cΔ* displays a synthetic genetic interaction with *trs33Δ*. We cannot yet exclude the possibility that isoforms of TRAPP containing either C2 or C2L bound to the C3-C5 interface form independently and associate during membrane transport events through the Golgi. Alternatively, sub-complexes of TRAPP, containing either C2L or C2, may associate to mediate distinct trafficking events.

2.4.3 Implications for SEDT

The skeletal disorder SEDT has been shown to be caused by mutations in C2. Our expression analysis raises the question: how do C2.19 and C2L affect the molecular basis of SEDT? We provide evidence that C2.19 is expressed and translated. We also show that it is expressed in primary chondrocytes from femoral condyles derived from female patients. Since factors such as weight-bearing load and neighboring tissue are known to influence gene expression (Ben-Ze'ev et al., 1988;Raab-Cullen et al., 1994;Little et al., 1996) and since SEDT is a sex-linked disorder, a more detailed expression analysis of C2 compared to C2.19 in affected males is needed.

We have shown that C2L is expressed in multiple mouse tissues and in human chondrocytes (Figure 2.4). Bioinformatic resources (e.g. http://www.genecards.org) similarly indicate broad expression of C2L in humans. With the same cautions mentioned above this may also point to a functional distinction between C2 and C2L. Like C2.19, this speculation also awaits analysis of SEDT patient chondrocytes. Sequence conservation of Asp47 between C2L and C2 implies that this residue, shown to be pathogenic in an SEDT patient, is important for the function of both proteins. Curiously, we have found that mutation of the Asp47 yeast equivalent in *TRS20* does not lead to a recognizable phenotype under standard laboratory conditions (unpublished observation) and the function of this residue remains unclear.

CHAPTER 3

A *trs20* mutation that mimics an SEDT-causing mutation blocks selective and non-selective autophagy: A model for TRAPP III organization

All of the work in this Chapter was recently published in the journal *Traffic* in July 2013. I am co-first author of this manuscript and my contribution is as follows: Figures 3.1-3.8, 3.11, 3.13, 3.16, and 3.20.

3.1 Introduction

The ability of a cell to properly localize its protein complement is critical for the cell to function correctly. Referred to as membrane transport, the process is mediated by vesicle carriers that move between various compartments. There are many factors involved in ensuring the fidelity of this process and defects in this trafficking process lead to numerous disorders (Aridor and Hannan, 2000 and 2002). Although strong defects in membrane traffic would be expected to result in embryonic lethality, more subtle mutations may lead to tissue-specific disorders.

The overall process involves tethering factors, small GTP-binding proteins of the Rab family, coat proteins that encompass the transport vesicles and SNARE proteins that are involved in vesicle fusion with the target membrane (Cai et al., 2007a) . Intimate connections between each of these factors have been identified in various transport steps. In transport between the endoplasmic reticulum (ER) and Golgi in yeast, the tethering factor TRAPP I binds to the coat protein Sec23p, thus acting to bridge the vesicle and the target membrane (Cai et al., 2007b;Lord et al., 2011). In addition, as a guanine nucleotide exchange factor (GEF), TRAPP I activates the GTPase Ypt1p (Jones et al., 2000;Wang et al., 2000). Although a direct

link between TRAPP I and SNAREs has yet to be demonstrated, SNARE complex assembly is impaired in a *bet3* mutant, a gene that encodes an essential TRAPP I subunit (Rossi et al., 1995). Thus, as a tethering factor, TRAPP I serves to link all of these processes to ensure proper targeting of ER-derived transport vesicles.

TRAPP I is composed of six distinct polypeptides (Bet5p, Bet3p, Trs20p, Trs23p, Trs31p, Trs33p) although the levels of Trs20p appear to be sub-stoichiometric in this complex (Sacher et al., 2001). Two related complexes called TRAPP II and III have also been described (Sacher et al., 2001;Lynch-Day et al., 2010). Each complex contains the TRAPP I core along with unique polypeptides: Trs65p, Tca17p, Trs120p and Trs130p for TRAPP II, and Trs85p for TRAPP III (Montpetit and Conibear 2009;Choi et al., 2011 ;Sacher et al., 2001;Lynch-Day et al., 2010). TRAPP II has been implicated in traffic at the late Golgi, endocytosis and macroautophagy (Cai et al., 2005;Zou et al., 2013; Sacher et al., 2001) and TRAPP III has been shown to function in selective autophagy (Meiling-Wesse et al., 2005;Lipatova et al., 2012a;Lynch-Day et al., 2010). Interestingly, Trs85p, the TRAPP III-specific subunit, has been implicated in ER-to-Golgi transport as well (Zou et al., 2012; Sacher et al., 2001). Since the TRAPP I core possesses Ypt1p GEF activity, both TRAPP II and III have also been shown to be capable of activating Ypt1p (Sacher et al., 2001;Lynch-Day et al., 2010). Indeed, Ypt1p has been implicated in the same membrane trafficking processes as TRAPP I, II and III (Jedd et al., 1995;Bacon et al., 1989;Sclafani et al., 2010;Segev et al., 1988;Lipatova et al., 2012a;Lynch-Day et al., 2010).

In humans, mutations in TRAPPC2 (C2), the homolog of the yeast TRAPP I core protein Trs20p, have been linked to the skeletal disorder spondyloepiphyseal dysplasia tarda (SEDT) (Shaw et al., 2003). This X-linked disorder affects bone growth in the spine and the ends of long bones in the arms and legs. Patients are of short stature and develop dysplasia of joints in the

shoulders, hips and knees. The disorder appears to result from an inability of chondrocytes to secrete collagen (Tiller et al., 2001). Indeed, given the size of pro-collagen (~300nm) and the diameter of an ER-derived carrier (~60nm) it has been an unanswered question as to how pro-collagen is transported between the ER and Golgi. Furthermore, understanding how a ubiquitously expressed protein such as C2 could lead to the phenotype seen in SEDT patients has been a major focus of researchers studying TRAPP. A recent report suggested that recruitment of C2 to ER exit sites by the pro-collagen receptor TANGO1 regulates the cycle of the GTPase Sar1, thus allowing carriers to achieve a size sufficient to accommodate the large pro-collagen molecule (Venditti et al., 2012).

While elegant, we speculated that the model put forth regarding the role of C2 in pro-collagen secretion may not explain the etiology of all SEDT mutations since yeast do not secrete collagen nor do they possess a readily identifiable homolog of the collagen receptor. Furthermore, C2-dependent Golgi fragmentation and collagen secretion are separable functions (Venditti et al., 2012;Scrivens et al., 2009), suggesting C2 may have several roles in the cell. Interestingly, an SEDT-causing missense mutation at D47 in C2 (C2D47Y) cannot suppress the lethality of a yeast *trs20Δ* mutation although wild type C2 can (Gecz et al., 2003). Since yeast do not produce collagen, this is an unexpected result if the sole function of C2 was in collagen transport. We therefore set out to characterize the interactions and function of the C2D47Y protein and its yeast homolog Trs20D46Y. Here we demonstrate an interaction between C2 and the SNARE protein Syntaxin 5 and show that this interaction is sensitive to the D47Y mutation. In yeast, Trs20D46Y is not involved in anterograde transport but is defective in endocytosis and both selective and non-selective autophagy, correlating with a destabilization of TRAPP III. We also show that the appearance of TRAPP III is dependent upon Atg9p and that the function of TRAPP III is influenced by palmitoylation of Bet3p, suggesting unexpected complexities in TRAPP III assembly and localization.

3.2 Materials and methods

3.2.1 Yeast strains and molecular biological techniques

All yeast strains were constructed using standard genetic techniques. *TRS20* mutations were introduced by site-directed mutagenesis using High-Fidelity Polymerase (Roche) and expressed in yeast under the endogenous *TRS20* promoter from a single-copy plasmid (pRS315 or pRS316). The C2D47Y mutation was constructed as above and cloned into the pRK5-myc plasmid facilitating detection of the mutant protein with anti-myc antibody. For yeast two-hybrid analysis, open reading frames were inserted into pGBKT7 or pGADT7 using either restriction enzyme cloning or Gateway cloning into modified, Gateway-compatible vectors (Scrivens et al., 2011).

3.2.2 Yeast two-hybrid analysis

Yeast cells (AH109 and Y187) were transformed with either pGBKT7 or pGADT7 constructs. The cells were mated overnight on YPD plates and then replicated to selective medium (-Leucine/-Tryptophan, -Leucine/-Tryptophan/-Histidine ± 2 mM 3-aminotriazole, -Leucine/-Tryptophan/-Histidine/-Adenine) to ensure that both plasmids were present and to test for an interaction. Growth was monitored daily for up to 8 days.

3.2.3 Cell culture and immunoprecipitation

HeLa and 293T cells were maintained in a humidified environment with 5% CO_2 at 37°C. Transfections were performed using the Ca_2PO_4 method and 10 µg of plasmid DNA per 10 cm dish. In certain cases cells were treated with 10 µM *N*-ethylmaleimide (NEM) during the time course indicated in Figures 3.7 and 3.8.

For immunoprecipitations, 500 mg of lysate prepared in lysis buffer (150 mM NaCl, 50 mM Tris pH 7.2, 1 mM DTT, 1% Triton X-100, 0.5 mM EDTA, 1 mini-tablet of protease inhibitor

cocktail (Roche) per 10 mL) was incubated with 0.4 µg of anti-Syntaxin 5 antibody (Santa Cruz) overnight on ice. The sample was then incubated with a 10 µL bed volume of protein A-agarose beads for 60 min in the cold. The beads were washed 3 times with lysis buffer and eluted by boiling with 25 µL SDS-PAGE sample buffer.

3.2.4 Yeast trafficking assays

The assay for carboxypeptidase Y (CPY) transport and GFP-Snc1p localization were performed as previously described (Brunet et al., 2012). For the CPY assay the cells were shifted to 37°C for 60 min.

For the general secretion assay, 2 OD_{600} units of cells were pre-shifted to 37°C for 30 min. The cells were then pulse-labeled with 100 µCi ^{35}S-methionine/cysteine for 15 min and chased with 10 mM unlabeled methionine and cysteine for 15 min. Before pelleting the cells NaN_3/NaF was added to the culture to a final concentration of 0.5 mM. The cells were pelleted and the growth medium was precipitated with 10% trichloroacetic acid on ice. The pellet was dissolved in SDS-PAGE sample buffer and fractionated by SDS-PAGE.

Calcofluor white (CFW) growth was monitored by spotting serial dilutions of cells on YPD ± 10 µg/mL CFW and incubating the plates at 30°C. Growth was monitored daily for up to 5 days.

Processing of pre-Ape1p was performed by monitoring the forms of the protein using western analysis (Klionsky et al., 1992). Cells were grown overnight to an $OD_{600} \leq 1$ in YPD and resuspended in prewarmed YPD medium at 37.5°C (for heat sensitive mutants) or 30°C for 1 h. For selective autophagy cells were immediately processed for lysis (see below). For macroautophagy cells were pelleted, washed in water and re-suspended in pre-warmed synthetic medium lacking nitrogen, incubated for 2-4 h at 37.5°C (for heat sensitive mutants) or 30°C, and then processed for lysis. Localization of GFP-Ape1p was performed on fixed cells according to the GFP-Snc1p protocol above.

3.2.5 Preparation of yeast cell lysates

Lysates for size exclusion chromatography were prepared as previously described (Brunet et al., 2012) and 2-5 mg of total protein was fractionated on a Superose 6 column. In some cases, 1% Triton X-100 was added to the lysis buffer and was included in the size exclusion column buffer. For pre-Ape1p processing, lysates were prepared by converting the cells to spheroplasts in medium containing 1.4 M sorbitol, 50 mM KP_i pH 7.5, 36 mM β-mercaptoethanol, 33 µg/mL zymolyase 100T for 30 min at 37.5°C. Spheroplasts were lysed in 1% SDS, boiled and cleared by centrifugation.

3.2.6 Optiprep gradient assay

A yeast lysate from *TRS85*-HA cells was prepared in the absence of detergent and fractionated on a Superose 6 column as described (Brunet et al., 2012). Fractions containing TRAPP III were pooled and a portion was supplemented with 1% Triton X-100 before incubating on ice for 30 min. A sample (100 µL) was combined with size exclusion column buffer to a final volume of 300 µL and then loaded on top of a step Optiprep gradient composed of 1 mL 15%, 1 mL 30%, 1 mL 40% 0.8 mL of 45% and 1.2 mL 54% Optiprep. The sample was centrifuged in an SW55 rotor at 36000 rpm for 16 h. Fractions were collected from the top of the tube and probed for Trs85p-HA with anti-HA antibody.

3.2.7 Recombinant protein expression and *in vitro* binding

Syntaxin 5 (amino acids 1-333) was recombined into pDEST15 (GST fusion vector) from a Gateway entry clone. C2 and C2D47Y were recombined into pDEST17 (His fusion vector) from Gateway entry clones. Protein was expressed by inducing with 1 mM IPTG in BL21 (DE3) cells overnight at 25°C. The protein was purified on glutathione-agarose resin or Ni^{2+}-NTA resin as per manufacturer's instructions.

In vitro binding assays contained 0.5 µM of GST-Syntaxin 5 with increasing amounts (0, 0.1, 0.2, 0.5 µM) of His-tagged C2 wild type or D47Y. Samples were made up to a total volume of 250 µL with 1x binding buffer (10 mM HEPES pH 7.4, 25 mM NaCl, 115 mM KCl, 2 mM $MgCl_2$, 0.1% Triton X-100) and left on ice at 4ºC for 1 h to allow binding. Pulldown employed 10 µL glutathione agarose resin (GE Healthcare) in the cold for 1 h. Samples were washed 3x with binding buffer and eluted by boiling with SDS-PAGE sample buffer. Western blotting was performed using horseradish peroxide-conjugated anti-His antibody (Qiagen).

3.2.8 Acyl-biotin exchange

Biotinylation of acylated proteins was performed essentially as described (Hou et al., 2005;Wan et al., 2007) with minor modifications. A wild type yeast lysate was prepared in the absence of detergent and fractionated on a Superose 6 column as described (Brunet et al., 2012). Fractions containing TRAPP I, II and III were separately pooled and incubated at 4°C for 30 min in 1% Triton X-100 with 25 mM *N*-ethylmaleimide. The proteins were precipitated two times using methanol/chloroform and resuspended in buffer A (2% SDS, 8 M urea, 100 mM NaCl, 50 mM Tris HCl, pH 7.4). Six volumes of a solution containing 1 M hydroxylamine and 300 µM biotin-BMCC (Pierce) was added and incubated for 2 h at 4°C. The proteins were precipitated one time using methanol/chloroform, resuspended in PBS containing 0.1% Triton X-100 and incubated with 15 µL of streptavidin-agarose beads (Sigma) for 1 h at room temperature. The beads were washed in PBS containing 0.5 M NaCl and 0.1% Triton X-100 after which the proteins were eluted by boiling in a 3:1 mix of buffer A: 4x SDS-PAGE sample buffer. Bet3p was detected by western analysis using anti-Bet3p IgG.

3.3 Results

3.3.1 Binding of C2 to Syntaxin 5 is dependent upon the D47 residue in C2

A recent study suggested that C2 participates in the export of pro-collagen by regulating the Sar1p GTPase cycle (Venditti et al., 2012). C2 is recruited to ER exit sites through an interaction with the collagen receptor Tango1. We reasoned that C2 has additional functions for the following reasons: (i) the yeast *Saccharomyces cerevisiae* does not have a recognizable Tango1 homolog nor a collagen-like molecule yet the yeast homolog of C2 (Trs20p) is encoded by an essential gene, and (ii) the role of C2 in collagen export and Golgi morphology can be separated based on the extent of C2 knockdown (Venditti et al., 2012;Scrivens et al., 2009). Since C2 is structurally related to longin-domain-containing SNARE proteins (Jang et al., 2002;Tochio et al., 2001;Gonzalez et al., 2001) we speculated that it may interact with SNAREs involved in the early secretory pathway of mammalian cells. Using a yeast two-hybrid assay, we screened for interactions between C2 and the early secretory pathway SNAREs Syntaxin 5, membrin, Sec22b, Ykt6, Bet1 and GS28. As shown in Figure 3.1, we detected an interaction between C2 and Syntaxin 5. The interaction was mediated through the SNARE domain of Syntaxin 5 (Figure 3.2).

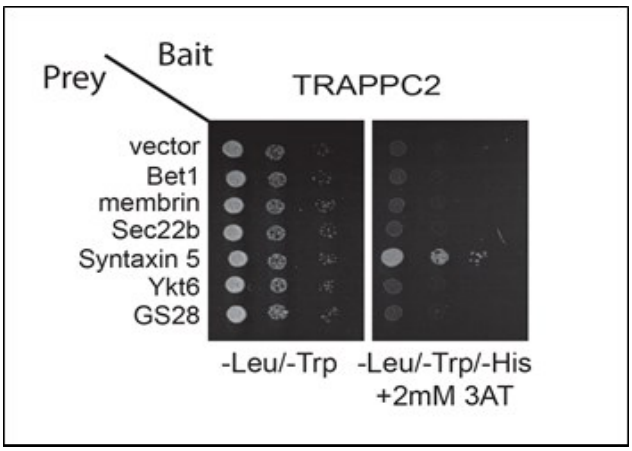

Figure 3.1 C2 binds to Syntaxin 5. C2 was cloned into the yeast two hybrid vector pGBKT7 and the SNAREs indicated were cloned into pGADT7. The plasmids were transformed into AH109

and Y187 cells, mated and spotted as serial dilutions onto SD-Leu/-Trp and SD-Leu/-Trp/-His/-Ade and grown at 30°C for ~3 days.

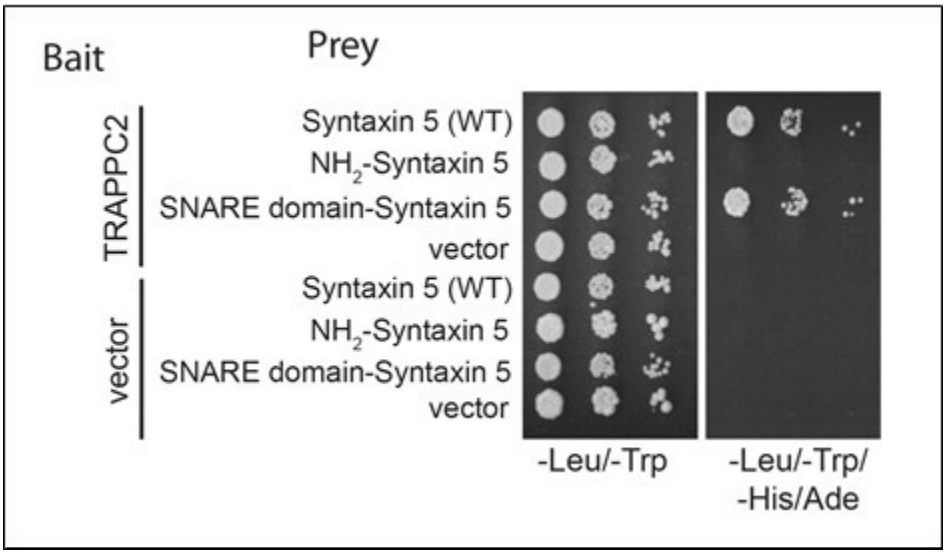

Figure 3.2 C2 binds to the SNARE domain of Syntaxin 5 in addition to the full length protein. Full length Syntaxin 5, the SNARE domain (amino acids 263-333) or the amino-terminal domain (amino acids 1-262) of Syntaxin 5 were cloned into pGADT7 and tested for an interaction by yeast two hybrid with C2 (or an empty pGBKT7 vector control) as described in (Figure 3.1).

This interaction was not simply due to the fact that C2 is a longin-domain-containing protein since C1 and C4, two other TRAPP components with longin domains, did not interact with Syntaxin 5 (Figure 3.3).

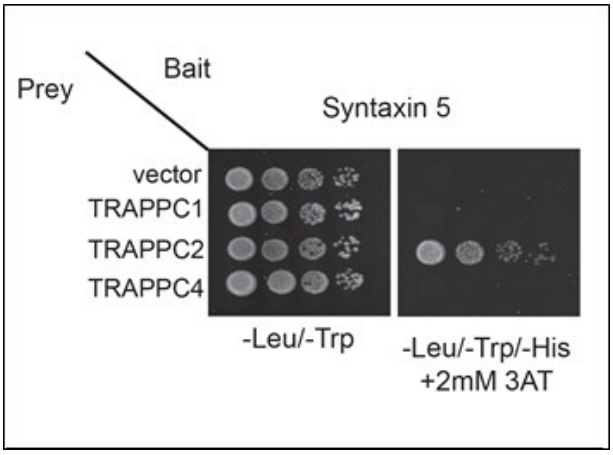

Figure 3.3 C2 interaction to Syntaxin 5 is specific. C2 in pGBKT7 was tested for its ability to interact with the indicated TRAPP proteins expressed in pGADT7 by yeast two hybrid.

In an attempt to define the region of C2 that participates in the interaction with Syntaxin 5 we found that the pathogenic missense mutation D47Y in C2 found in patients with SEDT significantly weakened the interaction (Figure 3.4). Mutations near D47, however, had no effect (Figure 3.4).

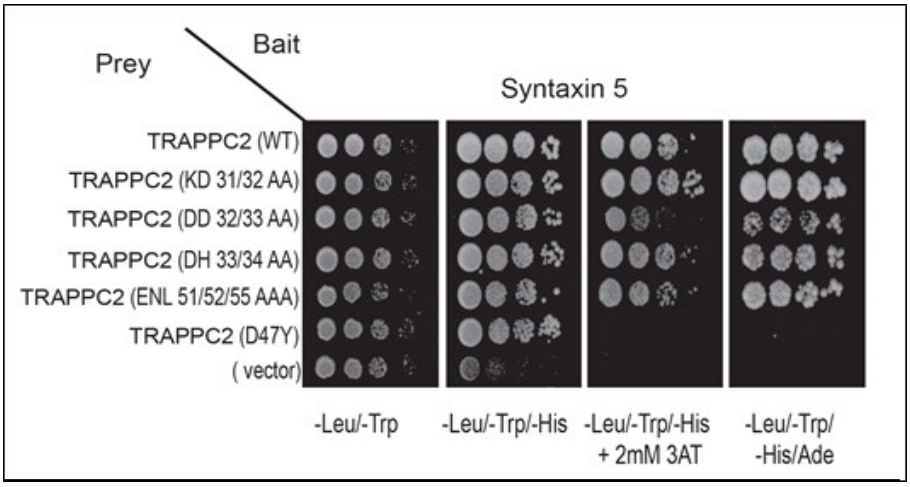

Figure 3.4 SEDT-causing residue in C2 is critical for interaction with Syntaxin 5. C2 or the indicated mutants were inserted into pGBKT7 and tested for their ability to interact with Syntaxin 5 cloned into pGADT7 by yeast two hybrid.

In order to confirm the interaction between C2 and Syntaxin 5, we performed *in vitro* binding studies with GST-tagged Syntaxin 5 and His-tagged C2. As shown in Figure 3.5, an interaction between the two proteins was detected in vitro. Consistent with the yeast two-hybrid assay above (Figure 3.4), the D47Y mutation in C2 weakened this interaction *in vitro* (Figure 3.5).

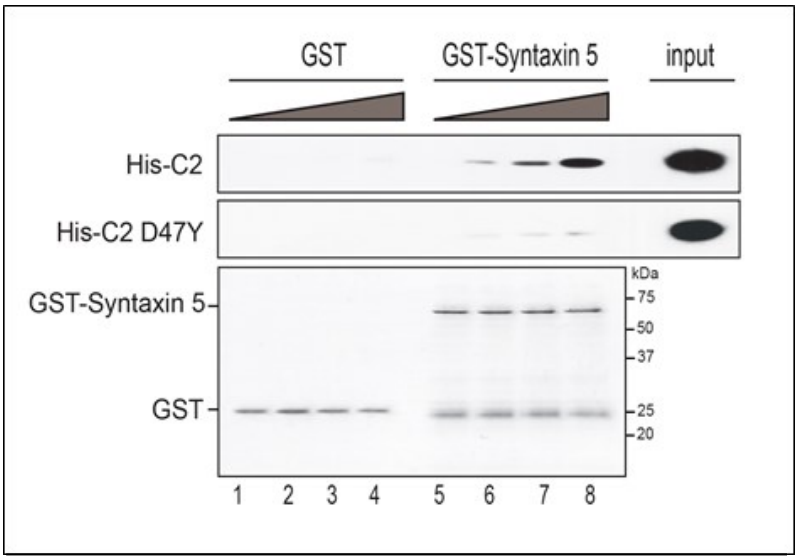

Figure 3.5 C2-Syntaxin 5 interaction and its perturbation with C2-D47Y are also observed *in vitro*. Increasing amounts of His-tagged C2 or C2D47Y (0, 0.1, 0.2, 0.5 μM) were incubated with 0.5 μM GST-tagged Syntaxin 5 as indicated in materials and methods. The bound C2 was detected by western analysis using anti-His IgG. An input representing 10% is shown. The lower panel shows a coomassie-stained gel of the bait proteins GST and GST-Syntaxin 5.

As a third confirmation of this interaction we expressed myc-tagged C2 or C2D47Y in HeLa cells, immunoprecipitated Syntaxin 5 from the lysates prepared from the transfected cells and probed the immunoprecipitates for the presence of myc-C2. Consistent with the first two assays, we noted an interaction between Syntaxin 5 and C2 that was weakened by the D47Y mutation in C2 (Figure 3.6).

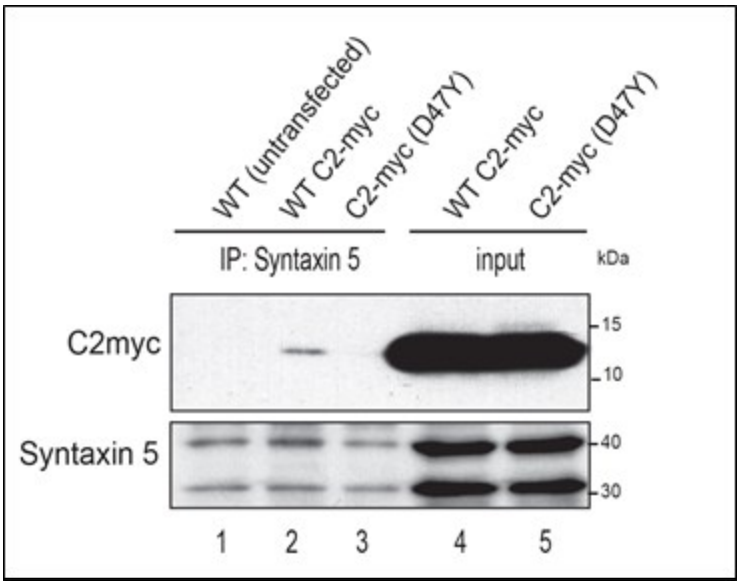

Figure 3.6 C2-Syntaxin 5 interaction and its perturbation with C2-D47Y are demonstrated in cell culture. Lysates from HeLa cells transfected with myc-tagged C2 or C2D47Y were treated with anti-Syntaxin 5 IgG and the immunoprecipitates were probed for the presence of myc-C2 and Syntaxin 5 by western analysis using anti-myc or anti-Syntaxin 5 IgG. A portion (10%) of the input is also shown.

Syntaxin 5 can be found as a component of a larger SNARE complex or free from other SNAREs (Williams et al., 2004). SNARE complex formation is increased by treatment of intact cells with *N*-ethyl maleimide (NEM) (Williams et al., 2004). In order to investigate whether C2 binds to Syntaxin 5 in a SNARE complex, HeLa cells were transfected with C2-myc and cells were either untreated or treated with 10 μM NEM, a concentration sufficient to induce SNARE complex formation (N.S. and M.S., unpublished observation), with increasing times. Lysates prepared from the cells were immunoprecipitated with Syntaxin 5 antibody and probed for C2-myc. Untreated cells showed a small amount of C2 co-precipitating with Syntaxin 5 (Figure 3.7).

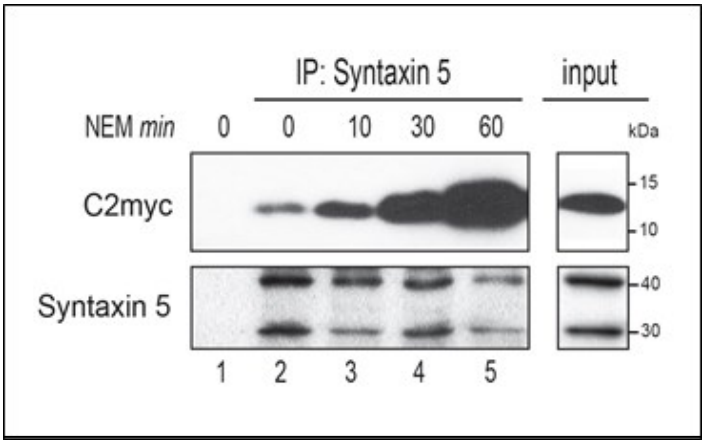

Figure 3.7 C2-Syntaxin 5 interaction increases in NEM-treated cells. HeLa cells were transfected with myc-tagged C2 and then treated for increasing times (indicated) with 10 μM NEM. Lysates were prepared and Syntaxin 5 was immunoprecipitated as in (Figure 3.6) (lanes 2-5). Lysate in lane 1 was from a non-transfected culture and subjected to precipitation with protein A-agarose beads (serves as a negative control). The bound, tagged C2 was detected using anti-myc IgG and Syntaxin 5 was detected using anti-Syntaxin 5 IgG. A portion (10%) of the input is shown.

The amount of co-precipitating C2 increased with increasing times of NEM treatment, suggesting that C2 binds to Syntaxin 5-containing SNARE complexes. Endogenous C2 was also shown to co-precipitate with Syntaxin 5 in HeLa cells in an NEM-dependent manner (Figure 3.8).

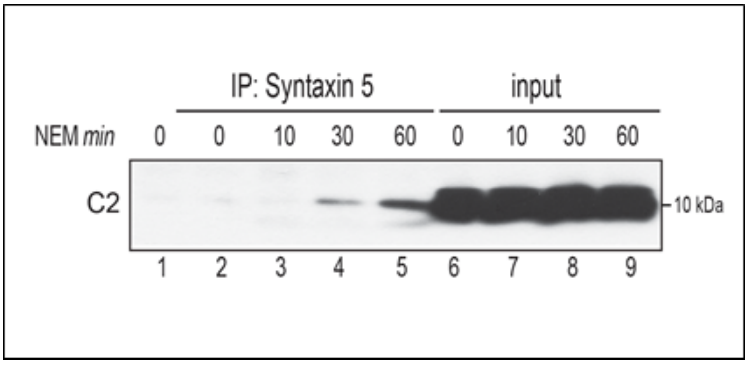

Figure 3.8 Endogenous C2-Syntaxin 5 interaction is elevated in NEM-treated cells. Non-transfected HeLa cells were treated for increasing times (indicated) with 10 μM NEM. Lysates

were prepared and processed as in (Figure 3.7). Lysate in lane 1 was not incubated with IgG during the precipitation and only received protein A-agarose beads. Endogenous C2 was detected using anti-C2 IgG. A portion (10%) of the input is shown.

3.3.2 The yeast mutant *trs20D46Y* does not prevent processing of carboxypeptidase Y

The yeast homologs of C2 and Syntaxin 5 are Trs20p and Sed5p, respectively. The interaction demonstrated above suggested that Trs20p and Sed5p may also interact to mediate transport in the secretory pathway. However, we were unable to detect an interaction between the yeast homologs. The human D47 residue that plays a role in its interaction with Syntaxin 5 is conserved in the yeast Trs20 protein at the D46 residue. In order to study this conserved residue and its role in membrane traffic we focused on the more easily tractable yeast system. We first constructed *trs20D46Y*, a yeast mutant patterned after the pathogenic human C2D47Y mutation. Although this mutant was slightly heat sensitive, it was not as severely-compromised as *trs20ts*, a mutant that was constructed by random mutagenesis (Figure 3.9). In order to investigate whether *trs20D46Y* blocked early secretory protein traffic we performed a pulse-chase experiment using the vacuolar hydrolase carboxypeptidase Y (CPY). This commonly used secretory marker protein is translated and inserted into the ER as a “p1” form. It then traffics to the Golgi where it migrates as a slower “p2” form before it is delivered to the vacuole as a faster-migrating “m” form (Stevens et al., 1982). As shown in Figure 3.10, neither *trs20D46Y* nor *trs20ts* displayed a defect in the processing of CPY. In addition, *trs85Δ*, a gene whose product has been reported to function in ER-to-Golgi transport but has more recently been implicated in selective autophagy, also processed CPY similar to wild type. These results suggest that *TRS20* may not be required for ER-to-Golgi traffic. If this is the case, Trs20p may function either as a component of TRAPP II and/or III, complexes that function at the late Golgi and in autophagy, respectively.

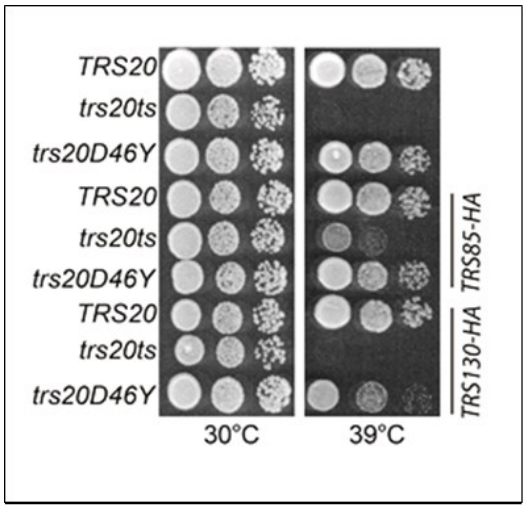

Figure 3.9 Temperature sensitive phenotype observed in *trs20D46Y* is exacerbated in a *TRA130*-HA background. A yeast strain with *trs20D46Y* as the sole copy of *TRS20* was spotted as a serial dilution on YPD plates and grown at either 30°C or 39°C. A *trs20ts* strain (Ben-Aroya et al., 2008) was also included. The same *trs20* mutations were introduced into a yeast strain with the sole copy of *TRS130* tagged with the HA epitope.

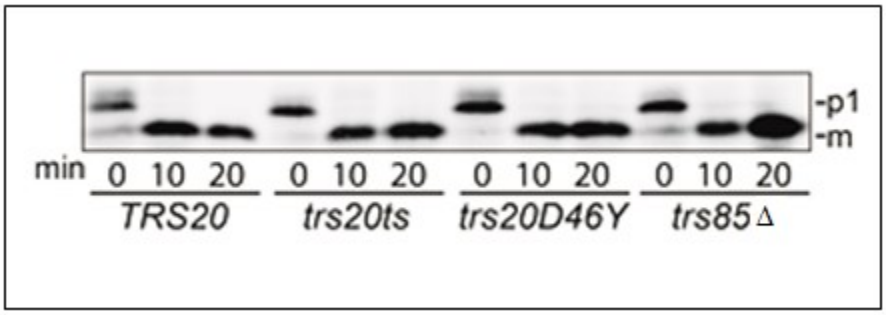

Figure 3.10 Trafficking of carboxypeptidase Y is unaffected in *trs20D46Y. trs20D46Y* does not block trafficking of CPY. Yeast strains indicated were pulsed with ^{35}S-methionine for 4 min and chased with unlabeled methionine for the times indicated as described in materials and methods. CPY was immunoprecipitated using anti-CPY IgG, and the forms of CPY were visualized by radioautography.

3.3.3 The *D46Y* mutation in *trs20* affects its interactions with TRAPP II and III proteins

To begin to understand where Trs20p functions, we compared the interactions of Trs20p and Trs20D46Yp with all known components of the TRAPP complex using the yeast two-hybrid assay. As shown in Figure 3.11, Trs20p interacted with Trs31p, Bet3p, Trs85p, Trs120p and Trs130p (all other interactions were negative). The first two proteins are components of the TRAPP core and these interactions were seen in the crystal structure of both the yeast and mammalian complexes (Cai et al., 2008;Kim et al., 2006). Trs85p is a component of TRAPP III while Trs120p and Trs130p are found in the TRAPP II complex. These results are consistent with a recent report suggesting that the mammalian Trs20p homolog C2 interacts with both the Trs120p and Trs85p homologs C9 and C8, respectively (Zong et al., 2011). Interestingly, while the D46Y mutation in Trs20p did not affect the interaction with neither Bet3p nor Trs31p, it did weaken the interaction between Trs20p and the TRAPP II/III-specific components Trs85p, Trs120p and Trs130p (Figure 3.11).

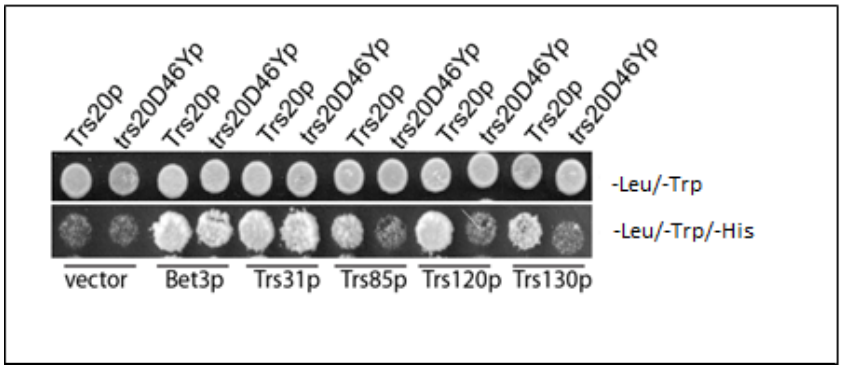

Figure 3.11 Genetic interactions affected by *trs20D46Y*. The open reading frames encoding *TRS20* and *trs20D46Y* were cloned into pGBKT7, transformed into AH109 yeast cells, and mated to Y187 yeast that harbored pGADT7 containing the indicated TRAPP open reading frames. The resulting diploids were spotted onto SD-Leu/-Trp (top panel) or SD-Leu/-Trp/-His.

We also used yeast genetic interactions to investigate the connection between *TRS20* and the TRAPP II and III complexes. Although *trs20D46Y* is mildly heat sensitive, the phenotype was more pronounced in the presence of HA-tagged Trs130p but not with HA-tagged Trs85p (Figure 3.9). Neither *trs20D46Y* nor *trs20ts* displayed genetic interactions with *trs85Δ*, although *trs20ts* was synthetically lethal with *trs65Δ* (a gene encoding a TRAPP II subunit) (Figure 3.12).

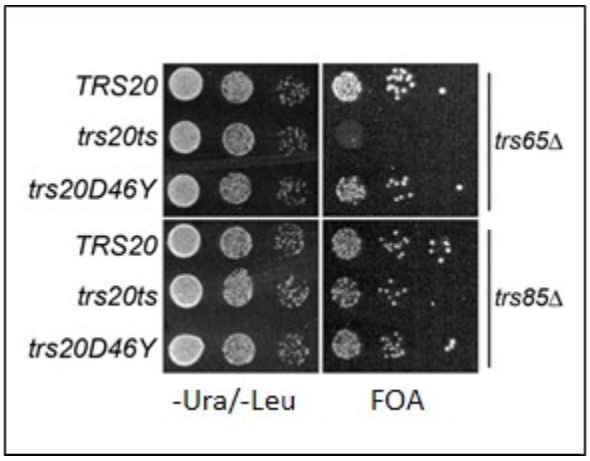

Figure 3.12 *trs20D46Y* does not display synthetic genetic interactions with *trs65Δ* or *trs85Δ*. The *trs20D46Y* mutation was introduced into a yeast strain in which the chromosomal copy of *TRS65* (*trs65*Δ) or *TRS85* (*trs85*Δ) was deleted and a copy of the respective wild type gene was maintained on a *URA3*-based plasmid. The plasmid was counter-selected on 5-fluoroorotic acid-containing plates.

Finally, using the more heat-sensitive *trs20D46Y* mutation in the *TRS130-HA* background, we found that, in addition to the expected suppression conferred by *TRS20* and *TRS130*, *TRS120* was capable of suppressing the temperature-sensitive growth phenotype (Figure 3.13). These results suggest that, although *trs20D46Y* does not have a strong growth phenotype, it does display interactions with genes encoding TRAPP II and III subunits.

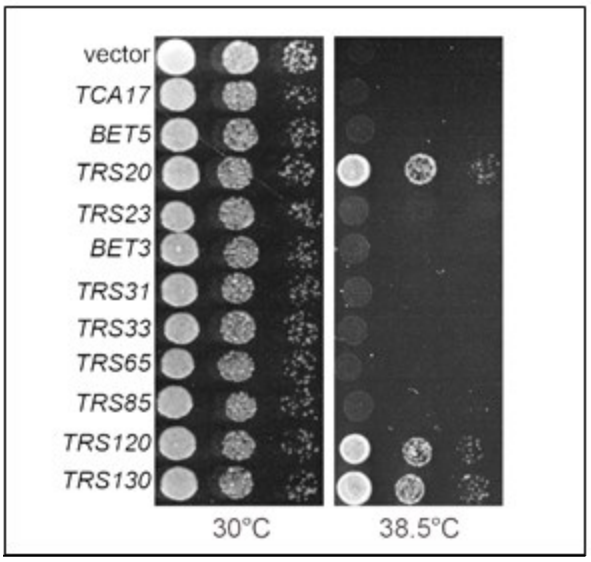

Figure 3.13 The temperature sensitive phenotype of a *trs20D46Y TRS130-HA* yeast strain is bypassed by overexpression of two TRAPP II-specific subunits. A yeast strain (*TRS130*-HA *trs20D46Y*; see Figure 3.9) was transformed with a plasmid containing the indicated TRAPP gene and grown on YPD plates at either 30°C or 38.5°C.

3.3.4 *trs20D46Y* phenocopies *trs85Δ* in both Snc1p-GFP recycling and calcofluor white (CFW) hypersensitivity

Since early secretory protein traffic was unaffected in *trs20D46Y* cells, we examined the cells for a general secretion defect. Included in these studies was the *trs85Δ* mutant since Trs20p showed a D46-dependent interaction with Trs85p (see Figure 3.11). Cells were pulsed with ^{35}S-methionine and then chased with cold methionine and the culture supernatant was assayed for secreted proteins. As expected, *sec18*, a gene involved in virtually all membrane trafficking steps, blocked the production of secreted proteins compared to wild type (Figure 3.14). In contrast, *trs20D46Y* appeared similar to wild type, suggesting that secretion is not defective in this mutant. A similar result was seen for *trs85Δ* (Figure 3.14) whereas *trs130ts* showed a partial block in secretion (not shown; see (13)). A partial block in secretion was also seen in *trs20ts* (Figure 3.14).

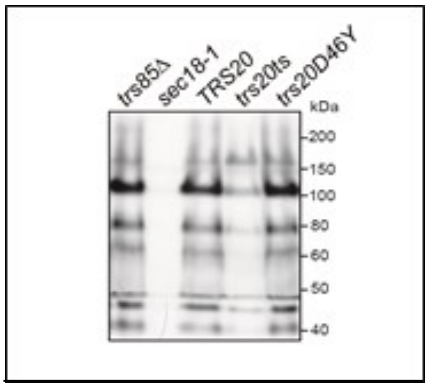

Figure 3.14 General secretion is not blocked in *trs20D46Y*. Yeast strains indicated were pulsed with ^{35}S-methionine for 15 min and chased with unlabeled methionine for 15 min. The yeast were separated from the growth medium during a brief centrifugation and proteins in the growth medium were precipitated with trichloroacetic acid. The precipitates were visualized by radioautography.

Calcofluor white (CFW) sensitivity is often used as a measure of activity of the endocytic pathway (Valdivia et al., 2002). This compound binds to chitin in the yeast cell wall, enters the cell and ultimately results in cell death. A defect in endocytosis leads to elevated chitin levels in the cell wall and a hypersensitivity of the cells to CFW while a defect in anterograde traffic results in CFW resistance. In the case of *trs20D46Y* the cells were hypersensitive to CFW (Figure 3.15). This was also the case for *trs20ts* and *trs85Δ*.

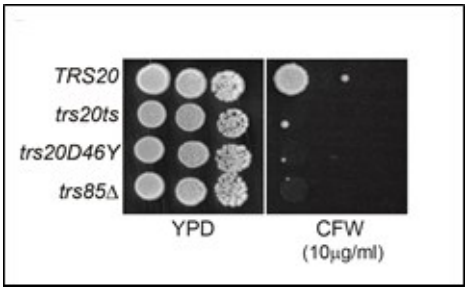

Figure 3.15 The endocytic pathway is compromised in *trs20D46Y*. The indicated yeast strains were spotted as serial dilutions on YPD plates either with or without 10 μg/mL CFW and grown at 30°C.

We next examined Snc1p-GFP localization in these cells. Snc1p is a SNARE protein that cycles between the Golgi and plasma membrane via the endocytic pathway. When fused to GFP, the protein localizes to the plasma membrane and to small buds in dividing cells (Figure 3.16). Previous studies have shown an accumulation of internal structures in *trs85Δ* cells (Montpetit and Conibear, 2009; Brunet et al., 2012) (Figure 3.16). Similarly, we found internal, Snc1p-GFP-positive structures in *trs20D46Y* and *trs20ts*. Collectively, our results suggest that *trs20D46Y* affects post-Golgi trafficking. The similar phenotype seen in *trs85Δ* and the interaction between Trs20p and the TRAPP III-specific component Trs85p suggests Trs20p may act in autophagy.

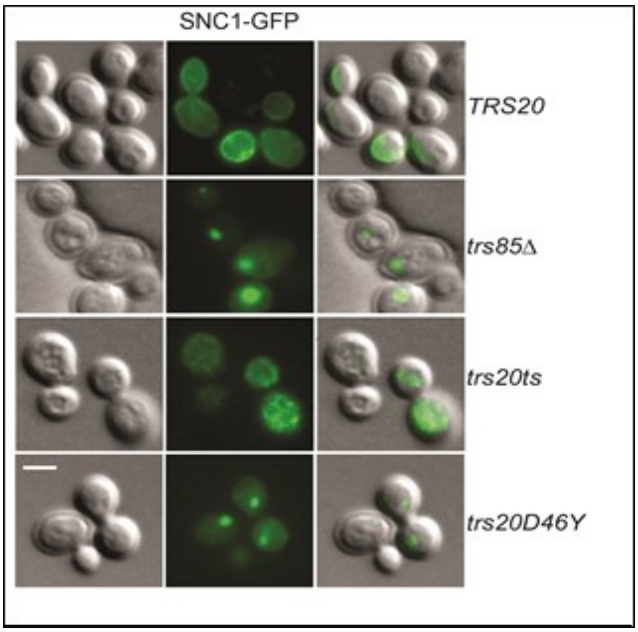

Figure 3.16 Snc1p-GFP recycling is affected in *trs20D46Y*. Yeast strains were transformed with a plasmid containing GFP-Snc1p. The cells were fixed with paraformaldehyde and the localization of GFP-Snc1p was assessed by fluorescence microscopy. Accumulation of GFP-Snc1p on internal structures is seen in 24±1%, 62±2%, 77±1% and 89±3% of wild type, *trs20ts*, *trs20D46Y* and *trs85Δ* cells, respectively (N=150 for each strain, performed in triplicate). The scale bar is 2 μm.

3.3.5 TRAPP III is destabilized in the *trs20D46Y* mutant

To better understand the trafficking step(s) affected in *trs20D46Y*, we examined the assembly state of the TRAPP complexes. First, yeast lysates from wild type or *trs20* mutants were probed for Trs20p, Trs23p (TRAPP I core protein), Trs130p-HA (TRAPP II subunit) and Trs85p-HA (TRAPP III subunit). As seen in Figure 3.17, Trs130p-HA levels were unaffected in *trs20D46Y* but were greatly reduced in *trs20ts* cells, suggesting destabilization of TRAPP II in the latter mutant. In addition, both mutants showed greatly reduced levels of Trs85p-HA. Only *trs20ts*, but not *trs20D46Y*, showed reduced Trs20p levels. Neither mutant displayed significant changes in the levels of Trs23p. These results suggest that the integrity of TRAPP III, but not TRAPP II, may be affected in *trs20D46Y*.

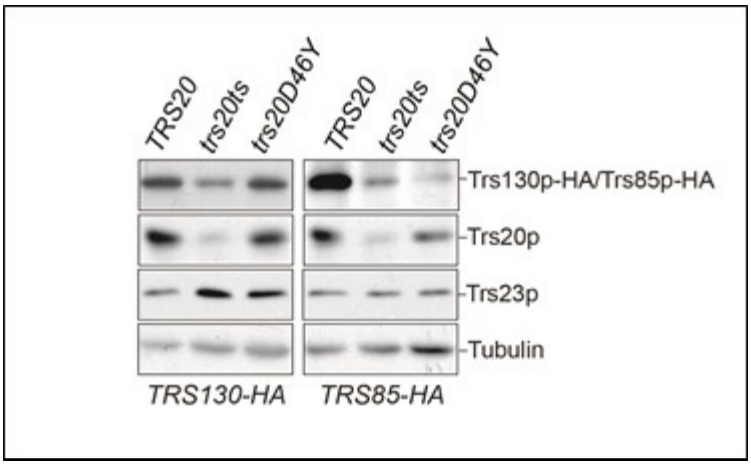

Figure 3.17 Stability of several TRAPP components is reduced in *trs20D46Y*. *TRS85* or *TRS130* was tagged with a 3XHA epitope in wild type, *trs20D46Y* and *trs20ts*. Lysates prepared from these strains were probed with anti-HA IgG, anti-Trs20p, anti-Trs23p and anti-tubulin (as a loading control).

To examine this, we fractionated lysates on a Superose 6 column that we previously showed efficiently separates TRAPP I, II and III (Choi et al., 2011;Brunet et al., 2012). The fractions from the column were probed with anti-Trs23p antibody. This protein is an integral

component of the TRAPP I core and, thus, is found in all three TRAPP complexes. As previously reported for wild type cells, Trs23p was detected in the fractions corresponding to TRAPP I, II and III (Figure 3.18). In the *trs20D46Y* mutant there was a striking loss in the Trs23p signal in only the TRAPP III fractions. In contrast to *trs20D46Y*, the Trs23p signal in both TRAPP II and III was reduced in *trs20ts* (Figure 3.18). Upon examination of Trs85p-HA, there was a decrease in this protein from the TRAPP peak in both *trs20D46Y* and *trs20ts*, consistent with the decrease in protein levels from whole cell lysates (Figure 3.18). The results from the Superose 6 column suggest that TRAPP III is selectively destabilized in the *trs20D46Y* mutant. This destabilization may be due to a weakened interaction between Trs20p and Trs85p in this mutant (see Figure 3.11).

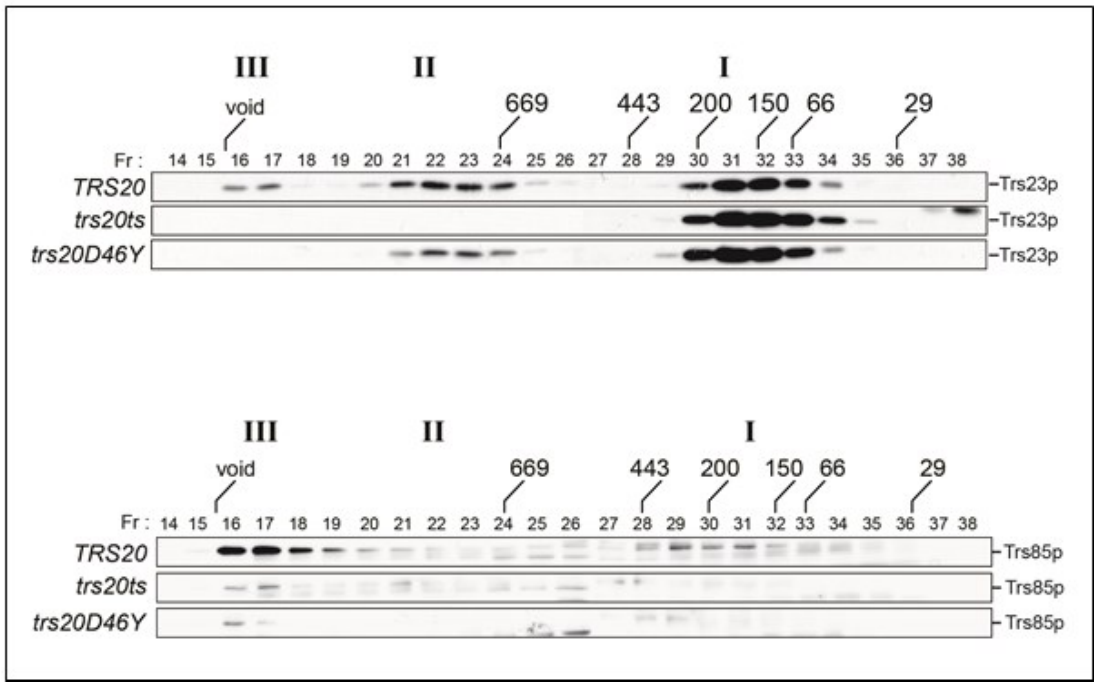

Figure 3.18 The TRAPP III peak is affected in *trs20D46Y*. Lysates from the Trs85p-HA-tagged strains in Figure 3.17 were fractionated on a Superose 6 size exclusion column in 300 mM NaCl and fractions were probed with anti- Trs23p (top panel) or anti-HA IgGto detect Trs85p-HA (lower panel). The location of the TRAPP I, II and III fractions are indicated as are the fractionation of molecular size standards.

3.3.6 Autophagy is defective in the *trs20D46Y* mutant

Based on the destabilization of TRAPP III, a complex involved in autophagy, we tested whether *trs20D46Y* affected autophagy. Growing cells in the presence or absence of a nitrogen allows one to distinguish between the selective Cytosol-to-vacuole (Cvt) autophagic pathway (+nitrogen) and the non-selective macroautophagy pathway (-nitrogen). We first probed for the marker protein Ape1p which uses the Cvt pathway in the presence of nitrogen but is transported to the vacuole in a non-selective manner in the absence of nitrogen (Scott et al., 1996). The processing of Ape1p is detected by examining the levels of the precursor form of the protein and the processed form that appears as a faster-migrating species by SDS-PAGE using an Ape1p antibody. Consistent with the destabilization of TRAPP III in *trs20D46Y*, Ape1p processing in the presence of nitrogen was completely blocked when compared to wild type (Figure 3.19, +N panel). In accordance with previous studies, *trs85Δ* and *atg1Δ* (genes that are critical for autophagy) also showed blocks in the Cvt pathway (Lynch-Day et al., 2010;Meiling-Wesse et al., 2005) as did *trs20ts* (Figure 3.19). In the absence of nitrogen, when Ape1p is processed by non-selective macroautophagy, a significant amount of mature Ape1p was detected in *trs20D46Y*, *trs20ts* and *trs85Δ* with small amounts of the precursor form also present, suggesting a defect in non-selective autophagy (Figure 3.19 -N panel).

To more carefully assess whether *trs20D46Y* affects macroautophagy, we examined the processing of GFP-Atg8p. Upon uptake into the vacuole under nitrogen starvation conditions, this fusion protein is cleaved, liberating GFP. This processing can be detected by western analysis. As seen in Figure 3.19, *trs20D46Y* as well as *trs20ts* displayed a defect in GFP-Atg8p processing in nitrogen starved medium (-N). A similar defect was also seen for *trs85Δ*, consistent with previous studies (Zou et al., 2013; Meiling-Wesse et al., 2005). Collectively, our results demonstrate that *trs20D46Y* affects both the selective (Cvt) and non-selective autophagic pathways without affecting anterograde transport.

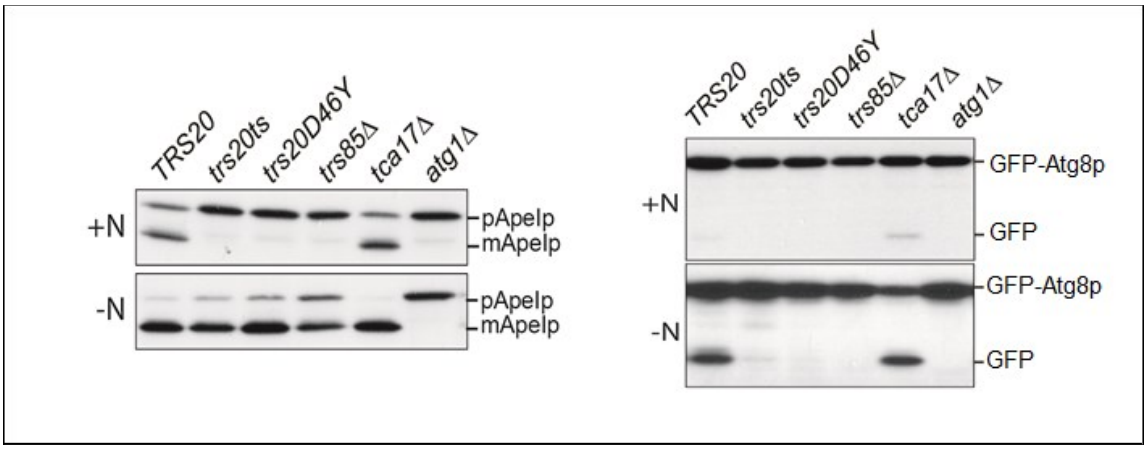

Figure 3.19 Both selective and non-selective autophagy are affected in *trs20D46Y*. The indicated yeast strains were grown in nitrogen rich (+N) or nitrogen starvation (-N) medium as described in materials and methods. Equal amounts of protein were fractionated by SDS-PAGE and analyzed by western analysis using anti-Ape1p IgG or anti-GFP (to monitor GFP-Atg8p processing) as indicated.

To further confirm autophagic defects in *trs20D46Y*, we examined the localization of Ape1p-GFP. In wild type cells, a single punctum of fluorescence is often detected that represents Ape1p in the preautophagosomal structure (PAS) (Shintani et al., 2002) (Figure 3.20). Interestingly, *trs20D46Y* showed a single but much larger punctum of Ape1p-GFP fluorescence suggesting the protein accumulates in the PAS. This is consistent with the autophagic defect seen by western analysis above. Furthermore, *trs85Δ* and *trs20ts* also displayed a similar phenotype of a single, but much larger, punctum of fluorescence (Figure 3.20). A single, large punctum such as that seen in *trs20D46Y* and *trs85Δ* has been reported in other mutants that block the Cvt pathway (Shintani et al., 2002).

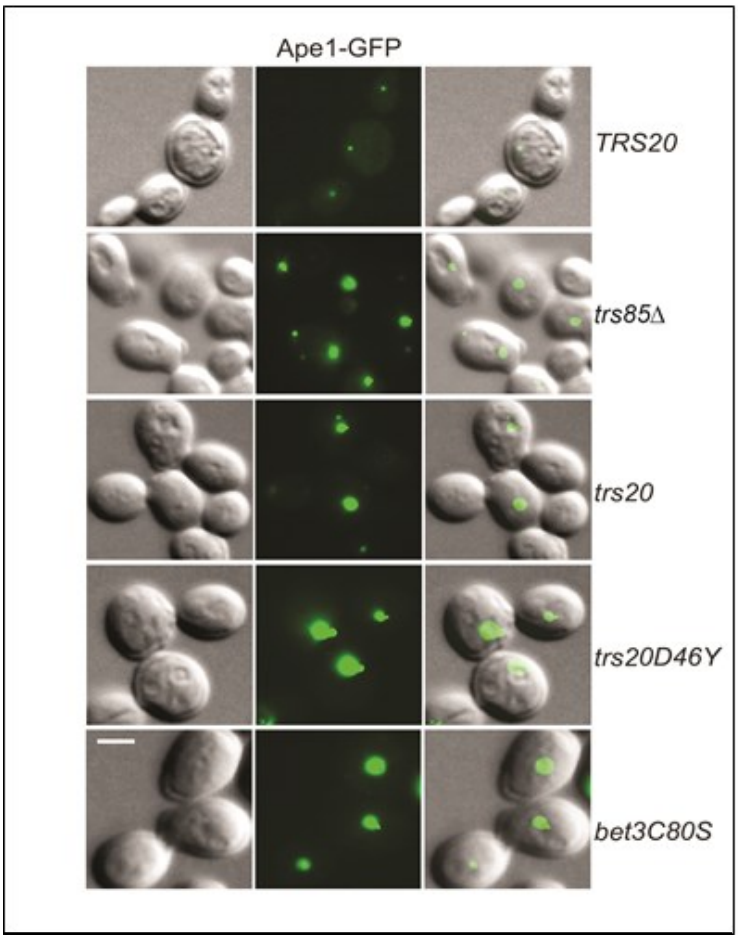

Figure 3.20 The appearance of Ape1p-GFP is affected in *trs20D46Y*. The strains indicated were transformed with GFP-Ape1p, fixed and visualized by fluorescence microscopy. The scale bar is 2 μm. Note the larger size of the GFP-Ape1p punctum in the mutants compared to wild type.

3.3.7 Trs20p and Tca17p have differing functions

Trs20p and its mammalian homolog C2 are phylogenetically and structurally related to a newly-identified TRAPP interacting protein called Tca17p in yeast (TRAPPC2L in higher eukaryotes) (Cai et al., 2008;Kim et al., 2006;Jang et al., 2002; Scrivens et al., 2009) (Protein Data Bank ID 3PR6). We therefore examined the interaction profile of Tca17p and the biochemical consequences in yeast of *tca17Δ* to that seen for Trs20p and *trs20D46Y*. By yeast two hybrid analysis, and in accordance with our previously reported genetic interaction

(Scrivens et al., 2009), when compared to the three TRAPP subunits whose interactions were affected by Trs20D46Yp (i.e. Trs85p, Trs120p and Trs130p), we found that Tca17p only interacted with Trs130p (Figure 3.21).

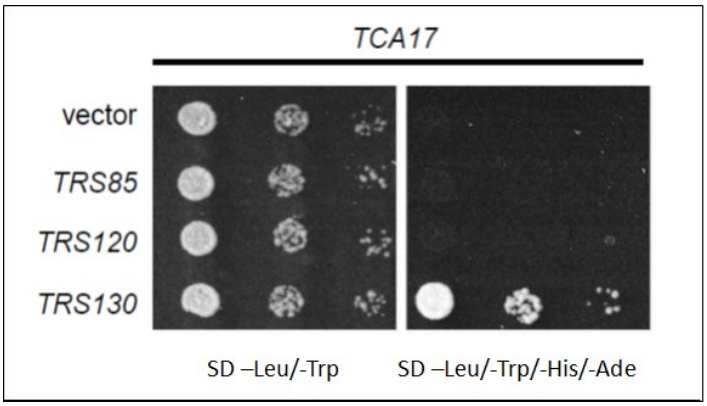

Figure 3.21 Tca17p interacts with Trs130p, but not with Trs120p or Trs85p. The open reading frame encoding *TCA17* was cloned into pGBKT7, transformed into AH109 yeast cells, and mated to Y187 yeast that harbored pGADT7 containing the open reading frame for either *TRS130*, *TRS120* or *TRS85*. Growth on SD-Leu/-Trp/-His/-Ade indicates that Tca17p binds to only Trs130p.

In addition, size exclusion chromatography showed that *tca17Δ* altered the integrity of the TRAPP II peak but did not alter the integrity of the TRAPP III peak (Figure 3.22) (Choi et al., 2011). Finally, in contrast to *trs20D46Y*, *tca17Δ* did not block the processing of Ape1p in rich medium nor of GFP-Atg8p in starvation medium (Figure 3.19). While this latter result is in contradiction to that recently reported for *tca17ts* (Zou et al., 2013), it is noteworthy that our mutant is a simple *tca17* deletion as compared to *tca17ts* which also includes modifications to *TRS120* and *TRS130*. In combination with our previous results showing that human C2, but not human C2L, could suppress *trs20Δ* (Scrivens et al., 2009), we suggest that Tca17p and Trs20p, although evolutionarily and structurally related, are functionally distinct.

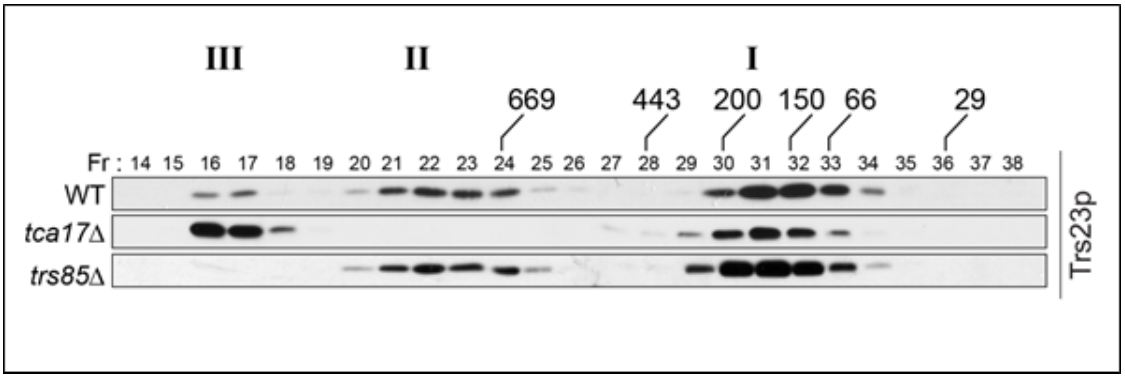

Figure 3.22 Deletion of TCA17 affects TRAPP II but does not affect TRAPP I and TRAPP III. Lysate prepared from *tca17Δ* or *trs85Δ* was fractionated on a Superose 6 size exclusion column in 300 mM NaCl. The peaks for TRAPP I, II and III are indicated. Also shown is the same wild type blot shown in Figure 3.18 for comparison. The Trs23p signal in the TRAPP II fractions is missing but remains in the TRAPP III fractions.

3.3.8 The molecular size of TRAPP III depends upon membranes and Atg9p

The composition of TRAPP III differs from that of TRAPP I by the addition of a single subunit, Trs85p. However, the molecular size of TRAPP III (>1MDa) is much greater than that of TRAPP I (~200kDa), and this difference cannot be accounted for by this single 85 kDa protein. A previous study did not identify any other polypeptides in this complex and oligomerization was also ruled out (Choi et al., 2011) (S.B. and M.S., unpublished observation). Suspecting that the large molecular size of TRAPP III was due to association with membranes, we examined the fractionation of Trs23p and Trs85p-HA in lysates prepared using Triton X-100. While Trs85p-HA shifted to a fraction with a smaller molecular size near TRAPP I, Trs23p spread out between the fractions spanning TRAPP III to II (Figure 3.23). This spreading of the Trs23p peak in Triton X-100 was independent of Trs85p since a similar pattern was seen in *trs85Δ* treated with the detergent (Figure 3.23). Such an effect was previously noted for Trs130p in a *tca17Δ* strain (Choi et al., 2011). Since Trs23p is absent from the TRAPP III fractions in *trs85Δ* prepared without detergent (Figure 3.22), this result suggests that the fractionation of Trs23p seen in the

presence of Triton X-100 is likely due to changes to TRAPP II. Our results indicate that, in the absence of detergent, TRAPP III is associated with Triton X-100-soluble membranes. Consistent with this notion, TRAPP III penetrated an Optiprep gradient further in the absence, as compared to the presence, of Triton X-100 (Figure 3.24).

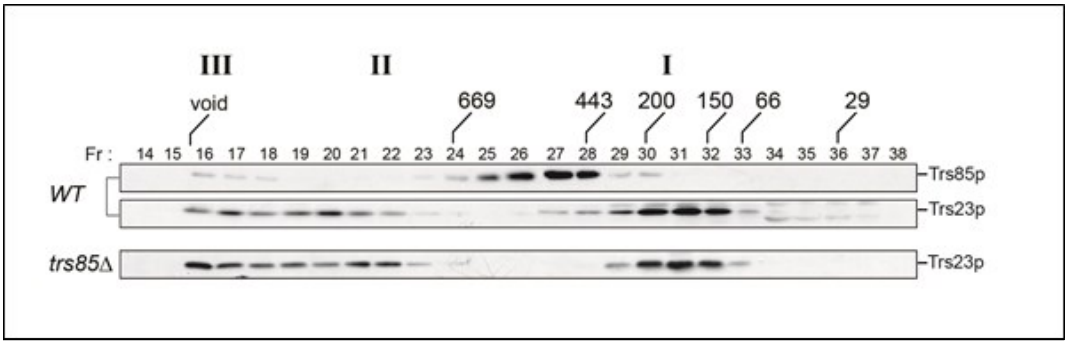

Figure 3.23 The molecular size of TRAPP III is dependent upon membranes. Lysate was prepared from *TRS85*-HA or *trs85Δ* strains with 300 mM NaCl/1% Triton X-100. The lysates were fractionated on a Superose 6 size exclusion column. The fractions were probed for Trs23p and Trs85p-HA as indicated.

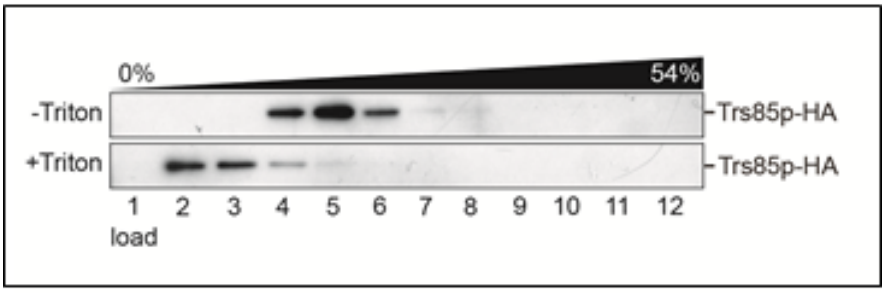

Figure 3.24 Trs85p-HA is bound to membranes. Pooled fractions from a Superose 6 column enriched in TRAPP III derived from a *TRS85*-HA strain that was not treated with Triton X-100 were loaded on top of an Optiprep step gradient prepared as described in materials and methods. The top-loaded sample was either left untreated or incubated with 1% Triton X-100 before centrifugation on the gradient. Fractions were collected from the top of the gradient and probed for Trs85p-HA.

We next set out to identify a putative TRAPP III receptor on autophagic membranes by screening *atgΔ* mutants for changes in the fractionation pattern of TRAPP III on a size exclusion column. Our studies led us to focus on *atg9Δ*. In whole cell lysates, the levels of Trs85p-HA, but not Trs23p, were dramatically reduced upon nitrogen starvation in *atg9Δ* (Figure 3.25, compare +/- nitrogen). Correspondingly, there was a decrease in the appearance of Trs85p-HA in the TRAPP III peak in nitrogen-starved *atg9Δ* cells relative to non-starved cells (Figure 3.26). Remarkably, Trs23p was also reduced in the TRAPP III fractions (Figure 3.26). This result is similar to that seen for *trs20D46Y* (see Figure 3.18) in which the levels of Trs85p-HA, but not Trs23p, are reduced yet the amounts of both proteins are reduced in TRAPP III. We next examined Atg17p since this protein has been reported to recruit Atg9p to autophagic membranes (Sekito et al., 2009). In a nitrogen-starved *atg17Δ* strain, we did not detect a significant decrease in the levels of neither Trs85p-HA nor of Trs23p (Figure 3.25) and there were no differences in the fractionation of these proteins in the TRAPP III peak (Figure 3.26) compared to non-starved cells. Collectively, our results suggest that the recruitment of TRAPP III during non-selective, but not during selective autophagy, requires Atg9p, and that an assembled TRAPP III complex is required for both selective and non-selective autophagy.

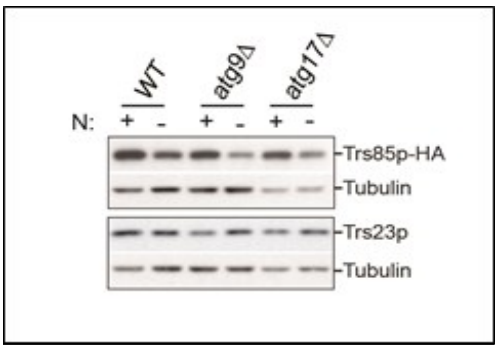

Figure 3.25 Starvation-induced reduction in the levels of Trs85p-HA in *atg9Δ*. Lysate in 300 mM NaCl was prepared from wild type, *atg9Δ*, *atg17Δ*, *atg9Δ TRS85*-HA or *atg17Δ* /*TRS85*-HA grown in YPD (+) or nitrogen starvation medium (-). Lysates were probed for either Trs23p, Trs85p-HA or tubulin (as a loading control).

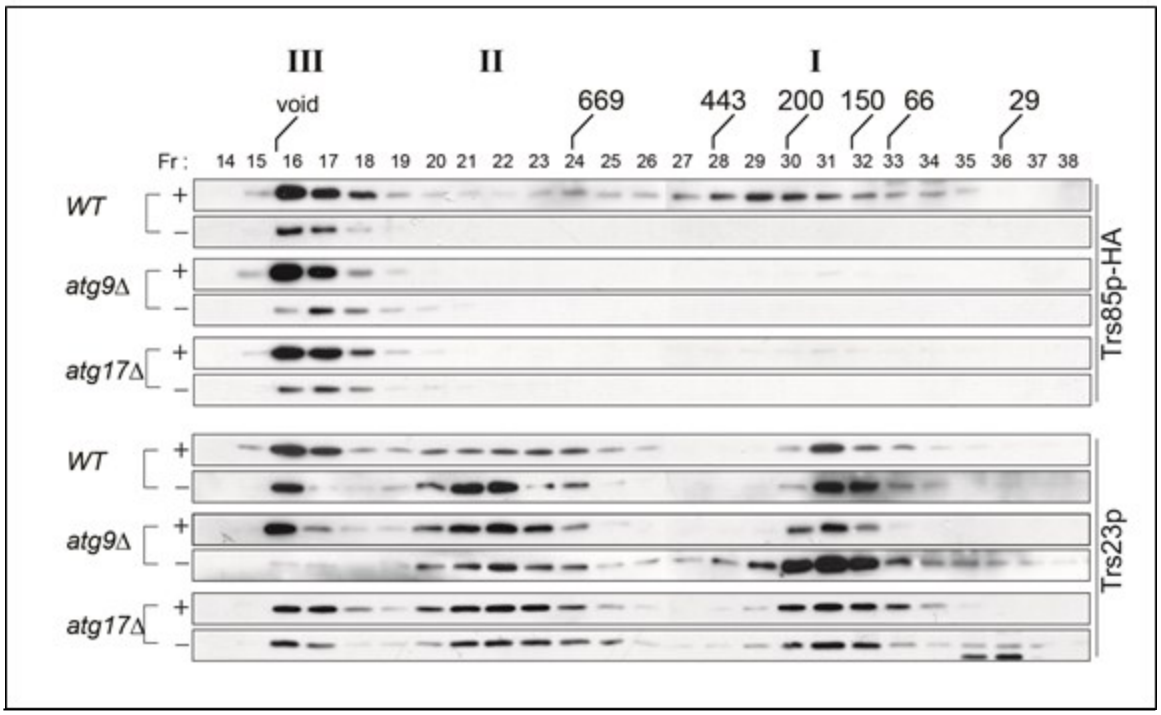

Figure 3.26 Starvation-induced disappearance of TRAPP III in *atg9Δ*. A total of 5 mg of lysate from the cells in (Figure 3.25) was fractionated on a Superose 6 column and probed for Trs23p or Trs85p-HA as indicated. + and – indicate nutrient rich and starvation conditions, respectively.

3.3.9 Palmitoylated Bet3p is enriched in TRAPP III

TRAPP III appears to be membrane associated while TRAPP I is more easily separated from membranes since fractionation of the latter on a size exclusion column is not affected by detergent. What can account for this difference? The TRAPP I core subunit Bet3p was shown to be lipid-modified by either palmitoylation or myristoylation (Kim et al., 2005b;Turnbull et al., 2005). The modified cysteine residue at position 80 in the yeast protein is highly conserved yet, surprisingly, mutation of this residue does not lead to any observable growth phenotype. We speculated that lipid-modified Bet3p may partially account for the association of the TRAPP III complex with PAS membranes. If this is the case, *bet3C80S*, a mutant that prevents Bet3p

palmitoylation (Kummel et al., 2006;Kim et al., 2005b;Turnbull et al., 2005), may block autophagy. Indeed, compared to wild type, *bet3C80S* displayed both a defect in Ape1p processing in the presence, but not the absence, of nitrogen and a starvation-induced block in GFP-Atg8p processing upon nitrogen starvation (Figure 3.27). In addition, *bet3C80S* also displayed an enlarged Ape1p-GFP punctum similar to that seen for *trs85Δ* and *trs20D46Y* (Figure 3.20). This suggests that palmitoylation of Bet3p is involved in the efficient functioning of TRAPP III in both selective and non-selective autophagy.

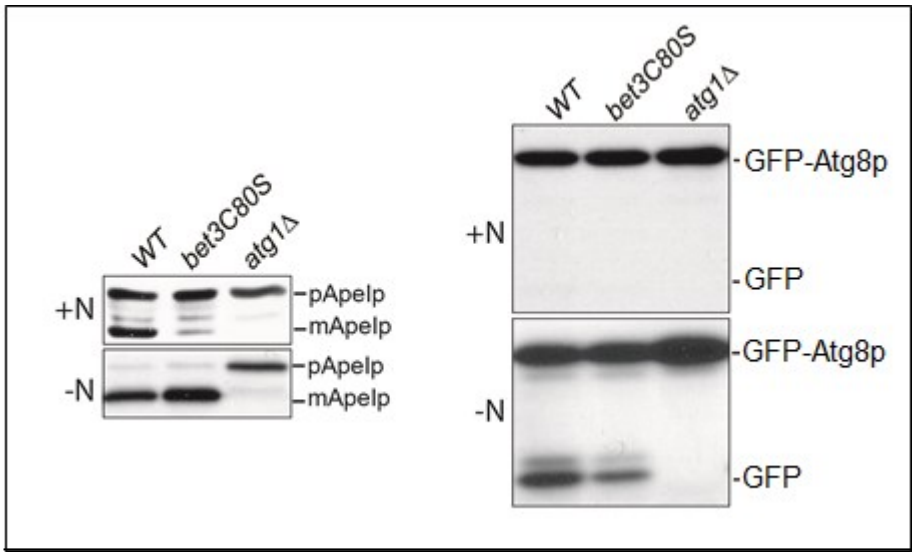

Figure 3.27 Both selective and non-selective autophagy are affected in *bet3C80S*. Lysates from wild type, *bet3C80S* and *atg1Δ* were prepared from cultures grown in YPD (+N) or nitrogen starvation (-N) medium as described in materials and methods and analyzed by western analysis with anti-Ape1p IgG or anti-GFP (to monitor GFP-Atg8p processing) as indicated.

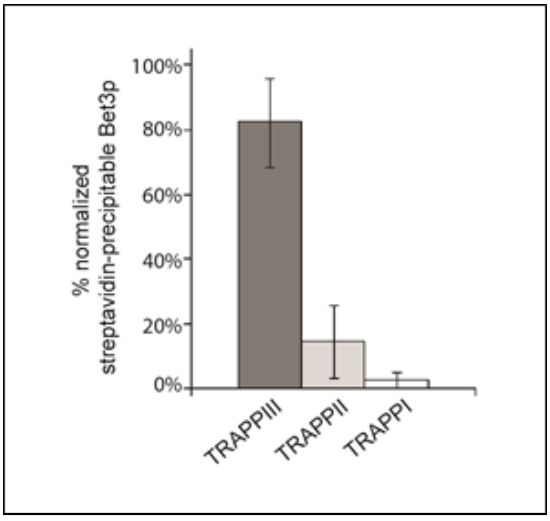

Figure 3.28 Lipidated Bet3p is predominantly found in TRAPP III. A wild type lysate was fractionated on a Superose 6 column and the peak of TRAPP I, II and III were pooled individually and subjected to acyl-biotin exchange as described in materials and methods. A portion of each input fraction, to enable normalization to Bet3p, along with the entire precipitate from the streptavidin-agarose beads was subjected to western analysis using anti-Bet3p serum and quantitated using Image J. Error bars indicate standard deviation.

Given the result above we speculated that palmitoylated Bet3p would be enriched in TRAPP III. To test this notion, a wild type lysate was fractionated by size exclusion chromatography and the fractions containing TRAPP I, II and III were pooled separately and subjected to acyl-biotin exchange. In this assay, acyl chains on proteins are exchanged for a biotin moiety which can then bind to streptavidin-agarose beads. Precipitation of proteins onto the beads indicates that the proteins were initially acylated. As shown in Figure 3.28, after normalization to Bet3p levels in the input, acylated Bet3p was greatly enriched in TRAPP III. Our results suggest that acylated Bet3p is important for the function and/or localization of the TRAPP III complex.

3.4 Discussion

Here we demonstrate that the mammalian TRAPP protein C2 binds to the SNARE protein Syntaxin 5. This interaction is weakened by the pathogenic D47Y mutation in C2 and led us to speculate that a yeast mutation patterned after this mutation in the C2 homolog Trs20p would affect early secretory pathway traffic. Instead this mutant (*trs20D46Y*) did not display anterograde trafficking defects but was defective in the selective (Cvt) and non-selective autophagy pathways. In addition, *trs20D46Y*, *atg9Δ* and *bet3C80S* mutants revealed complexities in the organization and function of the TRAPP III complex that is involved in these pathways. It should be stressed that, although the *trs20* mutants examined in this study did not display trafficking defects in the early secretory pathway, other residues in this protein may in fact impinge on this process.

3.4.1 Complexities in TRAPP III assembly and function

The subunit composition of TRAPP III differs from TRAPP I by just a single protein (Trs85p in TRAPP III), yet the molecular size of TRAPP III is much greater than that of TRAPP I (see Figures 3.17-3.18 and 3.23-3.26) (Choi et al., 2011;Brunet et al., 2012) and this is not due to oligomerization of Trs85p/TRAPP III (Choi et al., 2011) (S.B. and M.S., unpublished observation). We found that the levels of the TRAPP III-specific protein Trs85p-HA, but not the TRAPP I core protein Trs23p, were greatly diminished in *trs20D46Y* as well as in *atg9Δ*, but unaffected in *atg17Δ*. The former two mutants showed reduced levels of both Trs85p-HA and Trs23p in the TRAPP III fractions. Our results imply that, during macroautophagy, the recruitment of TRAPP III to autophagic membranes is dependent upon Atg9p (Figure 3.29, A). Our data do not address which, if any, subunit of TRAPP III interacts directly with Atg9p although a recent report suggested that Trs85p, but not other TRAPP I core subunits, binds directly to Atg9p (Kakuta et al., 2012). If this is the case, our results with *trs20D46Y* suggest that recruitment of the TRAPP I core to the Atg9p-Trs85p unit is mediated by Trs20p and particularly

by its conserved D46 residue. Our data leave open the possibility that the TRAPP I core may be recruited to membranes distinct from those containing Trs85p in which case their interaction to form TRAPP III may contribute to tethering (Figure 3.29, B). This would be similar to the mechanism of exocyst complex-mediated tethering in which vesicles are tethered to the plasma membrane via interactions between exocyst components on separate membranes (Boyd et al., 2004). Since the levels of Trs85p-HA and the appearance of Trs85p-HA and Trs23p in TRAPP III were not affected under rich growth conditions in *atg9Δ*, recruitment of TRAPP III to autophagic membranes during selective autophagy must be dependent on an as yet unidentified factor (Figure 3.29, C).

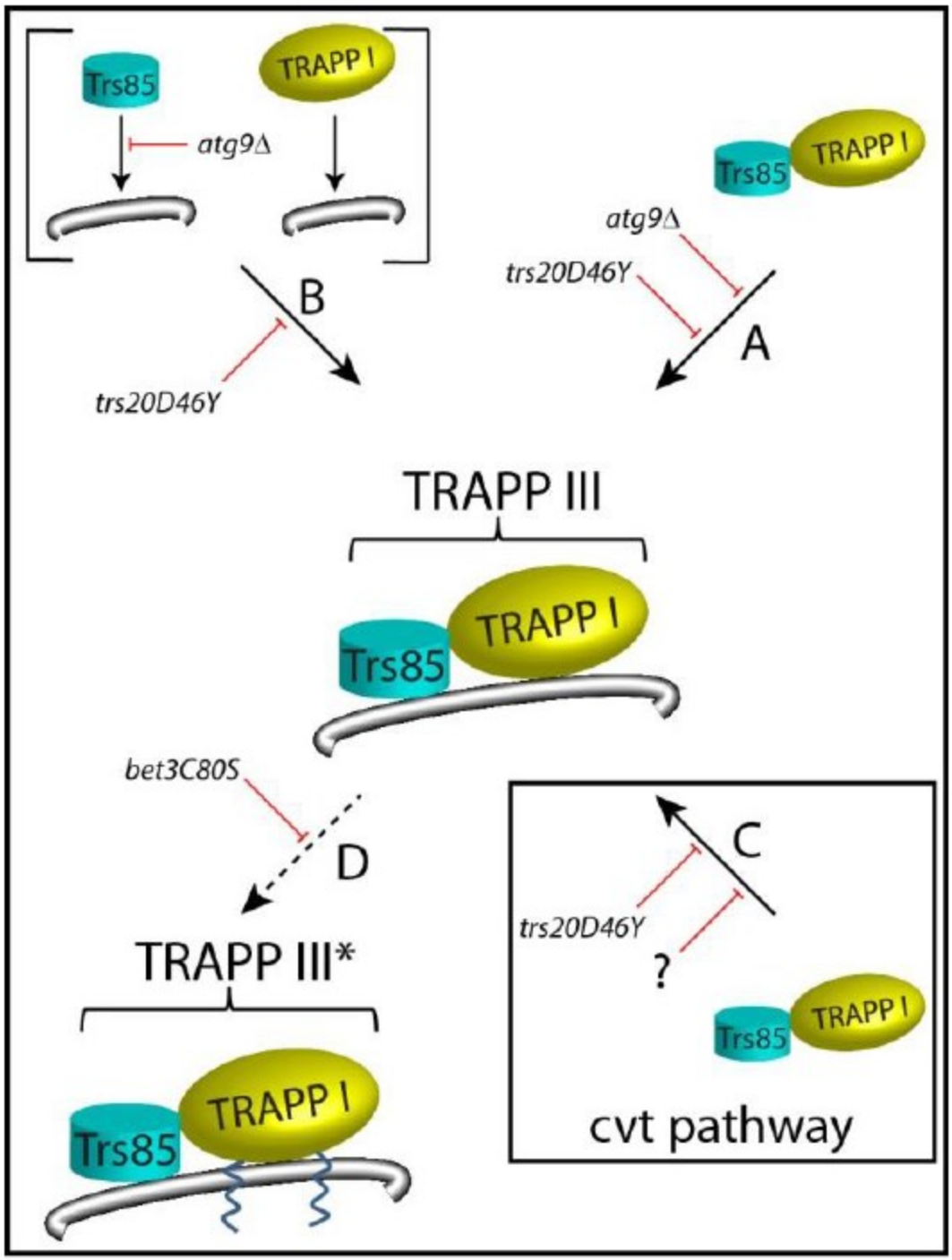

Figure 3.29 Model for the organization and assembly of TRAPP III. Assembly of TRAPP III is dependent upon an interaction between Trs20p and Trs85p and is mediated by the conserved D46 residue in Trs20p. Assembled TRAPP III is then recruited to autophagic membranes in an Atg9p-dependent manner (A). This may be mediated by a direct interaction between Trs85p and Atg9p as recently suggested (Kakuta et al., 2012). Alternatively, Trs85p and Trs23p may be

recruited to separate membranes, and their interaction to form TRAPP III is mediated by the same Trs20p-Trs85p interaction described above (B). Note that the involvement of Atg9p in this scenario is based on a recent study (Kakuta et al., 2012). Although TRAPP III assembly in the Cvt pathway is also mediated by a Trs20p-Trs85p interaction, recruitment to autophagic membranes does not appear to require Atg9p and some as yet unknown factor (denoted as ?) may be involved (C). In both cases (Cvt and macroautophagy) lipidation of Bet3p in TRAPP III increases the functional efficiency of the TRAPP III complex (denoted by TRAPP III*). The steps that are blocked by the various mutants used in this study are indicated by red lines.

Our results provide a clue as to the role of *trs20D46Y* in autophagy. Based on Ape1p processing in rich medium, this mutant affects the Cvt pathway. While there was only a minor defect in Ape1p processing under nitrogen-starved conditions, examination of GFP-Atg8p under these conditions indicated that non-selective autophagy was also strongly affected. Such a phenotype of a mild defect of Ape1p processing but a strong defect in GFP-Atg8p processing in starvation conditions has been reported for the TRAPP mutant *trs85Δ* as well as for *vac8Δ* (Cheong et al., 2005;Zou et al., 2013; Meiling-Wesse et al., 2005). In the latter mutant, autophagic bodies were reduced in both number and size. Our results, therefore, suggest that in *trs20D46Y* Cvt vesicles fail to form. However, in nitrogen-starved conditions, while some autophagosomes may form, their size is likely abnormally small.

What is the role of Bet3p lipidation in TRAPP III function? The enrichment of lipidated Bet3p in TRAPP III and the fact that TRAPP III remains membrane-associated in *bet3C80S* (S.B. and M.S., unpublished observation), suggests that lipidation alone cannot account for TRAPP III membrane attachment. It is tempting to speculate that lipidated Bet3p may localize the complex to a membrane sub-domain of authophagic vesicles. It is noteworthy that acylation of proteins is one mechanism that directs their intracellular localization (Moreau et al., 2011;Roskoski, 2003). Alternatively, lipidation of Bet3p/C3 has been postulated to alter its

structure (Kummel et al., 2006 and 2010;Turnbull et al., 2005), which may promote binding to these specialized membrane regions or increase the efficiency of TRAPP III function (Figure 3.29, D).

3.4.2 Trs20p as an adaptor protein

When compared to *tca17Δ*, our results with *trs20D46Y* suggest that Trs20p can act as an adaptor protein for the TRAPP II-specific subunit Trs120p and the TRAPP III-specific subunit Trs85p. This adaptor function of Trs20p is similar to that reported for the mammalian homolog C2 (Scrivens et al., 2009). Since Trs85p and Trs120p do not reside in the same complex, their interaction with Trs20p is not mutually exclusive. The fact that the D46Y mutation in Trs20p weakens both interactions suggests that these two TRAPP subunits interact with Trs20p in a similar fashion. The suggestion that Trs120p binds directly to Trs20p is in disagreement with the recently published electron microscopic structure of the TRAPP II complex, which suggested that Trs20p was in direct contact with Trs130p while Trs120p was on a side of the complex opposite to that of Trs20p (Yip et al., 2010; see Figure 1.9). While our results leave this possibility open, we do not believe this to be the case for the following reasons. The interaction between Trs20p and Trs130p is much weaker than that between Trs20p and Trs120p (M.S., unpublished observation). In addition, the similarity in structure between Trs20p and Tca17p leaves open the possibility that some Trs20p interactions occur due to the similar structure between these two proteins and do not take place *in vivo*. Indeed, Tca17p was found to bind only to Trs130p which is consistent with a previous study showing that Tca17p binds to the amino-terminus of Trs130p (Choi et al., 2011) and our earlier result showing a strong genetic interaction between *TCA17* and *TRS130* (Scrivens et al., 2009). We suggest that Tca17p may be the TRAPP subunit that interacts with Trs130p while Trs20p acts as an adaptor to allow either Trs85p or Trs120p to interact with the TRAPP I core complex. It remains unclear how Tca17p interacts with the TRAPP I core and how it is excluded from TRAPP III.

3.4.3 Implications for SEDT

The C2D47Y mutation was identified in a patient with spondyloepiphyseal dysplasia tarda (SEDT) (Shaw et al., 2003). A recent study suggested that C2 (called Sedlin) regulates the Sar1p GTPase cycle at ER exit sites to allow ER-derived carriers to grow to a size that can accommodate large cargo such as collagen (Venditti et al., 2012). It is the transport of pro-collagen that is believed to be defective in SEDT patients. Although we could not detect an interaction between Trs20p and the yeast Syntaxin 5 homolog Sed5p, it is possible that the mammalian Trs20p homolog C2 evolved the ability to interact with Syntaxin 5. In this case, pro-collagen release from the Golgi in patients with the C2D47Y mutation may not be affected but fusion of the megacarriers with the Golgi would be defective. Alternatively, Syntaxin 5 has been implicated in membrane traffic steps beyond the ER-to-Golgi portion of the secretory pathway including the endocytic pathway (Xu et al., 2002;Tai et al., 2004) and pro-collagen transport in patients with the C2D47Y mutation may be blocked at these later stages. It is noteworthy that defects in endocytosis could indirectly block anterograde transport, suggesting that the C2D47Y mutation may have an indirect effect on pro-collagen transport. At present, it is difficult to envision how a defect in autophagy could affect pro-collagen transport. Studies on the role of mammalian C2 in both endocytosis and autophagy will help address these possibilities.

CHAPTER 4

Binding of TRAPP to the tethering factor p115 affects its membrane association in the presence of an SEDT-causing mutant TRAPPC2D47Y

In Chapter 3, I presented evidence that there is a direct association between the TRAPP complex and the ER-Golgi fusion protein Syntaxin 5. In the following chapter, I will demonstrate further results, yet to be published, involving the stated TRAPP-SNARE interaction and in the course of this study I will demonstrate a novel association between two tethering factors TRAPP and p115.

4.1 Introduction

The first interaction between a vesicle and target membrane is called "tethering", a process mediated by a group of heterogeneous proteins known as tethering factors. Tethering factors are divided into two groups: multisubunit complexes and long coiled-coil proteins, and some of these proteins reside at the Golgi. The tethering factor p115 was originally identified through an *intra*-Golgi transport assay and was revealed to be essential in capturing coat protein I (COPI) transport vesicles on Golgi membranes (Clary and Rothman, 1990). Subsequent studies on the yeast p115 homolog Uso1p pointed to its involvement in ER-to-Golgi trafficking mediated by the coat protein II (COPII) coat. Additionally, the temperature sensitive *uso1-1* mutant was unable to support trafficking to the Golgi apparatus (Allan et al., 2000;Beard et al., 2005;Alvarez et al., 2001;Nakajima et al., 1991). Thus, p115/Uso1p has been implicated in interactions with both COPI- and COPII- coated vesicles and mediates different trafficking steps. Structural studies of p115 have documented two large N-terminal globular homology (H1-2) domains, also known as globular head region (GHR), which precede the central extended coiled-coiled domains (CC1 – CC4), followed by an acidic tail (AD) (Sapperstein, et al., 1995) (Figure 4.1). Golgi-SNARE proteins are also among the direct binding partners of p115 and their

interaction is mapped to the coiled-coil regions of p115, facilitating SNARE complex formation by directing anterograde transport of COPII vesicles towards the Golgi apparatus (Beard et al., 2005; Xu et al., 2004). A recent *in vivo* study in *Caenorhabditis elegans* has elegantly shed light on the simultaneous involvement of two SNARE-binding domains (CC1 and CC4) in the tethering event (Grabski et al., 2012a).

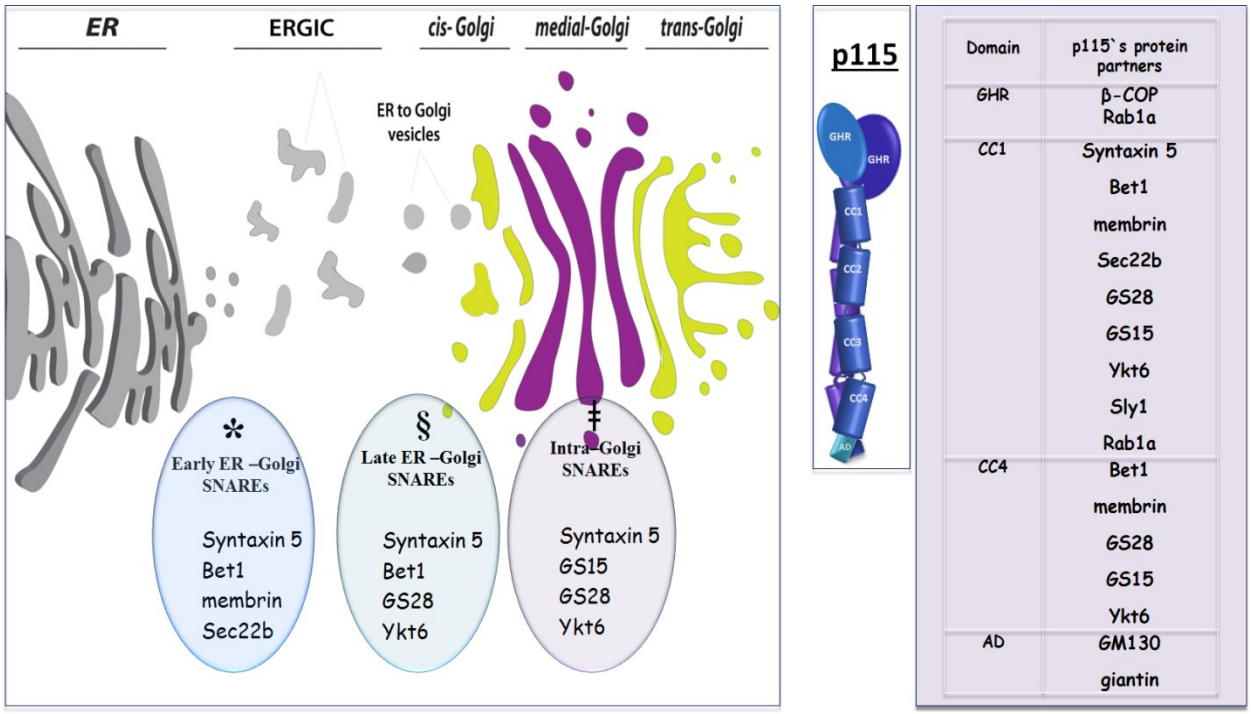

Figure 4.1 Multiple interactions in p115 with several proteins of the secretory machinery. Coiled-coil domains one and four (CC1 and CC4) directly bind to a number of SNARE proteins (left panel). Distinct combinations of these SNAREs make three different complexes of four SNARE proteins (right panel); complexes 1, 2, and 3 are symbolized by *, §, and ǂ, respectively. *Complex 1 has been reported to be involved early in the secretory pathway in homotypic fusion of COPII vesicles with ERGIC (Xu et al., 2000). § Complex 2 is implicated in tethering of anterograde transport carrier with *cis*-Golgi (Zhang et al., 2001). ǂ Complex 3 plays a role in *intra*-Golgi trafficking (Xu and Hay, 2004). Note that CC4 region does not bind to Syntaxin 5, Sly1, or Rab1a.

Homotypic fusion of COPII coated vesicles is believed to be mediated between the globular head region of p115 and Rab1a, with these interactions leading to the generation of vesicular tubular clusters (VTCs) (Beard et al., 2005). Sequential actions involved in COPII tethering occur as follows: (1) The TRAPP I complex associates via Bet3p/C3 with a component of COPII, Sec23p/Sec23 (Cai et al., 2007b), on the nascent vesicle; (2) Ypt1p/Rab1 is activated by the TRAPP I complex, serving as a Ypt1p/Rab1 GEF (Jones et al., 2000; Wang et al., 2000) which in turn recruits its effector, Uso1p/p115, to the COPII vesicle; and (3) The captured vesicle is brought toward the target Golgi membrane (Allan et al., 2000), although in mammals it is less clear whether the target membrane is ERGIC (VTCs) or Golgi. A recent study in yeast indicates that sequential Sec23p-Sec24p interactions first with TRAPP and then with a Golgi resident kinase Hrr25p that competes with TRAPP I to bind to Sec23p-Sec24p establishes the directionality of vesicle trafficking (Lord et al., 2011).

The tethering protein p115 is a cytoplasmic protein that cycles on and off of membranes (Brandon et al., 2006) and a cytosolic p115 dimer is recruited to the membrane through the small GTPase Rab1 (Brandon et al., 2006; Allan et al., 2000) and is implicated in SNARE complex formation in order to promote subsequent membrane bilayer fusion (Shorter et al., 2002; Allan et al., 2000; Puthenveedu et al., 2004; Bentley et al., 2006; Gmach and Wimmer, 2001). In support of this, GDI-mediated extraction of Ypt1p in yeast results in Uso1p dissociation from membranes (Cao et al., 1998). Moreover, membrane targeting of p115 is regulated by accessibility of free SNARE binding as persistence of the assembled SNARE complex due to mutation in SNARE-dissociation factors NSF or α-SNAP, prolongs p115 membrane residency (Bentley et al., 2006; Brandon et al., 2006). However, it is currently unknown whether the TRAPP complex affects membrane recruitment of p115. Here I present evidence that an SEDT-causing mutation of TRAPPC2 leads to stronger association of p115 with membranes. In addition I demonstrate that a TRAPP-Syntaxin 5 interaction (shown in

Chapter 3) is associated with COPII-coated vesicles. The association occurs in brefeldin A-(BFA-) resistant compartments thought to be ERGIC.

4.2 Materials and Methods

Methods listed below are unique to this chapter. All other methods can be found in the methods sections of Chapters 2, 3 and 5.

4.2.1 Preparation of total cell lysates

Lysates from HeLa cells for size exclusion chromatography were prepared as previously described in Chapter 2 and a total protein of 2-5 mg was fractionated on a Superose 6 column. High molecular weight fractions corresponding to TRAPP were identified by western blotting analysis and pooled together. The same was done for low molecular weight monomeric fractions. These fractions were subjected to co-immunoprecipitation (see Chapter 2) using 2 µL of Syntaxin 5 (18C8) antibody and probed with rabbit, home-made anti-C2 1:1000, mouse anti-p115 (1:1000, kind gift from Dr. Paul Melancon) and for positive and negative controls rabbit anti-Syntaxin 5 (1:1000, Santa Cruz) and rabbit anti-Sam68 (1:1000). In co-IP experiments, SNARE antibodies were anti-Bet1, anti-membrin, anti-Syntaxin 5 and anti-GS28 were generous gifts from Dr. James Rothman. In certain experiments cells were treated with BFA (10 µg/mL 30 minutes prior to harvesting) or NEM (see Chapter 2). Co-IPs were as above and probed with anti-Sec23 (1:1000, rabbit) courtesy of Dr. Randy Schekman. NEM-treated HeLa cells used for co-IP experiments were as described in Chapter 2. Immunofluorescence microscopy was performed as in Chapter 5.

4.2.2 Membrane and soluble fractionations

HeLa cells were grown in 10 cm dishes to 50-60% confluency at the time of transfection. Cells were then transfected with 10 µg of plasmid either with or without the Syntaxin 5 open reading frame and co-transfected either with myc-tagged C2 or C2 D47Y-myc. 48 hours post transfection, medium was removed and cells were collected by scraping. Samples were washed twice in wash buffer (140 mM NaCl, 10 mM EDTA, 25 mM Tris, and 30 mM KCl). Cells were

resuspended in homogenizing buffer (25 mM NaCl, 1 mM EGTA, 25 mM Tris ,and 30 mM KCl) and lysed by 10 passes with a dounce homogenizer and then through a 26 and 21 G needle, each with 10 strokes. After a brief spin to remove cell debris (3000*g*, 5 minutes), the postnuclear supernatant was centrifuged for 1 hour at 100,000*g* in an SW55Ti rotor. A volume of 700 µL of supernatant was removed (S fraction) and the pellet (P fraction) was washed with wash buffer. The supernatant received 700 µL of 2X Laemmli buffer while the pellet was resuspended in 1400 µL of 1X Laemmli buffer.

4.3 Results

4.3.1 Novel association between p115 and TRAPP is enhanced by SNARE complex formation

A recent review article by Yu and Liang (2012) on the TRAPP complex suggests the involvement of p115 once TRAPP has been released from an incoming vesicle. In order to reveal spatiotemporal relationships between key players in capturing vesicles, as well as further investigating the significance of the C2-Syntaxin 5 interaction (a novel association found in the course of this study; see Chapter 3), I performed co-IP experiments wherein Syntaxin 5 simultaneously precipitated both p115 and C2 (Figure 4.2). This result is in accordance with previous models suggesting the possibility of multiple tethers being involved in tethering vesicles (Kim et al., 2006). More interestingly, the association of TRAPP and p115 to Syntaxin 5 are both enhanced when the cells are treated with NEM, a reagent that prevents the disassembly of the four helix bundle of the SNARE complex, suggesting that these tethering factors bridge the cargo to the target membrane while also facilitating formation of SNARE complexes for the later fusion event (Figure 4.2).

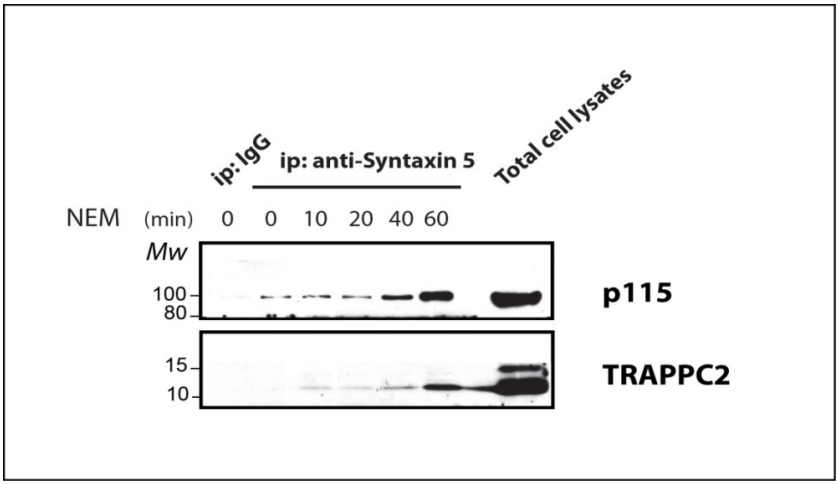

Figure 4.2 Syntaxin 5 associates with both p115 and C2. Immunoprecipitation of Syntaxin 5 reveals a novel association between p115 and TRAPP. Like the TRAPP complex, p115

association to Syntaxin 5 is increased by NEM and assessed by western analysis using antibodies against p115 and C2. During a time course of 60 minutes, HeLa cells were treated with 10 μM NEM. Total cell lysate represents 10% of the input lysate utilised in co-IP.

While Syntaxin 5 immuno-isolations (Figures 4.2) suggest p115 could also associate with TRAPP and Syntaxin 5 in distinct complexes, we considered the possibility that p115 and TRAPP are Syntaxin 5 protein partners and constituents of a single complex. To address this, anti-C2 was used to precipitate endogenous p115 along with Syntaxin 5. As shown in Figure 4.3 this antibody was able to precipitate both Syntaxin 5 and p115.Taken together with the results in Figure 4.2, it is possible that all three proteins (Syntaxin 5, C2 and p115) are components of a single complex although this has not been conclusively demonstrated.

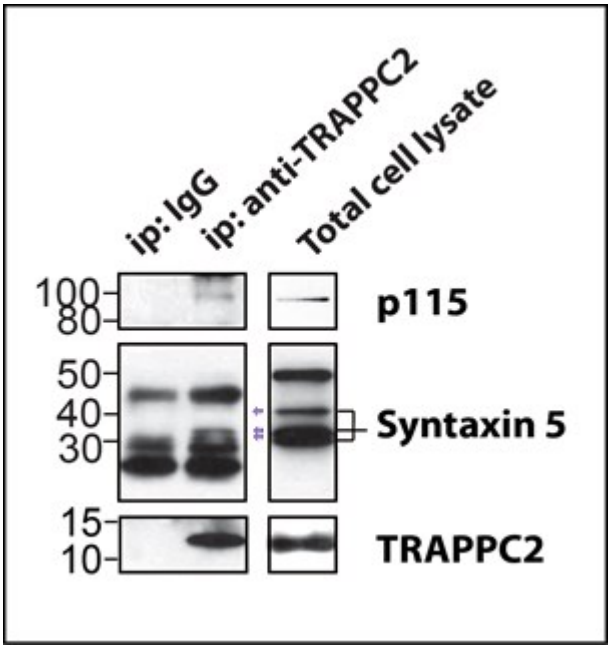

Figure 4.3 p115 and Syntaxin 5 are C2 binding partners that are associated together. HEK 293 cells were immunoprecipitated using C2 IgG and then subjected to western blot analysis to detect p115 (top panel), Syntaxin5 (middle panel) and C2 (bottom panel). Total cell lysate

indicates 10% of input used in the co-IP. Syntaxin 5 migrates at three different sizes: 30, 34, and 40 kDa (shown by pink arrows).

4.3.2 Unlike Syntaxin 5, p115 associates with C2-containing TRAPP complex and not with the monomeric form of C2

Since the two protein partners C2 and Syntaxin 5 are part of their own protein complex and can be also found in free/monomeric form (Sacher et al., 2000; Williams et al., 2004), the C2-Syntaxin 5 interaction may occur in the presence of their cognate protein complexes or in their monomeric forms. To distinguish between these possibilities, size exclusion chromatography was employed to separate TRAPP complexes from their monomeric components. Cell fractions corresponding to multimeric and monomeric forms were collected and subjected to immunoprecipitation with endogenous Syntaxin 5 antibody. While the C2 and Syntaxin 5 interaction was confirmed in both forms of C2 (with a preference for association with the complex form) (Figure 4.4; and shown in the *inset*), interestingly, an association of p115 with the complex form of C2 and not with its monomeric form was observed (compare lanes 3 and 4). This suggests that TRAPP and p115, two tethering factors, together may facilitate the capture of the t-SNARE Syntaxin 5. This is consistent with the subcellular distribution of p115, Syntaxin 5 and TRAPP (ERGIC, *cis*-Golgi and *intra*-Golgi compartments).

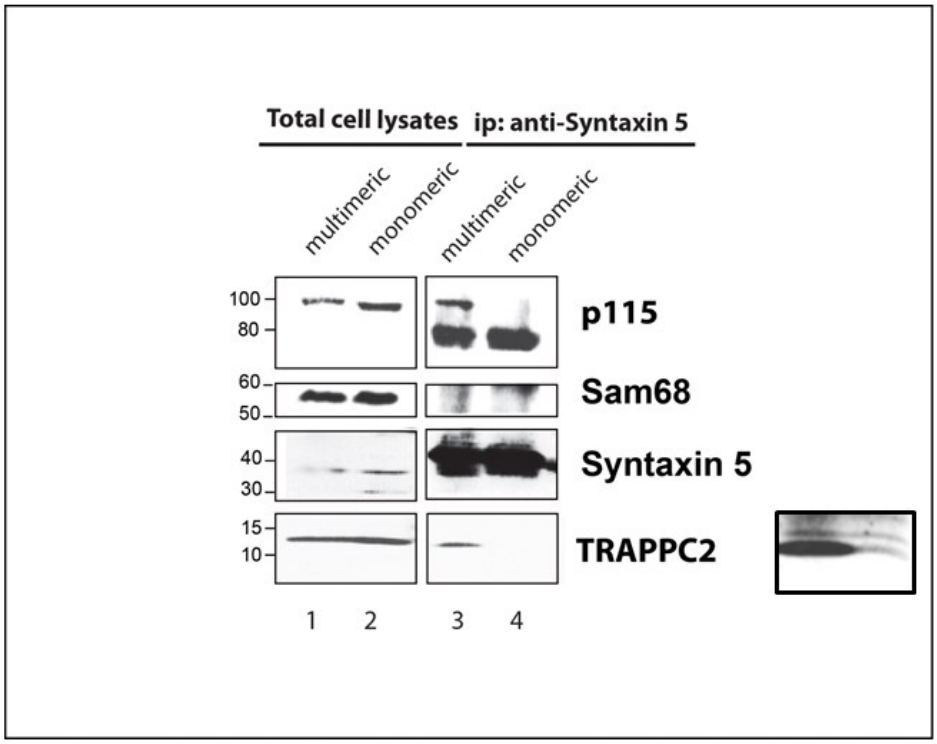

Figure 4.4 p115 and C2 associate with Syntaxin 5. Multimeric subunits of TRAPP complex interacts with an essential putative ER-Golgi tethering factor p115 along with ER-Golgi t-SNARE Syntaxin 5 in HEK293 cells. Total cell lysates are 10% of lysate subjected to co-IP (lanes 1 and 2). At higher exposure (shown on the right side of the C2 blot), a band for the monomeric form of C2 appears, but not for p115. Sam68 antibody is used as a negative control. Multimeric and monomeric populations are collected from fractions of high and low molecular weights respectively corresponding to TRAPP complex and monomers of TRAPP subunits and subsequently were used in co-IP (lanes 3 and 4).

4.3.3 Association of C2 with multiple Syntaxin 5-containing SNARE complexes

As previously mentioned (Figure 4.1), Syntaxin 5 is part of three distinct SNARE complexes. Thus, in order to assess whether a free form of Syntaxin 5 is associating with the TRAPP complex or interacting with its cognate SNARE complexes, immunoprecipitation analysis was performed using antibodies raised against SNARE proteins and probed for the

TRAPP complex component C2 as well as Syntaxin 5 (Figure 4.5). Immuno-isolation of Syntaxin 5 demonstrated that Bet1, membrin, Syntaxin 5 and GS28 were coprecipitated with C2. Bet1, membrin and Syntaxin 5 (Xu et al., 2000) are part of complex 1, acting in homotypic COPII vesicle fusion while GS28, Bet1 and Syntaxin 5 (Xu et al., 2000) constitute complex 2, proposed to be serving at the *cis*-Golgi interface. These data suggest that Syntaxin 5 interacts with TRAPP as part of a SNARE complex. Furthermore, TRAPP might be involved in multiple processes along with three distinct SNARE complexes.

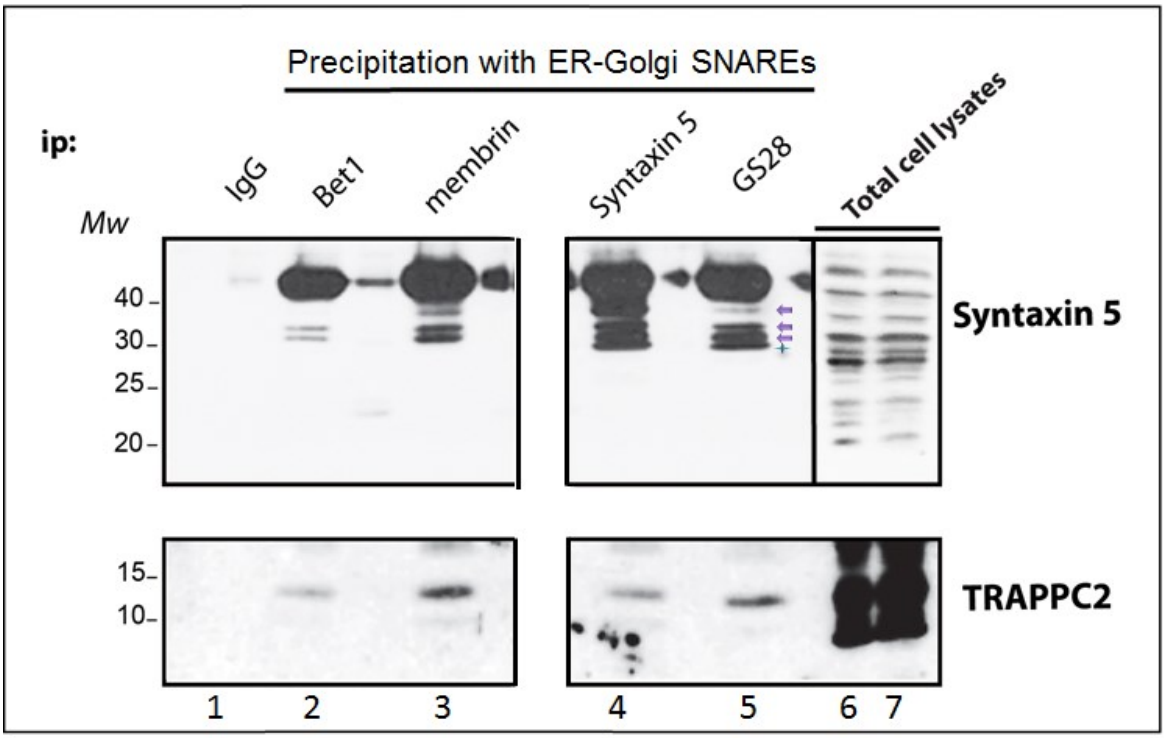

Figure 4.5 ER-Golgi SNARE complexes containing Syntaxin 5 coprecipitates with TRAPP. HeLa cells were lysed then the moncolonal Syntaxin 5 antibody was used to isolate endogenous ER-Golgi SNAREs (Bet1, membrin, Syntaxin 5, and GS28) along with a component of the TRAPP complex C2. Syntaxin 5 migrates at three different sizes: 30, 34, and 40 kDa (shown by pink arrows; green star is thought to be a degradation product). 10% of the inputs are shown in lanes 6 and 7 are subjected to co-IP.

4.3.4 TRAPP interacts with Syntaxin 5 while COPII vesicles are still coated

Coat depolymerisation was once thought to occur immediately upon COPII vesicle biogenesis. However subsequent studies indicated that coat proteins remains after budding. In support of this notion, TRAPP I (C3) was shown to directly interact with COPII subunit Sec23 (Cai et al., 2007b). Thus, this notion prompted me to determine whether TRAPP association to ER-Golgi SNAREs occurs in presence of transport vesicle coat proteins (shown in Figure 4.6). To test this idea, HeLa cells were treated with and without the fungal metabolite brefeldin A (BFA), which is known to disrupt the Golgi architecture (Klausner et al., 1992). Western blot analysis indicates that immunoprecipitation of anti-Syntaxin 5 not only pulls down C2 but it is also able to precipitate COPII component Sec23 (Figure 4.6).

These associations with Syntaxin 5 are BFA-resistant (Figure 4.6). In agreement with previous reports, C3 localization is also resistant to BFA (Yu et al., 2006). Since BFA induces dramatic morphological alterations in several intracellular compartments (Pelham, 1991), the BFA-resistance of C2 and Syntaxin 5 association with COPII suggests that this interaction might occur at BFA-resistant compartments such as ER exit site (ERES) or ERGIC and precludes the compartment sensitive to BFA treatment such as the *cis*-Golgi. Therefore, I postulate that TRAPP can act at the center of the membrane trafficking process by linking the components of the COPII machinery, small GTP-binding protein as well as membrane fusion at an early stage of the secretory pathway.

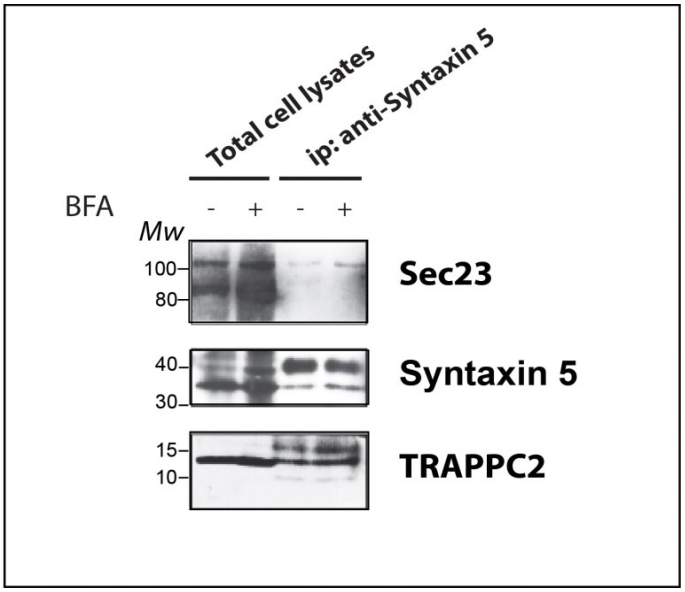

Figure 4.6 Syntaxin 5 binds to TRAPP and Sec23. This association is not disrupted in presence of BFA treatment. Prior to lysate preparation, HeLa cells were treated with or without BFA (10 µg/mL) and lysates were subjected to co-IP using Syntaxin 5 and probed for Sec23, Syntaxin 5 and C2.

4.3.5 SEDT-causing mutant C2D47Y enhances p115 membrane association

I then turned my attention to the membrane association and dissociation of tethering factor p115. The rationale for these experiments was that if p115 membrane targeting is regulated by Rab1 and SNARE complexes, then TRAPP may affect the cycle of on and off membrane dynamics of p115 due to its association with SNAREs. To test this hypothesis, C2-myc or the SEDT-causing C2D47Y-myc was overexpressed in HEK293 cells with or without Syntaxin 5 (Figure 4.7). Soluble and membrane fractions were separated by centrifugation and after loading equal amounts of total cell lysates in each set, the membrane- and soluble-associated form of p115 were assessed using p115 antibody. Interestingly, p115 membrane association was perturbed when the pathogenic D47Y-myc was overproduced (lanes 7-12); indicating that efficient cycling of membrane and cytosolic p115 is dependent upon C2. It further

suggests the membrane association of p115 in C2 D47Y-myc is antagonised by overexpression of Syntaxin 5 (compare lanes 9 to 12).

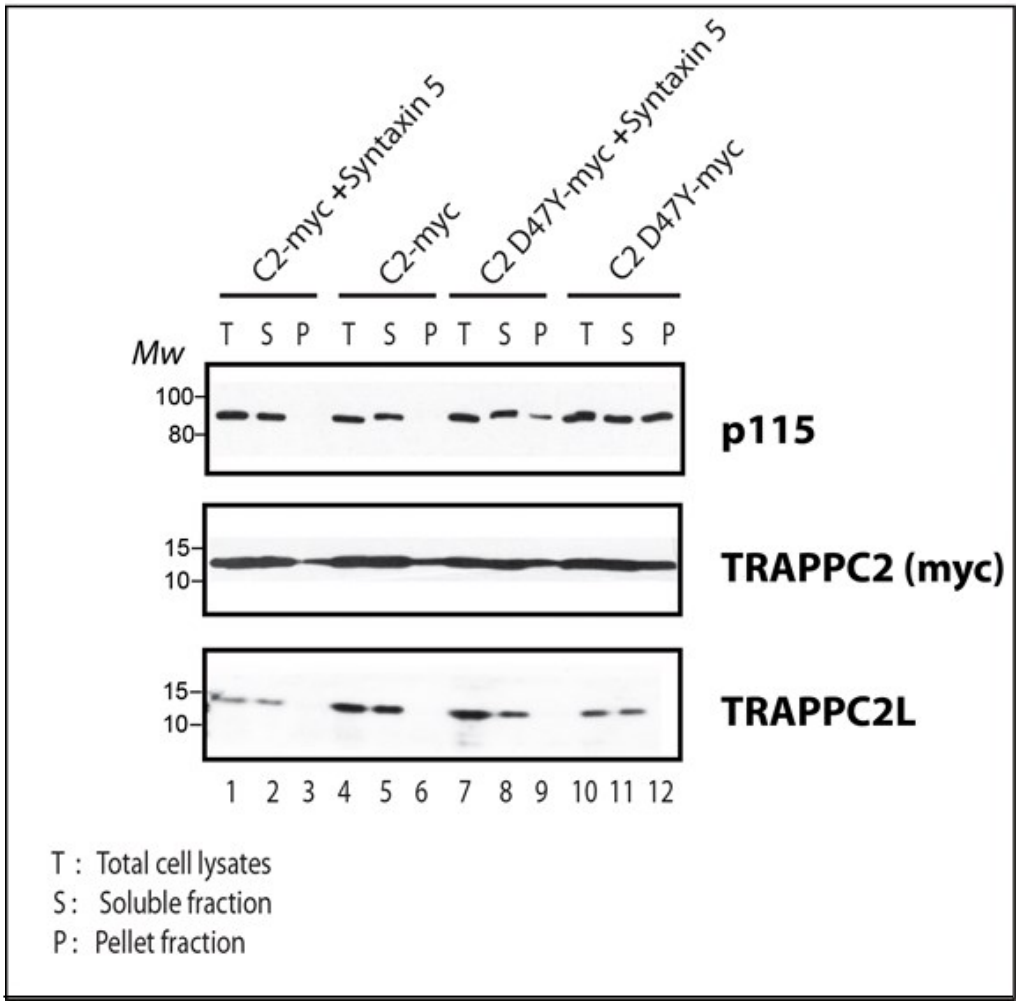

Figure 4.7 Membrane association of p115 requires C2. HeLa cells were transiently transfected with C2-myc with or without Syntaxin 5 (lanes 1-6); or X-linked SEDT causing mutation C2D47Y-myc in combination with or without Syntaxin 5 (lanes 7-12). Post-transfected cells were disrupted and subjected to cell fractionation. Membrane (pellet) and soluble fractions were separated and fractions were identified using antibodies against p115, myc and C2L.

4.3.6 C2 and p115 both have similar cellular distribution in human fibroblast cells

Because defining the localization of C2 using our home-made anti-C2 antibody was difficult in cultured cells such as HeLa and HEK293, primary cultures of skin fibroblasts were used (see Chapter 5). Interestingly, C2 and p115 staining showed a similar subcellular distribution (Figure 4.8). Co-localization is consistent with C2 and p115 association shown in Figures 4.2- 4.4.

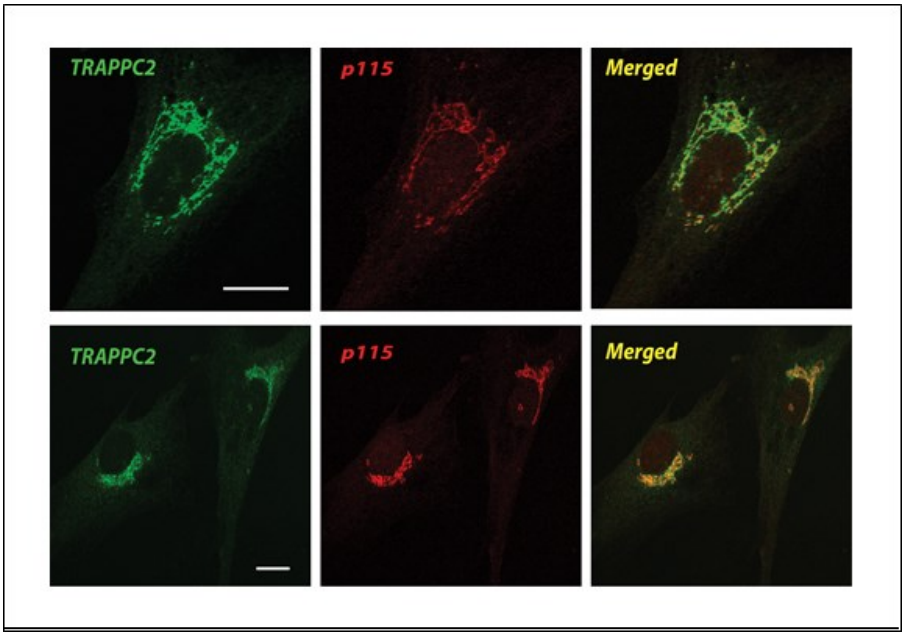

Figure 4.8 Co-localization of C2 and p115. Endogenous C2 and p115 co-localize in human primary skin fibroblast of a healthy volunteer; scale bars on top and bottom panels are 10 and 5 µm respectively.

4.4 Discussion

I previously showed that C2 binds to Syntaxin 5 (Chapter 3). Here I demonstrate a novel association between TRAPP and the ER-Golgi tethering factor p115. Syntaxin 5 antibody pulls down increasing amounts of p115 and C2 upon NEM treatment. Additionally, I presented evidence that these Syntaxin 5 binding partners are associating together. Further investigation is required to determine whether C2 and p115 are constituents of different Syntaxin 5-containing complexes or present in the same complex. In order to further characterize the state to which the C2-Syntaxin 5-p115 associates, I carried out gel filtration chromatography to discriminate TRAPP complexes from its monomeric species. The result indicated that p115 only associates with TRAPP in its complex form and not to its monomeric component C2.

I subsequently presented evidence in which Syntaxin 5 interacts with the TRAPP complex along with its cognate SNARE complexes (Figure 4.5). TRAPP may be involved in multiple processes in conjunction with three distinct SNARE complexes. The experiments were carried out with available antibodies against SNARE proteins and further examination is required to investigate the association of TRAPP with SNARE complexes (particularly using SNAREs specific to complex 2 and 3, Ykt6 and GS15, respectively).

Previous studies determined that TRAPP interacts with the COPII component Sec23 in yeast and mammals. Interestingly, while TRAPP binds to Syntaxin 5-containing SNAREs, the COPII subunit Sec23 also attached to a TRAPP-SNARE complex (Figure 4.6). Additionally, it was demonstrated that TRAPP-SNARE association to COPII is resistant to BFA treatment. Thus C2-Syntaxin 5-Sec23 association can potentially take place at ERES and/or ERGIC compartments. Along the same line, disruption of ERES using nocodazole or blockage of Sar1 activity would be useful to further distinguish the site of TRAPP-SNARE association to COPII.

Lastly, I have shown the SEDT-causing C2D47Y mutation enhances the membrane-bound fraction of p115 (Figure 4.7). This finding is significant since it reveals that the mechanism of p115 membrane retention involves C2. Considering the fact that p115 only associates with C2-containing TRAPP complex (Figure 4.4), it highlights a novel function of the TRAPP complex performed through the C2 subunit. p115 with its proposed function as a "flypaper" capturing free SNAREs (Grabski et al., 2012b) might facilitate the C2-Syntaxin 5 association and both TRAPP and p115 might be under the influence of SNARE proteins to be recruited to ERGIC and/or the Golgi membranes. Below I propose a preliminary model based on the current understanding in the field on multiple players of the early secretory pathway (Figure 4.9).

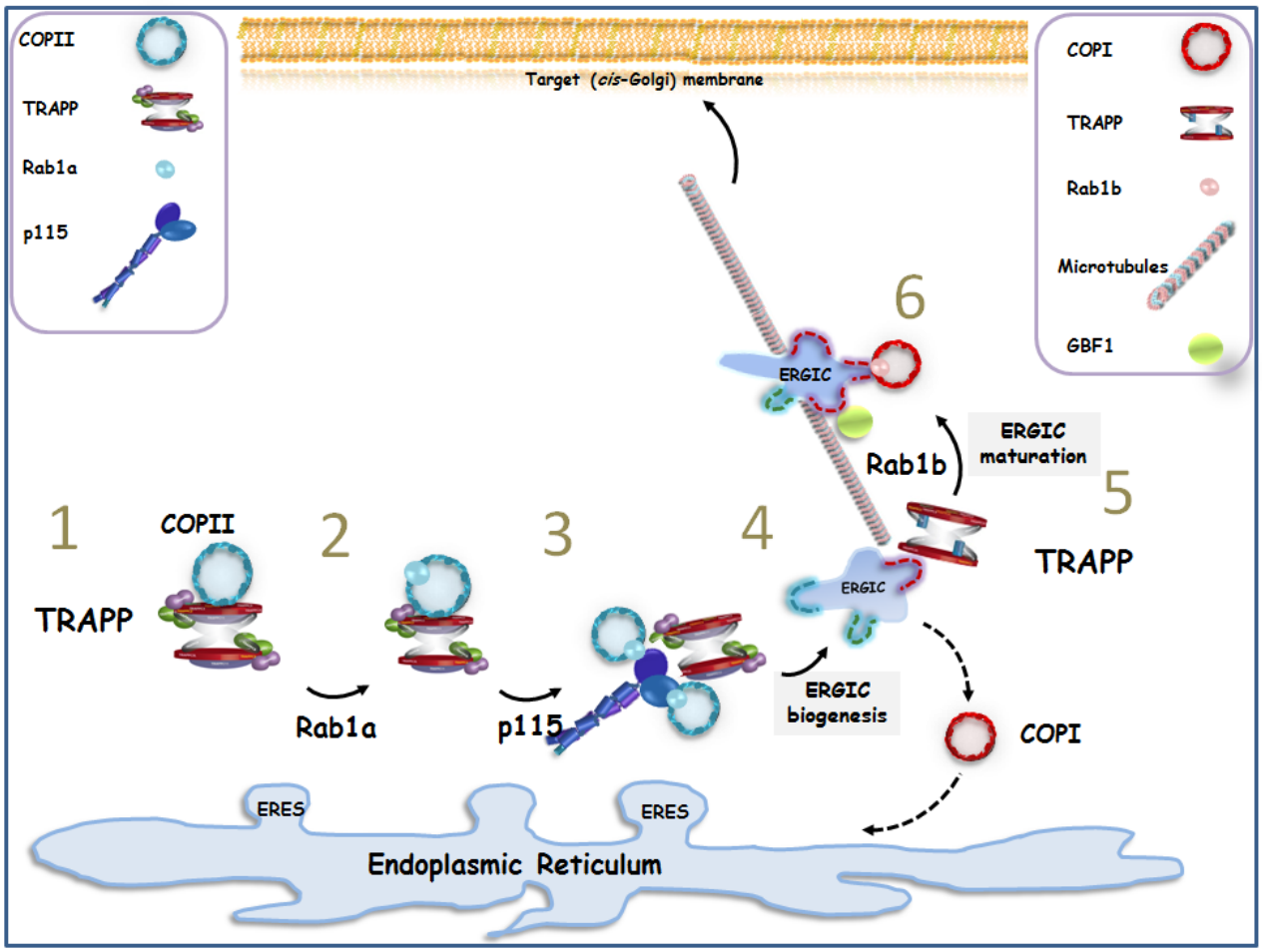

Figure 4.9 Schematic representation of the early secretory pathway. Traffic initiates at ER exit sites where COPII vesicles bud. (1) The TRAPP complex via its C3 subunit interacts with COPII vesicles (Yu et al., 2006). (2) Subsequently, TRAPP GEF activity results in activation of the small GTPase Rab1a (Yamasaki et al., 2009). (3) Activated Rab1a induces p115 recruitment onto COPII vesicles. (4) ERGIC formation results from homotypic fusion of COPII vesicles in a p115- and SNARE-dependent manner (Xu and Hay, 2004). Currently, it is not clear how anterograde trafficking of COPII vesicles, once fused with ERGIC membranes, continues its joinery toward the *cis*- Golgi. However there is evidence to suggest that during ERGIC maturation a number of proteins, in sequential transport stages, are recruited to this compartment thus providing acquisition of COPI vesicles onto the ERGIC. For instance, (5) TRAPP II via the C9 subunit interacts with components of minus-end-directed dynein to move these vesicles towards the *cis*- Golgi and the microtubule organizing center (Zong et al., 2012). (6) Rab1b recruits the Arf GEF GBF1 and activation of Arf1 GTPase is followed by COPI recruitment onto the ERGIC (Garcia et al., 2011). It is worth mentioning that GBF1, but not

Rab1b, recruitment is BFA-sensitive. Dashed lines indicate COPI vesicles originating from ERGIC recycling back to the ER to return ER-resident proteins. The relationship between ERGIC and the Golgi is not clear, however live cell microscopy showed that cargo is not diluted upon reaching the Golgi (Presley et al., 1997), indicating that ERGIC membranes fuse to each other as opposed to fusion of ERGIC to pre-existing Golgi. The positions depicted for TRAPP II and TRAPP III are not known. However in Chapter 2 I have presented data suggesting that a fraction of the TRAPP complex resides on very light density membrane, possibly COPII vesicles.

CHAPTER 5

Recessive *TRAPPC11* mutations cause a disease spectrum of limb girdle muscular dystrophy and myopathy with infantile hyperkinetic movements and intellectual disability

In the following chapter I will discuss our discoveries into the function of TRAPPC11, some of which have been incorporated in a publication in the *American Journal of Human Genetics* (Bogershausen et al., 2013). The genetic component of this work was conducted by our collaborators from Alberta who used homozygosity mapping in combination with exome sequencing in two affected siblings from a Hutterite family to find that the candidate gene is mutated in *TRAPPC11*. Two additional Syrian families with a *TRAPPC11* point mutation, though in a different region (C-terminus) compared to the Hutterite mutation, were also found and the results will be briefly discussed. My contribution to the figures is as follows: Figures 5.1- 5.15 were conducted by myself and live cell imaging was performed by myself and Gabriel Lapointe. Figures presented in this chapter are all published except for Figures 5.7, 5.14 and 5.15 and I am co-first author on this manuscript.

5.1 Introduction

Intellectual disability (ID) is defined as an intelligence quotient <70 and significant limitations in two or more adaptive skills identified in childhood and is found in 1-3% of the general population (Kaufman et al., 2010). ID is etiologically heterogeneous with genetic and non-genetic causes and can be found as the sole clinical feature in non-syndromic ID or as part of a syndrome with other clinical manifestations. Over the past decade much effort has gone into unravelling the genetic complexity of ID such that ID is now one of the most genetically heterogeneous disorders. Autosomal recessive, autosomal dominant and X-linked inheritance patterns have all been documented and over 100 responsible genes have been identified, yet the underlying cause of ID is found in only 15% of patients (de Ligt et al., 2012). Disruption of a

number of cellular and embryological processes have been linked to ID and include metabolism, transcription (including epigenetic modifications), translation, neuronal development and maturation (including transcription factors), development, intracellular signalling, as well as intracellular trafficking (van Bokhoven, 2011;Kaufman et al., 2010). We report on the clinical, molecular, and cellular phenotype of a novel ID pathway demonstrating that altered vesicle trafficking downstream of the Golgi results in a syndrome that includes intellectual disability, hyperkinetic movements, myopathy, and ataxia.

5.2 Materials and Methods

All experiments conducted in this chapter used skin primary fibroblast cells from control and patients (2:II-6 and 2:II-8). Cells were plated on 6-well dishes with coverslips in a 37°C incubator unless otherwise mentioned.

5.2.1 Fluorescence microscopy

Cells were grown to 60-70% confluency in Dulbecco's modified Eagle's medium (DMEM) containing 10% fetal bovine serum (FBS). For treatment with microtubule the disrupting agent (Figure 5.15), 10 μM of Nocodazole (gift from Dr. Alisa Piekny) was added to the cells for 1 hour. Cells were then washed with ice-cold phosphate-buffered saline (PBS), and fixed for 20 minutes at room temperature with freshly prepared 4% paraformaldehyde (PFA). Cells were then permeabilized with ice-cold methanol for 4 minutes at -20°C and washed thoroughly in PBS. Cells were subjected to one hour blocking solution (2% FBS, 2% bovine serum albumin (BSA), and 0.2% fish skin gelatin) at room temperature. Diluted primary antibodies were used as follows: GM130/ MLO7 at 1:250 (rabbit, kind gift of Dr. Martin Lowe); Mannosidase II at 1:300 (rabbit, kind gift of Dr. Kelley Mormen); EEA1 at 1:400 (mouse, BD Biosciences 610456); LAMP1 at 1:150 (rabbit, ab24170); Rab9 at 1:300 (mouse, ab2810), TGN46 at 1:150 (rabbit, AB16052). Immunostaining was conducted as described (Scrivens et al., 2011). All images were acquired on a Leica TCS SP2 laser scanning confocal microscope at 63X magnification except for Figure 5.3 which represents an epifluorescence image using a Zeiss Axioplan microscope.

5.2.2 Preparation of total cell lysates

Lysate for size exclusion chromatography was prepared with lysis buffer (150 mM NaCl, 0.5 mM EDTA, 50 mM Tris, pH 7.2, 1% Triton X-100, 1 mM dithiothreitol [DTT], one tablet of EDTA-free protease inhibitor) and a total protein of 2 mg were fractionated on a Superose 6

column. For western blot analysis the lysate was prepared as above and probed with TRAPPC11 antibody. Samples were heated for 2 minutes at 95°C with Laemmli sample buffer prior to loading on an SDS-polyacrylamide gel. Coimmunoprecipitations were conducted as previously described (Scrivens et al., 2011).

5.2.3 Transferrin trafficking assay

Cells were grown on a 6-well dish with coverslips. One hour prior to initiating the trafficking assay, cells were placed in serum free-DMEM. Subsequently cells were allowed to internalize Alexa-Fluor-448-EGF or Alexa-Fluor-546-transferrin (Tfn) (both courtesy of Dr. Peter McPherson) at 10 µg/mL for 15 and 30 minutes. Samples were prepared, for fluorescence microscopy as stated above.

5.2.4 ts045-VSV-G-GFP trafficking assay

Cells were infected by adenovirus (a generous gift from Dr. Martin Lowe) encoding a temperature-sensitive mutant of the vesicular stomatitis virus glycoprotein fused with GFP (ts045-VSV-G-GFP) and the cells were followed either in real time or fixed at specific times (Figure 5.1).

5.2.4.1 Preparation of ts045-VSV-G-GFP virus

HEK293 cells at 70% confluencey were prepared in collagen-coated 75 cm bottles. A 50 µL aliquot of ts045-VSV-G-GFP diluted with 2 mL DMEM (supplemented with 5% FBS) was added to the cells and incubated for 1 hour at 37 °C. At the end of 1 hour, 13 mL of DMEM + 5% FBS were added to the infected cells. After 4 days, the cells and culture supernatant were recovered in a 50 mL falcon tube. 6 cycles of freeze and thaw were applied using liquid N_2. The samples were centrifuged (3000 rpm, 10 minutes) and the supernatant was aliquoted.

5.2.4.2 ts045-VSV-G-GFP trafficking assay

Human skin fibroblasts were incubated with 50 µL of virus solution for each well in a 6-well dish for 1 hour at 37°C with occasional tilting. Following 1 hour of infection, 2 mL of DMEM + 10% FBS was added to the cells. The following day (~18 hours post-infection) the cells were transferred to a 40°C incubator for 6 hours to ensure that the ts045-VSV-G-GFP was retained in the ER. At the end of 6 hours, 10 µg/mL cycloheximide was added and rapidly transferred to a 32°C incubator to allow the release of trafficking. One coverslip was immediately fixed (0 time point). For the remainder of the coverslips, cells were fixed and prepared for immunostaining with the Golgi *medial* marker ManII at the time points indicated below. The Golgi was then counter stained using a *medial* Golgi marker and co-localization with ts045-VSV-G-GFP was assessed at 0, 30, and 120 minutes after shifting to the permissive temperature.

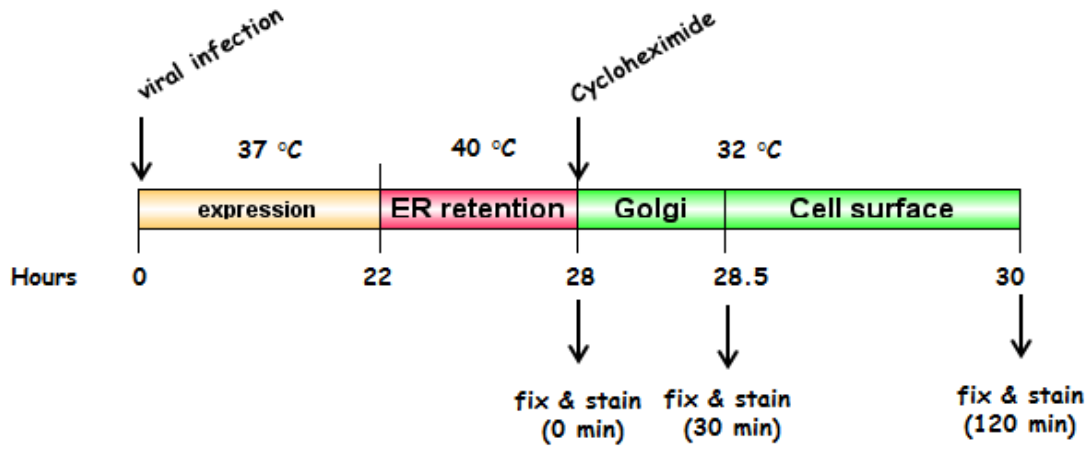

Figure 5.1 Schematic representation of the ts045-VSV-G-GFP trafficking assay. Cells were infected and allowed to express the GFP-tagged ts045-VSV-G. This was followed by a 6 hour incubation at restrictive temperature. After cycloheximide addition, the cells were shifted to permissive temperature and fixed and stained with the Golgi *medial* marker ManII at the indicated time points. The different time points were chosen empirically.

5.3 Results

5.3.1 Mutation in *TRAPPC11* causing a partial deletion in the highly-conserved *foie gras* domain

Two families with a total of five affected children were independently examined due to longstanding histories of moderate ID, ataxia and muscle weakness. These families are all of Hutterite ancestry (Hostetler et al., 1985;Boycott et al., 2008) and have remained largely genetically isolated from one another. Although the two families were not closely related, a founder mutation with an autosomal recessive mode of inheritance was suspected because of the Hutterite's history of genetic isolation. One family consists of two affected brothers (designated as 2:II-6 and 2:II-8) and their affected first cousin from the Hutterites of Alberta, in which the phenotypes of the two brothers at both the molecular and cellular levels will be presented in this chapter. The other family consists of two affected siblings (one male, one female) from the Hutterites of South Dakota.

As young adults all affected individuals now have obvious mild to moderate intellectual disability. As young children, they all had significant evidence of a hyperkinetic movement disorder. Age of walking was delayed and although the hyperkinetic movements have improved, all patients continue to have gross and fine motor difficulties. Mild muscle weakness with persistently elevated creatine kinase (CK) levels suggested an associated myopathy with non-specific myopathic changes uncovered by muscle biopsy.

TRAPPC11 (hereafter *C11*) is a 32-exon gene and the first pathogenic mutation to be reported for *C11* was identified in two brothers from Huteritte families by means of homozygosity mapping and exome sequencing. RT-PCR revealed that this mutation (C.1287+5G>A) results in mis-splicing and an in-frame deletion of 58 amino acids (372-429) comprising both exons 11 and 12, in the highly conserved *foie gras* domain of C11 (Figure 5.2).

Once the candidate gene was revealed to be *C11*, primary skin fibroblasts from the two affected brothers and from a healthy volunteer were obtained and cultured in our laboratory. My work in this portion of my thesis revolved around further biological and functional characterization of C11 from these samples.

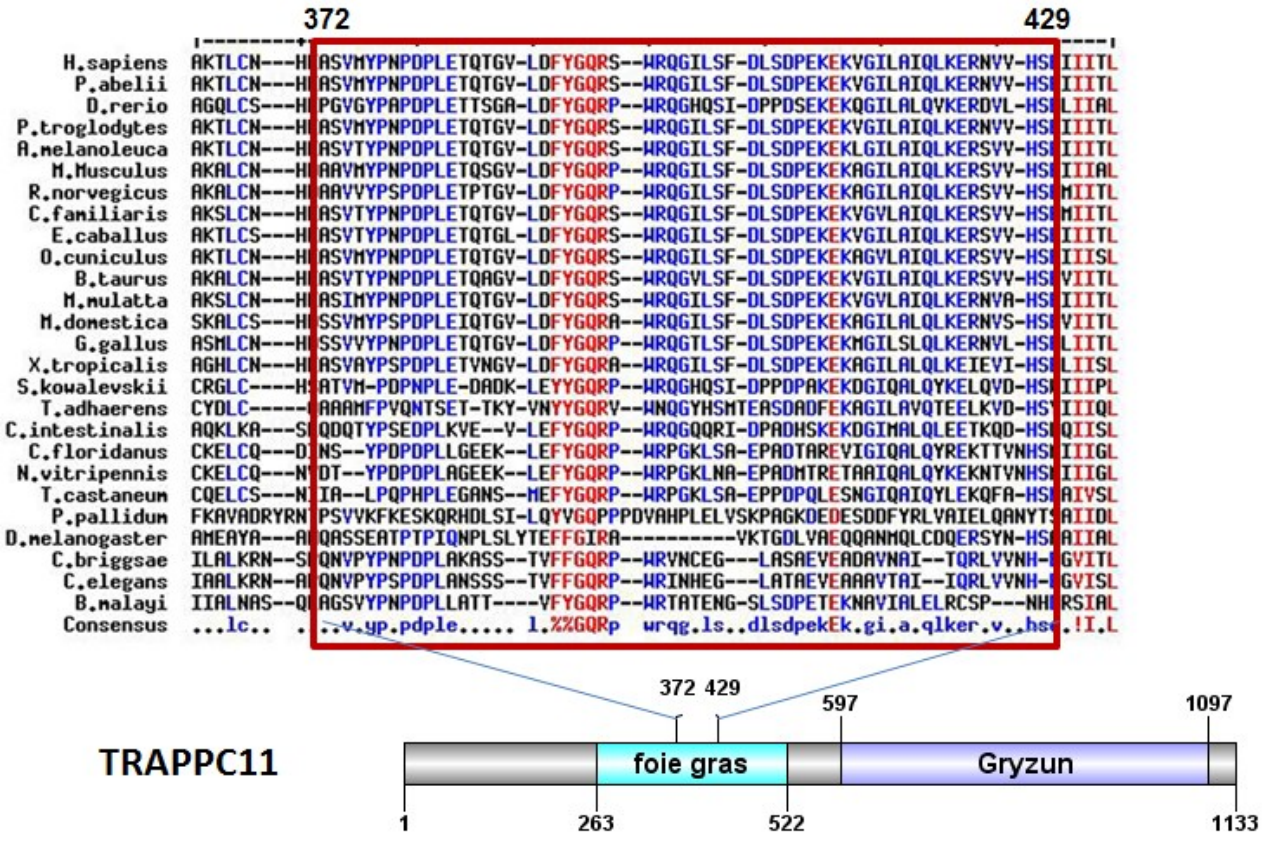

Figure 5.2 The *foie gras* domain of C11 is highly conserved. Multiple sequence alignment of C11 (adapted from R. Lamont) indicating conservation of this region across evolution, suggesting a critical role might be attributed to C11 in normal cellular function. A schematic of the C11 protein, indicating the highly-conserved foie gras domain and the region deleted due to the splicing defect (amino acids 372-429) is also shown.

C11 (transport protein particle complex 11) has been shown to play a role in vesicle trafficking to the membrane in both human and *Drosophila* cells (Scrivens et al., 2011; Wendler et al., 2010;) and was recently characterized as a component of TRAPP (transport protein particle), a multisubunit complex implicated in vesicle-mediated membrane trafficking (Yu and Liang, 2012;Sacher et al., 2008). C11 participates in numerous interactions with other TRAPP complex family members, most notably C2, C2L, C6, C10 and C12 (Scrivens et al., 2011). Mutations in TRAPP complex members, *C2* and *C9*, result in X-linked spondyloepiphyseal dysplasia tarda and non-syndromic ID, respectively (Gedeon et al., 1999; Mir et al., 2009; Najmabadi et al., 2007). Loss of function mutations in the zebrafish homolog of C11 have been found in the *foie gras* mutant, characterized by hepatomegaly from steatohepatitis and eye development defects (Sadler et al., 2005 ;Gross et al., 2005). We do not observe any liver or eye phenotypes in our patients; however, this may reflect complete loss of function in the zebrafish model compared to the presumed hypomorphic nature of the in-frame deletion identified in our patients.

5.3.2 Golgi organization is under influence of the intact TRAPP complex

Since small interfering RNA-mediated (siRNA) knockdown of *C11* leads to Golgi fragmentation (Scrivens et al., 2011), we examined the state of the Golgi in primary fibroblasts from the two brothers from family 1 (herein referred to as patients 2:II-6 and 2:II-8). Compared to control fibroblasts, the Golgi in both patients appeared more fragmented using the marker proteins GM130 (Figures 5.3) and Mannosidase II (ManII; data not shown). Quantitation of the fragmented phenotype indeed showed a higher percentage of cells with a fragmented Golgi (Figure 5.4), consistent with results from previous *C11* knockdown experiments. Three-dimensional reconstruction of the Golgi confirmed that the fragmentation was due to fewer and/or thinner connections between the GM130-positive structures (Figure 5.4).

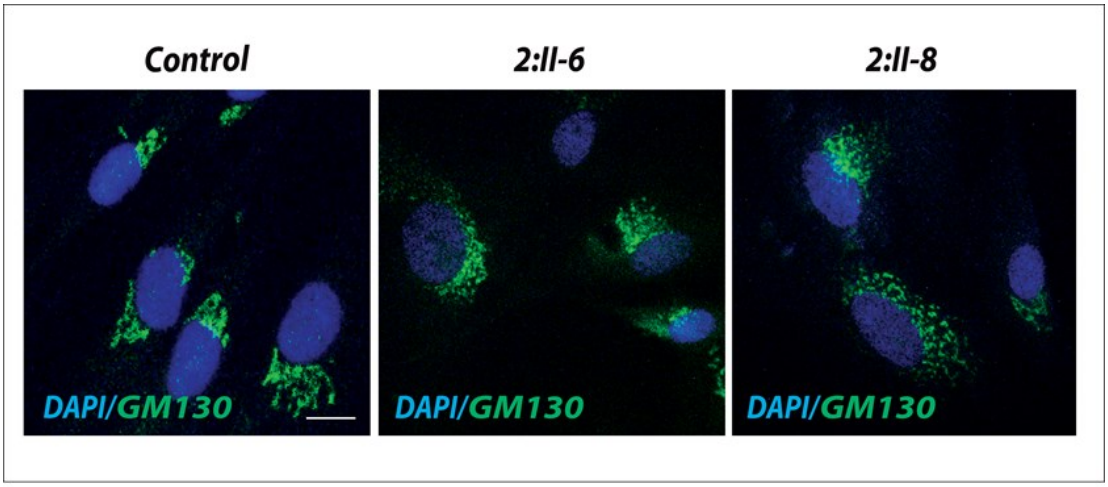

Figure 5.3 The Golgi integrity is dependent upon C11. Immunofluorescence of the Golgi apparatus and nucleus by GM130 and DAPI, respectively, in primary skin fibroblasts from affected (2:II-8, 2:II-6) and unaffected (control) individuals. Scale bar represents 10μm.

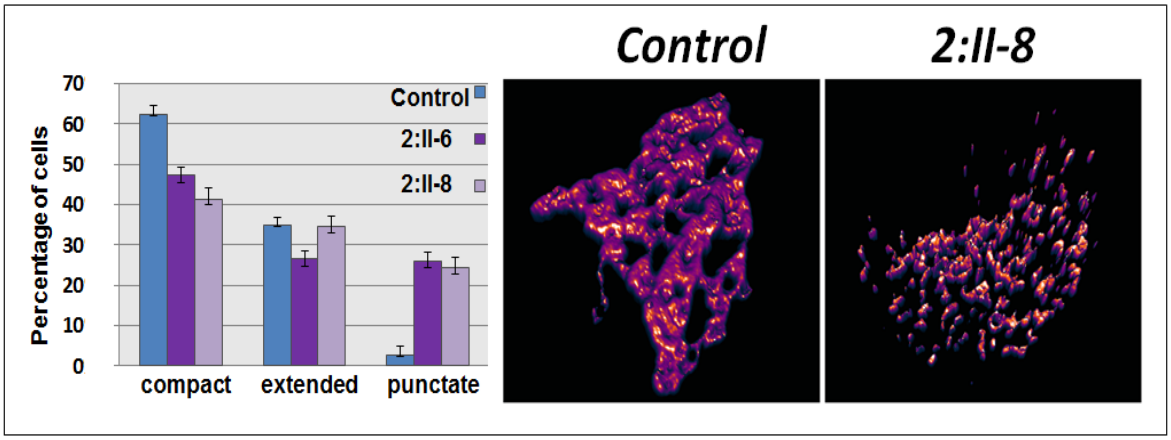

Figure 5.4 Quantification of Golgi morphology. Quantification of the Golgi morphology was performed using the same criteria as in Figure 2.17. Also shown is a three dimensional (3D) reconstruction of the Golgi apparatus using confocal z stack images generated in control and patient cells (2:II-8) by Fiji software. A minimum of 300 cells for each sample was quantified over three independent expriments.

5.3.3 Partial deletion of the *foie gras* domain results in C11 protein instability and perturbed assembly of the TRAPP complex

To assess the effect of the C11 in-frame deletion on the TRAPP complex, C11 was immunoprecipitated from lysates prepared from control and patient cells and probed for the TRAPP complex member C2 that co-precipitates with C11. Although equal amounts of C2 are present in the starting material, patient cells showed significantly less C2 co-precipitating with C11 (Figure 5.5), suggesting that C11 is either unstable or that the levels of C11-C2-containing TRAPP complexes are reduced. Consistent with the former notion, western blot analysis of lysates from control and patient cells indicate reduced levels of C11 in patient cells (Figure 5.6).

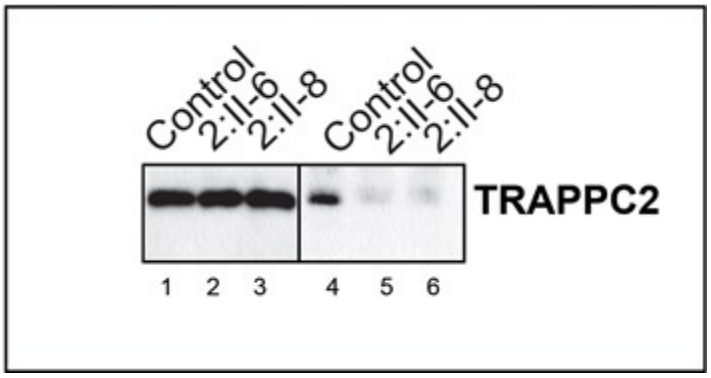

Figure 5.5 Loss of interaction of C11 with C2 in affected patient cells. Inputs (10%) were loaded (lanes 1-3) and equal amounts of total lysates in control and affected individuals were used in the immunoprecipitation.

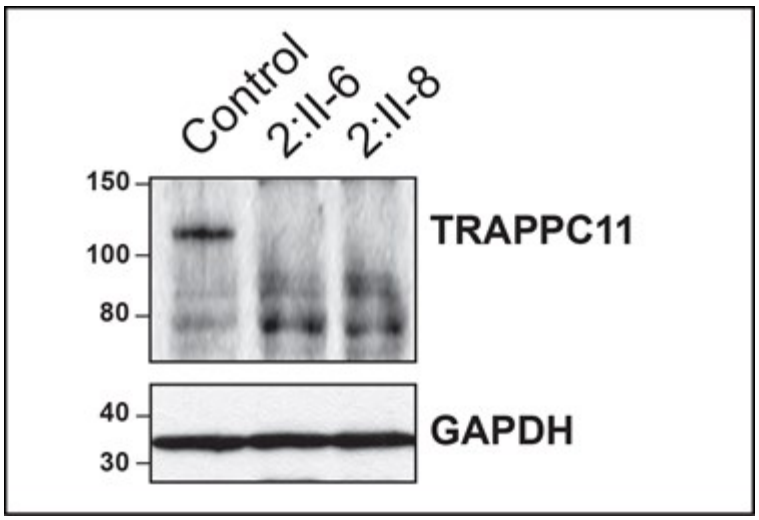

Figure 5.6 Partial deletion of the *foie gras* domain affects C11 stability. Total cellular level of C11 was estimated in control and affected (2:II-6, 2:II-8) individuals. GAPDH was used as a loading control. Note the loss of full-length C11 immunoreactivity and the appearance of presumably truncated versions of C11.

As a further confirmation that TRAPP assembly is compromised in the presence of this C11 mutation, we examined the fractionation of TRAPP in lysates prepared from affected and non-affected individuals using size exclusion chromatography. Consistent with Figure 5.6, a single band for C11 at fractions 16-19, where the mammalian TRAPP complex fractionates, was seen in the control sample while the affected individuals (2:II-6 and 2:II-8) exhibited multiple bands. In addition a subtle shift which begins trailing off in fractions 17 to 22 was also noted. Consistent with the fractionation of a C11 knock down observed in our previous publication (Scrivens et al., 2011), a subtle shift for the C2 protein was also seen (Figure 5.7). This suggests that the assembly of the TRAPP complex has been compromised in the patient cells.

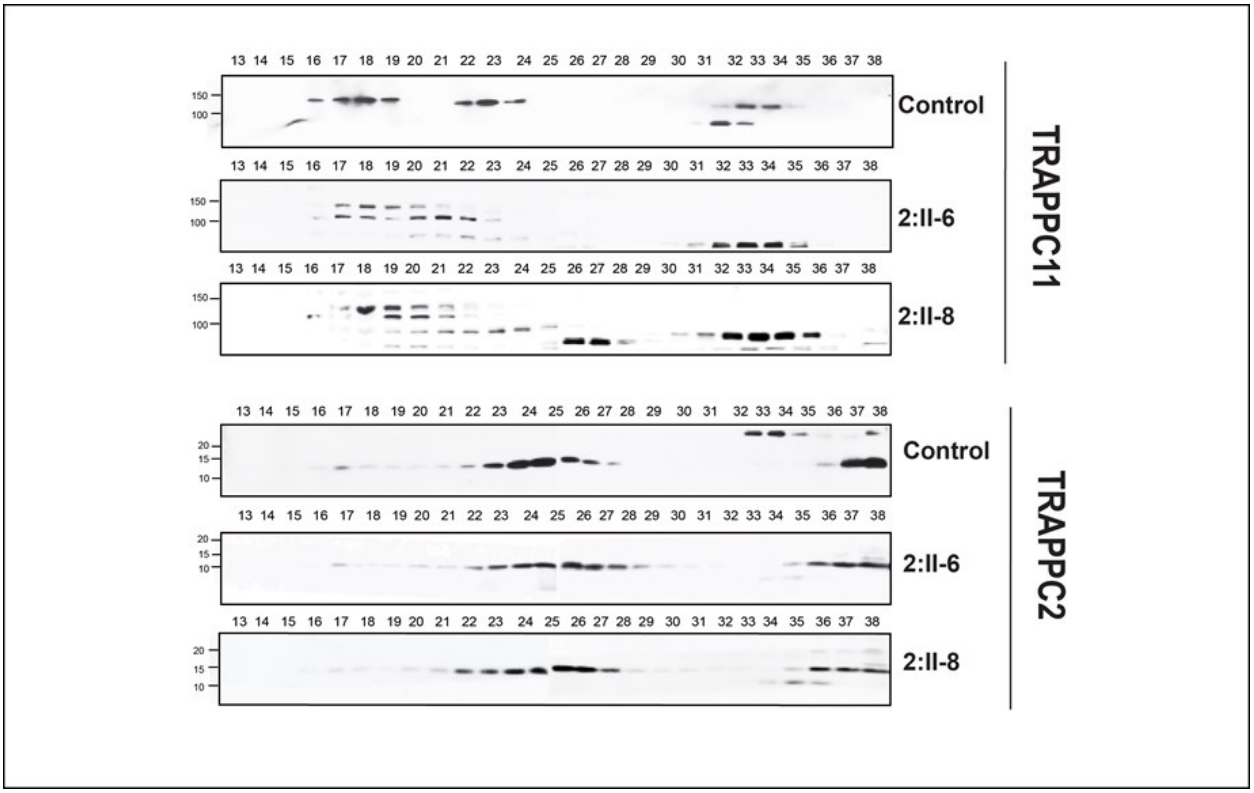

Figure 5.7 Partial deletion of the *foie gras* domain results in a perturbation of the TRAPP complex. Lysates from affected and unaffected individuals were fractionated on a Superose 6 column and fractions were probed for C2 and C11. Note the difference in fractions 16-19, where the TRAPP complex fractionates, between control and affected individual samples.

5.3.4 Partial deletion of the *foie gras* domain results in impaired exit from the Golgi

Scrivens et al. (2011) have shown that siRNA knockdown of *C11* leads to Golgi fragmentation and perturbed membrane trafficking between the endoplasmic reticulum (ER) and the Golgi (Scrivens et al., 2011). Thus, we investigated if patient cells also displayed a block in transport between these two compartments. We used the ts045-VSVG -GFP (VSV-G) marker to investigate transport along the secretory pathway. This commonly used marker protein mis-folds at elevated temperatures (40°C) and is retained in the ER. Upon shifting to lower temperature (32°C) and in the presence of the protein synthesis inhibitor cycloheximide, the ER-restricted material exits and is transported to the Golgi and ultimately to the cell surface (Bergmann et al.,

1983). The kinetics of this transport is well documented with appearance of the protein in the Golgi within minutes of release, where it can reside for up to 40 minutes before transport to the cell surface (Hirschberg et al., 1998). To determine the effect of the *C11* mutation on ER-Golgi trafficking, we assessed VSV-G localization at fixed intervals in patient and control fibroblasts, in conjunction with the Golgi marker ManII. After incubation at 40°C, VSV-G is found exclusively in the ER in both control and patient cells, displaying the typical diffuse, reticular pattern (Figure 5.8). Co-localization of VSV-G with the Golgi marker ManII is clearly seen after 30 minutes following release from the ER at 32°C in both control and patient cells (Figure 5.8). After 120 minutes, however, virtually all of the VSV-G is found on the cell surface of control cells while a significant amount of VSV-G remains in the Golgi of patient cells (Figure 5.8).

Live-cell imaging confirmed delayed VSV-G exit from the Golgi in patient cells, pronounced from approximately 90 minutes, consistent with the findings of the timed intervals above (http://www.cell.com/AJHG/supplemental/S0002-9297(13)00273-5). In the movie additional information was gained since vesicles or carriers moving in several directions and not fusing with the PM were observed. The delay of VSV-G exit from the Golgi in patient cells suggests that generalized trafficking of molecules through the Golgi may be delayed in patient fibroblasts as a result of the in-frame deletion within the *foie gras* domain of C11.

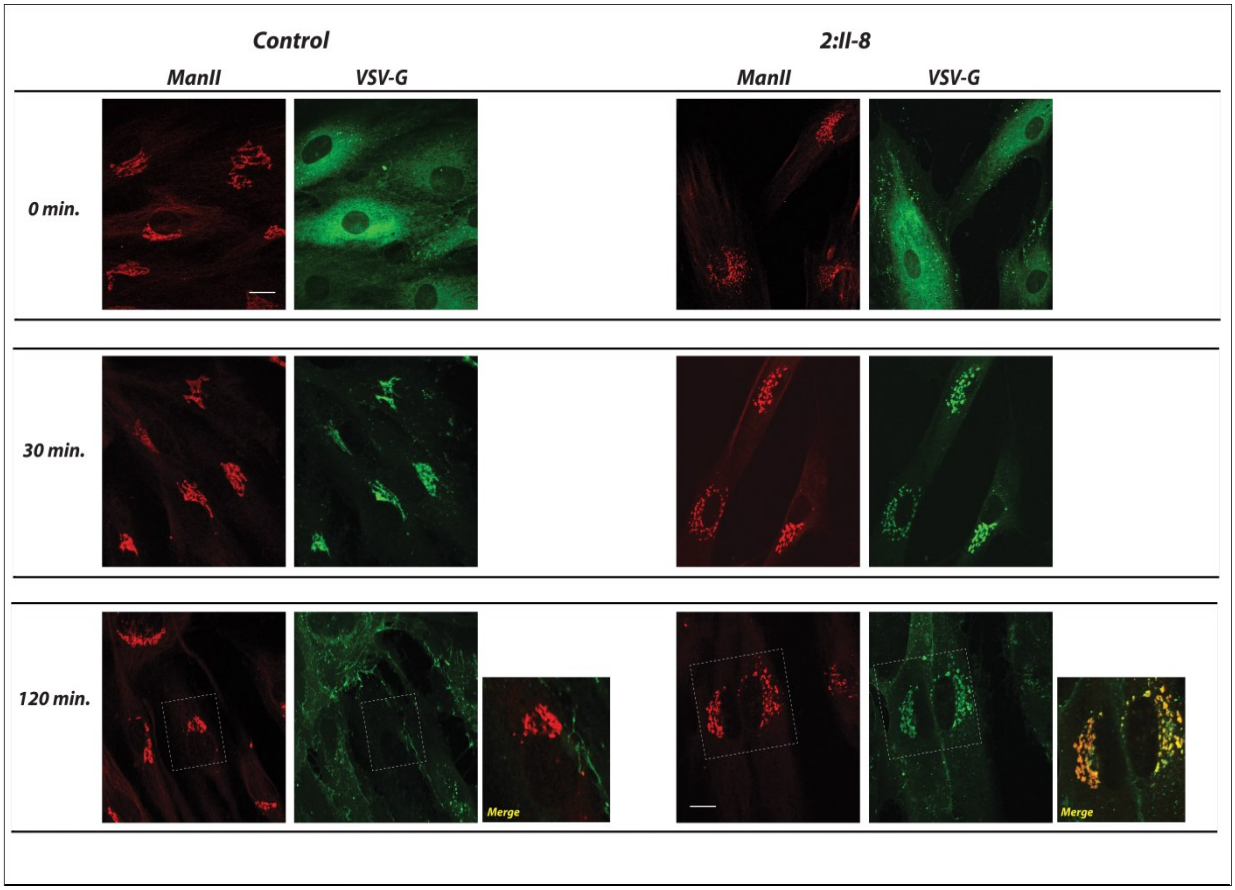

Figure 5.8 Transport of ts045-VSV-G-GFP is markedly reduced in patient cells lacking a portion of the *foie gras* domain. Note the white boxed area in patient cells at 120 minutes where ts045-VSV-G-GFP colocalized with the Golgi marker ManII, while in the control samples the ts045-VSV-G-GFP had reached the surface of the cells and none is colocalizing with the Golgi marker. The scale bar represents 10 μm.

5.3.5 Partial deletion of the *foie gras* domain from C11 does not interfere with internalization and early recycling pathways

Delayed exit from the Golgi could arise from a defect in anterograde traffic from the Golgi to the cell surface or indirectly from defects in the endocytic pathway that would fail to retrieve material from the Golgi needed for anterograde traffic. To determine if the trafficking defect observed in patient cells was due to defects in the endocytic pathway, we examined the

uptake of fluorescently-tagged transferrin (Figure 5.9) and EGF (data not shown) from the cell medium, but did not observe any uptake defects.

(A)

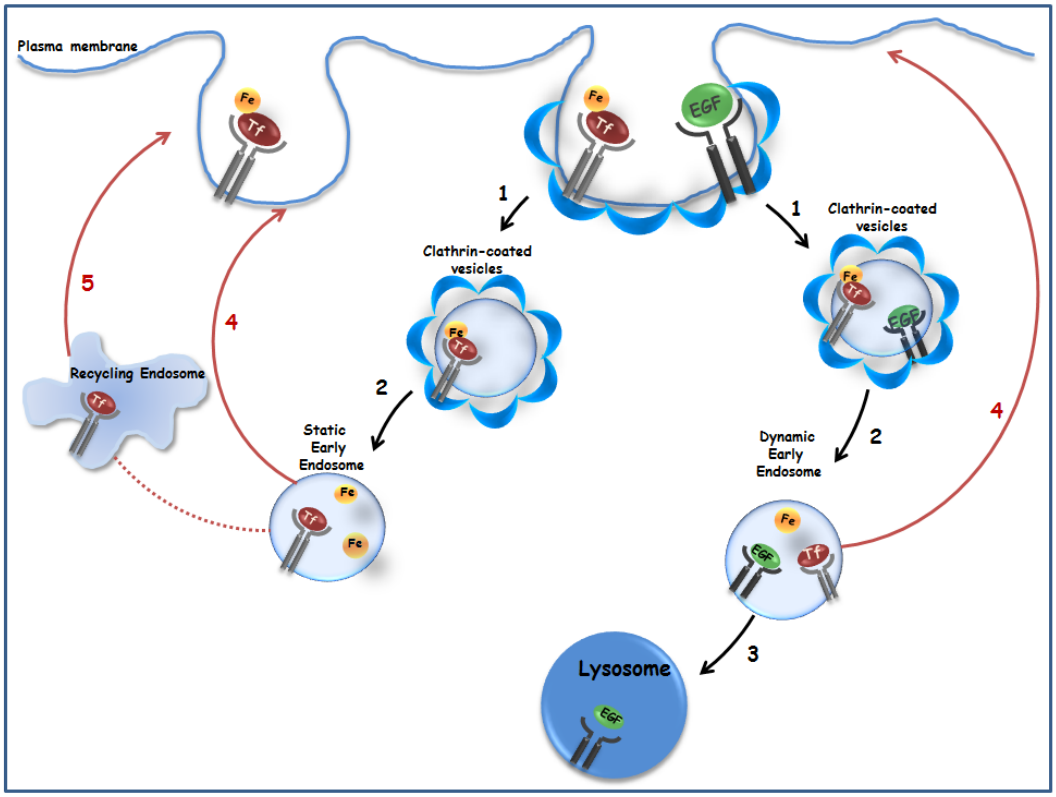

(B)

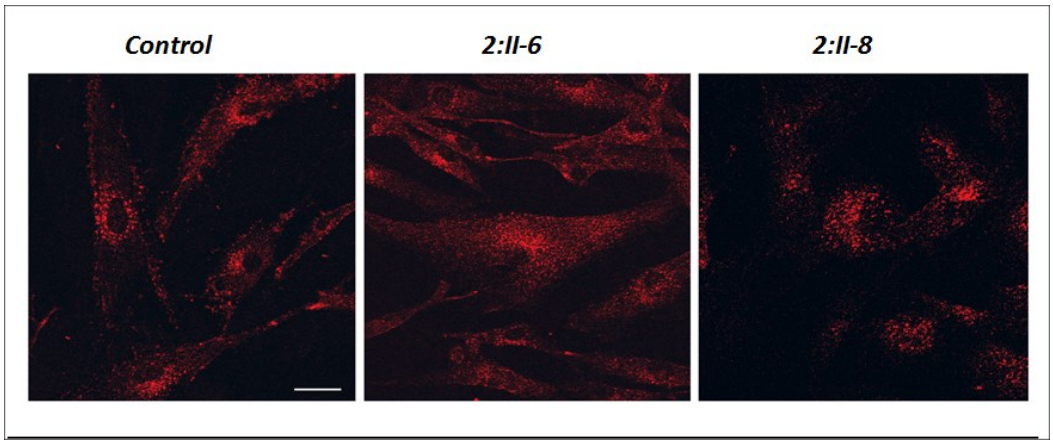

Figure 5.9 Partial loss of the *foie gras* domain does not affect transferrin uptake. (A) Internalization can occur by means of clathrin (Step 1) or clathrin-independent pathways. Tf-Tf receptor (TfR) complexes are present in both static and dynamic populations of early

endosomes (EE) (Step 2). Alternatively, EGF-EGF receptor complexes exist in dynamic EE which mature into lysosomes (Step 3). Tf-TfR complexes return to the cell surface from both forms of EE called fast recycling (Step 4), or after transit through recycling endosome known as slow recycling (Step 5). (B) Early recycling and internalization are normal in fibroblast patient cells. After a 15 minute incubation at 37°C with fluorescently-tagged surface ligand, transferrin did not display any alteration in patient cells compared to controls neither in internalization nor in recycling. The scale bar represents 10 μm.

5.3.6 Partial deletion of the *foie gras* domain from C11 interferes with late endosome/lysosomal trafficking

Having ruled out a defect in the early endocytic pathway, we next examined markers for other structures in the endocytic pathway including TGN46, Rab9, EEA1, and LAMP1. Staining patient cells for LAMP1, a marker of late endosomes/lysosomes, identified a striking difference in the localization pattern compared to control cells (Figure 5.10). LAMP1 in control cells was concentrated in puncta throughout the cell with the occasional deposition in a perinuclear region (24±1% of control cells (N=189)). Conversely, fibroblasts from patients displayed prominent perinuclear staining for LAMP1 in a high proportion of cells (78±2% and 87±3% of cells in patients 2:II-6 and 2:II-8, respectively (N=189 for all cases)) (Figure 5.11).

Immunostaining of patient cells as well as immunoblotting of patient cell lysates showed a reduced level of LAMP1 compared to control (Figures 5.10 and 5.12). Interestingly, as opposed to the broad molecular size seen in control cells, LAMP1 from patient cells was concentrated in the higher molecular size region, suggesting it may be more highly glycosylated (Figure 5.12). A similar phenotype was also observed for the related protein LAMP2, although the levels of the protein do not appear to be dramatically reduced as LAMP1 (Figure 5.12). Hyperglycosylation could result from either an increased residence time of LAMP1 and LAMP2

in the Golgi, in accordance with the VSV-G results above, or mis-localization of Golgi-resident glycosylation enzymes such that LAMP1 and LAMP2 continue to be glycosylated outside of the Golgi. In contrast, no obvious changes were observed in the distribution of the early endosomal marker EEA1 in patient fibroblasts (Figure 5.10).

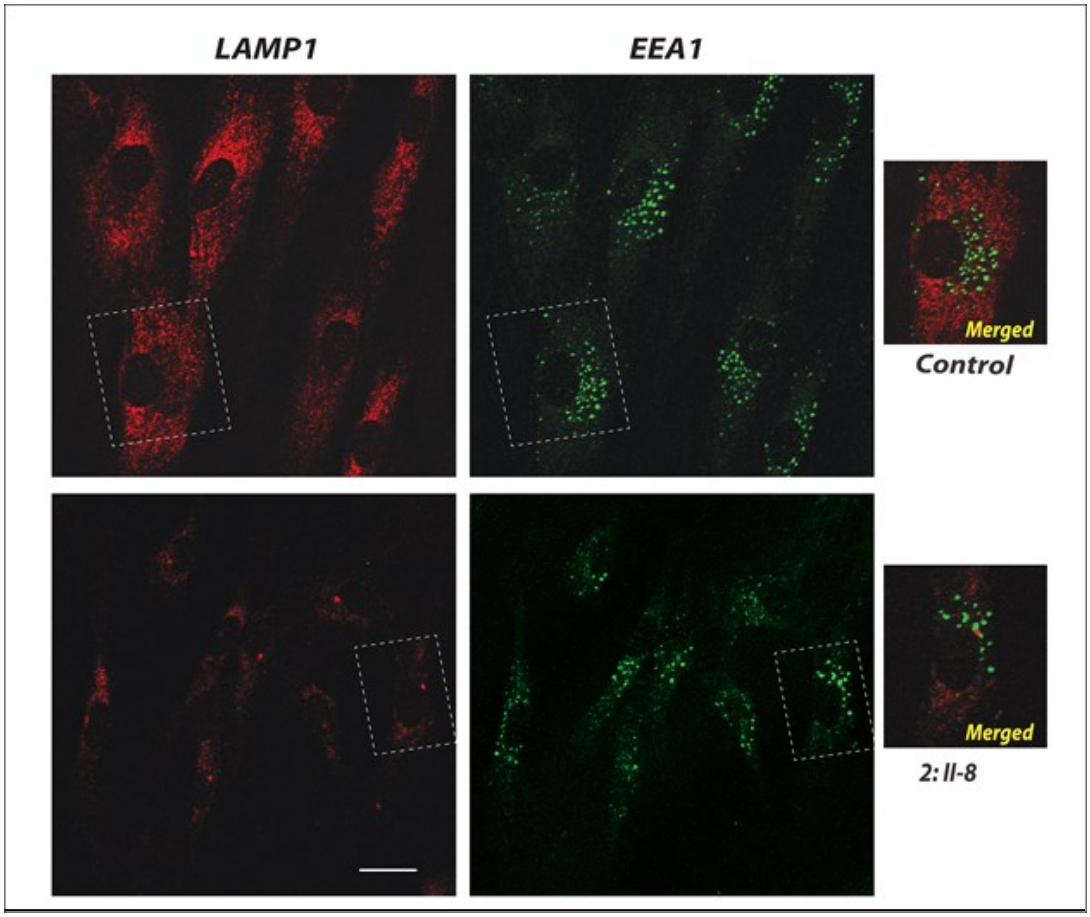

Figure 5.10 Distribution of late endosomes/lysosomes, but not early endosomes, is altered in patient cells. Immunofluorescence was performed using antibodies against early and late Golgi markers EEA1 and LAMP1, respectively, in control and affected primary fibroblast cells. Note perinuclear LAMP1 foci can be observed in affected cells (2:II-8). The scale bar represents 10 µm.

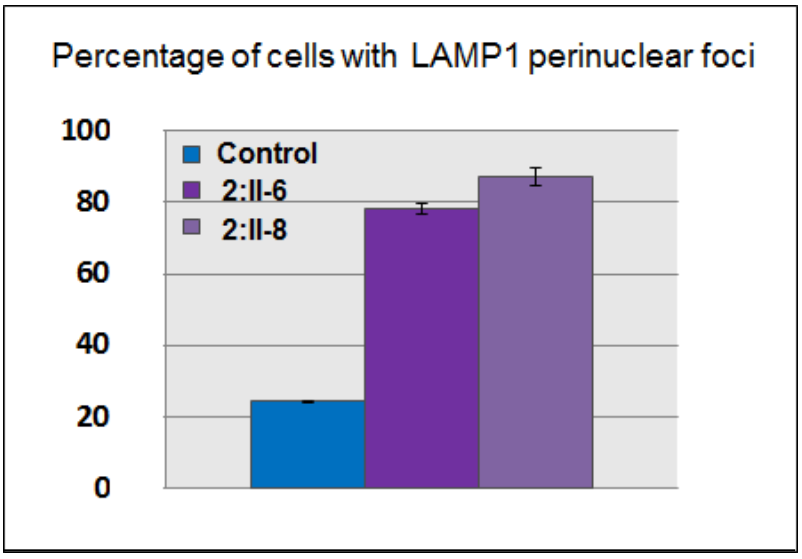

Figure 5.11 LAMP1 perinuclear foci are dramatically increased in patient cells. Quantification of the LAMP1 phenotype in control and patient (2:II-6 and 2:II-8) fibroblasts (N=189).

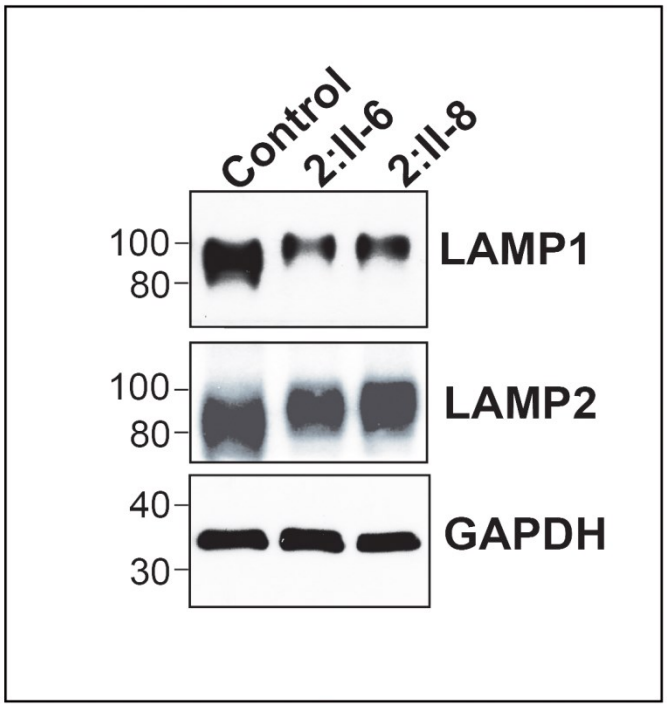

Figure 5.12 Altered protein and glycosylation levels of LAMP1 and LAMP2 in cells lacking a portion of the *foie gras* domain. Equal amounts of lysates were prepared from control and patient (2:II-6 and 2:II-8) fibroblasts. With respect to LAMP1 and LAMP2, bands with a diffuse

appearance are typical of highly glycosylated proteins. There are two differences in lysates of patient cells compared to control cells: (1) decreased level of the lysosomal membrane proteins LAMP1 and LAMP2, and (2) slower migration of LAMP1 and LAMP2, indicative of extensive glycosylation.

Given the fragmented nature of the membranes of *cis*- and *medial*- Golgi stack assessed by GM130 and ManII (refer to Figures 5.3 and 5.8, respectively), it was expected that the *trans* side of the Golgi would also be fragmented in the patient cells. Surprisingly, in addition to a TGN-fragmented phenotype shown by TGN46, perinuclear foci, similar to that observed for LAMP1 staining, were noted (Figure 5.13). Co-localization with Rab9 suggests these perinuclear foci may be *bona fide* late endosomes (Figure 5.13). In contrast, Rab9 signal is observed as a punctate staining seen throughout the cytoplasm in the control sample. This phenotype suggests that C11 may function in the late endocytic pathway.

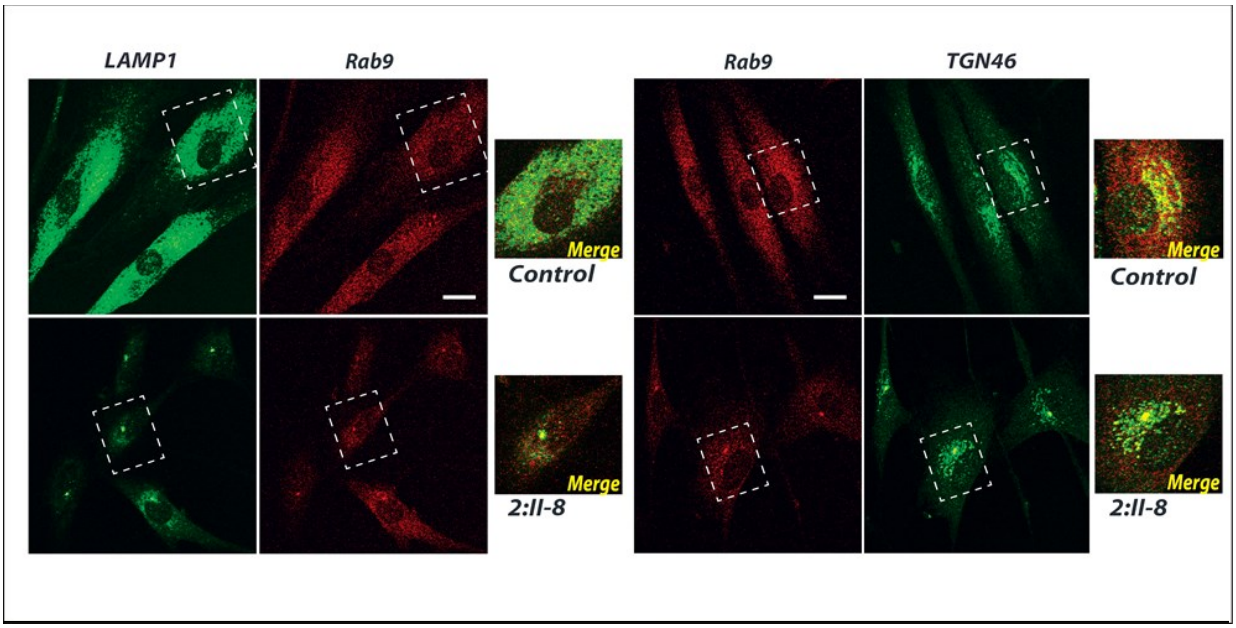

Figure 5.13 Perinuclear foci in LAMP1-positive organelles also co-localize with Rab9 and TGN46 markers. Skin fibroblasts were double labeled with LAMP1 and Rab9 or Rab9 and TGN46. Intriguingly, patient fibroblasts immunostained with both late endosomal and TGN

markers reveal perinuclear foci similar to that observed with LAMP1 antibody. The scale bar represents 10 μm.

5.3.7 LAMP1 perinuclear foci co-localise with γ-tubulin

Given the requirement for both LAMP1 and LAMP2 in lysosomal motility along microtubules (Huynh et al., 2007), together with the perinuclear foci found in the LAMP1-, Rab9-, and TGN46- positive organelles, we speculated that if the concentrated perinuclear region is clustered around the microtubule organizing centre (MTOC) minus-end, these foci should co-localise with the microtubule nucleation member γ–tubulin. Indeed, LAMP1-positive foci in patient samples were restricted to centrosomes where γ–tubulin is positioned (Figure 5.14).

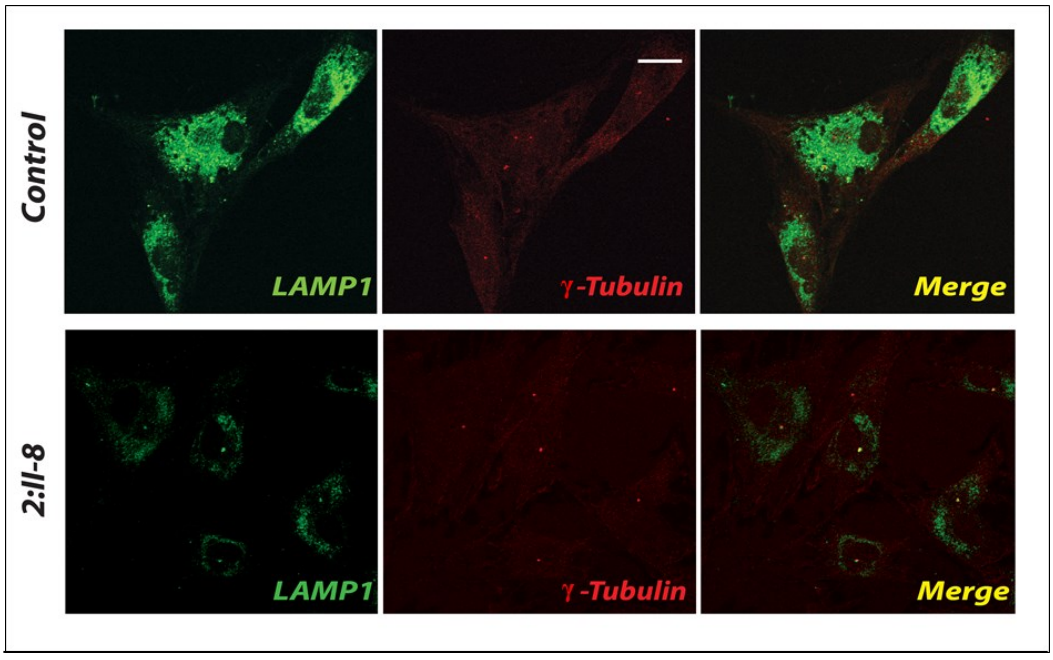

Figure 5.14 LAMP1 foci co-localize with γ-tubulin. Double immunostaining of primary skin fibroblasts in control and patient (2:II-8) samples with γ–tubulin and LAMP1.

5.3.8 LAMP1 perinuclear foci formation is dependent upon microtubules

To evaluate if juxtanuclear LAMP1 is reliant on microtubules, both patient and control samples were treated with the microtubule destabilizing drug nocodazole. While the LAMP1 staining remained unaltered in control cells, juxtanuclear foci in patient samples treated with nocodazole were disrupted (Figure 5.15).

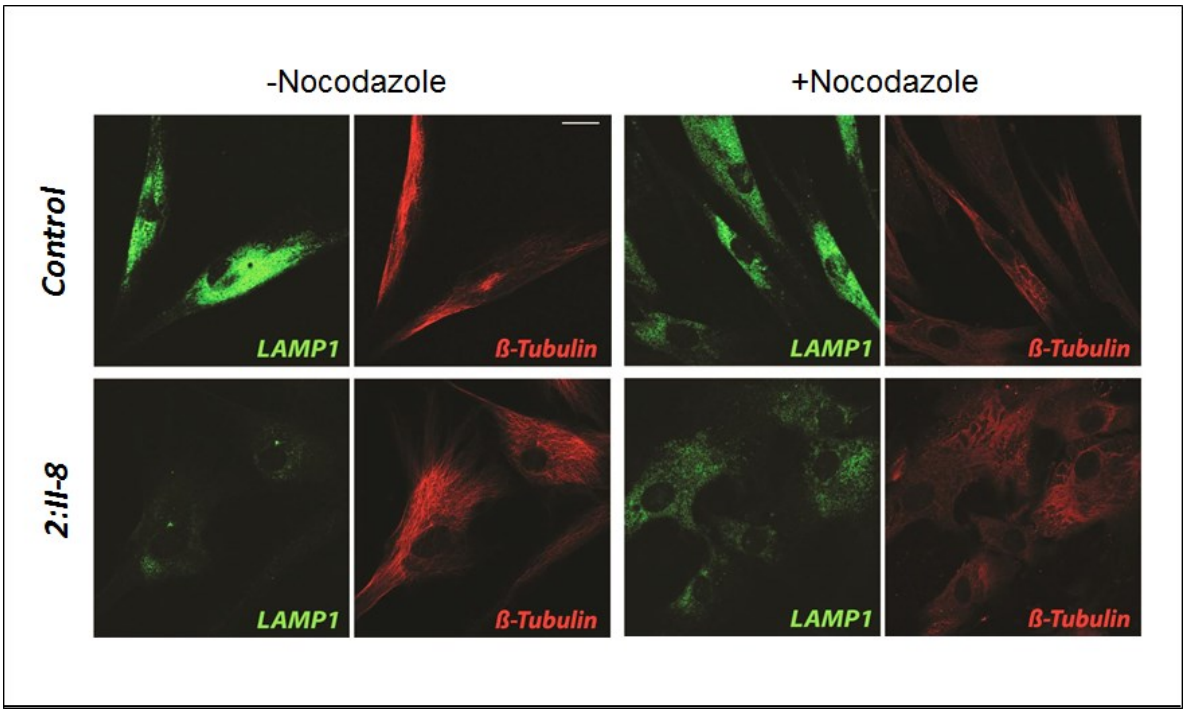

Figure 5.15 LAMP1 foci are dependent upon microtubules. Nocodazole treatment of affected (2:II-8) and unaffected (control) samples resulted in elimination of perinuclear foci of patient fibroblasts. The scale bar represents 10 μm.

5.4 Discussion

Retention of the human growth hormone marker protein GFP-F_M4-hGH in the Golgi of HeLa cells following knockdown of C11 was previously reported (Wendler et al., 2010). In addition, ablation of C11 by small interfering RNA was reported to result in accumulation of VSV-G in a brefeldin A-resistant compartment, interpreted to be related to the ERGIC (ER-Golgi intermediate compartment) (Scrivens et al., 2011). Our finding that partial deletion of the *foie gras* domain of C11 leads to defects in a post-Golgi compartment may be explained by the fact that only a portion of the protein is missing and represents a milder defect compared to knockdown of the entire protein. It is noteworthy that a recent study implicated the TRAPP complex in retrograde traffic originating at the cell surface, however, the precise cellular location where TRAPP acts in this pathway was not addressed (Moreau et al., 2011). Our present study suggests that a C11-containing TRAPP complex is involved in the formation and/or movement of late endosomes/lysosomes and implicates the *foie gras* domain of C11 in this process. A prominent perinuclear staining of LAMP1 has been observed in cells depleted of Rab9, leading to the suggestion that effector molecules required for late endosomal transport are not recruited in the absence of this GTPase (Ganley et al., 2004). In addition, Rab7 and the lipid composition of membranes has been implicated in the motility of late endosomes/lysosomes (Lebrand et al., 2002). It will be of interest to examine the relationship between a C11-containing TRAPP complex and various GTPases involved in late endosome dynamics. Interestingly, reduced LAMP1 levels and Golgi fragmentation have also been observed in Syrian patients with a missense mutation in *C11* (p.Gly980Arg) presenting with limb-girdle muscular dystrophy. This mutation shows a weakened interaction with several TRAPP proteins including C2, C2L, C6a, and C13.

Finally, a link to autophagy should also be considered. It has been suggested that lysosomal myopathies result from a buildup of autophagosomes (Malicdan et al., 2008). Given

recent studies suggesting the yeast TRAPP III complex is involved in autophagy (Zou et al., 2012;Lynch-Day et al., 2010;) and a study that suggests depletion of C11 leads to a reduction in autophagosome formation (Behrends et al., 2010), it will also be important to determine the molecular connection between autophagy and the phenotype we describe here.

Using whole exome sequencing we have identified a mutation in *C11*, resulting in a splicing defect that creates an in-frame deletion in five patients with ID, hyperkinetic movements, myopathy and ataxia from two Hutterite families. Functional studies using patient fibroblasts demonstrated a defect in vesicle trafficking through the Golgi. This finding represents the second TRAPP complex gene associated with ID and provides evidence for the involvement of Golgi trafficking to the expanding list of cellular processes that, when defective, can cause ID.

CHAPTER 6

Discussion

In Chapter 6, I will discuss the significance and implications of the results of the experiments that I conducted over the course of my PhD work. I also will outline questions that remain unanswered. I speculate further on the models that I introduced in Chapters 4 and 5 and I will propose future experiments. Finally, I will discuss possible explanations for the phenotype seen in C11 patients.

6.1 Tca17p and its related protein Trs20p exists in the same TRAPP complex

In Chapter 2 of this dissertation subsequent to the identification of YEL048cp, a new component of the TRAPP II complex now termed Tca17p, we suggested that Tca17p is located on a side of TRAPP opposite to that of Trs20p. The arrangement of Tca17p was based on *in vitro* binding as well as recombinant reconstitution of a TRAPP sub-complex. With respect to the core subunits of the TRAPP complex, Tca17p interacted with Trs33p-Bet3p as well as with Trs31p-Bet3p, the equivalent interface to which Trs20p binds. However Trs20p only interacted with Trs31p-Bet3p. The interaction of Tca17p with the Trs33p-Bet3p side of the complex was also observed in Dr. Elizabeth Conibear's laboratory. Since Trs20p only interacts with one side of the complex, and since Trs20p and Tca17p co-exist in the same complex, strongly suggest that these two proteins likely bind to opposite ends of the complex. The most likely explanation as to why Tca17p binds to Trs31p-Bet3p is that it is structurally similar to Trs20p (compare structure coordinates 1H3Q and 3PR6). This result was also observed in mammals for the proteins C2 and C2L.

More recently a physical interaction of Tca17p with TRAPP II-specific subunits (Trs65p, Trs120p and Trs130p) was described by yeast two-hybrid, and Tca17p was shown to directly

interact with the N-terminus of Trs130p (Choi et al., 2011). Given the proposed position of Trs130p deduced by electron microscopy of purified yeast TRAPP II (Yip et al., 2010) (Figure 1.9), Trs130p is located a substantial distance away from Trs33p-Bet3p, thus it is difficult to imagine how Tca17p can physically interact with Trs33p-Bet3p as well as with Trs130p. The comparably distant location of Trs33p-Bet3p to that of Trs130p is reminiscent of Trs31p-Bet3p to that of Trs120p, both of which interact with Trs20p (Taussig et al., 2013;Kim et al., 2005a). As stated in Chapter 1, although a number of laboratories have reported a direct interaction between Trs20p and Trs120p and their mammalian counterparts C2 and C9, yeast TRAPP II might assemble into a higher-order structure composed of multiple TRAPP II complexes that disassemble in the course of purification of yeast TRAPP II, thus the structure and the orientations of the larger specific components of TRAPP II (Trs120p and Trs130p), relative to the smaller subunits of the core TRAPP complex requires further investigation.

6.2 TRAPP proteins are present on two distinct membranes

As discussed in Chapter 2, we detected C2L, along with other subunits of TRAPP, on very light density membranes (VLDM) (Figure 2.14). VLDM is the only fraction that endogenous C2L shares with other TRAPP components because C2L is not found on Golgi membranes where other TRAPP proteins are present. There are two possible explanations for the existence of TRAPP on two different membranes: (1) light density membranes may represent Golgi to which TRAPP components are tethered. Interestingly, our data described in Chapter 3 suggested that the yeast TRAPP I core recruited to autophagic membranes is distinct from that of Trs85p-containing membranes (Figure 3.29). We postulated that this is similar to the mechanism of exocyst tethering of vesicles at the cell surface through interactions between components present on both vesicles and the plasma membrane. This might explain how the TRAPP complex assembles, an open question in the field, and whether the TRAPP complex assembles on membranes or in the cytosol. Thus the elucidation of the identity of VLDM could

help to explain the functional mechanism of the TRAPP complex. (2) Alternatively, light density membranes potentially come from COPII-coated vesicles. To test this, membrane isolation followed by equilibrium-gradient centrifugation, similar to that performed in Chapter 2, with different gradients (to obtain better resolution of the light density membranes) could be carried out. To this end, the inhibitor of COPII-coat assembly, H89, could be used to determine whether COPII-coated vesicles are the source of the C2L-containing VLDM.

6.3 TRAPP complexes and their implication in specific and non-specific autophagy

Several researchers have described the significant role played by the TRAPP complexes (TRAPP II and TRAPP III) in both Cvt and non-selective autophagy. There are numerous Atg proteins and components of intracellular machinery that act either in only one or in both of these pathways. In Chapter 3, we showed that TRAPP III, in addition to its role in non-specific autophagy, is involved in the proper localization of the Cvt complex to the PAS (Figures 3.19 and 3.20). We have also deciphered a model for TRAPP III assembly via interaction between the conserved D46 residue of Trs20p and Trs85p (Figure 3.29) which was supported by the recently-published EM structure of TRAPP III (Tan et al., 2013). In addition to Atg11p (Shintani et al., 2002), the multi tethering complex GARP has also been reported to be important for proper delivery of the Cvt complex to PAS, and its function is indispensable for autophagy (Reggiori et al., 2003). A recurring hypothesis is that membrane sources for Cvt and bulk autophagy pathways are distinct from one another. However it remains to be determined what the molecular machinery is that converts the specific/Cvt form of autophagy to non-specific/bulk autophagy. In this regard, hyperphosphorylation of Atg13p and the formation of a trimer of Atg17p-Atg29-Atg31p were hypothesized to be critical for favouring biogenesis of Cvt vesicles into much larger autophagosomes.

TRAPP III GEF activity acting on Ypt1p results in activation of Ypt1p, and Ypt1p-GTP has been recently been shown to associate with the Atg1p kinase. Intriguingly, the association between these two proteins is preserved in the absence and presence of nutrients. However, under starvation conditions the binding Ypt1p-GTP to Atg1p is enhanced. Along the same lines of evidence, overexpression of Ypt1p-GTP increases autophagy, which further supports the idea that there is a stronger association of the two proteins during nutrient deprivation (Wang et al., 2013). Interestingly Lipatova et al. (2012) examined the effects of Ypt1p in the regulation of selective autophagy, and under nutrient-rich conditions. Ypt1p-GTP interacted with the Cvt-specific subunit Atg11p. Thus, I propose that given the specific behaviour of activated Ypt1p, in terms of its interaction with two important Atg components (Atg1p and Atg11p), one implicated in bulk autophagy and the other in selective autophagy, that Ypt1p is an ideal candidate to study the molecular mechanism of transition between the two pathways. It is critical to map out the regions on Ypt1p sequences to which the two binding partners Atg1p and Atg11p associate and to better understand their binding affinity towards Ypt1p under vegetative and starvation conditions. This could indicate whether Ypt1p serves as a turning point in induction of selective and non-selective autophagy.

The possible role of yeast and mammalian TRAPP complexes in autophagy has been described. However, involvement of mammalian TRAPP in the Cvt pathway has not been studied. In yeast, Atg19p is a cargo receptor in the Cvt pathway that also binds to membrane-associated Atg8p-PE and promotes formation of Cvt vesicles (Noda et al., 2008). Like Atg8p, the mammalian homolog LC3 contains an evolutionarily conserved WXXL binding pocket critical for the Cvt pathway and not for bulk autophagy (Noda et al 2008). This region is responsible for interaction with the mammalian adaptor protein p62/SQSTM1 that then binds to ubiquitinated cargos. Interestingly, C8 harbours the WXXL motif and it is worth investigating, using various protein-protein interaction methods, whether under vegetative conditions the WXXL motif of C8

can associate with LC3. Nevertheless, while researchers are working to understand the molecular mechanism regulating autophagy, elucidation of the function of TRAPP complexes in this fundamental physiological process will be as fascinating as the discovery of this tethering complex.

6.4 The TRAPP complex and the ER-Golgi intermediate compartment (ERGIC)

C3 is required for homotypic fusion of COPII vesicles leading to ERGIC biogenesis (Yu et al., 2006). Our laboratory determined that siRNA-mediated depletion of C11 caused retention of secretory proteins in a BFA-resistant compartment thought to be the ERGIC compartment. In Chapter 4, the association of C2-Syntaxin 5 in the presence of the COPII component Sec23 was observed, and the interaction was not affected by BFA treatment (Figure 4.6). BFA treatment of cells causes Golgi structural collapse and the distribution of puncta that colocalize with the ERGIC (Lippincott-Schwartz et al., 1989), suggesting that the ERGIC, not the *cis*-Golgi, could be the site of Sec23-C2-Syntaxin 5 association. Interestingly, Syntaxin 5 and the SM protein Sly1 were reported to be involved in homotypic fusion of COPII vesicles and thus biogenesis of ERGIC (Xu and Hay, 2004).

It has been shown that once the ERGIC has been generated, an Arf GEF (GBF1) is recruited to ERGIC by Rab1 and in turn GBF1 activates the Arf1 GTPase, and both of these events are sensitive to BFA treatment (Garcia et al., 2011) (Figure 6.1). The fact that Sec23-C2-Syntaxin 5 association was resistant to BFA treatment suggests that the coat-tether-SNARE interaction must have occurred prior to Arf GTPase and/or GBF1 recruitment.The ERGIC depleting inhibitor H89 could be used to confirm the subcellular location where COPII-TRAPP-SNARE association takes place. If it is at the ERGIC, a compartment that has not yet been identified in yeast, it could explain why a physical interaction between their yeast counterparts (Trs20p and Sed5p) is absent in *S. cerevisiae*.

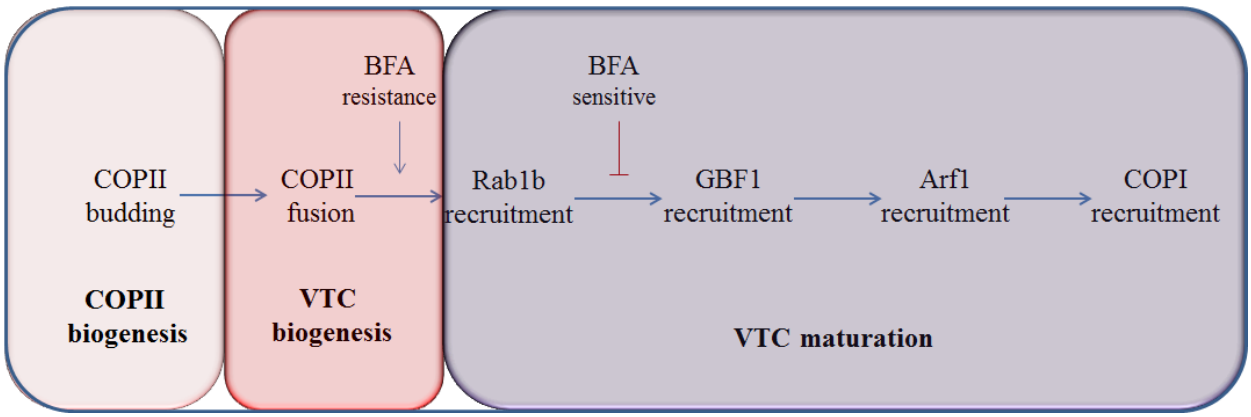

Figure 6.1 Schematic representation of ERGIC maturation.

6.5 Implications of SEDT

The tethering factor COG has been proposed to regulate the assembly of SNARE complexes, since the localization and stability of Golgi SNAREs are perturbed in cells with a defect in the COG complex (Laufman et al., 2011). As stated in Chapter 4, p115 cycles on and off membranes of Golgi and ERGIC, and the ER-Golgi SNARE protein GS28 colocalizes with p115 on the ERGIC (Brandon et al., 2006). In a series of elegant experiments, which included the use of fluorescence recovery after photobleaching (FRAP), the time required for the recovery of p115 onto the membrane was precisely measured. Interestingly, an inactive mutant form of NSF (NSF E329Q), which inhibits SNARE complex disassembly, increased the FRAP half time of p115 compared to that of wild type cells (20 vs 13 seconds) (Figure 6.2) (Bentley et al., 2006). In other words, the persistence of SNARE complex assembly in the cells treated with NSF E329Q decreased p115 membrane association, thus indicating that p115 membrane association is related to SNARE disassembly. In Chapter 4, I have also demonstrated that p115 membrane association in the SEDT-causing mutant C2D47Y is dramatically increased (Figure 4.7). In addition, in Chapter 3, I have shown that the C2D47Y interaction with Syntaxin 5 is reduced (Figures 3.4- 3.6), implying that the C2D47Y mutant could compromise p115 cycling through the disassembly of SNARE complexes. Interestingly the GTPase that TRAPP acts on,

Rab1, also influences the cycle of its effector p115, as the dominant negative form of Rab1 (Rab1 N121I) shortens FRAP of p115 to 8 seconds (see Figure 6.2). The cycling of p115 is summarized below:

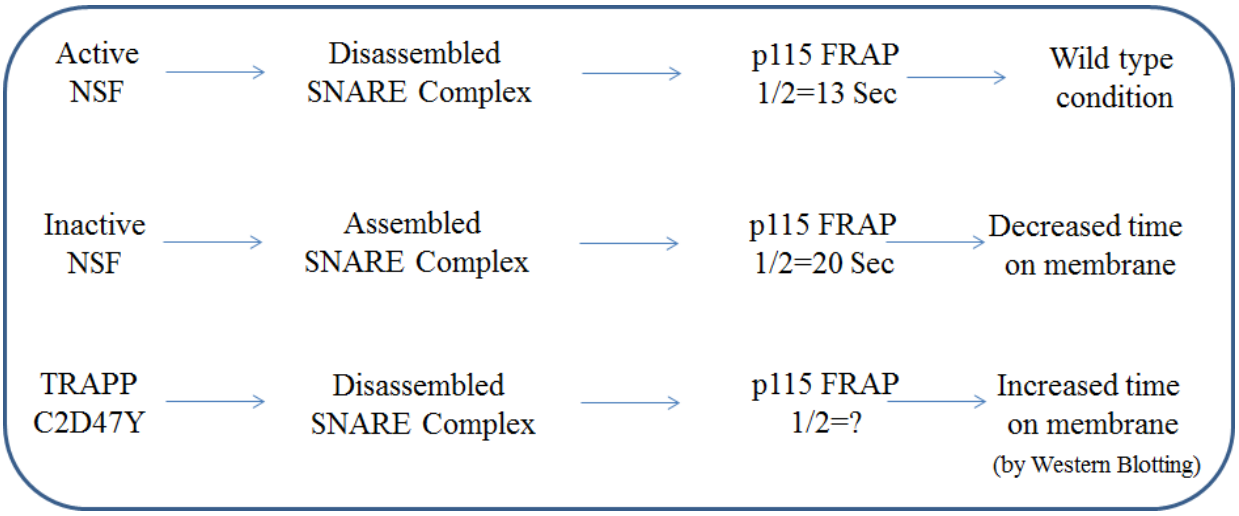

Figure 6.2 Schematic representation of p115 cycling between membrane and cytosol.

C2 is thought to be involved in the regulation of numerous intracellular processes from membrane trafficking to controlling gene expression as reflected by the vast number of its interacting partners. A link between membrane transport and cartilage development began to emerge when patients with a degenerative skeletal disorder causing SEDT were found to have mutations in the *C2* gene (Gedeon et al., 1999;Sacher, 2003). Currently, more than 40 different mutations in C2 have been reported to cause SEDT (Jeyabalan et al., 2010). To shed light on the etiology of SEDT, it will be useful to identify the protein interactions, among the many protein partners, that are impaired when C2 is mutated.

These proteins include intermolecular associations within the TRAPP complex such as C8, C9 (Zong et al., 2011), and C10 (my unpublished observations) which are also observed with their yeast counterparts (Figure 3.11;Taussig et al., 2013). While disruption of these

interactions caused by the C2D47Y mutation might compromise the dynamics of TRAPP complexes (TRAPP II/III), other protein partners of C2 are not part of the TRAPP complex, including Sar1-GTP and TANGO1. This is of interest as TANGO1 is the collagen receptor and recruits C2 to the ERES. ER-export of collagen is perturbed upon C2 depletion (Venditti et al., 2012). It would be interesting to examine collagen exit from the ER in the context of C2D47Y where its interaction with Syntaxin 5 is perturbed. The C2-Syntaxin 5 interaction is not observed in budding yeast, which does not produce collagen, and it is possible that in higher eukaryotes the TRAPP complex has gained the latter interaction to fulfil a novel function during the course of evolution. There is a strong possibility that in the C2D47Y mutant and in the intellectual disability-causing C9 truncation mutation the formation of TRAPP II and TRAPP III might be impaired. However it is difficult to know the consequences of the above dissociations in yeast. Thus far the only protein partner of C2 beyond the components of the TRAPP complex that does not bind to the C2D47Y SEDT-causing mutant is Syntaxin 5.

6.6 Models for the function of C11

Microscopic and biochemical analyses revealed a dramatic decrease and extensive glycosylation in cellular levels of LAMP1 in the presence of a mutation of C11 (Figures 5.10 and 5.12). There are several explanations for the observed phenotype. First, LAMP1 turnover might have been comprised in the affected individuals. It has been shown that the lysosomal hydrolase neuraminidase acts on sialic acid of LAMP1, which is a regulator of LAMP1 half-life and its subcellular distribution. Given the aberrant glycosylation of LAMP1 in patient samples, we speculate that alteration of the pattern of glycosylation, presumably sialylation which mostly occurs in the *trans*-Golgi, could explain why the expression level of LAMP1 is diminished, thus making cellular LAMP1 prone to degradation. Further experiments are needed to test this hypothesis.

Second, as stated in Chapter 5, recycling transport between endosomal compartments occurs via slow or fast recycling pathways. The slow circuit transits through recycling endosomes. Recycling endosomes accumulate around the microtubule organizing centre (MTOC) (Maxfield and McGraw, 2004), and the marker for recycling endosomes, Rab11, is found as a perinuclear focus similar to that seen for LAMP1 staining observed in the C11 patients lacking the *foie gras* domain. Thus we speculate that while a portion of cellular LAMP1 declines possibly by degradation, a second fraction of LAMP1 is distributed to perinuclear foci. Either the state of glycosylation or alteration of protein-protein interactions induced by partial deletion of the *foie gras* domain possibly redirects LAMP1-Rab9-TGN46- positive vesicles towards recycling endosomes.

Finally our proposal that compromised TRAPP function interferes with microtubule-mediated transport of the late endosomal/lysosomal compartment towards the MTOC is supported by experiments in which overexpression of multiple TRAPP components causes the microtubule minus end-directed component of dynactin p150 to move away from the MTOC (Zong et al., 2012). FYCO1 is one of the many Rab7 effectors decorating vesicles of late endosomes and lysosomes (Pankiv et al., 2010). FYCO1 via interaction with LC3 promotes anterograde transport of plus end-directed vesicles along microtubules. On the other hand, activated Rab7 also interacts with RILP and ORP1L to recruit the dynein-dynactin complex to the late endosome/ lysosomes (Johansson et al., 2007) (Figure 6.3 bottom boxed area). LAMP1 foci are observed in the partial deletion of *foie gras* domain of C11, which implies that wild-type C11 functions in favor of the plus end-directed kinesin motor machinery. Therefore, it would be worthwhile to examine whether the *foie gras* domain interacts with kinesin or alternatively associates with a kinesin-binding partner.

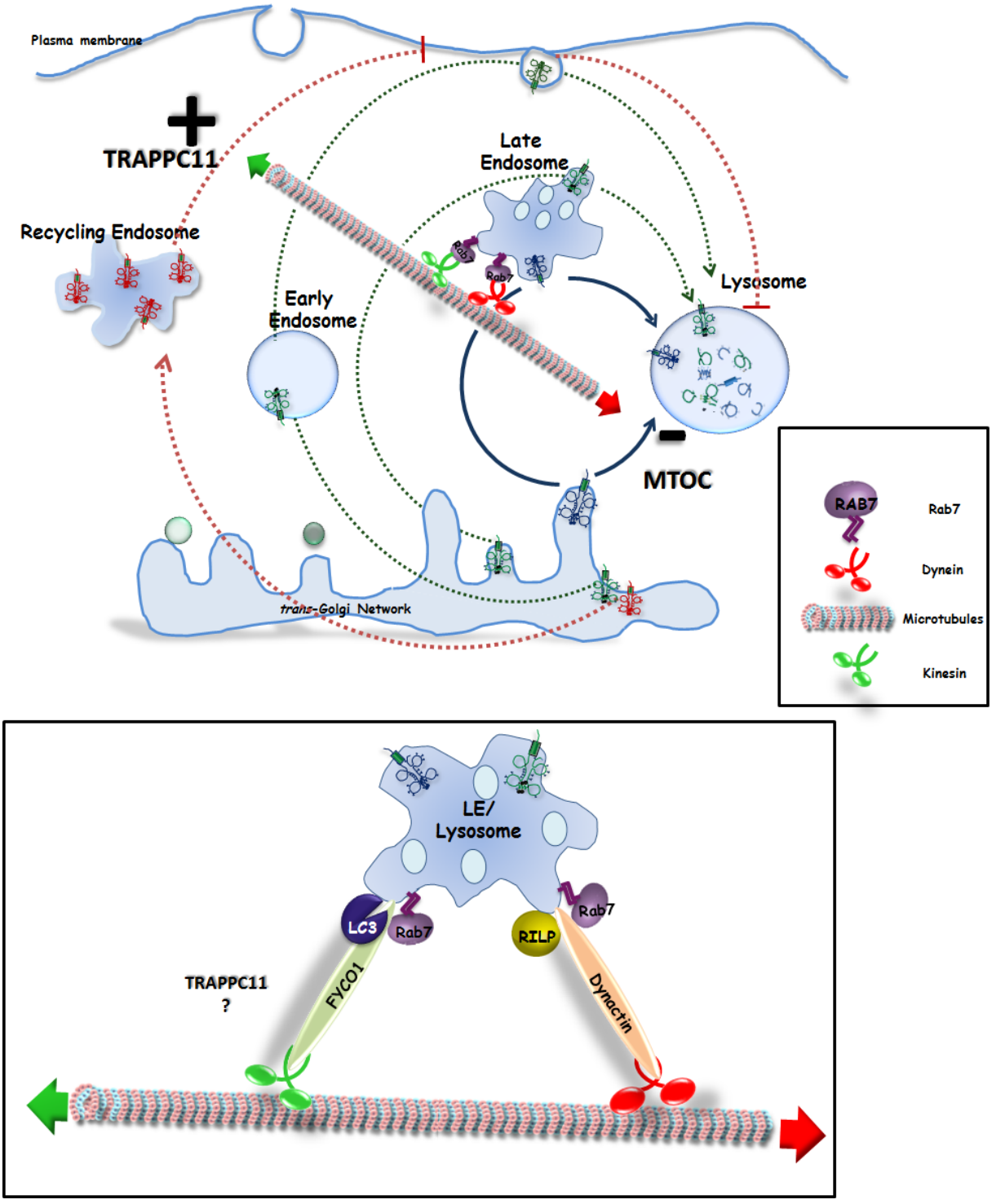

Figure 6.3 Model in favor of the TRAPP complex playing a role in plus end-directed anterograde (toward cell periphery) transport of late endosomal/lysosomal vesicles along microtubules (see text for details).

CHAPTER 7

References

Allan, B. B., Moyer, B. D., & Balch, W. E. (2000). Rab1 recruitment of p115 into a cis-SNARE complex: programming budding COPII vesicles for fusion. *Science, 289*(5478), 444-448.

Alvarez, C., Garcia-Mata, R., Hauri, H. P., & Sztul, E. (2001). The p115-interactive proteins GM130 and giantin participate in endoplasmic reticulum-Golgi traffic. *J Biol Chem, 276*(4), 2693-2700. doi: 10.1074/jbc.M007957200

Amessou, M., A. Fradagrada, T. Falguieres, J.M. Lord, D.C. Smith, L.M. Roberts, C. Lamaze, and L. Johannes (2007). Syntaxin 16 and syntaxin 5 are required for efficient retrograde transport of several exogenous and endogenous cargo proteins. *J Cell Sci, 120*(Pt 8), 1457-1468. doi: 10.1242/jcs.03436

Appenzeller-Herzog, C., & Hauri, H. P. (2006). The ER-Golgi intermediate compartment (ERGIC): in search of its identity and function. *J Cell Sci, 119*(Pt 11), 2173-2183. doi: 10.1242/jcs.03019

Aridor, M., Bannykh, S. I., Rowe, T., & Balch, W. E. (1995). Sequential coupling between COPII and COPI vesicle coats in endoplasmic reticulum to Golgi transport. *J Cell Biol, 131*(4), 875-893.

Aridor, M., & Hannan, L. A. (2000). Traffic jam: a compendium of human diseases that affect intracellular transport processes. *Traffic, 1*(11), 836-851.

Aridor, M., & Hannan, L. A. (2002). Traffic jams II: an update of diseases of intracellular transport. *Traffic, 3*(11), 781-790.

Baba, M., Osumi, M., Scott, S. V., Klionsky, D. J., & Ohsumi, Y. (1997). Two distinct pathways for targeting proteins from the cytoplasm to the vacuole/lysosome. *J Cell Biol, 139*(7), 1687-1695.

Bachinger, H. P., Doege, K. J., Petschek, J. P., Fessler, L. I., & Fessler, J. H. (1982). Structural implications from an electronmicroscopic comparison of procollagen V with procollagen I, pC-collagen I, procollagen IV, and a Drosophila procollagen. *J Biol Chem, 257*(24), 14590-14592.

Bacon, R. A., Salminen, A., Ruohola, H., Novick, P., & Ferro-Novick, S. (1989). The GTP-binding protein Ypt1 is required for transport in vitro: the Golgi apparatus is defective in ypt1 mutants. *J Cell Biol, 109*(3), 1015-1022.

Balch, W. E., Dunphy, W. G., Braell, W. A., & Rothman, J. E. (1984). Reconstitution of the transport of protein between successive compartments of the Golgi measured by the coupled incorporation of N-acetylglucosamine. *Cell, 39*(2 Pt 1), 405-416.

Barlowe, C., L. Orci, T. Yeung, M. Hosobuchi, S. Hamamoto, N. Salama, M.F. Rexach, M. Ravazzola, M. Amherdt, and R. Schekman. (1994). COPII: a membrane coat formed by Sec proteins that drive vesicle budding from the endoplasmic reticulum. *Cell, 77*(6), 895-907.

Barrowman, J., Sacher, M., & Ferro-Novick, S. (2000). TRAPP stably associates with the Golgi and is required for vesicle docking. *EMBO J, 19*(5), 862-869. doi: 10.1093/emboj/19.5.862

Bassik, M.C., M. Kampmann, R.J. Lebbink, S. Wang, M.Y. Hein, I. Poser, J. Weibezahn, M.A. Horlbeck, S. Chen, M. Mann, A.A. Hyman, E.M. Leproust, M.T. McManus, and J.S. Weissman. (2013). A systematic mammalian genetic interaction map reveals pathways underlying ricin susceptibility. *Cell, 152*(4), 909-922. doi: 10.1016/j.cell.2013.01.030

Beard, M., Satoh, A., Shorter, J., & Warren, G. (2005). A cryptic Rab1-binding site in the p115 tethering protein. *J Biol Chem, 280*(27), 25840-25848. doi: 10.1074/jbc.M503925200

Behrends, C., Sowa, M. E., Gygi, S. P., & Harper, J. W. (2010). Network organization of the human autophagy system. *Nature, 466*(7302), 68-76. doi: 10.1038/nature09204

Ben-Aroya, S., Coombes, C., Kwok, T., O'Donnell, K. A., Boeke, J. D., & Hieter, P. (2008). Toward a comprehensive temperature-sensitive mutant repository of the essential genes of Saccharomyces cerevisiae. *Mol Cell, 30*(2), 248-258. doi: 10.1016/j.molcel.2008.02.021

Bentley, M., Liang, Y., Mullen, K., Xu, D., Sztul, E., & Hay, J. C. (2006). SNARE status regulates tether recruitment and function in homotypic COPII vesicle fusion. *J Biol Chem, 281*(50), 38825-38833. doi: 10.1074/jbc.M606044200

Ben-Ze'ev, A., Robinson, G. S., Bucher, N. L., & Farmer, S. R. (1988). Cell-cell and cell-matrix interactions differentially regulate the expression of hepatic and cytoskeletal genes in primary cultures of rat hepatocytes. *Proc Natl Acad Sci U S A, 85*(7), 2161-2165.

Bergmann, J. E., & Singer, S. J. (1983). Immunoelectron microscopic studies of the intracellular transport of the membrane glycoprotein (G) of vesicular stomatitis virus in infected Chinese hamster ovary cells. *J Cell Biol, 97*(6), 1777-1787.

Bielli, A., Haney, C. J., Gabreski, G., Watkins, S. C., Bannykh, S. I., & Aridor, M. (2005). Regulation of Sar1 NH2 terminus by GTP binding and hydrolysis promotes membrane deformation to control COPII vesicle fission. *J Cell Biol, 171*(6), 919-924. doi: 10.1083/jcb.200509095

Blower, M. D., Feric, E., Weis, K., & Heald, R. (2007). Genome-wide analysis demonstrates conserved localization of messenger RNAs to mitotic microtubules. *J Cell Biol, 179*(7), 1365-1373. doi: 10.1083/jcb.200705163

Bogershausen, N., N. Shahrzad, J.X. Chong, J.C. von Kleist-Retzow, D. Stanga, Y. Li, F.P. Bernier, C.M. Loucks, R. Wirth, E.G. Puffenberger, R.A. Hegele, J. Schreml, G. Lapointe, K. Keupp, C.L. Brett, R. Anderson, A. Hahn, A.M. Innes, O. Suchowersky, M.B. Mets, G. Nurnberg, D.R. McLeod, H. Thiele, D. Waggoner, J. Altmuller, K.M. Boycott, B. Schoser, P. Nurnberg, C. Ober, R. Heller, J.S. Parboosingh, B. Wollnik, M. Sacher, and R.E. Lamont. (2013). Recessive TRAPPC11 Mutations Cause a Disease

Spectrum of Limb Girdle Muscular Dystrophy and Myopathy with Movement Disorder and Intellectual Disability. *Am J Hum Genet, 93*(1), 181-190. doi: 10.1016/j.ajhg.2013.05.028

Bonifacino, J. S., & Glick, B. S. (2004). The mechanisms of vesicle budding and fusion. *Cell, 116*(2), 153-166.

Bonifacino, J. S., & Lippincott-Schwartz, J. (2003). Coat proteins: shaping membrane transport. *Nat Rev Mol Cell Biol, 4*(5), 409-414. doi: 10.1038/nrm1099

Boycott, K.M., J.S. Parboosingh, B.N. Chodirker, R.B. Lowry, D.R. McLeod, J. Morris, C.R. Greenberg, A.E. Chudley, F.P. Bernier, J. Midgley, L.B. Moller, and A.M. Innes. (2008). Clinical genetics and the Hutterite population: a review of Mendelian disorders. *Am J Med Genet A, 146A*(8), 1088-1098. doi: 10.1002/ajmg.a.32245

Boyd, C., Hughes, T., Pypaert, M., & Novick, P. (2004). Vesicles carry most exocyst subunits to exocytic sites marked by the remaining two subunits, Sec3p and Exo70p. *J Cell Biol, 167*(5), 889-901. doi: 10.1083/jcb.200408124

Brandon, E., Szul, T., Alvarez, C., Grabski, R., Benjamin, R., Kawai, R., & Sztul, E. (2006). On and off membrane dynamics of the endoplasmic reticulum-golgi tethering factor p115 in vivo. *Mol Biol Cell, 17*(7), 2996-3008. doi: 10.1091/mbc.E05-09-0862

Brunet, S., B. Noueihed, N. Shahrzad, D. Saint-Dic, B. Hasaj, T.L. Guan, A. Moores, C. Barlowe, and M. Sacher. (2012). The SMS domain of Trs23p is responsible for the in vitro appearance of the TRAPP I complex in Saccharomyces cerevisiae. *Cell Logist, 2*(1), 28-42. doi: 10.4161/cl.19414

Brunet, S., Shahrzad, N., Saint-Dic, D., Dutczak, H., & Sacher, M. (2013). A trs20 Mutation That Mimics an SEDT-Causing Mutation Blocks Selective and Non-Selective Autophagy: A Model for TRAPP III Organization. *Traffic*. doi: 10.1111/tra.12095

Cai, H., Reinisch, K., & Ferro-Novick, S. (2007a). Coats, tethers, Rabs, and SNAREs work together to mediate the intracellular destination of a transport vesicle. *Dev Cell, 12*(5), 671-682. doi: 10.1016/j.devcel.2007.04.005

Cai, H., S. Yu, S. Menon, Y. Cai, D. Lazarova, C. Fu, K. Reinisch, J.C. Hay, and S. Ferro-Novick. (2007b). TRAPPI tethers COPII vesicles by binding the coat subunit Sec23. *Nature, 445*(7130), 941-944. doi: 10.1038/nature05527

Cai, H., Zhang, Y., Pypaert, M., Walker, L., & Ferro-Novick, S. (2005). Mutants in trs120 disrupt traffic from the early endosome to the late Golgi. *J Cell Biol, 171*(5), 823-833. doi: 10.1083/jcb.200505145

Cai, Y., H.F. Chin, D. Lazarova, S. Menon, C. Fu, H. Cai, A. Sclafani, D.W. Rodgers, E.M. De La Cruz, S. Ferro-Novick, and K.M. Reinisch. (2008). The structural basis for activation of the Rab Ypt1p by the TRAPP membrane-tethering complexes. *Cell, 133*(7), 1202-1213. doi: 10.1016/j.cell.2008.04.049

Cao, X., Ballew, N., & Barlowe, C. (1998). Initial docking of ER-derived vesicles requires Uso1p and Ypt1p but is independent of SNARE proteins. *EMBO J, 17*(8), 2156-2165. doi: 10.1093/emboj/17.8.2156

Cao, Y., Cheong, H., Song, H., & Klionsky, D. J. (2008). In vivo reconstitution of autophagy in Saccharomyces cerevisiae. *J Cell Biol, 182*(4), 703-713. doi: 10.1083/jcb.200801035

Caro, L. G., & Palade, G. E. (1964). Protein Synthesis, Storage, and Discharge in the Pancreatic Exocrine Cell. An Autoradiographic Study. *J Cell Biol, 20*, 473-495.

Carr, C. M., Grote, E., Munson, M., Hughson, F. M., & Novick, P. J. (1999). Sec1p binds to SNARE complexes and concentrates at sites of secretion. *J Cell Biol, 146*(2), 333-344.

Chen, S., Cai, H., Park, S. K., Menon, S., Jackson, C. L., & Ferro-Novick, S. (2011). Trs65p, a subunit of the Ypt1p GEF TRAPPII, interacts with the Arf1p exchange factor Gea2p to facilitate COPI-mediated vesicle traffic. *Mol Biol Cell, 22*(19), 3634-3644. doi: 10.1091/mbc.E11-03-0197

Cheong, H., & Klionsky, D. J. (2008). Dual role of Atg1 in regulation of autophagy-specific PAS assembly in Saccharomyces cerevisiae. *Autophagy, 4*(5), 724-726.

Cheong, H., Yorimitsu, T., Reggiori, F., Legakis, J. E., Wang, C. W., & Klionsky, D. J. (2005). Atg17 regulates the magnitude of the autophagic response. *Mol Biol Cell, 16*(7), 3438-3453. doi: 10.1091/mbc.E04-10-0894

Chiari, R., Foury, F., De Plaen, E., Baurain, J. F., Thonnard, J., & Coulie, P. G. (1999). Two antigens recognized by autologous cytolytic T lymphocytes on a melanoma result from a single point mutation in an essential housekeeping gene. *Cancer Res, 59*(22), 5785-5792.

Choi, C., Davey, M., Schluter, C., Pandher, P., Fang, Y., Foster, L. J., & Conibear, E. (2011). Organization and assembly of the TRAPPII complex. *Traffic, 12*(6), 715-725. doi: 10.1111/j.1600-0854.2011.01181.x

Choi, M. Y., Chan, C. C., Chan, D., Luk, K. D., Cheah, K. S., & Tanner, J. A. (2009). Biochemical consequences of sedlin mutations that cause spondyloepiphyseal dysplasia tarda. *Biochem J, 423*(2), 233-242. doi: 10.1042/BJ20090541

Choi, W. I., Qama, D., Lee, M. Y., & Kwon, K. Y. (2013). Pleural cancer antigen-125 levels in benign and malignant pleural effusions. *Int J Tuberc Lung Dis, 17*(5), 693-697. doi: 10.5588/ijtld.12.0635

Clary, D. O., & Rothman, J. E. (1990). Purification of three related peripheral membrane proteins needed for vesicular transport. *J Biol Chem, 265*(17), 10109-10117.

Conibear, E. (2011). Vesicle transport: springing the TRAPP. *Curr Biol, 21*(13), R506-508. doi: 10.1016/j.cub.2011.05.045

Cox, R., Chen, S. H., Yoo, E., & Segev, N. (2007). Conservation of the TRAPPII-specific subunits of a Ypt/Rab exchanger complex. *BMC Evol Biol, 7*, 12. doi: 10.1186/1471-2148-7-12

Cuervo, A. M. (2004). Autophagy: many paths to the same end. *Mol Cell Biochem, 263*(1-2), 55-72.

de Ligt, J., M.H. Willemsen, B.W. van Bon, T. Kleefstra, H.G. Yntema, T. Kroes, A.T. Vulto-van Silfhout, D.A. Koolen, P. de Vries, C. Gilissen, M. del Rosario, A. Hoischen, H. Scheffer, B.B. de Vries, H.G. Brunner, J.A. Veltman, and L.E. Vissers. (2012). Diagnostic exome sequencing in persons with severe intellectual disability. *N Engl J Med, 367*(20), 1921-1929. doi: 10.1056/NEJMoa1206524

Dulubova, I., Sugita, S., Hill, S., Hosaka, M., Fernandez, I., Sudhof, T. C., & Rizo, J. (1999). A conformational switch in syntaxin during exocytosis: role of munc18. *EMBO J, 18*(16), 4372-4382. doi: 10.1093/emboj/18.16.4372

Duncan, J. R., & Kornfeld, S. (1988). Intracellular movement of two mannose 6-phosphate receptors: return to the Golgi apparatus. *J Cell Biol, 106*(3), 617-628.

Fukuda, M., Viitala, J., Matteson, J., & Carlsson, S. R. (1988). Cloning of cDNAs encoding human lysosomal membrane glycoproteins, h-lamp-1 and h-lamp-2. Comparison of their deduced amino acid sequences. *J Biol Chem, 263*(35), 18920-18928.

Ganley, I. G., Carroll, K., Bittova, L., & Pfeffer, S. (2004). Rab9 GTPase regulates late endosome size and requires effector interaction for its stability. *Mol Biol Cell, 15*(12), 5420-5430. doi: 10.1091/mbc.E04-08-0747

Garcia, I. A., Martinez, H. E., & Alvarez, C. (2011). Rab1b regulates COPI and COPII dynamics in mammalian cells. *Cell Logist, 1*(4), 159-163. doi: 10.4161/cl.1.4.18221

Gavin, A.C., M. Bosche, R. Krause, P. Grandi, M. Marzioch, A. Bauer, J. Schultz, J.M. Rick, A.M. Michon, C.M. Cruciat, M. Remor, C. Hofert, M. Schelder, M. Brajenovic, H. Ruffner, A. Merino, K. Klein, M. Hudak, D. Dickson, T. Rudi, V. Gnau, A. Bauch, S. Bastuck, B. Huhse, C. Leutwein, M.A. Heurtier, R.R. Copley, A. Edelmann, E. Querfurth, V. Rybin, G. Drewes, M. Raida, T. Bouwmeester, P. Bork, B. Seraphin, B. Kuster, G. Neubauer, and G. Superti-Furga. (2002). Functional organization of the yeast proteome by

systematic analysis of protein complexes. *Nature, 415*(6868), 141-147. doi: 10.1038/415141a

Gecz, J., Hillman, M. A., Gedeon, A. K., Cox, T. C., Baker, E., & Mulley, J. C. (2000). Gene structure and expression study of the SEDL gene for spondyloepiphyseal dysplasia tarda. *Genomics, 69*(2), 242-251. doi: 10.1006/geno.2000.6326

Gecz, J., Shaw, M. A., Bellon, J. R., & de Barros Lopes, M. (2003). Human wild-type SEDL protein functionally complements yeast Trs20p but some naturally occurring SEDL mutants do not. *Gene, 320*, 137-144.

Gedeon, A.K., A. Colley, R. Jamieson, E.M. Thompson, J. Rogers, D. Sillence, G.E. Tiller, J.C. Mulley, and J. Gecz. (1999). Identification of the gene (SEDL) causing X-linked spondyloepiphyseal dysplasia tarda. *Nat Genet, 22*(4), 400-404. doi: 10.1038/11976

Gedeon, A.K., G.E. Tiller, M. Le Merrer, S. Heuertz, L. Tranebjaerg, D. Chitayat, S. Robertson, I.A. Glass, R. Savarirayan, W.G. Cole, D.L. Rimoin, B.G. Kousseff, H. Ohashi, B. Zabel, A. Munnich, J. Gecz, and J.C. Mulley. (2001). The molecular basis of X-linked spondyloepiphyseal dysplasia tarda. *Am J Hum Genet, 68*(6), 1386-1397. doi: 10.1086/320592

Ghosh, A. K., Majumder, M., Steele, R., White, R. A., & Ray, R. B. (2001). A novel 16-kilodalton cellular protein physically interacts with and antagonizes the functional activity of c-myc promoter-binding protein 1. *Mol Cell Biol, 21*(2), 655-662. doi: 10.1128/MCB.21.2.655-662.2001

Ghosh, A. K., Steele, R., & Ray, R. B. (2003). Modulation of human luteinizing hormone beta gene transcription by MIP-2A. *J Biol Chem, 278*(26), 24033-24038. doi: 10.1074/jbc.M211982200

Gillingham, A. K., & Munro, S. (2003). Long coiled-coil proteins and membrane traffic. *Biochim Biophys Acta, 1641*(2-3), 71-85.

Gonzalez, L. C., Jr., Weis, W. I., & Scheller, R. H. (2001). A novel snare N-terminal domain revealed by the crystal structure of Sec22b. *J Biol Chem, 276*(26), 24203-24211. doi: 10.1074/jbc.M101584200

Grabski, R., Z. Balklava, P. Wyrozumska, T. Szul, E. Brandon, C. Alvarez, Z.G. Holloway, and E. Sztul. (2012a). Identification of a functional domain within the p115 tethering factor that is required for Golgi ribbon assembly and membrane trafficking. *J Cell Sci, 125*(Pt 8), 1896-1909. doi: 10.1242/jcs.090571

Grabski, R., Hay, J., & Sztul, E. (2012b). Tethering factor P115: A new model for tether-SNARE interactions. *Bioarchitecture, 2*(5).

Gross, J.M., B.D. Perkins, A. Amsterdam, A. Egana, T. Darland, J.I. Matsui, S. Sciascia, N. Hopkins, and J.E. Dowling. (2005). Identification of zebrafish insertional mutants with defects in visual system development and function. *Genetics, 170*(1), 245-261. doi: 10.1534/genetics.104.039727

Gwynn, B., Smith, R. S., Rowe, L. B., Taylor, B. A., & Peters, L. L. (2006). A mouse TRAPP-related protein is involved in pigmentation. *Genomics, 88*(2), 196-203. doi: 10.1016/j.ygeno.2006.04.002

Hirschberg, K., Miller, C. M., Ellenberg, J., Presley, J. F., Siggia, E. D., Phair, R. D., & Lippincott-Schwartz, J. (1998). Kinetic analysis of secretory protein traffic and characterization of golgi to plasma membrane transport intermediates in living cells. *J Cell Biol, 143*(6), 1485-1503.

Hostetler, J. A. (1985). History and relevance of the Hutterite population for genetic studies. *Am J Med Genet, 22*(3), 453-462. doi: 10.1002/ajmg.1320220303

Hou, H., K. Subramanian, T.J. LaGrassa, D. Markgraf, L.E. Dietrich, J. Urban, N. Decker, and C. Ungermann. (2005). The DHHC protein Pfa3 affects vacuole-associated palmitoylation of the fusion factor Vac8. *Proc Natl Acad Sci U S A, 102*(48), 17366-17371. doi: 10.1073/pnas.0508885102

Howarth, D. L., Passeri, M., & Sadler, K. C. (2011). Drinks like a fish: using zebrafish to understand alcoholic liver disease. *Alcohol Clin Exp Res, 35*(5), 826-829. doi: 10.1111/j.1530-0277.2010.01407.x

Hughson, F. M. (1999). Membrane fusion: structure snared at last. *Curr Biol, 9*(2), R49-52.

Huynh, K. K., Eskelinen, E. L., Scott, C. C., Malevanets, A., Saftig, P., & Grinstein, S. (2007). LAMP proteins are required for fusion of lysosomes with phagosomes. *EMBO J, 26*(2), 313-324. doi: 10.1038/sj.emboj.7601511

Hyttinen, J. M., Niittykoski, M., Salminen, A., & Kaarniranta, K. (2013). Maturation of autophagosomes and endosomes: a key role for Rab7. *Biochim Biophys Acta, 1833*(3), 503-510. doi: 10.1016/j.bbamcr.2012.11.018

Itakura, E., Kishi-Itakura, C., Koyama-Honda, I., & Mizushima, N. (2012). Structures containing Atg9A and the ULK1 complex independently target depolarized mitochondria at initial stages of Parkin-mediated mitophagy. *J Cell Sci, 125*(Pt 6), 1488-1499. doi: 10.1242/jcs.094110

Jahn, R., Lang, T., & Sudhof, T. C. (2003). Membrane fusion. *Cell, 112*(4), 519-533.

Jahn, R., & Scheller, R. H. (2006). SNAREs--engines for membrane fusion. *Nat Rev Mol Cell Biol, 7*(9), 631-643. doi: 10.1038/nrm2002

Jang, S. B., Kim, Y. G., Cho, Y. S., Suh, P. G., Kim, K. H., & Oh, B. H. (2002). Crystal structure of SEDL and its implications for a genetic disease spondyloepiphyseal dysplasia tarda. *J Biol Chem, 277*(51), 49863-49869. doi: 10.1074/jbc.M207436200

Janvier, K., & Bonifacino, J. S. (2005). Role of the endocytic machinery in the sorting of lysosome-associated membrane proteins. *Mol Biol Cell, 16*(9), 4231-4242. doi: 10.1091/mbc.E05-03-0213

Jedd, G., Richardson, C., Litt, R., & Segev, N. (1995). The Ypt1 GTPase is essential for the first two steps of the yeast secretory pathway. *J Cell Biol, 131*(3), 583-590.

Jeyabalan, J., Nesbit, M. A., Galvanovskis, J., Callaghan, R., Rorsman, P., & Thakker, R. V. (2010). SEDLIN forms homodimers: characterisation of SEDLIN mutations and their interactions with transcription factors MBP1, PITX1 and SF1. *PLoS One, 5*(5), e10646. doi: 10.1371/journal.pone.0010646

Johannes, L., Tenza, D., Antony, C., & Goud, B. (1997). Retrograde transport of KDEL-bearing B-fragment of Shiga toxin. *J Biol Chem, 272*(31), 19554-19561.

Johansson, M., N. Rocha, W. Zwart, I. Jordens, L. Janssen, C. Kuijl, V.M. Olkkonen, and J. Neefjes. (2007). Activation of endosomal dynein motors by stepwise assembly of Rab7-RILP-p150Glued, ORP1L, and the receptor betalll spectrin. *J Cell Biol, 176*(4), 459-471. doi: 10.1083/jcb.200606077

Jones, S., Newman, C., Liu, F., & Segev, N. (2000). The TRAPP complex is a nucleotide exchanger for Ypt1 and Ypt31/32. *Mol Biol Cell, 11*(12), 4403-4411.

Kakuta, S., Yamamoto, H., Negishi, L., Kondo-Kakuta, C., Hayashi, N., & Ohsumi, Y. (2012). Atg9 vesicles recruit vesicle-tethering proteins Trs85 and Ypt1 to the autophagosome formation site. *J Biol Chem, 287*(53), 44261-44269. doi: 10.1074/jbc.M112.411454

Kaufman, L., Ayub, M., & Vincent, J. B. (2010). The genetic basis of non-syndromic intellectual disability: a review. *J Neurodev Disord, 2*(4), 182-209. doi: 10.1007/s11689-010-9055-2

Kim, M.S., M.J. Yi, K.H. Lee, J. Wagner, C. Munger, Y.G. Kim, M. Whiteway, M. Cygler, B.H. Oh, and M. Sacher. (2005a). Biochemical and crystallographic studies reveal a specific interaction between TRAPP subunits Trs33p and Bet3p. *Traffic, 6*(12), 1183-1195. doi: 10.1111/j.1600-0854.2005.00352.x

Kim, Y.G., S. Raunser, C. Munger, J. Wagner, Y.L. Song, M. Cygler, T. Walz, B.H. Oh, and M. Sacher. (2006). The architecture of the multisubunit TRAPP I complex suggests a model for vesicle tethering. *Cell, 127*(4), 817-830. doi: 10.1016/j.cell.2006.09.029

Kim, Y.G., E.J. Sohn, J. Seo, K.J. Lee, H.S. Lee, I. Hwang, M. Whiteway, M. Sacher, and B.H. Oh. (2005b). Crystal structure of bet3 reveals a novel mechanism for Golgi localization of tethering factor TRAPP. *Nat Struct Mol Biol, 12*(1), 38-45. doi: 10.1038/nsmb871

Klausner, R. D., Donaldson, J. G., & Lippincott-Schwartz, J. (1992). Brefeldin A: insights into the control of membrane traffic and organelle structure. *J Cell Biol, 116*(5), 1071-1080.

Klionsky, D. J. (2005). The molecular machinery of autophagy: unanswered questions. *J Cell Sci, 118*(Pt 1), 7-18. doi: 10.1242/jcs.01620

Klionsky, D. J., Cueva, R., & Yaver, D. S. (1992). Aminopeptidase I of Saccharomyces cerevisiae is localized to the vacuole independent of the secretory pathway. *J Cell Biol, 119*(2), 287-299.

Komatsu, M., S. Waguri, T. Ueno, J. Iwata, S. Murata, I. Tanida, J. Ezaki, N. Mizushima, Y. Ohsumi, Y. Uchiyama, E. Kominami, K. Tanaka, and T. Chiba. (2005). Impairment of starvation-induced and constitutive autophagy in Atg7-deficient mice. *J Cell Biol, 169*(3), 425-434. doi: 10.1083/jcb.200412022

Kornfeld, S., & Mellman, I. (1989). The biogenesis of lysosomes. *Annu Rev Cell Biol, 5*, 483-525. doi: 10.1146/annurev.cb.05.110189.002411

Koumandou, V. L., Dacks, J. B., Coulson, R. M., & Field, M. C. (2007). Control systems for membrane fusion in the ancestral eukaryote; evolution of tethering complexes and SM proteins. *BMC Evol Biol, 7*, 29. doi: 10.1186/1471-2148-7-29

Kummel, D., Muller, J. J., Roske, Y., Henke, N., & Heinemann, U. (2006). Structure of the Bet3-Tpc6B core of TRAPP: two Tpc6 paralogs form trimeric complexes with Bet3 and Mum2. *J Mol Biol, 361*(1), 22-32. doi: 10.1016/j.jmb.2006.06.012

Kummel, D., Muller, J. J., Roske, Y., Misselwitz, R., Bussow, K., & Heinemann, U. (2005). The structure of the TRAPP subunit TPC6 suggests a model for a TRAPP subcomplex. *EMBO Rep, 6*(8), 787-793. doi: 10.1038/sj.embor.7400463

Kummel, D., Oeckinghaus, A., Wang, C., Krappmann, D., & Heinemann, U. (2008). Distinct isocomplexes of the TRAPP trafficking factor coexist inside human cells. *FEBS Lett, 582*(27), 3729-3733. doi: 10.1016/j.febslet.2008.09.056

Laufman, O., Hong, W., & Lev, S. (2011). The COG complex interacts directly with Syntaxin 6 and positively regulates endosome-to-TGN retrograde transport. *J Cell Biol, 194*(3), 459-472. doi: 10.1083/jcb.201102045

Lebrand, C., M. Corti, H. Goodson, P. Cosson, V. Cavalli, N. Mayran, J. Faure, and J. Gruenberg. (2002). Late endosome motility depends on lipids via the small GTPase Rab7. *EMBO J, 21*(6), 1289-1300. doi: 10.1093/emboj/21.6.1289

Lee, J.H., J.L. Silhavy, J.E. Lee, L. Al-Gazali, S. Thomas, E.E. Davis, S.L. Bielas, K.J. Hill, M. Iannicelli, F. Brancati, S.B. Gabriel, C. Russ, C.V. Logan, S.M. Sharif, C.P. Bennett, M. Abe, F. Hildebrandt, B.H. Diplas, T. Attie-Bitach, N. Katsanis, A. Rajab, R. Koul, L. Sztriha, E.R. Waters, S. Ferro-Novick, C.G. Woods, C.A. Johnson, E.M. Valente, M.S. Zaki, and J.G. Gleeson. (2012). Evolutionarily assembled cis-regulatory module at a human ciliopathy locus. *Science, 335*(6071), 966-969. doi: 10.1126/science.1213506

Lee, M. C., Orci, L., Hamamoto, S., Futai, E., Ravazzola, M., & Schekman, R. (2005). Sar1p N-terminal helix initiates membrane curvature and completes the fission of a COPII vesicle. *Cell, 122*(4), 605-617. doi: 10.1016/j.cell.2005.07.025

Letourneur, F., E.C. Gaynor, S. Hennecke, C. Demolliere, R. Duden, S.D. Emr, H. Riezman, and P. Cosson. (1994). Coatomer is essential for retrieval of dilysine-tagged proteins to the endoplasmic reticulum. *Cell, 79*(7), 1199-1207.

Levine, T. P., Daniels, R. D., Wong, L. H., Gatta, A. T., Gerondopoulos, A., & Barr, F. A. (2013). Discovery of new Longin and Roadblock domains that form platforms for small GTPases in Ragulator and TRAPP-II. *Small GTPases, 4*(2).

Lewis, M. J., Nichols, B. J., Prescianotto-Baschong, C., Riezman, H., & Pelham, H. R. (2000). Specific retrieval of the exocytic SNARE Snc1p from early yeast endosomes. *Mol Biol Cell, 11*(1), 23-38.

Liang, Y., Morozova, N., Tokarev, A. A., Mulholland, J. W., & Segev, N. (2007). The role of Trs65 in the Ypt/Rab guanine nucleotide exchange factor function of the TRAPP II complex. *Mol Biol Cell, 18*(7), 2533-2541. doi: 10.1091/mbc.E07-03-0221

Lipatova, Z., Belogortseva, N., Zhang, X. Q., Kim, J., Taussig, D., & Segev, N. (2012a). Regulation of selective autophagy onset by a Ypt/Rab GTPase module. *Proc Natl Acad Sci U S A, 109*(18), 6981-6986. doi: 10.1073/pnas.1121299109

Lipatova, Z., & Segev, N. (2012b). A Ypt/Rab GTPase module makes a PAS. *Autophagy, 8*(8), 1271-1272. doi: 10.4161/auto.20872

Lippincott-Schwartz, J., & Liu, W. (2003). Membrane trafficking: coat control by curvature. *Nature, 426*(6966), 507-508. doi: 10.1038/426507a

Lippincott-Schwartz, J., Yuan, L. C., Bonifacino, J. S., & Klausner, R. D. (1989). Rapid redistribution of Golgi proteins into the ER in cells treated with brefeldin A: evidence for membrane cycling from Golgi to ER. *Cell, 56*(5), 801-813.

Little, C. B., Ghosh, P., & Bellenger, C. R. (1996). Topographic variation in biglycan and decorin synthesis by articular cartilage in the early stages of osteoarthritis: an experimental study in sheep. *J Orthop Res, 14*(3), 433-444. doi: 10.1002/jor.1100140314

Liu, W., & Parpura, V. (2010). SNAREs: could they be the answer to an energy landscape riddle in exocytosis? *ScientificWorldJournal, 10*, 1258-1268. doi: 10.1100/tsw.2010.137

Loh, E., Peter, F., Subramaniam, V. N., & Hong, W. (2005). Mammalian Bet3 functions as a cytosolic factor participating in transport from the ER to the Golgi apparatus. *J Cell Sci, 118*(Pt 6), 1209-1222. doi: 10.1242/jcs.01723

Lord, C., D. Bhandari, S. Menon, M. Ghassemian, D. Nycz, J. Hay, P. Ghosh, and S. Ferro-Novick. (2011). Sequential interactions with Sec23 control the direction of vesicle traffic. *Nature, 473*(7346), 181-186. doi: 10.1038/nature09969

Lynch-Day, M.A., D. Bhandari, S. Menon, J. Huang, H. Cai, C.R. Bartholomew, J.H. Brumell, S. Ferro-Novick, and D.J. Klionsky. (2010). Trs85 directs a Ypt1 GEF, TRAPPIII, to the phagophore to promote autophagy. *Proc Natl Acad Sci U S A, 107*(17), 7811-7816. doi: 10.1073/pnas.1000063107

Lynch-Day, M. A., & Klionsky, D. J. (2010). The Cvt pathway as a model for selective autophagy. *FEBS Lett, 584*(7), 1359-1366. doi: 10.1016/j.febslet.2010.02.013

Mahfouz, H., Ragnini-Wilson, A., Venditti, R., De Matteis, M. A., & Wilson, C. (2012). Mutational analysis of the yeast TRAPP subunit Trs20p identifies roles in endocytic recycling and sporulation. *PLoS One, 7*(9), e41408. doi: 10.1371/journal.pone.0041408

Malicdan, M. C., Noguchi, S., Nonaka, I., Saftig, P., & Nishino, I. (2008). Lysosomal myopathies: an excessive build-up in autophagosomes is too much to handle. *Neuromuscul Disord, 18*(7), 521-529. doi: 10.1016/j.nmd.2008.04.010

Mallard, F., Antony, C., Tenza, D., Salamero, J., Goud, B., & Johannes, L. (1998). Direct pathway from early/recycling endosomes to the Golgi apparatus revealed through the study of shiga toxin B-fragment transport. *J Cell Biol, 143*(4), 973-990.

Margittai, M., Fasshauer, D., Pabst, S., Jahn, R., & Langen, R. (2001). Homo- and heterooligomeric SNARE complexes studied by site-directed spin labeling. *J Biol Chem, 276*(16), 13169-13177. doi: 10.1074/jbc.M010653200

Mari, M., Griffith, J., Rieter, E., Krishnappa, L., Klionsky, D. J., & Reggiori, F. (2010). An Atg9-containing compartment that functions in the early steps of autophagosome biogenesis. *J Cell Biol, 190*(6), 1005-1022. doi: 10.1083/jcb.200912089

Mari, M., & Reggiori, F. (2010). Atg9 reservoirs, a new organelle of the yeast endomembrane system? *Autophagy, 6*(8), 1221-1223. doi: 10.1083/jcb.200912089

Marra, P., T. Maffucci, T. Daniele, G.D. Tullio, Y. Ikehara, E.K. Chan, A. Luini, G. Beznoussenko, A. Mironov, and M.A. De Matteis. (2001). The GM130 and GRASP65 Golgi proteins cycle through and define a subdomain of the intermediate compartment. *Nat Cell Biol, 3*(12), 1101-1113. doi: 10.1038/ncb1201-1101

Martinez-Menarguez, J. A., Prekeris, R., Oorschot, V. M., Scheller, R., Slot, J. W., Geuze, H. J., & Klumperman, J. (2001). Peri-Golgi vesicles contain retrograde but not anterograde proteins consistent with the cisternal progression model of intra-Golgi transport. *J Cell Biol, 155*(7), 1213-1224. doi: 10.1083/jcb.200108029

Massey, A. C., Zhang, C., & Cuervo, A. M. (2006). Chaperone-mediated autophagy in aging and disease. *Curr Top Dev Biol, 73*, 205-235. doi: 10.1016/S0070-2153(05)73007-6

Maxfield, F. R., & McGraw, T. E. (2004). Endocytic recycling. *Nat Rev Mol Cell Biol, 5*(2), 121-132. doi: 10.1038/nrm1315

Meiling-Wesse, K., U.D. Epple, R. Krick, H. Barth, A. Appelles, C. Voss, E.L. Eskelinen, and M. Thumm. (2005). Trs85 (Gsg1), a component of the TRAPP complexes, is required for the organization of the preautophagosomal structure during selective autophagy via the Cvt pathway. *J Biol Chem, 280*(39), 33669-33678. doi: 10.1074/jbc.M501701200

Mir, A., L. Kaufman, A. Noor, M.M. Motazacker, T. Jamil, M. Azam, K. Kahrizi, M.A. Rafiq, R. Weksberg, T. Nasr, F. Naeem, A. Tzschach, A.W. Kuss, G.E. Ishak, D. Doherty, H.H. Ropers, A.J. Barkovich, H. Najmabadi, M. Ayub, and J.B. Vincent. (2009). Identification of mutations in TRAPPC9, which encodes the NIK- and IKK-beta-binding protein, in nonsyndromic autosomal-recessive mental retardation. *Am J Hum Genet, 85*(6), 909-915. doi: 10.1016/j.ajhg.2009.11.009

Mizushima, N., & Komatsu, M. (2011). Autophagy: renovation of cells and tissues. *Cell, 147*(4), 728-741. doi: 10.1016/j.cell.2011.10.026

Mizushima, N., Yoshimori, T., & Levine, B. (2010). Methods in mammalian autophagy research. *Cell, 140*(3), 313-326. doi: 10.1016/j.cell.2010.01.028

Mochida, G.H., M. Mahajnah, A.D. Hill, L. Basel-Vanagaite, D. Gleason, R.S. Hill, A. Bodell, M. Crosier, R. Straussberg, and C.A. Walsh. (2009). A truncating mutation of TRAPPC9 is associated with autosomal-recessive intellectual disability and postnatal microcephaly. *Am J Hum Genet, 85*(6), 897-902. doi: 10.1016/j.ajhg.2009.10.027

Montpetit, B., & Conibear, E. (2009). Identification of the novel TRAPP associated protein Tca17. *Traffic, 10*(6), 713-723. doi: 10.1111/j.1600-0854.2009.00895.x

Moreau, D., Kumar, P., Wang, S. C., Chaumet, A., Chew, S. Y., Chevalley, H., & Bard, F. (2011). Genome-wide RNAi screens identify genes required for Ricin and PE intoxications. *Dev Cell, 21*(2), 231-244. doi: 10.1016/j.devcel.2011.06.014

Morozova, N., Y. Liang, A.A. Tokarev, S.H. Chen, R. Cox, J. Andrejic, Z. Lipatova, V.A. Sciorra, S.D. Emr, and N. Segev. (2006). TRAPPII subunits are required for the specificity switch of a Ypt-Rab GEF. *Nat Cell Biol, 8*(11), 1263-1269. doi: 10.1038/ncb1489

Mumberg, D., Muller, R., & Funk, M. (1995). Yeast vectors for the controlled expression of heterologous proteins in different genetic backgrounds. *Gene, 156*(1), 119-122.

Mumm, S., Zhang, X., Vacca, M., D'Esposito, M., & Whyte, M. P. (2001). The sedlin gene for spondyloepiphyseal dysplasia tarda escapes X-inactivation and contains a non-canonical splice site. *Gene, 273*(2), 285-293.

Nair, U., A. Jotwani, J. Geng, N. Gammoh, D. Richerson, W.L. Yen, J. Griffith, S. Nag, K. Wang, T. Moss, M. Baba, J.A. McNew, X. Jiang, F. Reggiori, T.J. Melia, and D.J. Klionsky. (2011). SNARE proteins are required for macroautophagy. *Cell, 146*(2), 290-302. doi: 10.1016/j.cell.2011.06.022

Nair, U., & Klionsky, D. J. (2011). Autophagosome biogenesis requires SNAREs. *Autophagy, 7*(12), 1570-1572.

Najmabadi, H., M.M. Motazacker, M. Garshasbi, K. Kahrizi, A. Tzschach, W. Chen, F. Behjati, V. Hadavi, S.E. Nieh, S.S. Abedini, R. Vazifehmand, S.G. Firouzabadi, P. Jamali, M. Falah, S.M. Seifati, A. Gruters, S. Lenzner, L.R. Jensen, F. Ruschendorf, A.W. Kuss,

and H.H. Ropers. (2007). Homozygosity mapping in consanguineous families reveals extreme heterogeneity of non-syndromic autosomal recessive mental retardation and identifies 8 novel gene loci. *Hum Genet, 121*(1), 43-48. doi: 10.1007/s00439-006-0292-0

Nakajima, H., Hirata, A., Ogawa, Y., Yonehara, T., Yoda, K., & Yamasaki, M. (1991). A cytoskeleton-related gene, uso1, is required for intracellular protein transport in Saccharomyces cerevisiae. *J Cell Biol, 113*(2), 245-260.

Nakatogawa, H., Ichimura, Y., & Ohsumi, Y. (2007). Atg8, a ubiquitin-like protein required for autophagosome formation, mediates membrane tethering and hemifusion. *Cell, 130*(1), 165-178. doi: 10.1016/j.cell.2007.05.021

Nazarko, T. Y., Huang, J., Nicaud, J. M., Klionsky, D. J., & Sibirny, A. A. (2005). Trs85 is required for macroautophagy, pexophagy and cytoplasm to vacuole targeting in Yarrowia lipolytica and Saccharomyces cerevisiae. *Autophagy, 1*(1), 37-45.

Noda, N.N., H. Kumeta, H. Nakatogawa, K. Satoo, W. Adachi, J. Ishii, Y. Fujioka, Y. Ohsumi, and F. Inagaki. (2008). Structural basis of target recognition by Atg8/LC3 during selective autophagy. *Genes Cells, 13*(12), 1211-1218. doi: 10.1111/j.1365-2443.2008.01238.x

Nordmann, M., Cabrera, M., Perz, A., Brocker, C., Ostrowicz, C., Engelbrecht-Vandre, S., & Ungermann, C. (2010). The Mon1-Ccz1 complex is the GEF of the late endosomal Rab7 homolog Ypt7. *Curr Biol, 20*(18), 1654-1659. doi: 10.1016/j.cub.2010.08.002

Novick, P., Ferro, S., & Schekman, R. (1981). Order of events in the yeast secretory pathway. *Cell, 25*(2), 461-469.

Novick, P., Field, C., & Schekman, R. (1980). Identification of 23 complementation groups required for post-translational events in the yeast secretory pathway. *Cell, 21*(1), 205-215.

O'Donnell, J., Maddox, K., & Stagg, S. (2011). The structure of a COPII tubule. *J Struct Biol, 173*(2), 358-364. doi: 10.1016/j.jsb.2010.09.002

Orci, L., M. Ravazzola, A. Volchuk, T. Engel, M. Gmachl, M. Amherdt, A. Perrelet, T.H. Sollner, and J.E. Rothman. (2000). Anterograde flow of cargo across the golgi stack potentially mediated via bidirectional "percolating" COPI vesicles. *Proc Natl Acad Sci U S A, 97*(19), 10400-10405. doi: 10.1073/pnas.190292497

Orsi, A., Razi, M., Dooley, H. C., Robinson, D., Weston, A. E., Collinson, L. M., & Tooze, S. A. (2012). Dynamic and transient interactions of Atg9 with autophagosomes, but not membrane integration, are required for autophagy. *Mol Biol Cell, 23*(10), 1860-1873. doi: 10.1091/mbc.E11-09-0746

Otte, S., & Barlowe, C. (2004). Sorting signals can direct receptor-mediated export of soluble proteins into COPII vesicles. *Nat Cell Biol, 6*(12), 1189-1194. doi: 10.1038/ncb1195

Otto, H., Hanson, P. I., & Jahn, R. (1997). Assembly and disassembly of a ternary complex of synaptobrevin, syntaxin, and SNAP-25 in the membrane of synaptic vesicles. *Proc Natl Acad Sci U S A, 94*(12), 6197-6201.

Palade, G. (1975). Intracellular aspects of the process of protein synthesis. *Science, 189*(4206), 867. doi: 10.1126/science.189.4206.867-b

Pankiv, S., E.A. Alemu, A. Brech, J.A. Bruun, T. Lamark, A. Overvatn, G. Bjorkoy, and T. Johansen. (2010). FYCO1 is a Rab7 effector that binds to LC3 and PI3P to mediate microtubule plus end-directed vesicle transport. *J Cell Biol, 188*(2), 253-269. doi: 10.1083/jcb.200907015

Pankiv, S., T.H. Clausen, T. Lamark, A. Brech, J.A. Bruun, H. Outzen, A. Overvatn, G. Bjorkoy, and T. Johansen. (2007). p62/SQSTM1 binds directly to Atg8/LC3 to facilitate degradation of ubiquitinated protein aggregates by autophagy. *J Biol Chem, 282*(33), 24131-24145. doi: 10.1074/jbc.M702824200

Pelham, H. R. (1991). Multiple targets for brefeldin A. *Cell, 67*(3), 449-451.

Perez-Victoria, F. J., & Bonifacino, J. S. (2009). Dual roles of the mammalian GARP complex in tethering and SNARE complex assembly at the trans-golgi network. *Mol Cell Biol, 29*(19), 5251-5263. doi: 10.1128/MCB.00495-09

Pfeffer, S., & Aivazian, D. (2004). Targeting Rab GTPases to distinct membrane compartments. *Nat Rev Mol Cell Biol, 5*(11), 886-896. doi: 10.1038/nrm1500

Pfeffer, S. R. (2001). Rab GTPases: specifying and deciphering organelle identity and function. *Trends Cell Biol, 11*(12), 487-491.

Podar, M., Wall, M. A., Makarova, K. S., & Koonin, E. V. (2008). The prokaryotic V4R domain is the likely ancestor of a key component of the eukaryotic vesicle transport system. *Biol Direct, 3*, 2. doi: 10.1186/1745-6150-3-2

Pratelli, R., Sutter, J. U., & Blatt, M. R. (2004). A new catch in the SNARE. *Trends Plant Sci, 9*(4), 187-195. doi: 10.1016/j.tplants.2004.02.007

Presley, J. F., Cole, N. B., Schroer, T. A., Hirschberg, K., Zaal, K. J., & Lippincott-Schwartz, J. (1997). ER-to-Golgi transport visualized in living cells. *Nature, 389*(6646), 81-85. doi: 10.1038/38001

Puthenveedu, M. A., & Linstedt, A. D. (2004). Gene replacement reveals that p115/SNARE interactions are essential for Golgi biogenesis. *Proc Natl Acad Sci U S A, 101*(5), 1253-1256. doi: 10.1073/pnas.0306373101

Raab-Cullen, D. M., Thiede, M. A., Petersen, D. N., Kimmel, D. B., & Recker, R. R. (1994). Mechanical loading stimulates rapid changes in periosteal gene expression. *Calcif Tissue Int, 55*(6), 473-478.

Reggiori, F., Wang, C. W., Stromhaug, P. E., Shintani, T., & Klionsky, D. J. (2003). Vps51 is part of the yeast Vps fifty-three tethering complex essential for retrograde traffic from the early endosome and Cvt vesicle completion. *J Biol Chem, 278*(7), 5009-5020. doi: 10.1074/jbc.M210436200

Ren, Y., Yip, C. K., Tripathi, A., Huie, D., Jeffrey, P. D., Walz, T., & Hughson, F. M. (2009). A structure-based mechanism for vesicle capture by the multisubunit tethering complex Dsl1. *Cell, 139*(6), 1119-1129. doi: 10.1016/j.cell.2009.11.002

Riederer, M. A., Soldati, T., Shapiro, A. D., Lin, J., & Pfeffer, S. R. (1994). Lysosome biogenesis requires Rab9 function and receptor recycling from endosomes to the trans-Golgi network. *J Cell Biol, 125*(3), 573-582.

Roskoski, R., Jr. (2003). Protein prenylation: a pivotal posttranslational process. *Biochem Biophys Res Commun, 303*(1), 1-7.

Rossi, G., Kolstad, K., Stone, S., Palluault, F., & Ferro-Novick, S. (1995). BET3 encodes a novel hydrophilic protein that acts in conjunction with yeast SNAREs. *Mol Biol Cell, 6*(12), 1769-1780.

Rubinsztein, D. C., Codogno, P., & Levine, B. (2012). Autophagy modulation as a potential therapeutic target for diverse diseases. *Nat Rev Drug Discov, 11*(9), 709-730. doi: 10.1038/nrd3802

Sacher, M. (2003). Membrane traffic fuses with cartilage development. *FEBS Lett, 550*(1-3), 1-4.

Sacher, M., Barrowman, J., Schieltz, D., Yates, J. R., 3rd, & Ferro-Novick, S. (2000). Identification and characterization of five new subunits of TRAPP. *Eur J Cell Biol, 79*(2), 71-80. doi: 10.1078/S0171-9335(04)70009-6

Sacher, M., Barrowman, J., Wang, W., Horecka, J., Zhang, Y., Pypaert, M., & Ferro-Novick, S. (2001). TRAPP I implicated in the specificity of tethering in ER-to-Golgi transport. *Mol Cell, 7*(2), 433-442.

Sacher, M., & Ferro-Novick, S. (2001). Purification of TRAPP from Saccharomyces cerevisiae and identification of its mammalian counterpart. *Methods Enzymol, 329*, 234-241.

Sacher, M., Y. Jiang, J. Barrowman, A. Scarpa, J. Burston, L. Zhang, D. Schieltz, J.R. Yates, 3rd, H. Abeliovich, and S. Ferro-Novick. (1998). TRAPP, a highly conserved novel

complex on the cis-Golgi that mediates vesicle docking and fusion. *EMBO J, 17*(9), 2494-2503. doi: 10.1093/emboj/17.9.2494

Sacher, M., Kim, Y. G., Lavie, A., Oh, B. H., & Segev, N. (2008). The TRAPP complex: insights into its architecture and function. *Traffic, 9*(12), 2032-2042. doi: 10.1111/j.1600-0854.2008.00833.x

Sadler, K. C., Amsterdam, A., Soroka, C., Boyer, J., & Hopkins, N. (2005). A genetic screen in zebrafish identifies the mutants vps18, nf2 and foie gras as models of liver disease. *Development, 132*(15), 3561-3572. doi: 10.1242/dev.01918

Sapperstein, S. K., Walter, D. M., Grosvenor, A. R., Heuser, J. E., & Waters, M. G. (1995). p115 is a general vesicular transport factor related to the yeast endoplasmic reticulum to Golgi transport factor Uso1p. *Proc Natl Acad Sci U S A, 92*(2), 522-526.

Schegg, B., Hulsmeier, A. J., Rutschmann, C., Maag, C., & Hennet, T. (2009). Core glycosylation of collagen is initiated by two beta(1-O)galactosyltransferases. *Mol Cell Biol, 29*(4), 943-952. doi: 10.1128/MCB.02085-07

Sclafani, A., Chen, S., Rivera-Molina, F., Reinisch, K., Novick, P., & Ferro-Novick, S. (2010). Establishing a role for the GTPase Ypt1p at the late Golgi. *Traffic, 11*(4), 520-532. doi: 10.1111/j.1600-0854.2010.01031.x

Scott, S. V., Baba, M., Ohsumi, Y., & Klionsky, D. J. (1997). Aminopeptidase I is targeted to the vacuole by a nonclassical vesicular mechanism. *J Cell Biol, 138*(1), 37-44.

Scott, S. V., Guan, J., Hutchins, M. U., Kim, J., & Klionsky, D. J. (2001). Cvt19 is a receptor for the cytoplasm-to-vacuole targeting pathway. *Mol Cell, 7*(6), 1131-1141.

Scott, S. V., Hefner-Gravink, A., Morano, K. A., Noda, T., Ohsumi, Y., & Klionsky, D. J. (1996). Cytoplasm-to-vacuole targeting and autophagy employ the same machinery to deliver proteins to the yeast vacuole. *Proc Natl Acad Sci U S A, 93*(22), 12304-12308.

Scrivens, P. J., Noueihed, B., Shahrzad, N., Hul, S., Brunet, S., & Sacher, M. (2011). C4orf41 and TTC-15 are mammalian TRAPP components with a role at an early stage in ER-to-Golgi trafficking. *Mol Biol Cell, 22*(12), 2083-2093. doi: 10.1091/mbc.E10-11-0873

Scrivens, P. J., Shahrzad, N., Moores, A., Morin, A., Brunet, S., & Sacher, M. (2009). TRAPPC2L is a novel, highly conserved TRAPP-interacting protein. *Traffic, 10*(6), 724-736. doi: 10.1111/j.1600-0854.2009.00906.x

Seaman, M. N., Marcusson, E. G., Cereghino, J. L., & Emr, S. D. (1997). Endosome to Golgi retrieval of the vacuolar protein sorting receptor, Vps10p, requires the function of the VPS29, VPS30, and VPS35 gene products. *J Cell Biol, 137*(1), 79-92.

Segev, N., Mulholland, J., & Botstein, D. (1988). The yeast GTP-binding YPT1 protein and a mammalian counterpart are associated with the secretion machinery. *Cell, 52*(6), 915-924.

Sekito, T., Kawamata, T., Ichikawa, R., Suzuki, K., & Ohsumi, Y. (2009). Atg17 recruits Atg9 to organize the pre-autophagosomal structure. *Genes Cells, 14*(5), 525-538. doi: 10.1111/j.1365-2443.2009.01299.x

Sharpe, L. J., Luu, W., & Brown, A. J. (2011). Akt phosphorylates Sec24: new clues into the regulation of ER-to-Golgi trafficking. *Traffic, 12*(1), 19-27. doi: 10.1111/j.1600-0854.2010.01133.x

Shaw, M.A., N. Brunetti-Pierri, L. Kadasi, V. Kovacova, L. Van Maldergem, D. De Brasi, M. Salerno, and J. Gecz. (2003). Identification of three novel SEDL mutations, including mutation in the rare, non-canonical splice site of exon 4. *Clin Genet, 64*(3), 235-242.

Shen, J., Tareste, D. C., Paumet, F., Rothman, J. E., & Melia, T. J. (2007). Selective activation of cognate SNAREpins by Sec1/Munc18 proteins. *Cell, 128*(1), 183-195. doi: 10.1016/j.cell.2006.12.016

Shestakova, A., Zolov, S., & Lupashin, V. (2006). COG complex-mediated recycling of Golgi glycosyltransferases is essential for normal protein glycosylation. *Traffic, 7*(2), 191-204. doi: 10.1111/j.1600-0854.2005.00376.x

Shintani, T., Huang, W. P., Stromhaug, P. E., & Klionsky, D. J. (2002). Mechanism of cargo selection in the cytoplasm to vacuole targeting pathway. *Dev Cell, 3*(6), 825-837.

Shintani, T., & Klionsky, D. J. (2004). Autophagy in health and disease: a double-edged sword. *Science, 306*(5698), 990-995. doi: 10.1126/science.1099993

Shorter, J., Beard, M. B., Seemann, J., Dirac-Svejstrup, A. B., & Warren, G. (2002). Sequential tethering of Golgins and catalysis of SNAREpin assembly by the vesicle-tethering protein p115. *J Cell Biol, 157*(1), 45-62. doi: 10.1083/jcb.200112127

Sollner, T., Bennett, M. K., Whiteheart, S. W., Scheller, R. H., & Rothman, J. E. (1993b). A protein assembly-disassembly pathway in vitro that may correspond to sequential steps of synaptic vesicle docking, activation, and fusion. *Cell, 75*(3), 409-418.

Sollner, T., Whiteheart, S. W., Brunner, M., Erdjument-Bromage, H., Geromanos, S., Tempst, P., & Rothman, J. E. (1993a). SNAP receptors implicated in vesicle targeting and fusion. *Nature, 362*(6418), 318-324. doi: 10.1038/362318a0

Soppina, V., Rai, A. K., Ramaiya, A. J., Barak, P., & Mallik, R. (2009). Tug-of-war between dissimilar teams of microtubule motors regulates transport and fission of endosomes. *Proc Natl Acad Sci U S A, 106*(46), 19381-19386. doi: 10.1073/pnas.0906524106

Stevens, T., Esmon, B., & Schekman, R. (1982). Early stages in the yeast secretory pathway are required for transport of carboxypeptidase Y to the vacuole. *Cell, 30*(2), 439-448.

Sudhof, T. C., Baumert, M., Perin, M. S., & Jahn, R. (1989). A synaptic vesicle membrane protein is conserved from mammals to Drosophila. *Neuron, 2*(5), 1475-1481.

Suzuki, K., Kirisako, T., Kamada, Y., Mizushima, N., Noda, T., & Ohsumi, Y. (2001). The pre-autophagosomal structure organized by concerted functions of APG genes is essential

for autophagosome formation. *EMBO J, 20*(21), 5971-5981. doi: 10.1093/emboj/20.21.5971

Sztul, E., & Lupashin, V. (2006). Role of tethering factors in secretory membrane traffic. *Am J Physiol Cell Physiol, 290*(1), C11-26. doi: 10.1152/ajpcell.00293.2005

Szul, T., & Sztul, E. (2011). COPII and COPI traffic at the ER-Golgi interface. *Physiology (Bethesda), 26*(5), 348-364. doi: 10.1152/physiol.00017.2011

Tan, D., Y. Cai, J. Wang, J. Zhang, S. Menon, H.T. Chou, S. Ferro-Novick, K.M. Reinisch, and T. Walz. (2013). The EM structure of the TRAPPIII complex leads to the identification of a requirement for COPII vesicles on the macroautophagy pathway. *Proc Natl Acad Sci U S A, 110*(48), 19432-19437. doi: 10.1073/pnas.1316356110

Taussig, D., Lipatova, Z., Kim, J. J., Zhang, X., & Segev, N. (2013). Trs20 is Required for TRAPP II Assembly. *Traffic, 14*(6), 678-690. doi: 10.1111/tra.12065

Tiller, G.E., V.L. Hannig, D. Dozier, L. Carrel, K.C. Trevarthen, W.R. Wilcox, S. Mundlos, J.L. Haines, A.K. Gedeon, and J. Gecz. (2001). A recurrent RNA-splicing mutation in the SEDL gene causes X-linked spondyloepiphyseal dysplasia tarda. *Am J Hum Genet, 68*(6), 1398-1407. doi: 10.1086/320594

Tochio, H., Tsui, M. M., Banfield, D. K., & Zhang, M. (2001). An autoinhibitory mechanism for nonsyntaxin SNARE proteins revealed by the structure of Ykt6p. *Science, 293*(5530), 698-702. doi: 10.1126/science.1062950

Townley, A. K., Feng, Y., Schmidt, K., Carter, D. A., Porter, R., Verkade, P., & Stephens, D. J. (2008). Efficient coupling of Sec23-Sec24 to Sec13-Sec31 drives COPII-dependent collagen secretion and is essential for normal craniofacial development. *J Cell Sci, 121*(Pt 18), 3025-3034. doi: 10.1242/jcs.031070

Turnbull, A.P., D. Kummel, B. Prinz, C. Holz, J. Schultchen, C. Lang, F.H. Niesen, K.P. Hofmann, H. Delbruck, J. Behlke, E.C. Muller, E. Jarosch, T. Sommer, and U. Heinemann. (2005). Structure of palmitoylated BET3: insights into TRAPP complex

assembly and membrane localization. *EMBO J, 24*(5), 875-884. doi: 10.1038/sj.emboj.7600565

Valdivia, R. H., Baggott, D., Chuang, J. S., & Schekman, R. W. (2002). The yeast clathrin adaptor protein complex 1 is required for the efficient retention of a subset of late Golgi membrane proteins. *Dev Cell, 2*(3), 283-294.

van Bokhoven, H. (2011). Genetic and epigenetic networks in intellectual disabilities. *Annu Rev Genet, 45*, 81-104. doi: 10.1146/annurev-genet-110410-132512

Venditti, R., T. Scanu, M. Santoro, G. Di Tullio, A. Spaar, R. Gaibisso, G.V. Beznoussenko, A.A. Mironov, A. Mironov, Jr., L. Zelante, M.R. Piemontese, A. Notarangelo, V. Malhotra, B.M. Vertel, C. Wilson, and M.A. De Matteis. (2012). Sedlin controls the ER export of procollagen by regulating the Sar1 cycle. *Science, 337*(6102), 1668-1672. doi: 10.1126/science.1224947

Verhage, M., A.S. Maia, J.J. Plomp, A.B. Brussaard, J.H. Heeroma, H. Vermeer, R.F. Toonen, R.E. Hammer, T.K. van den Berg, M. Missler, H.J. Geuze, and T.C. Sudhof. (2000). Synaptic assembly of the brain in the absence of neurotransmitter secretion. *Science, 287*(5454), 864-869.

Wan, J., Roth, A. F., Bailey, A. O., & Davis, N. G. (2007). Palmitoylated proteins: purification and identification. *Nat Protoc, 2*(7), 1573-1584. doi: 10.1038/nprot.2007.225

Wang, C. W., & Klionsky, D. J. (2003). The molecular mechanism of autophagy. *Mol Med, 9*(3-4), 65-76.

Wang, J., Menon, S., Yamasaki, A., Chou, H. T., Walz, T., Jiang, Y., & Ferro-Novick, S. (2013). Ypt1 recruits the Atg1 kinase to the preautophagosomal structure. *Proc Natl Acad Sci U S A, 110*(24), 9800-9805. doi: 10.1073/pnas.1302337110

Wang, W., Sacher, M., & Ferro-Novick, S. (2000). TRAPP stimulates guanine nucleotide exchange on Ypt1p. *J Cell Biol, 151*(2), 289-296.

Wendler, F., A.K. Gillingham, R. Sinka, C. Rosa-Ferreira, D.E. Gordon, X. Franch-Marro, A.A. Peden, J.P. Vincent, and S. Munro. (2010). A genome-wide RNA interference screen identifies two novel components of the metazoan secretory pathway. *EMBO J, 29*(2), 304-314. doi: 10.1038/emboj.2009.350

Westlake, C.J., L.M. Baye, M.V. Nachury, K.J. Wright, K.E. Ervin, L. Phu, C. Chalouni, J.S. Beck, D.S. Kirkpatrick, D.C. Slusarski, V.C. Sheffield, R.H. Scheller, and P.K. Jackson. (2011). Primary cilia membrane assembly is initiated by Rab11 and transport protein particle II (TRAPPII) complex-dependent trafficking of Rabin8 to the centrosome. *Proc Natl Acad Sci U S A, 108*(7), 2759-2764. doi: 10.1073/pnas.1018823108

Whitney, J. A., Gomez, M., Sheff, D., Kreis, T. E., & Mellman, I. (1995). Cytoplasmic coat proteins involved in endosome function. *Cell, 83*(5), 703-713.

Whyte, J. R., & Munro, S. (2002). Vesicle tethering complexes in membrane traffic. *J Cell Sci, 115*(Pt 13), 2627-2637.

Williams, A. L., Ehm, S., Jacobson, N. C., Xu, D., & Hay, J. C. (2004). rsly1 binding to syntaxin 5 is required for endoplasmic reticulum-to-Golgi transport but does not promote SNARE motif accessibility. *Mol Biol Cell, 15*(1), 162-175. doi: 10.1091/mbc.E03-07-0535

Woollard, A. A., & Moore, I. (2008). The functions of Rab GTPases in plant membrane traffic. *Curr Opin Plant Biol, 11*(6), 610-619. doi: 10.1016/j.pbi.2008.09.010

Xie, Z., & Klionsky, D. J. (2007). Autophagosome formation: core machinery and adaptations. *Nat Cell Biol, 9*(10), 1102-1109. doi: 10.1038/ncb1007-1102

Xu, D., & Hay, J. C. (2004). Reconstitution of COPII vesicle fusion to generate a pre-Golgi intermediate compartment. *J Cell Biol, 167*(6), 997-1003. doi: 10.1083/jcb.200408135

Xu, D., Joglekar, A. P., Williams, A. L., & Hay, J. C. (2000). Subunit structure of a mammalian ER/Golgi SNARE complex. *J Biol Chem, 275*(50), 39631-39639. doi: 10.1074/jbc.M007684200

Xu, Y., Martin, S., James, D. E., & Hong, W. (2002). GS15 forms a SNARE complex with syntaxin 5, GS28, and Ykt6 and is implicated in traffic in the early cisternae of the Golgi apparatus. *Mol Biol Cell, 13*(10), 3493-3507. doi: 10.1091/mbc.E02-01-0004

Yamakawa, K., S. Mitchell, R. Hubert, X.N. Chen, S. Colbern, Y.K. Huo, C. Gadomski, U.J. Kim, and J.R. Korenberg. (1995). Isolation and characterization of a candidate gene for progressive myoclonus epilepsy on 21q22.3. *Hum Mol Genet, 4*(4), 709-716.

Yamasaki, A., S. Menon, S. Yu, J. Barrowman, T. Meerloo, V. Oorschot, J. Klumperman, A. Satoh, and S. Ferro-Novick. (2009). mTrs130 is a component of a mammalian TRAPPII complex, a Rab1 GEF that binds to COPI-coated vesicles. *Mol Biol Cell, 20*(19), 4205-4215. doi: 10.1091/mbc.E09-05-0387

Yip, C. K., Berscheminski, J., & Walz, T. (2010). Molecular architecture of the TRAPPII complex and implications for vesicle tethering. *Nat Struct Mol Biol, 17*(11), 1298-1304. doi: 10.1038/nsmb.1914

Young, A.R., E.Y. Chan, X.W. Hu, R. Kochl, S.G. Crawshaw, S. High, D.W. Hailey, J. Lippincott-Schwartz, and S.A. Tooze. (2006). Starvation and ULK1-dependent cycling of mammalian Atg9 between the TGN and endosomes. *J Cell Sci, 119*(Pt 18), 3888-3900. doi: 10.1242/jcs.03172

Yu, I. M., & Hughson, F. M. (2010). Tethering factors as organizers of intracellular vesicular traffic. *Annu Rev Cell Dev Biol, 26*, 137-156. doi: 10.1146/annurev.cellbio.042308.113327

Yu, S., & Liang, Y. (2012). A trapper keeper for TRAPP, its structures and functions. *Cell Mol Life Sci*. doi: 10.1007/s00018-012-1024-3

Yu, S., Satoh, A., Pypaert, M., Mullen, K., Hay, J. C., & Ferro-Novick, S. (2006). mBet3p is required for homotypic COPII vesicle tethering in mammalian cells. *J Cell Biol, 174*(3), 359-368. doi: 10.1083/jcb.200603044

Zhang, T., & Hong, W. (2001). Ykt6 forms a SNARE complex with syntaxin 5, GS28, and Bet1 and participates in a late stage in endoplasmic reticulum-Golgi transport. *J Biol Chem, 276*(29), 27480-27487. doi: 10.1074/jbc.M102786200

Zhao, S.L., J. Hong, Z.Q. Xie, J.T. Tang, W.Y. Su, W. Du, Y.X. Chen, R. Lu, D.F. Sun, and J.Y. Fang. (2011). TRAPPC4-ERK2 interaction activates ERK1/2, modulates its nuclear localization and regulates proliferation and apoptosis of colorectal cancer cells. *PLoS One, 6*(8), e23262. doi: 10.1371/journal.pone.0023262

Zhu, H., Liang, Z., & Li, G. (2009). Rabex-5 is a Rab22 effector and mediates a Rab22-Rab5 signaling cascade in endocytosis. *Mol Biol Cell, 20*(22), 4720-4729. doi: 10.1091/mbc.E09-06-0453

Zolov, S. N., & Lupashin, V. V. (2005). Cog3p depletion blocks vesicle-mediated Golgi retrograde trafficking in HeLa cells. *J Cell Biol, 168*(5), 747-759. doi: 10.1083/jcb.200412003

Zong, M., A. Satoh, M.K. Yu, K.Y. Siu, W.Y. Ng, H.C. Chan, J.A. Tanner, and S. Yu. (2012). TRAPPC9 mediates the interaction between p150 and COPII vesicles at the target membrane. *PLoS One, 7*(1), e29995. doi: 10.1371/journal.pone.0029995

Zong, M., Wu, X. G., Chan, C. W., Choi, M. Y., Chan, H. C., Tanner, J. A., & Yu, S. (2011). The adaptor function of TRAPPC2 in mammalian TRAPPs explains TRAPPC2-associated SEDT and TRAPPC9-associated congenital intellectual disability. *PLoS One, 6*(8), e23350. doi: 10.1371/journal.pone.0023350

Zou, S., Y. Chen, Y. Liu, N. Segev, S. Yu, Y. Liu, G. Min, M. Ye, Y. Zeng, X. Zhu, B. Hong, L.O. Bjorn, Y. Liang, S. Li, and Z. Xie. (2013). Trs130 participates in autophagy through GTPases Ypt31/32 in Saccharomyces cerevisiae. *Traffic, 14*(2), 233-246. doi: 10.1111/tra.12024

Zou, S., Y. Liu, X.Q. Zhang, Y. Chen, M. Ye, X. Zhu, S. Yang, Z. Lipatova, Y. Liang, and N. Segev. (2012). Modular TRAPP complexes regulate intracellular protein trafficking

through multiple Ypt/Rab GTPases in Saccharomyces cerevisiae. *Genetics, 191*(2), 451-460. doi: 10.1534/genetics.112.139378